Bank Erosion Problem in Large Braided River and its Solution

A thesis submitted in partial fulfilment of the requirement for the award of the degree of

Doctor of Philosophy

By

Ranjit Deka

Roll No. 166104021

Under the Supervision of

Prof. Arup Kumar Sarma

Department of Civil Engineering

Indian Institute of Technology Guwahati

September 2024

Dedicated To My Wife Maina

Declarations

I do hereby declare that the content embodied in this thesis entitled **"Bank Erosion Problem in Large Braided River and its Solution"** is the result of investigation carried out by me at IIT Guwahati. Experimental works were carried out at NEHARI, Brahmaputra Board, Ministry of Jal Shakti, Government of India under the guidance of Prof. Arup Kumar Sarma.

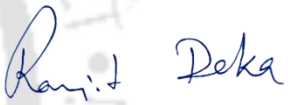

Ranjit Deka

Roll No 166104021

Department of Civil Engineering

Indian Institute of Technology Guwahati

Guwahati, Assam, India

September, 2024

Certificate

This is to certify that the work described in this thesis entitled "**Bank Erosion Problem in Large Braided River and its Solution**," submitted by Mr. **Ranjit Deka** (Roll No 166104021) in partial fulfilment of the requirements for the award of the degree of Doctoral of Philosophy is an authentic record of the results obtained from the research work carried out under my supervision in the Department of Civil Engineering, Indian Institute of Technology Guwahati, India and this work has not been submitted elsewhere for a degree.

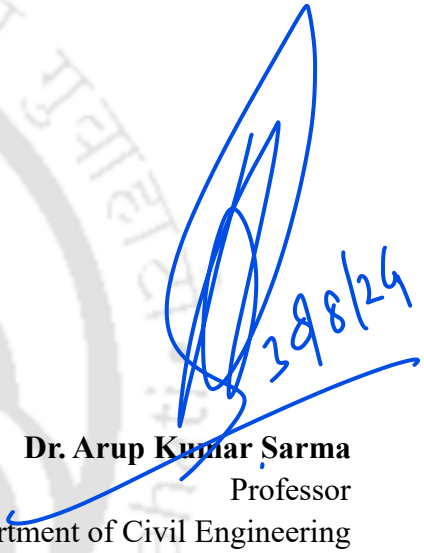

Dr. Arup Kumar Sarma
Professor
Department of Civil Engineering
Indian Institute of Technology Guwahati
Guwahati-781039

Acknowledgments

I would like to express my heartfelt gratitude and sincere thanks to my thesis supervisor Dr. Arup Kumar Sarma, Professor, Department of Civil Engineering, Indian Institute of Technology, Guwahati, for his invaluable guidance and full cooperation throughout all the aspects of this research work. It was a privilege to work under his supervision and humble guidance.

I attribute this achievement to my parents Late Bhabendra Deka and Smt. Labanyamoyee Deka, my wife Smt. Gitima Deka and my daughter Miss Abhilasha Deka. Without their blessing and support, I couldn't have made this possible.

I would like to acknowledge the Brahmaputra Board, Govt. Of India for providing NOC to pursue PhD programme. I am also indebted to officer and staff of NEHARI for their support during laboratory investigation, report preparation and field officers of Brahmaputra Board for their logistic support during the field investigation.

I would also like to express my heartfelt thanks and reverence to the Chairman of the Doctoral Committee, Dr. Rajib Kumar Bhattacharjya, Professor, Department of Civil Engineering, Indian Institute of Technology, Guwahati, for his valuable suggestions and all the help that I have received during the various stages of my research work. I am also indebted to Dr. Suresh A. Kartha, Professor, Department of Civil Engineering, Indian Institute of Technology, Guwahati, and Dr Sreedeep S., Professor, Geotechnical Engineering, Department of Civil Engineering, Indian Institute of Technology, Guwahati, for their keen interest, valuable suggestions, and guidance provided to complete my research work as members of the doctoral committee.

I would like to acknowledge Mr. Prasad S Kunjeer, Scientist, CWPRS, Pune, Dr. Anupal J Baruah and Dr. Dipsikha Devi, University of Alabama, USA for their support during my Ph.D. tenure.

I would also like to acknowledge that the Hydrological Result used in this study based on originally data collected by Central Water Commission, Govt. Of India.

I express my sincere thanks to the staff members of the Civil Engineering Department, Indian Institute of Technology, Guwahati, for their kind cooperation during my research work.

Finally, I would like to thank God for giving me strength, patience, and ability to carry out my PhD work with a sound mind and in good health.

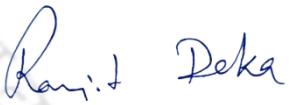

Ranjit Deka

Roll No 166104021

Department of Civil Engineering

Indian Institute of Technology Guwahati

Guwahati, Assam, India

September, 2024

ABSTRACT

The Brahmaputra River system commands a catchment area spanning 580,000 sq. km, making it one of the largest river basins in the region. For this study, the catchment areas of Brahmaputra River and its tributaries are delineated from freely available SRTM (Shuttle Radar Topography Mission) data. It is observed that catchment areas of north bank tributaries surpass those of their counterparts on the south bank, with higher rainfall in the former leading to a greater discharge contribution to the main river. While several river training works have been tried to manage the devastating impacts of erosion with experience of both success and failure, dredging is one of the measures at present under high priority. As dredging involves study of suspended and bed sediment movement, mathematical simulation become quite uncertain, as most of these sediment transport equations involve empirical parameters, whose applicability in a braided river like Brahmaputra needs to be verified with extensive field investigation. Such field investigations are not only time consuming and cumbersome, but also quite costly for a developing country like India. Physical model analysis has been an effective tool for good engineering judgement in selecting technically viable solutions, particularly for those situations where analytical study involves several empirical parameters difficult to be determined.

Satellite based study carried out in this research has shown that in Brahmaputra River, characterized by complex channel networks and frequent changes in channel morphology, bank erosion occurs not only along the main channel banks but also along the margins of secondary channels and bars. The lateral migration of channels, a common phenomenon in Brahmaputra River, leads to the progressive undermining and retreat of the adjacent banks, resulting in the lateral expansion of channels and the creation of new channels as the eroded sediment is redeposited downstream. High flow events, such as floods or sudden channel avulsions, can accelerate bank erosion rates by intensifying the erosive power of the water and mobilizing larger volumes of sediment. From soil characteristic study, it can be concluded that the bank erosion in Brahmaputra River is dependent on flow pattern and flow direction in channels and it is not much dependent on bank soil properties where clay or rock is not available.

Bank erosion problem of river Brahmaputra is studied in this research work starting with bank line study and soil characteristics study. The present research examines the characteristics of the river bank soil of the Brahmaputra River and investigates how they contribute to bank erosion. Also,

anthropogenic activities like construction of bridges etc., changes plan form configuration of the river and can lead to imbalance in the vicinity of such structure. Normally, rivers disperse immediately downstream of a bridge and this tendency of the river is popularly referred as fanning out of the river. Several initiatives are being implemented to safeguard the banks downstream of a bridge. However, there are few modelling-based research to explore whether downstream channelization can help reducing bank erosion at downstream of a bridge. Model study is carried out to investigate impacts of a mid-channel, created at downstream, on fanning out phenomenon at downstream of bridge. Three critical reaches of river Brahmaputra near Majuli, Tezpur and Guwahati are studied in this work. The Majuli reach is just downstream of a proposed bridge whereas the reaches near Guwahati and Tezpur are just downstream of existing bridge of river Brahmaputra. For deciding location of the dredged channel, time series satellite image analysis was undertaken to investigate the dynamics of large-scale sand bars. To evaluate sand bar motions over time, geo-referenced satellite pictures from 2015 to 2020 were overlay. Use of Landsat series data and Sentinel-1 Synthetic Aperture Radar (SAR) data has helped in identifying best location and orientation of dredging channels, as SAR data can capture river status even in a cloudy day during April to November. In the current study, it is imperative to acknowledge certain limitations associated with the mobile bed simulation feature implemented in mathematical models for modelling rivers with sediment transport. Hence, physical model study with mobile bed is conducted in parallel for the above-mentioned reaches of river Brahmaputra to understand the dynamics of bed of dredging channel. The comparison of velocities before and after providing the dredging channel is measured in the physical models. Also, deposition of the sand in the dredged channel with time is experimented to understand the sediment deposition rate. The study though has shown encouraging result, maintenance of the dredged channel is necessary for obtaining effective results in long run and thus impose a recurring expenditure.

Porcupine screen is also a commonly used river training works for deflecting flow and promoting near bank sedimentation in the Brahmaputra River. Physical model study is also conducted to check performance of dredging channel in reducing the near bank flow and in increasing flow concentration away from the bank. Performance of such dredged channel with and without porcupine screen, placed at appropriate location, is also investigated. Performance of porcupine screen alone is also investigated for one site in physical model. Although a thorough investigation using both experimental or mathematical model studies has not been conducted for these cases, the experimental study has shown potential of using dredged channel and porcupine or other similar river training work together to achieve the targeted goal of increasing flow concentration away from

the bank. A physical model study is conducted for a solution of bank erosion problem near Salmara in Majuli. Velocities are observed in physical model before and after laying scaled down porcupine screens. The best alignment for porcupine screens is finalized after observation of velocities in required location where deposition of sediment was expected. The porcupine screens are laid in actual field and observed deposition of sediment as required. It is concluded that the physical model study is an important tool in planning for solution of bank erosion problem in critical reaches of braided river.

There is relatively little research on movement of suspended sediment in braided rivers, yet it is possible that suspended sediment may have an impact on the dredging channel. Suspended sediment transport study is also conducted in one of proposed channel. The sediment transport dynamics within dredging channels are paramount for efficient management of hydraulic infrastructure. This study conducts a detailed analysis of sedimentation processes using a physical model approach. By meticulously examining the settling characteristics of suspended particles and establishing a similarity criterion for settling velocity between the model and prototype, this research ensures the accurate replication of sediment transport behaviour. The selection of Polyvinyl Chloride (PVC) powder as the suspended sediment material, matched carefully to the specific gravity requirements, further enhances the fidelity of the model. Through scaled sediment injection and systematic observation of sedimentation patterns at varying concentrations and discharge levels, this study provides valuable insights into sediment transport processes.

This research mainly emphasizes on physical model study for possible dredging work in river Brahmaputra. The study has shown potential of creating an appropriate dredged channel to reduce flow thrust at river bank. The approach developed in the study will help the decision-makers to execute effective anti-erosion measure in braided river.

Keywords: Braided river, River bank erosion, Anti-erosion measure, Dredging, Model study, Brahmaputra

Table of Contents

ABSTRACT V

LIST OF FIGURES XIV

LIST OF TABLES XVIII

LIST OF SYMBOLS XX

LIST OF ABBREVIATIONS XXII

1. INTRODUCTION 1

1.1 BACKGROUND 1

1.2 ORGANIZATION OF THE THESIS 5

2. LITERATURE REVIEW 7

2.1 INTRODUCTION 7

2.2 PREVIOUS STUDY ON RIVER BANK EROSION 8

2.2.1 STUDY ON RIVER BANK EROSION IN MEANDER RIVER 8

2.2.2 STUDY ON RIVER BANK EROSION IN BRAIDED RIVER 10

2.3 PREVIOUS GEOINFORMATICS STUDY TO UNDERSTAND MORPHOLOGICAL CHARACTERISTICS OF RIVER 13

2.4 PREVIOUS STUDY ON DREDGING OF RIVER 15

2.5 PREVIOUS MODEL STUDY TO UNDERSTAND CHARACTERISTICS OF RIVER FLOW 18

2.6 MOTIVATION AND OBJECTIVES FOR THE STUDY 20

OBJECTIVE 1: 21

OBJECTIVE 2: 21

OBJECTIVE 3: 22

OBJECTIVE 4: 22

OBJECTIVE 5: 23

3. BANKLINE STUDY TO QUANTIFY EROSION-DEPOSITION TREND IN BRAHMAPUTRA RIVER AND TO EXAMINE ITS RELATION WITH THE BANK MATERIAL 24

3.1 GIS BASED EROSION DEPOSITION STUDY ____ 24
3.2 DETAILED STUDY ON EROSION-DEPOSITION PATTERN OF MAJULI ISLAND ____ 30
3.2.1 BANKLINE STUDY NEAR MAJULI ____ 30
3.3 RIVER SAND BAR ANALYSIS ____ 35
3.4 SOIL CHARACTERISTIC STUDY OF RIVER BRAHMAPUTRA ____ 36
3.5 DISCUSSION AND CONCLUSION ____ 44

4. APPLICATION OF MATHEMATICAL MODEL FOR SIMULATING FLOW IN BRAIDED RIVER ____ 51

4.1 INTRODUCTION ____ 51
4.2 DEVELOPMENT OF BATHYMETRY ____ 51
4.2 SURVEY IN RIVER BRAHMAPUTRA FOR THE MODEL STUDY ____ 52
4.2.1 SURVEY OF RIVER BRAHMAPUTRA IN GUWAHATI REACH FOR THE MODEL STUDY ____ 53
4.2.2 SURVEY NEAR TEZPUR IN RIVER BRAHMAPUTRA FOR THE MODEL STUDY ____ 57
4.3 HYDROLOGICAL DATA ANALYSIS ____ 60
4.4 MATHEMATICAL MODEL APPLICATION ____ 64
4.5 MODEL APPLICATION FOR CREATION OF DREDGING CHANNEL AND DISCUSSIONS ____ 71
4.6 DISCUSSION AND CONCLUSION ____ 75

5. STUDY ON SUSTAINABILITY OF DREDGING CHANNEL IN RIVER BRAHMAPUTRA IN PHYSICAL MODEL ____ 77

5.1 INTRODUCTION ____ 77
5.2 LABORATORY SETUP AND EQUIPMENT USED FOR STUDY ____ 85
MEASUREMENT OF VELOCITY ____ 87
GAUGE MEASUREMENT ____ 88
5.2.1 DEVELOPMENT OF PHYSICAL MODEL OF RIVER BRAHMAPUTRA IN REACH NEAR GUWAHATI ____ 89
5.2.2 DEVELOPMENT OF PHYSICAL MODEL STUDY OF RIVER BRAHMAPUTRA IN REACH NEAR TEZPUR ____ 98
MOVABLE BED DESIGN ____ 102
5.3 DREDGING CHANNEL AT RIVER BRAHMAPUTRA ____ 104

5.4 STUDY OF SCOUR HOLE OF BRIDGES IN PHYSICAL MODEL OF RIVER BRAHMAPUTRA ____ 116
5.5 DISCUSSION AND CONCLUSION ____ 122
DISCUSSION AND CONCLUSION ON PHYSICAL MODEL STUDY OF PROPOSED DREDGING CHANNEL NEAR GUWAHATI ____ 122
DISCUSSION AND CONCLUSION ON PHYSICAL MODEL STUDY OF PROPOSED DREDGING CHANNEL NEAR TEZPUR ____ 123
6. NEED AND SCOPE OF USING PORCUPINE SCREEN AND DREDGING INDEPENDENTLY OR IN COMBINATION. ____ 126
6.1 STUDY ON USE OF PORCUPINE SCREEN ALONG WITH PROPOSED DREDGING CHANNEL FOR A REACH IN RIVER BRAHMAPUTRA NEAR MAJULI. ____ 126
PRELIMINARY ALIGNMENT OF DREDGING CHANNEL CONSIDERING RIVER SAND BAR DYNAMICS. ____ 129
RADAR DATA ANALYSIS FOR PROPOSED DREDGING CHANNEL: ____ 129
FINALIZATION OF POSSIBLE DREDGING CHANNEL AFTER SENTINEL 1 DATA ANALYSIS ____ 131
6.2 SURVEY DATA FOR THE MODEL STUDY: ____ 133
6.3 HYDROLOGICAL DATA FOR THE MODEL STUDY: ____ 139
6.4 DESIGN OF SCALE AS PER FROUDIAN SIMILITUDE: ____ 162
6.5 UAV STUDY ON PHYSICAL MODEL OF RIVER BRAHMAPUTRA ____ 165
6.6 OBSERVATION OF DEPTH AND VELOCITY IN THE PRESENT PHYSICAL MODEL STUDY ____ 167
6.7 STUDY ON USE OF PORCUPINE SCREEN AS ANTI-EROSION MEASURE FOR A CRITICAL LOCATION IN RIVER BRAHMAPUTRA NEAR MAJULI. ____ 171
6.8 DISCUSSION AND CONCLUSION ____ 173
DISCUSSION AND CONCLUSION FOR PHYSICAL MODEL STUDY FOR A REACH IN RIVER BRAHMAPUTRA NEAR MAJULI AT NORTH BANK AND NEMATI GHAT AT SOUTH BANK ____ 173
DISCUSSION AND CONCLUSION FOR PHYSICAL MODEL STUDY TO USE PORCUPINE SCREEN AS ANTI-EROSION MEASURE FOR A CRITICAL LOCATION AT SALMARA, MAJULI ____ 175
7. SEDIMENT TRANSPORT STUDY FOR PROPOSED DREDGING CHANNEL OF RIVER BRAHMAPUTRA ____ 177

7.1 INTRODUCTION ____ 177
7.2 SCALING OF SEDIMENT SIZE AND RATE FOR THE PHYSICAL MODEL STUDY 182
7.3 OBSERVATION OF SEDIMENTATION IN THE PROPOSED DREDGING CHANNEL IN THE PHYSICAL MODEL ____ 186
7.4 DISCUSSION AND CONCLUSION ____ 192
8. CONCLUSION AND GENERAL DISCUSSION FOR FUTURE STUDIES ____ 194
8.1 A BRIEF REVIEW OF WORK DONE ____ 194
OBJECTIVE 1: TO STUDY THE ROLE OF MORPHOLOGY AND SOIL PROPERTIES IN BANK EROSION OF BRAHMAPUTRA RIVER. ____ 194
OBJECTIVE 2.1: TO STUDY THE FORMATION OF SCOUR HOLE IN BRAHMAPUTRA RIVER AND COMPARE IT WITH THE CALCULATED SCOUR DEPTH AND WIDTH BY EMPIRICAL FORMULA. ____ 195
OBJECTIVE 2.2: TO CONDUCT MODEL STUDY FOR MANAGEMENT OF RIVER AT DOWNSTREAM OF BRIDGE BY PROVIDING MID CHANNEL. ____ 195
OBJECTIVE 3: TO INVESTIGATE THE POSSIBILITY OF REDUCTION IN RIVER BANK EROSION BY IMPLEMENTING DREDGED CHANNEL IN BRAIDED RIVER. ALSO, TO STUDY THE EFFICACY OF PORCUPINE SCREEN WITH DREDGING CHANNEL THROUGH PHYSICAL MODEL STUDY. ____ 196
OBJECTIVE 4: TO ANALYSE RADAR DATA FOR PLANNING OF ANTI-BANK EROSION WORK IN BRAIDED RIVER. ____ 196
OBJECTIVE 5: TO STUDY THE SUSPENDED SEDIMENT DEPOSITION IN PROPOSED DREDGING CHANNEL. ____ 196
8.2 RECOMMENDATIONS FOR FUTURE WORK ____ 197
REFERENCES ____ 198
LIST OF PUBLICATIONS ____ 204
ANNEXURE I: ____ 205
ANNEXURE II: ____ 207

List of Figures

Figure 3. 1 Satellite image showing Brahmaputra River in Assam 24
Figure 3. 2 Methodology for estimation of erosion or deposition 25
Figure 3.3 Right Bank Erosion (RBE) of River Brahmaputra 26
Figure 3.4 Left Bank Erosion (LBE) of River Brahmaputra..... 27
Figure 3.5 Right Bank Deposition (RBD) of River Brahmaputra..... 28
Figure 3.6 Left Bank Deposition (LBD) of River Brahmaputra 29
Figure 3.7 LISS IV imagery of study area 31
Figure 3.8 River bank line and main channel of the year 1988 32
Figure 3.9 River bank line and main channel of the year 2005 32
Figure 3.10 River bank line and main channel of the year 2012 33
Figure 3.11 River bank line and main channel of the year 2019..... 33
Figure 3.12 River Sand bar between Majuli and Nimati Ghat..... 36

Figure 4.1 Photographs taken during bathymetry survey near Guwahati _____ 55
Figure 4.2 Photographs taken during bathymetry survey near Guwahati _____ 55
Figure 4.3 Cross Section for survey of river Brahmaputra near Guwahati _____ 56
Figure 4.4 Flow chart for survey work at Tezpur _____ 59
Figure 4.5 Cross-section for survey near Tezpur _____ 59
Figure 4.6 Photographs taken during bathymetry survey near Tezpur _____ 60
Figure 4.7 Mathematical Model in HEC RAS 2D for a reach near Guwahati _____ 65
Figure 4.8 Water surface elevation map (For Q=51319.000 m3/sec) _____ 66
Figure 4.9 Velocity map (For Q=51319.000 m3/sec) _____ 67
Figure 4.10 Depth map (For Q=51319.000 m3/sec) _____ 67
Figure 4.11 Mathematical Model in HEC RAS 2D for a reach near Tezpur _____ 68
Figure 4.12 Water surface elevation map (For Q=50024 m3/sec) _____ 69
Figure 4.13 Velocity map (For Q=50024 m3/sec) _____ 70
Figure 4.14 Depth map (For Q=50024 m3/sec) _____ 70
Figure 4.15 Study in HEC RAS 2D with proposed channel near Guwahati _____ 71
Figure 4.16 Study in HEC RAS 2D with proposed channel near Tezpur _____ 72

Figure 5.1 An Aerial View of Hydraulic Models Tray 86
Figure 5.2 Twin rectangular weir at Hydraulic Laboratory 86
Figure 5.3 Photo of Propeller type Velocity Meter 87
Figure 5.4 Photo of Acoustic Doppler Velocity meter (ADV) 88
Figure 5.5 Photo of Gauge Scale 88
Figure 5.6 Plan of Model Survey Data 89
Figure 5.7 A Photo of Model prior to run (Dry State) 90
Figure 5.8 A Photo of Model at the Run 90
Figure 5.9 Plan of model tray Auto-CAD 91
Figure 5.10 Soil Grading Curve for Prototype Riverbed. 93
Figure 5.11 Shield Incipient Motion Graph. 94
Figure 5.12 Soil Grading Curve of Model Sand 96
Figure 5.13 Gauge – Discharge Curve for Pandu GDS 97
Figure 5.14 Plan of Model Survey Data 98
Figure 5.15 A Photo of Model Tray during Run 99
Figure 5.16 Plan of Model Tray Auto-CAD 99
Figure 5.17 Soil Grading Curve for Prototype River bank 101
Figure 5.18 Shield Incipient Motion Graph. 102
Figure 5.19 Soil Grading curve of model sand 103
Figure 5.20 Satellite Images of the Study Area for various years 104
Figure 5.21 Comparison of Velocity at 30000 cumec before and after dredging channel near Guwahati 105
Figure 5.22 Comparison of Velocity at 40000 cumec before and after dredging channel near Guwahati 106
Figure 5.23 Comparison of Velocity at 50000 cumec before and after dredging channel near Guwahati 106
Figure 5.24 Photo of Physical Model showing cross section near Guwahati 107
Figure 5.25 Deposition with respect to time in cross-section no. 15 Near Guwahati. 108
Figure 5.26 Deposition with respect to time in cross-section no. 11 Near Guwahati. 109
Figure 5.27 Comparison of Velocity at 30000 cumec before and after dredging channel near Tezpur 110
Figure 5.28 Comparison of Velocity at 40000 cumec before and after dredging channel near Tezpur 111

Figure 5.29 Comparison of Velocity at 50000 cumec before and after dredging channel near Tezpur 111
Figure 5.30 Photo of Physical Model showing cross-section near Tezpur 112
Figure 5.31 Deposition with respect to time in cross-section no. 18 Near Tezpur. 113
Figure 5.32 Deposition with respect to time in cross-section no. 15 Near Tezpur. 114
Figure 5.33 Deposition with respect to time in cross-section no. 10 Near Tezpur. 115
Figure 5.34 Empirical Scour Width (After Singh et al. (2020)) 120
Figure 5.35 Photo of scour hole around pier no. 5 of bridge near Guwahati 121
Figure 5.36 Photo of scour hole around pier no. 19 of bridge near Tezpur 121

Figure 6. 1 Methodology used to propose and finalise the dredging channel 128
Figure 6. 2 Preliminary dredging alignment near Majuli 129
Figure 6.3 Flowchart of the methodology 131
Figure 6.4 River channel maps of the study area from April, 2020 to September, 2020. 132
Figure 6.5 Image showing 56 nos. Cross sections for Bathymetry Survey 133
Figure 6.6 Image showing area of Physical Model Study 133
Figure 6.7 Cross-Sections of River Brahmaputra used in Physical Model Study 138
Figure 6.8 Maximum WL for the period 1976 to 1996 at Bessamara 144
Figure 6.9 Water Level for the period 1976 to 1996 at Bessamara 145
Figure 6.10 Maximum Discharge for the period 1976 to 1993 at Bessamara 151
Figure 6.11 Maximum Discharge for the period 1976 to 1993 at Bessamara 152
Figure 6.12 Rating Curve of Bessamara Site 153
Figure 6.13 Yearly Maximum Water Level of Brahmaputra River at Nimati Ghat 157
Figure 6.14 Monthly Maximum, Minimum and Average Water Level of Brahmaputra River at Nimati Ghat from 2014 to 2019 157
Figure 6.15 Maximum Water Level for the period 2008 to 2020 at Kamalabari 160
Figure 6.16 Maximum Water Level for the period 2008 to 2020 at Kamalabari 161
Figure 6.17 A photo during use of UAV to generate Digital Surface Models (DSMs) of model bed 165
Figure 6.18 UAV ortho-mosaic image and DSM of Model area before dredging 166
Figure 6.19 UAV ortho-mosaic image and DSM of Model area after dredging 166
Figure 6.20 Erosion problem near Salmara, Majuli 171
Figure 6.21 Velocity distribution from model study for Salmara reach (at 20000 cumec) 172
Figure 6.22 Velocity distribution from model study for Salmara reach (at 30000 cumec) 172

Figure 6.23 Velocity distribution from model study for Salmara reach (at 40000 cumec) _____ 173

Figure 7.1 Location of Dredging Channel for Model Study _____ 182
Figure 7.2 Construction of Dredging Channel in Physical Model _____ 183
Figure 7.3 Graph for specific gravity vs D_{50}Proto/D_{50}Model _____ 184
Figure 7.4 Observation at 50 PPM Suspended Sediment _____ 187
Figure 7.5 Observation at 90 PPM Suspended Sediment _____ 187
Figure 7.6 Sediment in percentage Flushed out of Channel at 50 PPM _____ 188
Figure 7.7 Sediment in percentage Flushed out of Channel at 90 PPM _____ 188
Figure 7.8 Collection of PVC at 10000 cumecs discharge _____ 189
Figure 7.9 Collection of Sand at 10000 cumecs discharge _____ 189
Figure 7.10 Collection of PVC at 20000 cumecs discharge _____ 190
Figure 7.11 Collection of Sand at 20000 cumecs discharge _____ 190
Figure 7.12 Collection of PVC at 30000 cumecs discharge _____ 191
Figure 7.13 Collection of Sand at 30000 cumecs discharge _____ 191

List of Tables

Table 3.1 Right Bank Erosion of River Brahmaputra 26
Table 3.2 Left Bank Erosion of River Brahmaputra 27
Table 3.3 Right Bank Deposition of River Brahmaputra 28
Table 3.4 Left Bank Deposition of River Brahmaputra 29
Table 3.5 Results of soil classification 40
Table 3.6 Results of Mechanical Analysis and Atterberg limits tests 41
Table 3.7 Results of Proctor Compaction and Specific Gravity 42
Table 3.8 Results of permeability test 43

Table 4.1 Coordinate of control points for survey near Guwahati 54
Table 4. 2 Details of the Bench mark (near Guwahati) 54
Table 4.3 Details of the Bench mark (near Tezpur) 57
Table 4.4 Coordinate of control points for survey near Tezpur 58
Table 4.5 Maximum flow corresponding to different return periods at Pandu 62
Table 4.6 Annual mean flow rate corresponding to different return periods at Pandu 62
Table 4.7 WL corresponding to different return periods at Pandu 63
Table 4.8 Maximum flow corresponding to different return periods at Bhomoraguri 63
Table 4.9 Annual mean flow rate corresponding to different return periods at Bhomoraguri 63
Table 4.10 The recorded event at Pandu site considered for validation of the model 66
Table 4.11 The recorded events at Bhromaguri site considered for validation of the model 69

Table 5.1 Model parameters of Physical Model of River Brahmaputra in Reach near Guwahati 92
Table 5.2 Model Parameters of Physical Model of River Brahmaputra in Reach near Tezpur 100
Table 5.3 Changes in Bed of Proposed Dredging Channel in Model Study 107
Table 5.4 Changes in Bed of Proposed Dredging Channel in Model Study 112
Table 5.5 Scour depth calculation 117
Table 5.6 Scour Depth Calculation Considering the Flow Concentration Through the Primary Channels 117
Table 5.7 Observed scour depth at various piers in model for Guwahati area. 119
Table 5.8 Observed scour depth at various piers in model for Tezpur area. 119

Table 6.1 Monthly Maximum, Minimum and Average Water Level of river Brahmaputra at Bessamara 139
Table 6.2 Yearly Maximum Water Level of Brahmaputra River at Bessamara 144
Table 6.3 Monthly Maximum, Minimum and Average Water Level of Brahmaputra River at Bessamara from 1976 to 1993 145
Table 6.4 Monthly Maximum, Minimum and Average Discharge Data of river Brahmaputra at Bessamara 146
Table 6.5 Yearly Maximum Discharge Data of Brahmaputra River at Bessamara 151
Table 6.6 Monthly Maximum, Minimum and Average Discharge Data of Brahmaputra River at Bessamara from 1976 to 1993 152
Table 6.7 Yearly Maximum, Minimum Discharge Data of Brahmaputra River at Bessamara 156
Table 6.8 Monthly Maximum, Minimum and Average Water Level of Brahmaputra River at Kamalabari 158
Table 6.9 Yearly Maximum Water Level of Brahmaputra River at Kamalabari 160
Table 6.10 Monthly Maximum, Minimum and Average Water Level of Brahmaputra River at Kamalabari from 2014 to 2019 161
Table 6.11 Velocities before and after dredging without porcupine. 168
Table 6.12 Velocities before and after dredging with porcupine 169

Table 7.1 Reading for 50 PPM Suspended Sediments 186
Table 7.2 Reading for 90 PPM Suspended Sediments 186

List of Symbols

SYMBOLS	DESCRIPTIONS
ρ	is the density of water,
g	is the acceleration due to gravity,
D	is the median particle diameter of the sediment.
x_T	is the value of variate with a return period T
$\bar{x}$	is the mean of the variate
K	is the frequency factor expressed as $K = (y - y_n)/S_n$
y	is the reduced variate expressed as $ln\left\{ln\left[\frac{T}{(T-1)}\right]\right\}$
T	is the return period
y_n	is the Gumbel's reduced mean variable
S_n	is the standard deviation
f	is the coefficient of friction
nb (Base Value)	is the fundamental value for a straight, uniform, and smooth channel within natural materials.
n1 (Surface Irregularities Correction)	is the correction factor accounting for the influence of surface irregularities on the channel.
n2 (Cross-Sectional Shape and Size)	is the value encapsulates the variations in both the shape and size of the channel's cross-section.
n3 (Obstruction Impact)	is the factor incorporates the effects of obstructions within the channel.
n4 (Vegetation and Flow Conditions)	is the impact of vegetation and the prevailing flow conditions on the channel.
m (Meandering Correction Factor)	is the correction factor accounts for the meandering tendencies of the channel.

$\tau*$	is the Shields Parameter (dimensionless shear stress),
τ	is the Shear Stress Exerted by the Flow on the Bed,
ρs	is the Density of Sediment Particles,
L_r	is the Horizontal Scale Ratio
D_r	is the Vertical Scale Ratio
SP-SM	is the Poorly Graded Sand with Silt
ML	is the Sandy Silts, Clayey Silts, or Inorganic Silts with Relatively Low Plasticity
MI	is the Silt of Intermediate Plasticity
SP	is the Gravelly or Sandy with Little to no Fines

List of Abbreviations

Terms	ABBREVIATIONS
1D	One Dimensional
2D	Two Dimensional
3D	Three Dimensional
A	Acceleration
ADCP	Acoustic Doppler Current Profilers
BIS	Bureau of Indian Standards
BRAHMA	Braided River Aid: Hydro-Morphological Analyzer
BM	Bench Mark
CWC	Central Water Commission
DEM	Digital Elevation Model
DGPS	Differential Global Positioning System
DSM	Digital Surface Model
ESA	European Space Agency
EW	Extra Wide
F	Force
F_i	Inertia force
GCP	Ground Control Point
GIS	Geographic Information System
GPS	Global Positioning System
HEC-RAS	Hydrologic Engineering Centre's River Analysis System
IS	Indian Standards

IW	Interferometric Wide
KML	Keyhole Markup Language
LiDAR	Light Detection and Ranging
M	Mass
MIKE	Modelling Integrated Catchment Hydrology
NEHARI	North Eastern Hydraulic and Allied Research Institute
NRSC	National Remote Sensing Centre
PPM	Parts Per Million
PVC	Poly Vinyl Chloride
R.L	Reduced Level
RTK	Real Time Kinematics
SAC	Space Application Centre
SAR	Synthetic Aperture Radar
SONAR	Sound Navigation and Ranging
SRTM	Shuttle Radar Topography Mission
SM	Strip Map
SNAP	Sentinel Application Platform
VH	Vertical Transmit- Horizontal Receive Polarization
VV	Vertical Transmit-Vertical Receive Polarization.

1.

Introduction

1.1 Background

The records of the last century show a general trend of widening of the river Brahmaputra in Assam. The widening trend is clearly visible when comparing erosion and accretion rates over different periods. Long-term observations on width changes of the river are available, although data from different authors are not directly comparable. In general, the losses due to erosion show an increasing trend. Reports available with Water Resources Department indicate that 3,860 km of land were lost since 1954, with a rate of about 80 km per year. The erosion wiped out more than 2,500 villages and 18 towns, including sites of cultural heritage and tea gardens affecting the lives of nearly half a million people. About 130 river reaches are presently classified as being under moderate to severe erosion and 25 as very severe. While suffering of people due to flood cannot be underestimated, suffering of rural agricultural community due to erosion of their land is much more disastrous.

Because of their distinct channel dynamics, sediment transport, and hydrological patterns, meandering and braided rivers' erosion processes show both parallels and contrasts. To understand river morphology and the resulting landscapes, one must have a thorough understanding of these processes. The interplay of water flow and sediment transport causes erosion in both types of rivers, although the patterns and results of these processes vary greatly between them. In meandering rivers, erosion primarily occurs on the outer bends, known as cut banks, where the flow velocity is highest. This high-velocity water scours the bank, creating lateral erosion and gradually shifting the meander bends over time. This process is balanced off by sediment deposition on the inner bends, or point bars, where the flow velocity drops and sediment accumulates. The end product is a sinuous waterway that flows through the floodplain, forming a sequence of loops and bends. Erosion and deposition in meandering rivers are relatively predictable and follow a consistent, cyclical pattern. When the river breaks through a tiny stretch of land during a high flow event, it can cut off a meander bend from the main channel, resulting in the formation of oxbow lakes over time. In contrast, braided rivers are made up of several interwoven channels that are divided by silt bars and islands. These rivers are commonly found in areas with heavy silt loads and fluctuating water flow. Erosion in

braided rivers is more dynamic and geographically varied than in meandering rivers. The large sediment load and frequent fluctuations in water flow cause both lateral and vertical erosion of the riverbed and banks. Channels in braided rivers vary often, resulting in rapid changes in river shape. The braided character of these rivers results in a wider, shallower channel than the deep, tight channels of meandering rivers. The unpredictability in braided rivers frequently results in a more extensive and distributed pattern of erosion, with bars and islands eroding and reforming on a regular basis. Despite their differences, meandering and braided rivers are shaped by the same fundamental processes: erosion and deposition. In both cases, water movement causes shear stress on the riverbed and banks, trapping material and pushing it downstream. The river's ability to erode and carry material is determined by variables such as water velocity, discharge, sediment size, and sediment supply. Meandering rivers' continuous and relatively constant flow allows for the formation of well-defined erosion and deposition patterns, whereas braided rivers' variability in flow and sediment supply leads to more chaotic and extensive erosion and deposition. In conclusion, whereas both meandering and braided rivers are shaped by the interaction of erosion and deposition, their mechanics differ dramatically due to differing channel dynamics and sediment transportation processes. Meandering rivers have more consistent and predictable erosion and deposition patterns, resulting in the construction of sinuous channels and oxbow lakes. Braided rivers, on the other hand, are distinguished by their highly dynamic and complicated erosion processes, which produce larger, shallower channels with frequent morphological changes. Understanding these distinctions is critical for effective river management and erosion control.

Understanding the dynamic nature of a large braided river like Brahmaputra is crucial for addressing the erosion challenges. Formation of braiding pattern is quite common in case of any wide river with gentle slope in alluvial flood plains. Even in the straight reaches, formation of the multi-thread flow can be found very often. In a system of multi-channel flow, the configuration of side channel is responsible for the bank erosion. In the erosion prone river reaches the side channel generally make a curvature to cause the erosion on its outward side like that of a meandering river. The close interrelationship between the river flow and channel formation governs many river channel processes such as meander planform, bed topography, bank erosion and lateral migration, which in turn provide the basis for analysis and hydrodynamic and sediment transport modelling in a curved channel (Chang et al., 1989). Under the influence of the centrifugal acceleration, the flow in the curved channel experiences secondary current leading to spiral motion of the flow directed normal to the main flow. The secondary current, which develops upon entering a channel bend, will eventually reach an equilibrium condition if sufficient bend length is available. In that state the flow

is called as fully developed and the river profile does not change unless there is significant change in the discharge or other influential parameters such as sediment influx.

As far as the erosion problem of Brahmaputra River is concern, thickly populated areas like Palashbari, Sualkushi, Rohmoria, Morigaon, South Salmara and more importantly, the Majuli Island, the largest habitat river island of the world are facing extensive erosion. The flow discharge and sediment load of the river undergo significant seasonal fluctuations, particularly during the monsoon season, which typically lasts from June to September. These fluctuations are driven by heavy rainfall in the catchment area, including the Himalayas and the hills of Assam. Increased flow rates during monsoon intensify its erosive power along the banks. Erosive force of the sediment-laden water contributes to the erosion of the riverbanks. Bank erosion is particularly pronounced in areas where the river bends or meanders, as these sections are more vulnerable to lateral erosion and channel migration. Erosion is also experienced at immediate downstream of bridges due to fanning out of the river emerging out from a constricted bridge width. Moreover, the Brahmaputra carries a substantial sediment load, comprised of sand, silt, clay, and organic matter, sourced from erosion and weathering processes in the catchment area. This sediment load fluctuates seasonally due to factors such as rainfall intensity and land use changes. During the monsoon, the heightened flow rates mobilize more sediment downstream, exacerbating erosion processes. Therefore, effective erosion control and management strategies must consider the dynamic nature of the Brahmaputra River and sediment transport processes along with impact of any anthropogenic activities.

To tackle the problem of erosion of river Brahmaputra various agencies including state, central government and autonomous institutions are engaged in planning and execution of flood and erosion management programs in the north eastern region. To achieve effective flood management programs a variety of structural and non-structural measures are adopted. These result in reasonable degree of protection to the flood prone areas in the Brahmaputra valley. However, due to the inherent widening characteristic of the Brahmaputra River they do not sustain and in many cases adversely affect the benefits anticipated while implementing the flood control and anti-erosion works.

Many problems in fluvial geomorphology involve complex, multivariate situations, often at large spatial and temporal scales. These topics have traditionally been addressed through detailed fieldwork combined with theoretical and numerical modelling. Whilst mathematical models have promoted major advances in our understanding of the complex interrelationships involved in sediment production, transfer and deposition in dynamic fluvial environments, they necessarily involve simplifications and use of empirical coefficients derived from limited input data. A

complementary technique that has developed in parallel with these computational simulations is physical modelling, which has two principal advantages. First, the formative processes can be observed, usually in a reduced time-frame, within a controlled and manageable laboratory environment. Second, physical models may allow incorporation of variables which are not known a priori and which may have markedly non-linear effects on the resultant dynamics or morphology. Of course, physical model also has some limitations, particularly in large braided river. Thus, use of both physical and mathematical model can always provide information helpful for decision makers.

The Brahmaputra River's braided nature has a substantial influence on bank erosion through a variety of methods. The Brahmaputra's many interwoven channels, which fluctuate often, induce lateral erosion and riverbank collapse. High discharge events amplify these effects because the forceful flow scours bank materials more aggressively. The Brahmaputra's riverbed and banks are constantly changing due to the river's dynamic sediment transport and ongoing cycles of deposition and erosion. Because of this, it is challenging for vegetation to grow and sustain the banks, increasing the risk of erosion. Bank erosion occurs in a highly dynamic environment that is characterized by shifting channels, variable flow, sediment transport, and weakened vegetation stability. The nearby regions are severely impacted by this erosion, which affects infrastructure, agriculture, and settlements. Consequently, continuous management and mitigation measures are required to safeguard vulnerable areas. In order to handle the substantial sediment transport and unpredictable flow patterns of the braided Brahmaputra River, dredging may be deemed an essential anti-erosion measure. Severe bank erosion is caused by the Brahmaputra's distinctive numerous intertwining channels and heavy sediment load. Strategically removing sediment from the riverbed through dredging can effectively assist mitigate these problems. Dredging can be used to deepen the Brahmaputra's main channel, which will stabilize and concentrate the river's flow and lessen its tendency to shift laterally. By concentrating the flow, the effect on riverbanks is reduced, which reduces erosion. Dredging can also assist in controlling the development of sandbars and islands in the river, which are common in braided systems such as the Brahmaputra. These formations can be regulated by removing surplus silt, which will result in a more stable river channel with decreased bank erosion. Additionally, secondary channels and floodplains are created or maintained by strategic dredging, which reduces the erosive stress against the banks by allowing excess water to spread out during heavy flow periods. This study examines three crucial Brahmaputra River reaches adjacent to Majuli, Tezpur, and Guwahati. To understand the dynamics of the dredging channel bed, physical model research with movable bed is carried out for the aforementioned stretches of the Brahmaputra River. In the physical models, the velocity difference between before and after the dredging channel is measured. In order to determine the rate of sediment deposition, experiments

are also conducted with the sand deposition over time in the dredged channel. Investigations are also conducted into the functionality of such dredging channels, both with and without porcupine screens, when oriented properly. Due to its dynamic sediment deposition and flow patterns, it becomes apparent that frequent maintenance of dredging is important for large braided rivers like the Brahmaputra. When paired with additional structural measures and thoughtful design, efficient dredging techniques can greatly improve the stability of riverbanks and shield nearby infrastructure and communities from the damaging impacts of erosion.

1.2 Organization of the Thesis

The complete work is divided into several stages and is presented in different chapters, as shown below

 Chapter-1 presents the introduction of the thesis, basically highlighting importance of the study and motivation for carrying out the research work.

 Chapter-2 contains a brief literature review on previous studies on river bank erosion. The literature regarding study on river bank erosion in Meander River as well as braided river is incorporated. Various literatures on geoinformatics study to understand morphological characteristics of river, dredging of river and model study to understand characteristics of river flow are reviewed and explained in this chapter. Based on the literature review, specific objectives of the study are finalized in this chapter.

 Chapter-3 presents the Geoinformatics study to understand morphological characteristics of river Brahmaputra and its temporal change. The Bankline Study and detailed Soil Characteristic Study of River Brahmaputra is presented here. A critical reach near Majuli Island is studied extensively. River bank line and Main River channel analysis of the reach and Sand bar analysis of the area is done using Landsat data and presented here. Similar study conducted for reaches near Guwahati and Tezpur where bridges exist are described here.

 Chapter-4 describes application of mathematical model for simulating flow in braided river. 2-dimensional mathematical model study is conducted on two important reaches of river Brahmaputra. Bathymetry surveys which are done for these reaches are described in this chapter. Soil testing and hydrological analysis of gauge discharge data are detailed in this chapter. Two channels are excavated in Hydrologic Engineering Centre's River Analysis System (HEC-RAS) 2D

model for Guwahati and Tezpur reach, covering length of 7 km and width of 350 m and length of 5.5 km and width of 450 m respectively. Studies have been done on how river flow changes in different discharges due to excavation of the channel. River flow velocities at different discharge are analysed from the bank to the dredging channel.

 Chapter-5 contains physical model study of selected reaches of river Brahmaputra. Design of scale as per Froudian Similitude and requirements of Field Data for Physical River Model Experiments are described in this chapter. Analysis of sand particle used for the Model Study are incorporated in this chapter. Physical model studies are conducted for proposed dredging channels near Guwahati and Tezpur. The efficacy of proposed dredging channel is studied in this chapter. The scour hole formation for pier of bridges near Guwahati and Tezpur are also studied.

 Chapter-6 presents possible solution measures and along with identification of best combination anti-erosion measure at vulnerable reach of river Brahmaputra. Study is done for the dredging possibility near Nimatighat, from the model application. The standalone and combined effects of proposed dredging channel and porcupines near Nimatighat are discussed in this chapter. In addition, efficiency of porcupine screens as immediate anti-erosion measure is also observed.

 Chapter-7 explains sediment transport study for proposed dredging channel of river Brahmaputra. Scaling of sediment size is designed and sediment rate for the proposed dredging channel in physical model is calculated. Observation of sedimentation in the proposed dredging channel in the physical model is explained in this chapter.

 Chapter-8 summarizes the discussion, conclusion, and future scope of the research work.

2.

Literature Review

2.1 Introduction

In alluvial river, sediment is frequently eroded from the curved banks. This sediment is deposited either on the subsequent convex side or form a bar. With a variation in level, there is a significant impact on the degradation of riverbank, the shifting of bed loads, and the position of deposition. The erosion and deposition of the bed and banks influence the cross-sectional form and gradient of the river. The energy caused by the internal frictions, as well as the energy needed to move the sediment, counterbalance the available energy in rivers. These elements interact in such a way that there is a constant desire to achieve stability. A stream operating with a constant discharge, comes very near to reaching this state in laboratory condition, even though it is never entirely accomplished in nature. But, the set of circumstances in the river are ever-changing. A river's characteristics, including its level, discharge, silt and other factors, vary and the stream rarely reaches equilibrium. Further, the location and direction of velocity, in a cross-section of a river, affect the channel characteristics. The river will be prone to bed scour, for example, if the bed is made of sand and the banks are made of the cohesive material. Again, if the banks are made of sandy particle, lateral erosion will often occur.

Complex issues are frequently faced due to sediment deposition in river channels. The raising river beds, which increases storm peaks and creates flood. In some cases, rivers have to divert from their original courses and flow along new ones. Habitable and agricultural lands are eroded due to this complex issue. A stream that runs in several, movable channels for parts of its course is said to be braided. Long-term river migration throughout the whole floodplain occurs in braided rivers, while small channel migration often occurs within the flowing bed (Harding, 2016). For channel pattern predictions, empirical and mechanical channel pattern discriminators are usually applied. But so far, despite the floodplain features having a significant impact on channel pattern, have a tendency to overlook them (Candel et al., 2021).

2.2 Previous Study on River Bank Erosion

2.2.1 Study on River Bank Erosion in Meander River

A meandering river is one that follows curved channel that frequently includes loops and bends. Meandering rivers are those that run in a flat or moderately sloping terrain with distinctive characteristics. A number of variables, such as the geometry and gradient of the streambed, the rate and quantity of flowing water, and the kind of silt in the river, all have an impact on how meandering rivers develop. The river starts changing its path and creates a fresh meander as it moves downwards, eroding the outermost banks of the bend and depositing material on the internal sides.

Research was done the formation of river bends, corroborating existing theories surrounding the interplay of flow dynamics and bed instability, particularly accentuated by bend flow phenomena. Additionally, a groundbreaking concept termed "self-constraining" emerges, shedding light on the evolutionary trajectory of low-energy meandering rivers as they develop tortuous planforms characterized by sharp bends. This notion underscores the gradual accumulation of self-formed deposits, progressively restricting channel mobility and shaping the river's morphology over time. Termed "self-constraining," this mechanism underscores the intrinsic adaptive capacity of rivers to shape their course and morphology. Significantly, this self-constraining process enhances the system's resilience against bank erosion, albeit revealing susceptibility to unforeseen increases in erosion should the river's energy exceed a critical threshold. These findings contribute to a deeper understanding of the intricate dynamics governing river morphology and evolution, offering valuable insights into how low-energy rivers respond to environmental changes, including the impacts of climate variability. Low-energy rivers with meandering paths may be able to control its own planform by preserving deposits that are more resistant to erosion. This technique explains why low-energy rivers typically have convoluted planforms. (Candel et al., 2020). A study of bank erosion patterns along the Meuse River was done particularly concerning the formation of oblique embayment following the removal of protective structures. Notably, the presence of trees, is found to correlate with areas of diminished retreat, attributed to the reinforcing effects of roots and chemical soil strengthening. However, the fact that erosion extends beyond certain tree locations suggests that other factors are at play. The floodplain's diverse composition, combined with tilted strata oriented obliquely to the current channel, emerges as a significant determinant of deposition during flood events, thus influencing erosion and accretion dynamics. The alignment between the orientation of strata and historical bank lines spanning from 1912 to 2017 suggests a historical context of river migration and sediment deposition shaping present-day strata and embayment’s.

Furthermore, the study highlights the critical role of deposit characteristics, with variations in structure and strata orientation significantly impacting the rates and patterns of bank retreat, emphasizing the multifaceted nature of geological influences on erosion dynamics. Soil features, which serve as a main influence on the extent of erosion, determine how well root systems of trees may reduce bank loss (Duró et al., 2020). Research focuses on investigating morphological changes along the Barak River in Assam, employing sinuosity index and bank erosion metrics as key analytical tools. Utilizing Landsat data spanning from 1990 to 2020, along with SARIMA (Seasonal Autoregressive Integrated Moving Average) models, the study predicts river discharge trends up to 2025. The findings indicate an inverse correlation between sinuosity index and bank erosion, suggesting that as sinuosity increases, bank erosion decreases. Moreover, the analysis forecasts a potential rise in future discharge levels, which could exacerbate erosion along the riverbanks. Consequently, the study underscores the necessity for robust riverbank protection structures to effectively manage the dynamics of meandering rivers and mitigate associated flood risks. The study meticulously examines various SARIMA models, determining the most fitting model for forecasting river discharge at Annapurnaghat and Badarpurghat stations based on criteria such as AIC (Akaike Information Criterion) and BIC (Bayesian Information Criterion) values. Additionally, the segment-by-segment morphological assessment of the Barak River highlights areas of heightened vulnerability due to the anticipated surge in discharge rates, emphasizing the urgent need for strategic planning and intervention measures. An established model SARIMA was used to forecast the future morphological evaluation (Nath and Ghosh, 2022). Rahman et. al. (2021) used Geographic Information System (GIS) and Remote Sensing technology to assess bank erosion and human effects along the Kirtankhola River in Barishal, Bangladesh in his research study. The study aims to detect human-induced variables leading to riverbank instability and to identify patterns of bank erosion through the use of geospatial tools, field surveys, and Landsat satellite images. The main conclusions show that erosion is more common on the left bank whereas accretion rates are greater on the right bank. Interestingly, the study finds that the main human-caused factor aggravating erosion near riverbanks is the high waves produced by watercraft. These results highlight how important it is to combine sophisticated spatial analytic software with field surveys in order to fully evaluate and manage the intricate dynamics of riverbank erosion.

A ship travelling around a circumferential meander at a rapid rate creates a significant centrifugal motion as a consequence of strong hydraulic waves that strike the riverbanks repeatedly and strongly, promoting damage to the banks (RAHMAN et al., 2021). Examination is done for the ramifications of rapid bank erosion on sediment budgeting within the lower Gangetic plains, with a specific focus on the Malda district in West Bengal. Employing a methodological approach that incorporates

Landsat imagery spanning from 1987 to 2019, the study utilizes ArcGIS and a MATLAB-based tool known as RivMAP to comprehensively assess patterns of river migration and sediment reworking. The findings of the research underscore a substantial net land loss of approximately 140 km² over the course of three decades, with an average annual loss of 4.5 km². Additionally, the study elucidates a sediment yield of approximately 30 million tons per year attributable to riverbank erosion. Moreover, the implications of the research shed light on the pronounced influence of peak annual discharge on riverbank erosion dynamics, suggesting the pivotal role of climate in governing processes of river migration and bank erosion. Furthermore, the study underscores the critical importance of alluvial plains as a significant sediment source within the broader sediment budget of the Ganges River system. Overall, these findings underscore the urgent need for effective management strategies to address the escalating challenges posed by rapid bank erosion in the lower Gangetic plains. Institutions on the two banks of the Ganges may face danger from developing meander arcs in the coming years (Dey et al., 2022). It is also explored the scientific and socio-economic importance of river meanders, including their ecological effects and the challenges posed by their movement. It attributes the migration of meandering rivers to the interaction between erosion and collapse of the outer bank, as well as accretion of the inner bank, influenced by the curvature of the river. Past theoretical research on meander morpho dynamics is then reviewed, with a focus on developing mathematical frameworks to describe the evolution of meanders. Additionally, it introduces a numerical model explicitly addressing bank collapse, highlighting its role in accelerating meander migration and maintaining a consistent channel width. This model provides valuable insights into the complex processes governing the behaviour of meandering rivers, aiding in the development of effective management strategies. Occasional failure occurrences, due to impact of the curvature-migration relation for the same bend, increasing local migration rate based on regional curvature (Zhao, 2021).

2.2.2 Study on River Bank Erosion in Braided River

It doesn't seem possible to forecast how changes in discharge will likely modify the drainage characteristics of braided rivers. In a study investigating braided rivers in New Zealand, a comprehensive examination was conducted on the Ashley, Hurunui, Rakaia, and Ahuriri Rivers. Through meticulous data collection of various physical attributes including depth, velocity, and sediment type along each river, intriguing findings emerged. Notably, a power function relationship between water surface width and discharge was identified, indicating a direct correlation where increased discharge leads to wider river spans. Furthermore, variations in cross-sectional area were observed, influenced by factors such as bank stability and vegetation cover. The study also revealed

insights into water depth dynamics, with mean and maximum depths exhibiting consistent relationships with discharge. Similarly, water velocity displayed a trend of decreasing with diminishing discharge, which has implications for fish habitat suitability. A novel index termed the Weighted Usable Area (WUA) was developed to assess habitat suitability, demonstrating an increase with discharge, albeit at a decreasing rate for most species. The study also examined the shifting proportions of channel sub environments like riffles, pools, and runs with varying discharge levels, noting accelerated widening of riffles due to their positioning on flat riverbeds. Additionally, the analysis of bed sediment size distributions revealed minimal alterations with increasing discharge unless sediment transport processes were active. Overall, this research underscores the inherent complexity of braided river systems, emphasizing the importance of detailed, site-specific analyses for a comprehensive understanding of their dynamics (Zealand, 1983). Recognising the unique characteristics of the braided fluvial morphology in the context of sand body interactivity and the depositional influence is a key issue for braided river. Key concerns such braid bar initiation, confluence-diffluence dynamics, sedimentary facies, and the impact of flow stage are highlighted in research to better understand the dynamics and sedimentary deposits of braided rivers. Understanding braided rivers' dynamics and deposition processes is essential since they are common in upland and proglacial settings and play a significant role in the development of landscapes. The study highlights the value of multidisciplinary cooperation and suggests interesting directions for further investigation (Bristow and Best, 1993).

Three different braided rivers—the Brahmaputra in Bangladesh and the Aichilik and Hulahula in Alaska—are the subject of a research that focuses on their spatial scaling characteristics. The methodology looked at self-affinity and fractal exponents, and it analysed spatial scaling using a logarithmic correlation integral approach. They showed comparable spatial scaling patterns despite changes in bed materials, slopes, and sizes. These findings imply that common characteristics underlie the development of spatial patterns in braided rivers. It was also observed that a type of fractal objects situated between river networks and single-channel rivers are braided rivers. These results have consequences for how we think about the dynamics of rivers and the evolution of landscapes. Readers are referred to the original source for a thorough understanding. (Victor Sapozhnikova, 1996) . Braided river floodplains are teeming with a diverse array of interconnected habitats, ranging from main channels to side braids, springs, and ponds. Despite the ever-changing physical conditions such as temperature and turbidity, invertebrate communities persist resiliently in these dynamic environments. Common taxa such as *Deleatidium mayflies*, *Chironomids*, and *Hydrobiosid caddisflies* thrive amidst the instability. Notably, springs and hyporheic zones foster rich and varied communities. However, these ecosystems face significant threats from human

activities, particularly flow regulation due to impoundments. Dams alter habitat dynamics, impeding channel migration and disrupting floodplain connectivity. Additionally, the escalating water demand for irrigation and hydroelectricity exacerbates these pressures. Despite these challenges, braided river floodplains remain crucial biodiversity hotspots, offering refuge and sustenance to a multitude of species. Their high habitat heterogeneity and diverse invertebrate communities underscore their ecological significance. It should be established how the physical characteristics of braided rivers influence the variety of species and ecological processes to successfully conserve and restore them (Harding, 2016). While flood instances are undoubtedly the main factors influencing how islands evolve, a number of climatic factors may be crucial for retaining of fine particles and the formation of the sand bar (Harding, 2016). The process of bar colonization by vegetation and subsequent island formation stands as a pivotal mechanism in the evolutionary trajectory of fluvial landscapes. A study focuses on investigating the dynamics of river islands along the Tagliamento River in Italy. Over the years, pioneer islands have exhibited rapid aggradation, accompanied by an increase in vegetation canopy height and a shift in sediment composition from gravel to silty-sand. The bio-geomorphological trajectory of island evolution is contingent upon various factors including sediment and seed delivery, climate patterns, and the establishment of vegetation. The initiation of islands in the Tagliamento River occurs through the deposition of uprooted trees during flood events, with the elevation of deposition sites influencing their subsequent development. Notably, trees deposited at lower elevations tend to experience better access to water and exhibit rapid growth. Following deposition, a period devoid of significant floods allows for the establishment of vegetation and subsequent island aggradation. As islands aggrade, they expand laterally through aggradation and coalescence, while sediment dynamics are influenced by increasing elevation and vegetation cover. Wind storms also contribute to sediment transport onto islands, shaping their morphology over time. Importantly, understanding these processes holds implications for river restoration and management, emphasizing the need to incorporate island dynamics into management strategies. Numerical models offer a promising avenue for forecasting the evolutionary trajectories of vegetated landforms under varying environmental conditions (Harding, 2016). Avulsions may be affected by complicated interactions of various elements, including as shear stress, connecting the discharge process, riverbed slope, and upstream channel layout (Yang, 2020). Rivers showcase a diverse array of channel patterns, ranging from braided to meandering configurations. The comprehension of these patterns holds paramount importance for both river restoration endeavours and forecasting their responses to climate change. Typically, rivers are classified based on parameters like discharge and valley gradient using channel pattern discriminators. However, a novel approach that integrates the influence of cohesive floodplains, utilizing the average silt-plus-clay

fraction of river banks as a key determinant. Understanding the relationship between channel patterns and bank strength is crucial; empirical observations suggest that certain channel patterns can only exist above specific lower limits. For instance, rivers with scroll bars may coexist within the domain of meandering rivers with scroll bars, but not vice versa. New channel pattern predictor incorporates bank strength as a third axis, significantly enhancing prediction accuracy across all channel pattern types. This advancement represents a valuable tool for river restoration efforts and deepening the understanding of morpho-dynamics. However, it's worth noting that our approach does not account for the effects of vegetation on channel patterns, and future research should encompass peatland rivers and cohesive banks for a comprehensive analysis (Zealand, 1983).

2.3 Previous Geoinformatics Study to Understand Morphological Characteristics of River

Many studies aimed to explore the effectiveness of Geographic Information Systems (GIS) in mapping changes in river channel configurations and assessing the likelihood of bank erosion. Leveraging Graf's methodology as a foundation, the researchers scrutinized the erosion probability of floodplain cells by considering their proximity to the active river channel and the intensity of flood events. To refine the approach, additional geomorphic variables such as river bank morphology, sediment composition, and floodplain vegetation were integrated. The investigation focused on the River Tummel in Scotland, renowned for its meandering gravel-bed characteristics, serving as an ideal testbed for the methodology. The findings underscored the utility of GIS in generating erosion hazard maps and gauging the repercussions of altered flood patterns and land use practices. However, the researchers acknowledged the complexities inherent in predicting erosion for cohesive silt banks. Moreover, the study capitalized on a robust dataset derived from aerial photographs with minimal temporal gaps between each capture. This comprehensive dataset was made attainable through a dedicated airborne remote sensing campaign, a rarity in regions like the UK where aerial surveys are often conducted at more protracted intervals. Additionally, the researchers explored the potential of spaceborne remote sensing systems, which offer a viable means of scrutinizing medium and large rivers with a repeat cycle of less than five weeks. This approach streamlined the co-registration of images from diverse dates and facilitated spatial analysis by harnessing the inherently raster format of satellite data. Through the application of GIS, the researchers successfully delineated erosion probabilities, identifying vulnerable floodplain sectors and honing the methodology for broad applicability across rivers of various scales and temporal dynamics. The accurate mapping of erosion probabilities bears substantial ramifications for river management, facilitating the delineation of floodplain erosion risks and enabling predictions regarding the impacts of alterations in flood patterns, bank stabilization initiatives, and land use

transformations (Archana et al., 2012). Study conducted by analysis of river bank erosion hazard attributed to morphometric changes in the Ganga River upstream of the Farakka Barrage up to Rajmahal. Utilizing morphometric parameters extracted from Landsat and Indian Remote Sensing (IRS) satellite imagery spanning from 1955 to 2005, the investigation revealed significant trends. Over the observed period, the river exhibited increased meandering, leading to elevated sinuosity values. Furthermore, there was a notable shift towards greater braidedness, indicating sediment deposition and lateral erosion dynamics. A substantial expansion in the area covered by islands was also identified, consequently impacting agricultural land. Various factors were identified as contributing to bank failure, including soil stratification, the presence of hard rocky areas, sediment load, and the obstruction of natural river flow by the Farakka Barrage. The repercussions of erosion were particularly evident in the Manikchak and Kaliachak-II blocks of Malda district, where approximately 1,670 hectares of agricultural land have been lost since 1977 (Archana et al., 2012). A study focusing on the instability and shifting nature of the Ganga River banks in the Manikchak Diara of Malda District, West Bengal, has been conducted. Employing the Bank Erosion Hazard Index (BEHI) alongside remote sensing and GIS techniques, the study aims to evaluate the stability of river banks. It highlights the severe impact of erosion on areas such as Pashim Narayanpur, South Chandipur, and Gopalpur. Notably, the leftward shifting of the river bank has been pronounced since 1973, leading to significant land loss in the region. The migration of the Ganga River, especially upstream of the Farakka Barrage, is attributed to engineering interventions. The study underscores the absence of long-term solutions grounded in geomorphic understanding and emphasizes the importance of floodplain zoning for effectively managing river dynamics and enhancing river health (Mandal, 2017). The River Brahmaputra is one of the world's biggest alluvial river, with periodic bank erosion causing stream pattern alterations and bank line movement (Archana et al., 2012). According to satellite image estimates, overall loss of land due to erosion in Brahmaputra ranged from 72.5 to 80 sq. km./year from 1997 to 2007–2008 (Das et al., 2014). Between 1991 and 1998, a total of 2745 hectares of land were lost to erosion in Majuli Island (Mani et al., 2003). To safeguard this region, an adequate strategy that considers all aspects of flood and river bank erosion is essential (Sarma, 2013). Despite continued erosion in patches, a significant portion of the island's land mass has been restored. Government agencies constructed rock armoured solid deflecting spurs / groynes at areas identified by river model studies in order to prevent flood and erosion in the long run (Sarma, 2014). A number of case studies using Geosynthetics in the River Brahmaputra's critical reaches for Bank Erosion Mitigation were discussed (Maurya et al., 2022). . The bank erosion is caused by changes in thalweg locations in the Brahmaputra, as well as the existing bank material, which is mostly poorly graded soil (SP) with minimal clay, indicating that the materials have weak binding

power (Krobicki, 2010). Using GIS software, riverbank mapping is done where the erosion is most severe, to forecast the cause of the erosion and offer appropriate actions to avoid additional erosion. Otherwise, the local engineering departments would have gone undiscovered about these places (Sarma and Dutta, 2016).

2.4 Previous Study on Dredging of River

Dredging is generally adopted to improve or maintain the discharge or flow carrying capacity of rivers, channels and / or natural waterways by enlarging or maintaining the cross-section or by realignment of the watercourses. The document titled "Understanding Dredging: Navigating Through Techniques, Environmental Concerns, and Applications" provides a comprehensive exploration of the multifaceted realm of dredging. It delves into the historical evolution of dredging, initially targeting developing nations in 1983 but now boasting a global audience. Dredging objectives, ranging from navigation enhancement to environmental remediation and mining support, are meticulously examined, underscoring its pivotal role across various industries. Furthermore, the document sheds light on the management of dredged material, advocating for its beneficial reuse in land reclamation and landscaping endeavours. Emphasizing the significance of waterborne transport, it elucidates how dredging maintains ports and facilitates global trade. Environmental considerations are paramount throughout, with an emphasis on sustainable practices and mitigation strategies for adverse impacts. Detailed discussions on dredging equipment types, including mechanical and hydraulic dredgers, elucidate their specific applications and operational constraints. The document also highlights the importance of proper placement of dredged material, favouring beneficial use whenever feasible. Lastly, it underscores the necessity of robust monitoring and maintenance regimes to ensure the long-term effectiveness of dredging projects. Dredging is also done to retain or increase the dimension of streams and redirect creeks, or build control infrastructure like embankments to upkeep or enhance the discharge or flow capacity of these streams (Dredging for development, 1991). River management must address the river's inherent dynamics (Smedes et al., 2006). In the context of managing the Rhine River for flood protection and navigation, the Netherlands and Germany heavily rely on Inland Water Transport (IWT). However, challenges such as riverbed degradation, reduced biodiversity, and conflicting interests persist. Notably, the Waal Project serves as a comprehensive initiative aimed at enhancing navigation conditions along the Waal River. Through measures like bend improvements utilizing fixed layers and bend way weirs, the project seeks to increase fairway dimensions while addressing ecological concerns. Systematic dredging in the Middle Waal, implemented as an alternative to normalization, is a key aspect of the project's strategy, necessitating dynamic approaches due to evolving river conditions. Dredging

serves as a recurrent measure to maintain a navigable fairway, albeit requiring long-term funding and facing challenges in consistency. Pilot dredging projects conducted between Nijmegen and Zaltbommel have provided valuable insights into sediment dynamics and shoal re-emergence, informing the development of a dredging strategy that distinguishes between profile and spot dredging. Sediment management and dumping techniques, including sustainable practices like dumping in groyne fields, have been explored to mitigate environmental impacts. Additionally, a Decision Support System (DSS) has been developed to aid in dredging decisions, particularly as fairway dimensions evolve. The Sustainable Fairway Rhine Delta (SFR) project further underscores the commitment to a sustainable approach, incorporating measures such as modifying normal widths, adapting groyne structures, and implementing sediment management practices to maintain a navigable and ecologically sound fairway (Smedes et al., 2006). In Bangladesh, where a dense population and extensive river network characterize the landscape, water transport serves as a vital mode of transportation. Dredging and land reclamation efforts are pivotal for enhancing waterways, thus fostering socio-economic development in the region. Maintenance dredging, conducted regularly to preserve river navigability, and development dredging, which involves excavating sediment to revive nearly stagnant waterways, are crucial types of dredging activities undertaken. However, challenges arise from the siltation of rivers and canals due to sand and clay deposits, hindering water passage. To address these issues, the government has devised a comprehensive 50-year mega plan for river training and capital dredging, emphasizing the importance of thorough pre- and post-dredging investigations for project success. Additionally, land reclamation from the sea has become imperative to accommodate the rapid population growth, with Bangladesh aiming to reclaim approximately 12,000 sq. km of land. Effective planning and harnessing the natural flow of silt are essential strategies to optimize land reclamation endeavours. In conclusion, sustainable dredging and land reclamation projects necessitate integrated planning, vigilant monitoring, and active public engagement to ensure long-term success and environmental stewardship. Dredging and land reclamation should be done in conjunction with thorough and comprehensive pre- and post-dredging studies and surveys (Sultana et al., 2017). Research was done to investigate the negative effects of sand dredging operations on Bangladesh's Payra River bed. The research was notably spurred by the government's effort to turn a freshly created sedimentary point bar, colloquially known as "Char," into a developed region. Results show that, regardless of the distance to the dredge site, dredging activities on any of the bars cause changes in the flow field. By giving priority to areas that have the least amount of influence on erosion along river banks, the research identifies areas with less erosion occurring upstream and downstream. It does, however, highlight the necessity of more research on the long-term effects on other river segments. The research emphasises the need for ongoing

monitoring and regulated dredging techniques, and it calls for actions to lessen negative impacts on the environment (Sultana et al., 2017). Examination is done for the dynamics of the Jamuna River in Bangladesh, a significant braided river system with notable hydrological influence on its surrounding areas. It observes recurring phenomena of erosion, sedimentation, and flow fluctuations throughout the year. Initiated by the Bangladesh Water Development Board in 2011-2012, a pilot capital dredging project aimed to manage flow patterns and mitigate risks to urban areas and infrastructure, notably the Jamuna Bridge. Utilizing numerical modelling techniques, researchers assessed erosion-sedimentation dynamics, revealing heightened sedimentation rates (ranging from 60% to 80%) at locations where dredging intersected existing sandbars and chars. Additionally, the study noted shifts in channel morphology following river training efforts. Satellite image analysis spanning from 2000 to 2018 revealed discernible shifts in bank lines and the formation of new channels, attributed in part to the construction of flow diverting structures. The research findings carry implications for understanding river behaviour and are instrumental in formulating management strategies aimed at promoting the sustainability of river ecosystems (Mossa and Chen, 2021). The Apalachicola River in Florida underwent dredging for navigation purposes, resulting in the formation of spoil mounds within its floodplain. However, poor placement of these mounds led to geomorphological changes, notably erosion of intermittent sediment pulses that altered the river's channel morphology, causing it to become wider and shallower. The transformation of the river's channel, attributed to artificial cutoffs and dredging activities, resulted in a three-fold increase in the width-depth ratio, fundamentally altering its original shape. Erosion of a large spoil mound, contributed to sediment input into the river, particularly at its downstream end. These changes adversely impacted navigation by reducing the river's depth, posing challenges for vessels. Despite dredging efforts in the 1970s and 1980s, navigation conditions did not improve significantly. Furthermore, the ecological implications of these alterations were notable, affecting habitat for freshwater mussels and Gulf Sturgeon. Lessons drawn from these experiences carry relevance for other rivers undergoing dredging or mining activities, stressing the importance of proper spoil placement and consideration of downstream impacts. Because the river will acquire sinuosity, dredging debris in cut-off channels near the river might be hazardous. In addition, locations on the outside bends of meanders are more prone to erosion, and site just upstream of issue portions will feed material into the problem reach (Mossa and Chen, 2021). The Pussur River, located in southwestern Bangladesh, hosts the Mongla Port along its banks, which has been grappling with navigational challenges due to siltation. To assess morphological changes, researchers analysed available hydrographic survey charts. Following capital dredging in 2014, the upstream portion near the MPA jetty area exhibited heightened susceptibility to siltation. Before dredging, the inner bar

area displayed minimal alteration in bed topography between 2010 and 2013; however, notable backfilling rates were observed post-dredging. At the outer bar, constituting the river mouth, the current navigational channel experiences annual siltation rates ranging from 0.1 to 0.25 meters. Contributing factors to these navigational issues include a decrease in upstream flow, occurrences of shipwrecks, and disturbances caused by human activities along the river route. Dredge materials can be utilised to raise existing embankments or elevate mud plinths (Valentine and Wilson, 2022).

2.5 Previous Model Study to Understand Characteristics of River Flow

A hydraulic and geometric replica of the field prototype can be produced using a properly scaled model and permitting reasonable relaxation in the grain Reynolds numbers (Ashworth etal., 1994). The Froude, Reynolds, Weber, Cauchy, and Euler numbers are the most significant force ratios for determining dynamic similarity (Taylor and Heller, 2011). Physical model analysis has been considered to be an effective tool for good engineering judgement for arriving at technically viable solutions. The suggestions based on the physical modelling research results should be executed in a timely and correct manner, and post-construction management should be performed to ensure sustainability (Islam, 2008). Although the lengthy heritage of physical hydraulic modelling, there is no work in which all essential parameters were downsized to the model (Taylor and Heller, 2011). The objective of the article is to explore scale effects in physical hydraulic models, stemming from discrepancies in force ratios between the model and its real-world counterpart. Various similarity criteria, including mechanical, Froude, and Reynolds similarities, are discussed to achieve similarity between the model and prototype. However, challenges arise as scale effects can lead to deviations between observations from upscaled models and actual prototype behaviour. To address these challenges, several methods are proposed. Inspectional analysis involves scrutinizing hydrodynamic force balances, while dimensional analysis reduces the problem to dimensionless parameters for better comparison. Calibration involves aligning model results with available prototype data to refine accuracy. Additionally, conducting tests at different scales, known as scale series, allows for quantification of scale effects and their impact on model accuracy. It is not feasible to build a model that is exactly like the original, but the likeness that may be attained is sufficient for all practical reasons. Researchers discovered that using this technology to solve various hydraulic issues that are not accessible to analytical solutions is reasonable. The performance of a variety of hydraulic structures globally and built appropriately (De, 2021).

The diversion of flow by providing spurs was studied using a distorted hydraulic model on a movable bed for the Kosi River at Central Water and Power Research Station (CWPRS), Pune with a

horizontal scale of 1/500 and a vertical scale of 1/70. The Kosi River, originating in Tibet and traversing through Nepal and India, has a history of significant shifts, leading to erosion and widespread devastation. To mitigate these issues, spurs—structures built perpendicular to the river flow—have been employed for bank protection. Typically constructed from impermeable materials such as earth or rockfill, these spurs serve to attract, repel, or deflect flow from the river bank. Model studies were conducted, utilizing a hydraulic model of the Kosi River. The study proposed the installation of two new spurs along the Western Kosi Main Canal (WKMC) at 3.75 km and 3.50 km, effectively deflecting flow away from vulnerable embankments and reducing the impact on existing structures. The findings indicated that these spurs improved river training and erosion protection measures. Velocity measurements confirmed their efficacy in reducing flow intensity near susceptible embankments. Overall, this study contributes to enhancing flood protection and management strategies along the Kosi River.(Burele et al., 2012). The Old Rhine's non uniform sediment flow, river erosion, and bank collapse were reinvestigate using an undistorted, movable-bed physical model (El et al., 2013). It will be feasible to better comprehend the complex processes caused by changing forcing within fluvial systems across a wider variety of time scales by enhancing physical modelling skills and connecting physical and numerical models. The interactions between water, sediment, and biology within fluvial systems are intricate, influenced by multiple forcing mechanisms across various scales. With the anticipation of extreme meteorological events due to climate change, there is a growing concern for the impact on riverscapes and ecosystems. Physical modelling plays a crucial role in comprehending both biotic and abiotic processes within fluvial systems. Various approaches, ranging from 1:1 experiments to analogue models that compress spatial scales, are utilized. However, existing capabilities often lack representation over relevant time scales necessary for managing climate change impacts. Addressing this challenge requires research to bridge knowledge gaps related to time scales, variable forcing, and biological processes. By enhancing physical modelling capabilities and integrating them with numerical models, a better understanding of the complex interactions within fluvial systems can be achieved across a broader range of time scales, thus improving management strategies (Baynes et al., 2018). A physical model project improves understanding of hydraulic phenomena and able to address numerous problems more realistically and inexpensively. The purpose of physical hydraulic models is to predict the behaviour of hydraulic phenomena, optimize designs, and enhance safety considerations. These models, often scaled down versions, facilitate quick investigation and modification of designs. Specific studies include the Pump Sump Model, which addresses surface and subsurface vortex issues in water pumps, utilizing Computational Fluid Dynamics (CFD) for prediction. Another example is the Spillway Dam model, where the spillway structure's safety in dams is crucial. Model

similitude at a scale of 1:20 is employed for design validation. In conclusion, it is recommended to combine simulation models with physical hydraulic models for comprehensive analysis. Experience gained from physical hydraulic projects further enhances understanding and problem-solving in hydraulic engineering (Firdaus Zulkefly et al., 2019). Physical model were studied out with the various alternatives for channelizing the Kosi river from Chatra to the Kosi barrage (Burele et al., 2018). At Gujarat Engineering Research Institute (GERI), a 3D physical model with a geometrical equivalent scale of 1:80 was observed and calibrated using HEC-RAS for a 3-kilometre Sabarmati River reach. The objective of the study was to assess the hydraulic performance of the proposed Hirpura barrage, utilizing both a 3D physical model and HEC-RAS 5.0.7. Through calibration, the HEC-RAS model was aligned with observed water levels from the physical model, demonstrating close agreement. Analysis revealed that a horizontal apron type of energy dissipating arrangement was suitable for the barrage. Scour depths downstream of the end sill were evaluated, with the provision of cutoff depth deemed adequate. Recommendations were made to enhance safety measures, including extending approach embankments beyond the abutments and implementing measures to safeguard against sand lifting and dislodging (Khan and Mujumdar, 2021).

2.6 Motivation and Objectives for the study

The characteristics of braided river is unique. It is very difficult to analyse the flow pattern of large braided river, where the seasonal variation of discharge and sediment load is quite high. While mathematical model study can help in having some understanding, setting up of bathymetry itself is quite challenging. There are still some challenges in creating proper bathymetry with sediment transport in mathematical model in case of large braided river. Various studies have been conducted to understand the process of erosion in braided river like Brahmaputra. Many physical experiments have been undertaken to investigate the flow velocity, channel bed form and channel morphology development. Many experiments have been carried out since the pioneering work by Friedkin in 1945. Need of a large model to minimize scale effect is a major challenge to conduct physical model study of large braided river and it calls for preparation of a large size model tray to conduct such physical model study for river like Brahmaputra. Physical modelling for braided river has not been attempted by many researchers whereas there are many physical model studies for meandering river. The reason is due to the many complex phenomenon occurring in the braided river which are highly sensitive to many parameters of the flow and soil characteristics. In large braided river, even with a constant discharge at an inflow section, flow remain unsteady in various sub channels due to presence of confluences and bifurcation. Only a limited number of studies are available in the published literature for physical model study for such river. Comprehensive study for solving bank

erosion problem by establishing dredged channel for river like Brahmaputra is very limited. Studies are necessary to seek answer to questions like a) can a dredged channel executed centrally downstream of a bridge reduce the fanning effect or strength of the side channel current? b) Can a dredged channel help taking the flow away from the erosion effected bank? To have answer to all such questions, efforts need to be made for carrying out such study using both physical and mathematical model.

Complexities of the erosion problem, as discussed above has motivated to explore scope of using some innovative approach like dredging in combination with other conventional methods to mitigate erosion problem in a large braided river like that of Brahmaputra taking recourse to both physical and mathematical model. Following is some of the specific points that have inspired the present study:

By considering the previous research, problems and their solutions, the following objectives are proposed.

Objective 1:

Soil investigation for bank of braided river was done earlier in many projects and studies. Again, many morphology studies based on remote sensing data are done to understand the braiding nature of river. However, the influence of bank material in erosion phenomenon of braided river is not exclusively studied. Systematic study is also necessary to understand impacts of bank material, if any, on the erosion process. The first objective of the present study is to apply geo-informatics to identify erosion prone area of Brahmaputra River and to study trend and extent of erosion in some of the important site and to investigate the soil properties of river bank to examine its role in bank erosion, if any.

Objective 2:

Rivers are normally spread out just downstream of a bridge. This behaviour of river is known as fanning out of river. A lot of schemes are being executed for protection of bank at downstream of bridges. But there is less model study whether downstream channelization can be the solution of this problem. Applicability of mathematical model with empirical formula for such study also needs to be established. To compare results of physical and mathematical model for such alluvial channel

having bridge, comparison of scour around the bridge piers can be a convenient way. Therefore, two sub objectives are considered under this study.

Sub-Objective 2.1:

To study formation of the scour hole around the piers in the physical model of Brahmaputra River and to compare it with the computed scour depth and width obtained by using empirical formula with the simulated velocity and depth.

Sub-Objective 2.2:

To conduct model study for management of river bank erosion due to fanning out of river by providing mid channel in river at downstream of the bridge.

Objective 3:

The river bank protection for braided river has been done with various types of river training works. Dredging of Channel is also done as river training work in some places. Apparently, it appears that it should be possible to take water flow away from the river bank by providing dredging channel. However, in-depth study through experimental/model study has not been done for such work. Similarly, the Reinforced Concrete (RCC) Porcupine screens are being used for anti-erosion work in braided river. From the literature review, it is clear that there is no model study in large scale model in this regard. Thus, the third objective is to investigate the possibility of reducing river bank erosion by implementing dredged channel and porcupine screen independently and in combination through physical model study.

Objective 4:

Optical satellite images are affected by the cloud cover. In Brahmaputra basin average cloud is more than 50% for the month from April to November in a year, which limits the use of optical sensors in this area significantly. Synthetic Aperture Radar (SAR) has the advantage of operating at wavelengths not impeded by cloud cover or a lack of illumination and can acquire data over a site during day or night time under all weather conditions. As the bank erosion occurs in Brahmaputra Basin during April to November, the fourth objective is to investigate scope of using SAR data for better planning of anti-bank erosion work in Brahmaputra River.

Objective 5:

There is very less study on suspended sediment movement in braided river. It can be apprehended that there may be effect of suspended sediment in dredging channel but there is no such experimental study. The fifth objective is therefore, to study the suspended sediment deposition in experimental dredging channel in river Brahmaputra.

3.

Bankline Study to Quantify Erosion-Deposition Trend in Brahmaputra River and to Examine Its Relation with the Bank Material

3.1 GIS based Erosion Deposition Study

The morphological changes of river Brahmaputra along the study reach have been analysed and trends has been analysed through both quantitative analysis and qualitative interpretation. For this purpose, satellite images are collected from 1988 to 2020. Most of images are downloaded through earth explorer (Landsat series data). Linear Imaging Self-Scanning Sensor (LISS) III and LISS IV Imagery of study area are collected from two projects; namely, "Construction of anti-erosion works for protection of Majuli Island from flood and erosion" taken up by Brahmaputra Board independently and "Mathematical Model Study of river Brahmaputra with Emphasis on Climate Change", taken up by Indian Institute of Technology (IIT) Guwahati with funding from Brahmaputra Board.

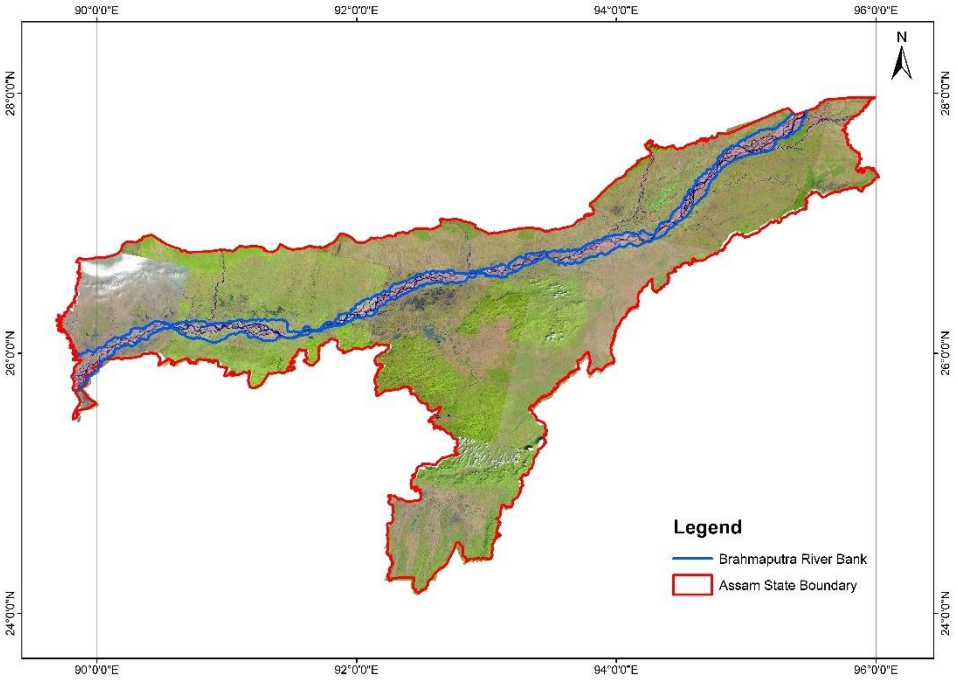

Figure 3. 1 Satellite image (2020) showing Brahmaputra River in Assam

Figure 3.2 shows a flowchart of the methodology for estimation of erosion or deposition.

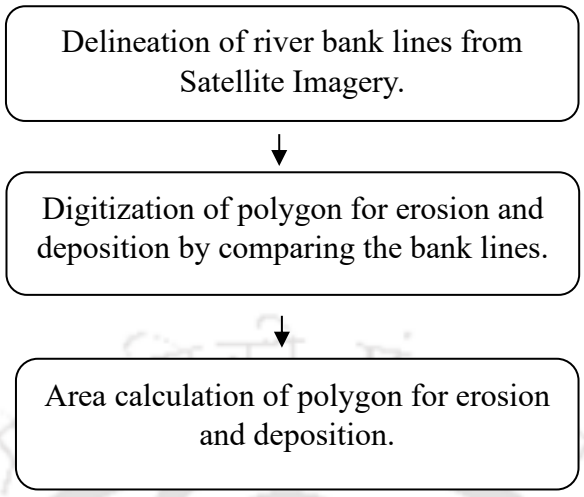

Figure 3. 2 Methodology for estimation of erosion or deposition

The bank lines of entire stretch of the Brahmaputra River in Assam have been digitized using satellite imagery (Landsat) for the year 1990 and 2020. By comparing the bank-lines of 1990 and 2020, overall erosion and deposition map of Brahmaputra is obtained between these two periods. Erosion of Brahmaputra on its North bank is found to be about 181 sq. km. and that on its South bank is found to be about 415 sq. km. with overall erosion of more than 596 sq. km. area. The deposition along North bank in the same period is found to be about 56 sq. km. on its South bank is 130 sq. km. with overall deposition of 186 sq. km. It is also found that the first Nodal point is the Bogibeel Bridge (Guide Bunds), followed by Salmara, Silghat Bridge Location, Pandu, and Pancharatna. Except at Bessamara (Salmara) point, where there is little erosion, there is no displacement on either of the Banks of the Brahmaputra at these Nodal Points. Erosion with associated deposition generally takes place within these nodal points. River reach undergoing erosions and deposition are shown in the Figure 3.3 through 3.6 along with details of eroded and deposited area are in Table 3.1 to 3.4.

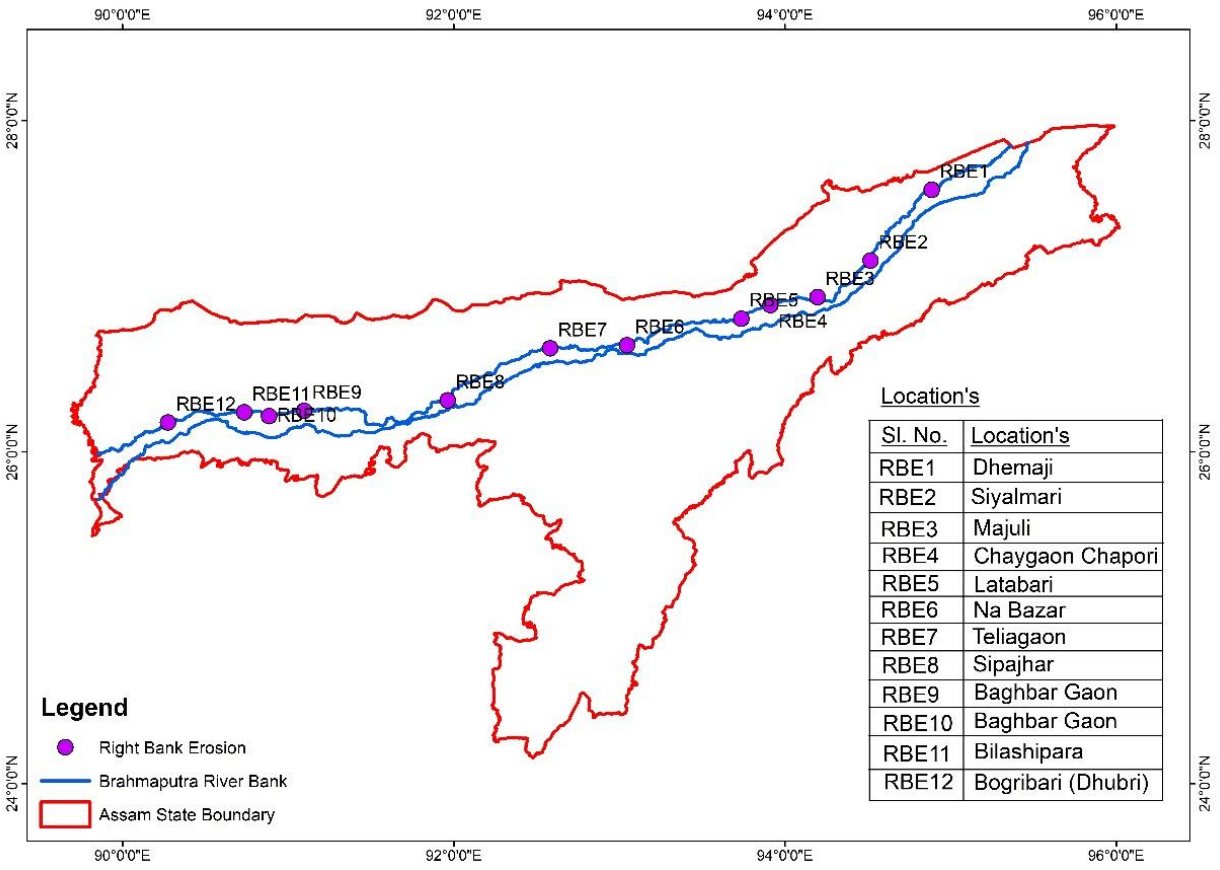

Figure 3.3 Right Bank Erosion (RBE) of River Brahmaputra

Table 3.1 Right Bank Erosion of River Brahmaputra			
SL No.	**Place**	**Area**	**Unit**
RBE1	Dhemaji	21.08	Sq.km
RBE2	Siyalmari	16.48	Sq.km
RBE3	Majuli	6.34	Sq.km
RBE4	Chaygaon Chapori	13.02	Sq.km
RBE5	Latabari	5.81	Sq.km
RBE6	Na Bazar	27.19	Sq.km
RBE7	Telia Gaon	9.67	Sq.km
RBE8	Sipajhar	24.04	Sq.km
RBE9	Baghbar Gaon	32.38	Sq.km
RBE10	Baghbar Gaon	7.00	Sq.km
RBE11	Bilashipara	7.29	Sq.km
RBE12	Bogribari (Dhubri)	11.50	Sq.km
	Total Area =	181.80	Sq.km

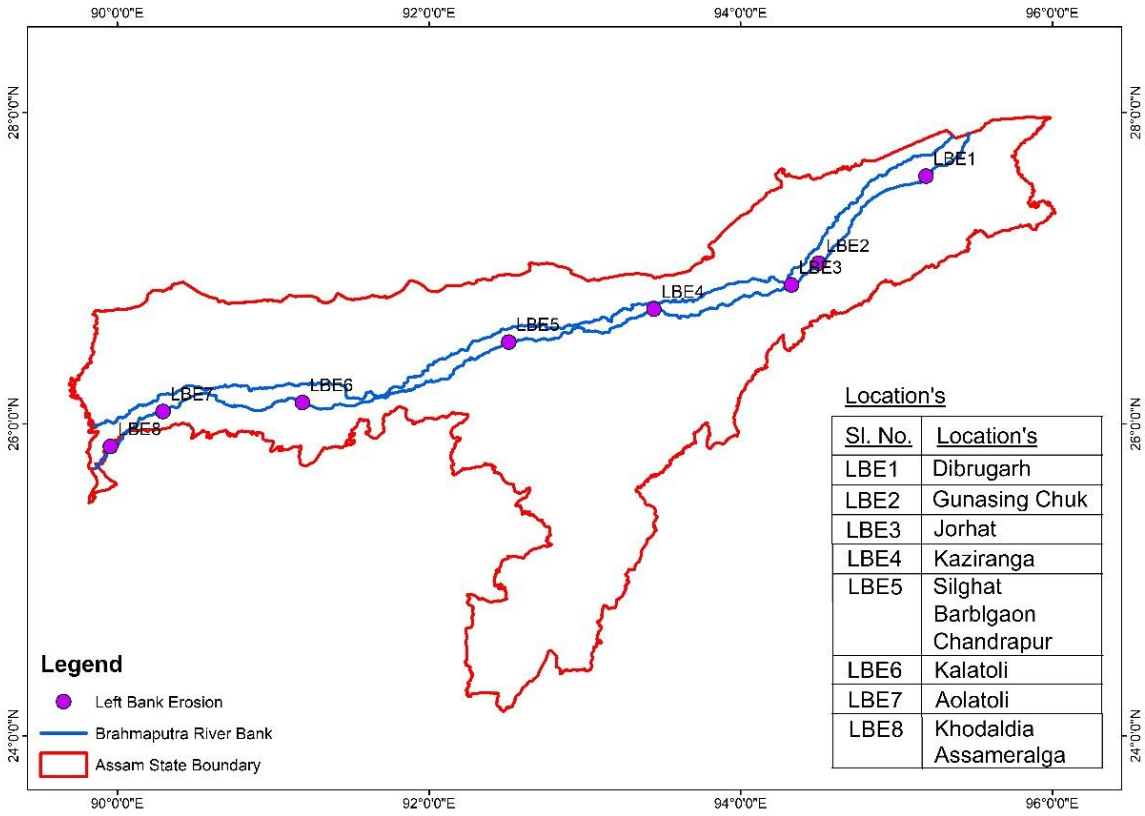

Figure 3.4 Left Bank Erosion (LBE) of River Brahmaputra

Table 3.2 Left Bank Erosion of River Brahmaputra

SL No.	Location	Area	Unit
LBE1	Dibrugarh	68.43	Sq.km
LBE2	Gunasing Chuk	7.10	Sq.km
LBE3	Jorhat	6.45	Sq.km
LBE4	Kaziranga	32.11	Sq.km
LBE5	Silghat	169.70	Sq.km
	Barbilgaon		
	Chandrapur		
LBE6	Kalatoli (Opp. Bhangamari)	17.60	Sq.km
LBE7	Aolatoli	27.70	Sq.km
LBE8	Khodaldia	86.12	Sq.km
	Assameralga		
	Total Area =	415.21	Sq.km

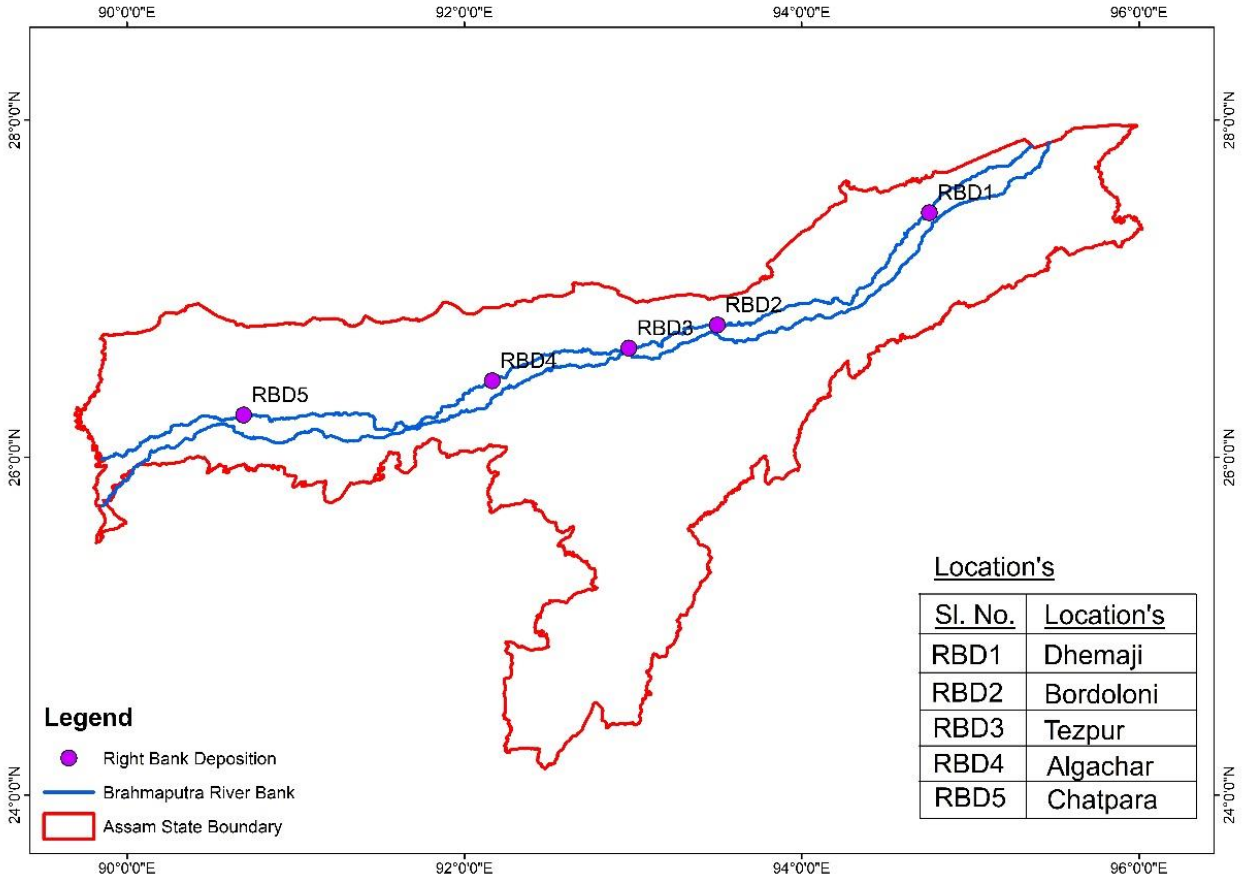

Figure 3.5 Right Bank Deposition (RBD) of River Brahmaputra

Table 3.3 Right Bank Deposition of River Brahmaputra

SL No.	**Place**	**Area**	**Unit**
LBD1	Neemati Ghat (Jorhat)	5.07	Sq. km
LBD2	Dergao (Golaghat)	15.70	Sq. km
LBD3	Aolatoli	35.60	Sq. km
	Total Area =	56.37	Sq. km

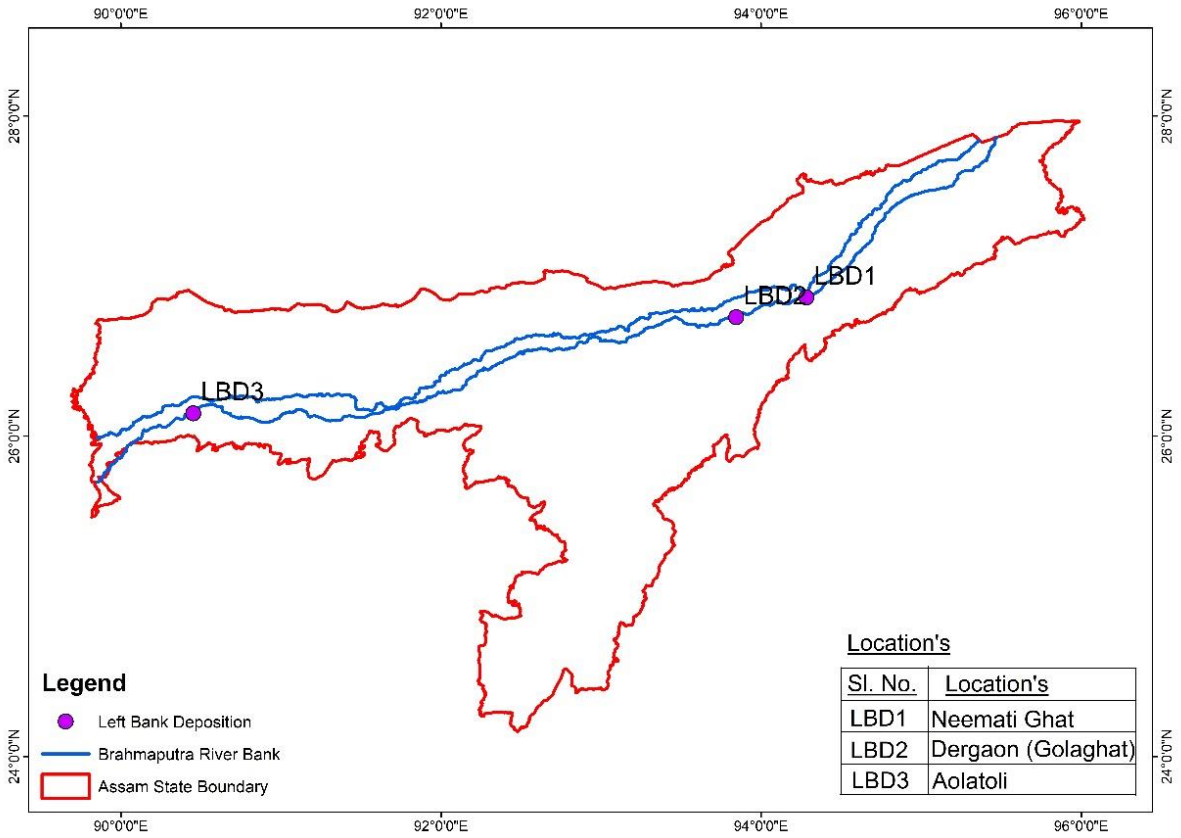

Figure 3.6 Left Bank Deposition (LBD) of River Brahmaputra

Table 3.4 Left Bank Deposition of River Brahmaputra

SL No.	Place	Area	Unit
RBD1	Dhemaji	26.98	Sq. km
RBD2	Bordoloni	8.19	Sq. km
RBD3	Tezpur	18.31	Sq. km
RBD4	Algachar	36.65	Sq. km
RBD5	Chatpara	39.80	Sq. km
	Total Area =	129.93	Sq. km

The erosion in the Right Bank of Brahmaputra of the region under consideration is 181.80 sq. km, with various specific areas contributing to this total. Dhemaji covers an area of 21.08 sq. km, Siyalmari spans 16.48 sq. km, Majuli occupies 6.34 sq. km, and Chaygaon Chapori encompasses 13.02 sq. km. Latabari covers 5.81 sq. km, while Na Bazar extends over 27.19 sq. km. Telia Gaon covers 9.67 sq. km, and Sipajhar spans 24.04 sq. km. The area of Baghbar Gaon is divided into two parts - one measuring 32.38 sq. km and the other 7.00 sq. km. Bilashipara covers an area of 7.29 sq. km, and Bogribari in Dhubri has an area of 11.50 sq. km. In summary, the region consists of various areas with different sizes, contributing to a total area of 181.80 sq. km.

The erosion in the Left Bank of Brahmaputra of the region covered in this assessment is 415.21 sq. km, with various locations contributing to this overall figure. Dibrugarh occupies an area of 68.43 sq. km, while Gunasing Chuk spans 7.10 sq. km and Jorhat covers 6.45 sq. km. Kaziranga National Park extends over 32.11 sq. km, and Silghat encompasses a significantly larger area of 169.70 sq. km. Barbilgaon and Chandrapur are also part of the region but specific area measurements are not provided for them in the given data. Kalatoli (Opposite of Bhangamari) covers 17.60 sq. km, Aolatoli spans 27.70 sq. km, and Khodaldia extends over 86.12 sq. km. The area of Assameralga is not provided. In summary, these various locations together contribute to a total area of 415.21 sq. km, with each area playing a unique role in the overall landscape of the region.

The total area of the Right Bank Deposition region is 56.37 sq. km, with specific locations contributing to this overall figure. Neemati Ghat in Jorhat covers an area of 5.07 sq. km, while Dergao in Golaghat spans 15.70 sq. km. Aolatoli also plays a significant role in this region, occupying 35.60 sq. km. In summary, these locations within the Right Bank Deposition area collectively make up a total area of 56.37 sq. km, each area contributing to the overall landscape and characteristics of the region. The Left Bank Deposition region has a total area of 129.93 sq. km, with several specific locations contributing to this overall figure. Dhemaji covers an area of 26.98 sq. km, while Bordoloni spans 8.19 sq. km and Tezpur occupies 18.31 sq. km. Algachar extends over 36.65 sq. km, and Chatpara encompasses 39.80 sq. km. In summary, these designated areas within the Left Bank Deposition region collectively make up a total area of 129.93 sq. km, each playing a unique role in the overall composition and features of the region.

3.2 Detailed Study on Erosion-Deposition Pattern of Majuli Island

Majuli, the largest habitat river island of the globe, is facing serious erosion problem. Because of its importance as a heritage site and a place reach culture, detail geoinformatics study is conducted to understand the erosion patter of this island and presented below:

3.2.1 Bankline Study Near Majuli

Several investigators have used remotely sensed data for ascertaining channel changes of Brahmaputra River and its tributaries. National Remote Sensing Agency (NRSA) (1980) has done the river migration study of the Brahmaputra using airborne scanner survey and to carry out repetitive survey to monitor changes in land use, river channels and banks to provide a base for estimating the response of the rivers to flood events. Space Application Centre (SAC), Ahmedabad

and Brahmaputra Board (1996) jointly took up a study to access the extent of river erosion in Majuli island in order to identify and delineate the areas of the island which have undergone changes along the bank-line due to dynamic behaviour of the river. Based on this report and other collateral data, Brahmaputra Board (1997) has prepared a status report on the erosion problem of Majuli Island.

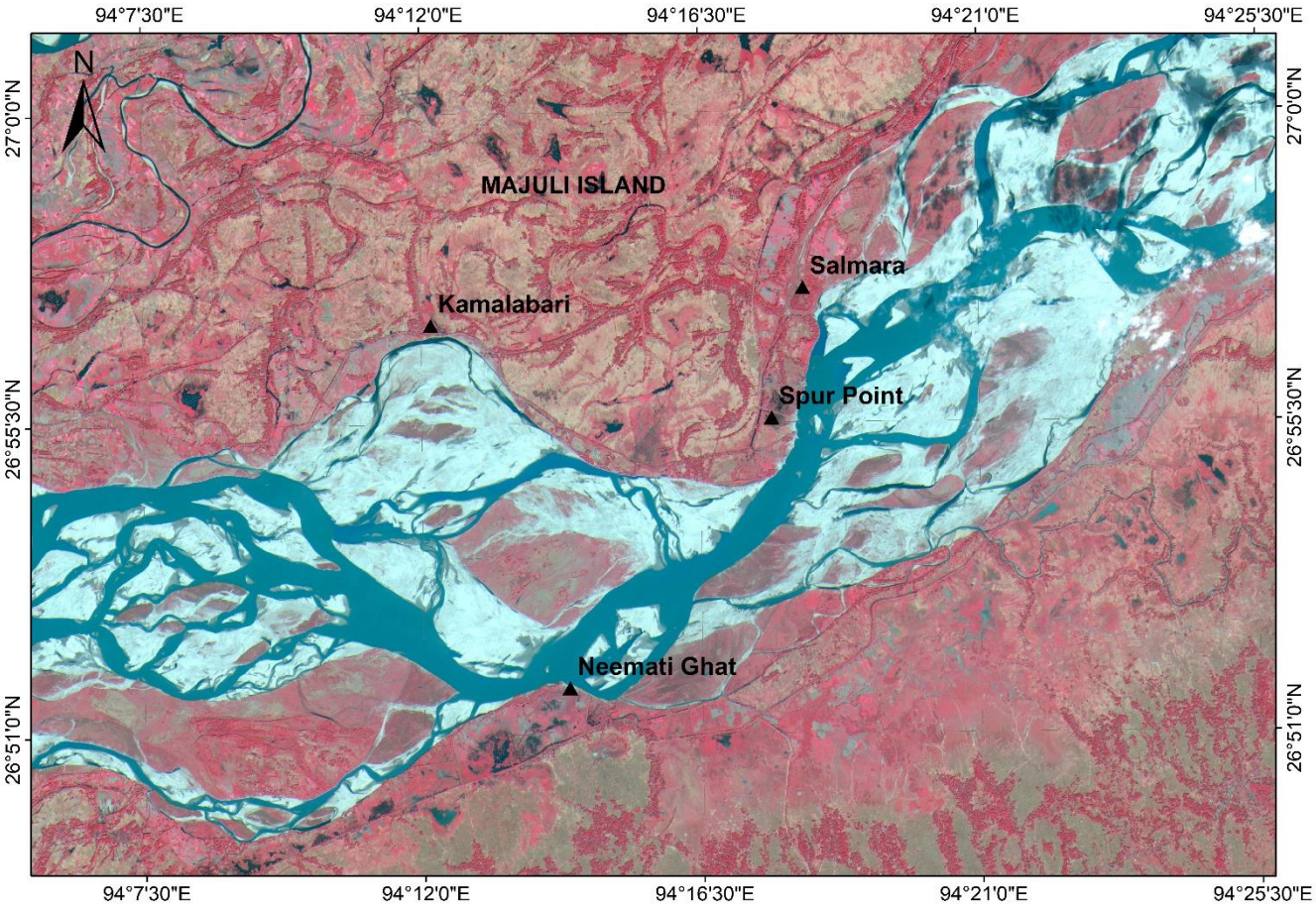

Figure 3.7 LISS IV imagery of study area

The LISS IV Imagery (2016) of study area is shown in Figure 3.7. NDWI (Normalized Difference Water Index) technique was initially tried to get the river bank line from cloud free Landsat series imageries. However, as the results were not very clear, river bank line and main channel are finally digitized manually on imageries of 04.10.1988, 02.01.2005, 30.01.2012 & 14.03.2019 and are shown in Figure 3.8, Figure 3.9, Figure 3.10 & Figure 3.11 respectively.

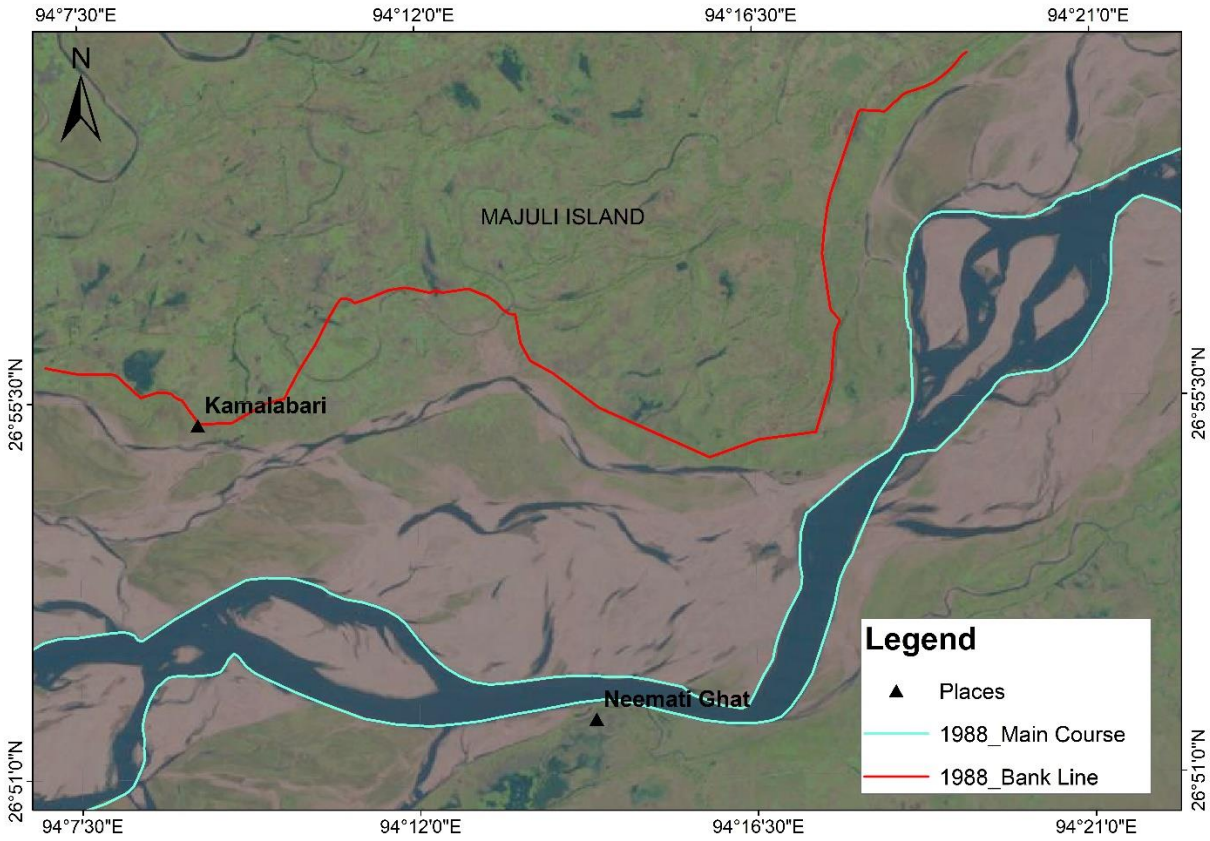

Figure 3.8 River bank line and main channel of the year 1988

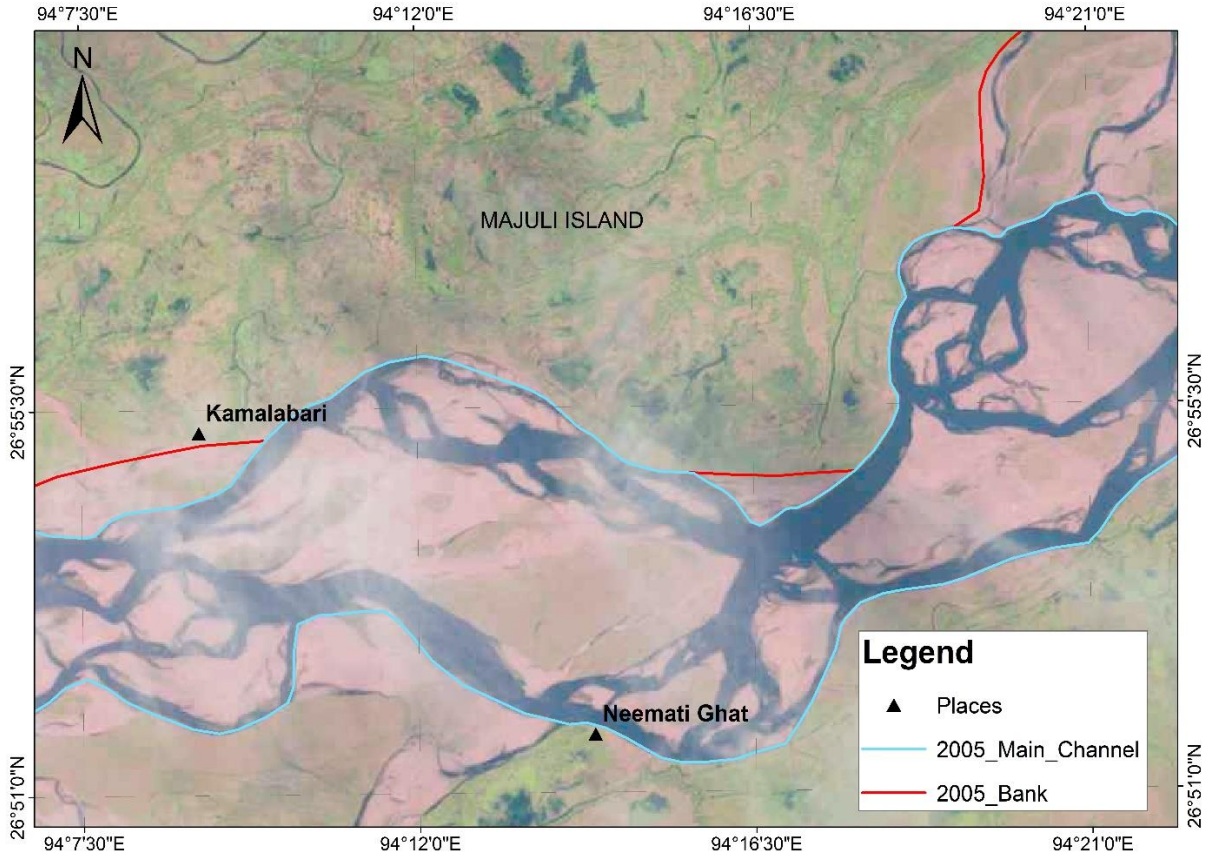

Figure 3.9 River bank line and main channel of the year 2005

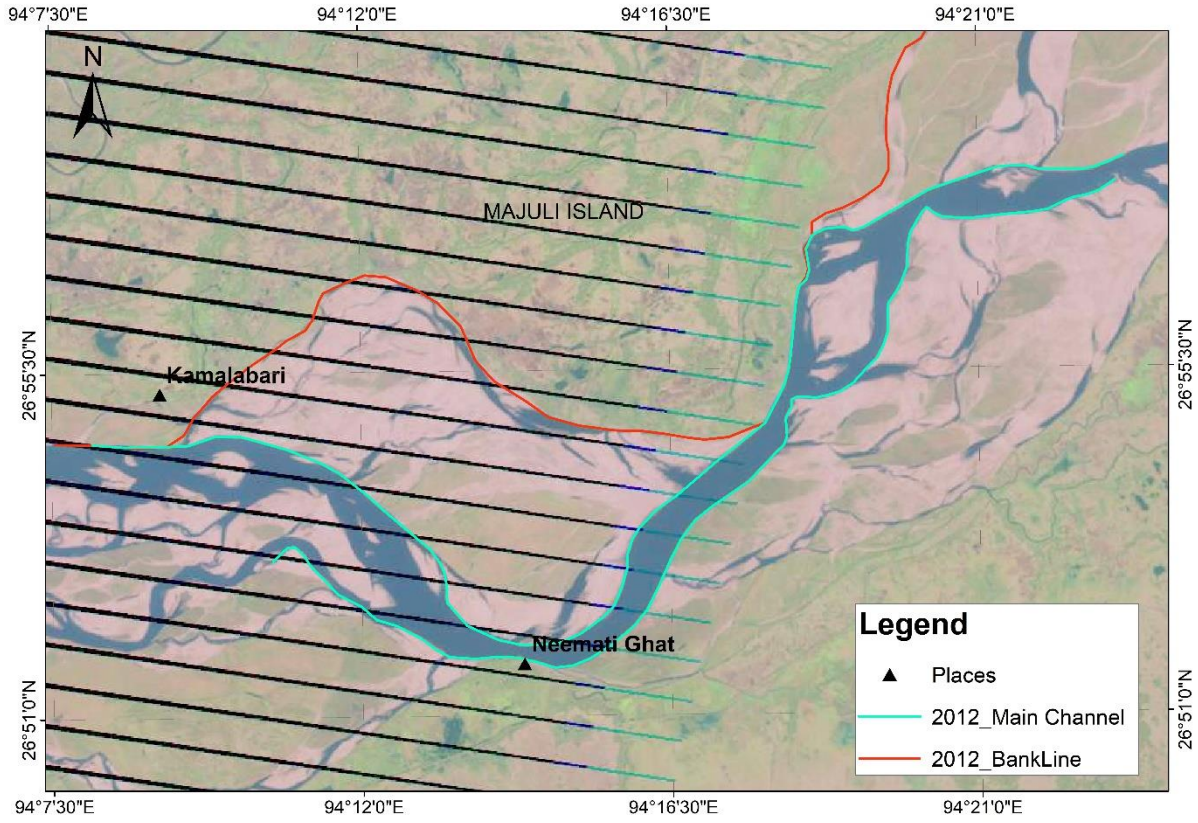

Figure 3.10 River bank line and main channel of the year 2012

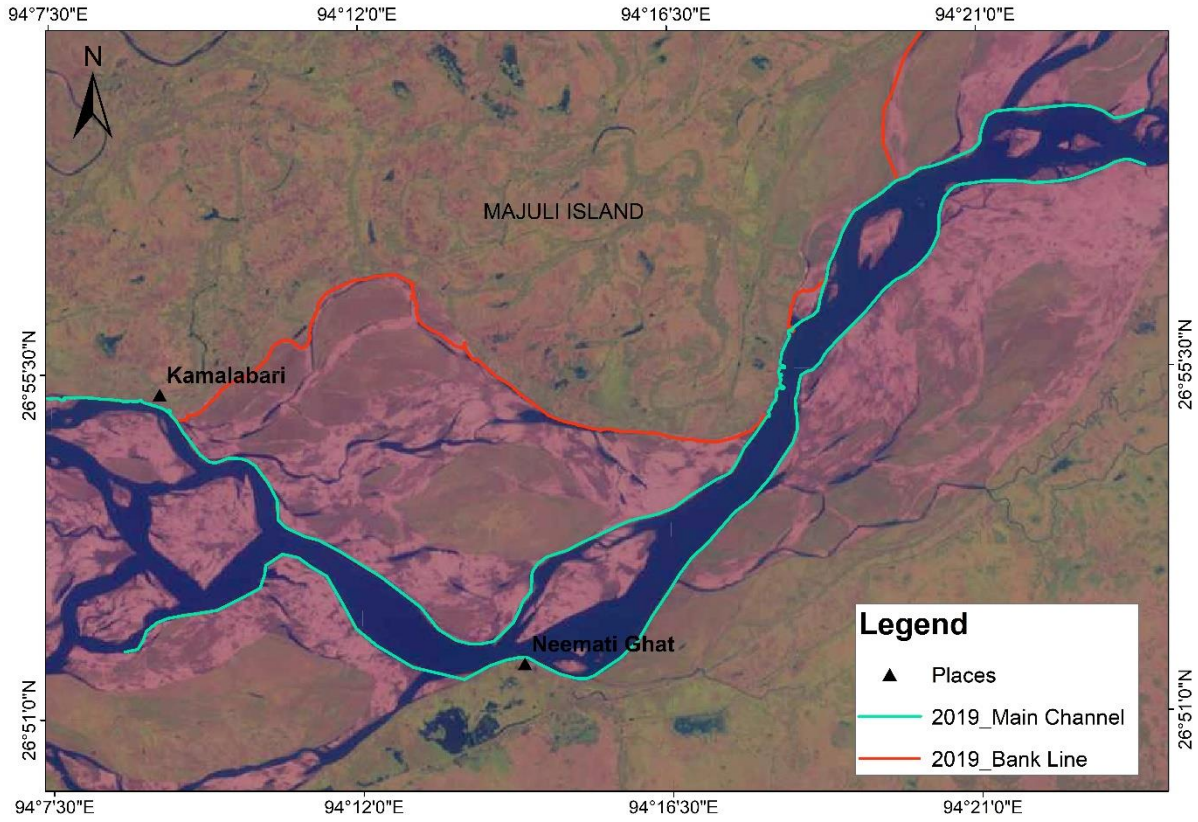

Figure 3.11 River bank line and main channel of the year 2019.

From satellite images of 1988, it can be clearly observed that there is a very small channel from Salmara to Kamalabari, on the northern bank of river Brahmaputra. Means, in the beginning the Sumoimari channel was very insignificant, but later it carried substantial flood water with high velocity. As per Detailed Project Report (DPR) for the work "Protection of Majuli Island form Flood & Erosion", the Majuli dyke was breached in August, 1993. The breach opening initially was of 2.00km length, later, it was increased to about 2.60km. The channel has been shifting towards Tuni River and joined the Tuni River in August, 1994 at Nam Sonowal village. The Breach opening has caused flooding of the area lying around Kamalabari Township and Kamalabari Satra including bank erosion near Kamalabari Police Station during its receding stage. Erosion of bank by channel was also noticed R/B embankment from Kamalabari to Burakalita. Erosion of bank at upstream of Dhakhinpat and at Bechamara had also been noticed during 1994. Further erosion of bank at Jengraimukh by kherkatiasuti had also been noticed during the flood of 1993 and 1994. From satellite images of 2000 onwards Sumoimari channel from Salmara to Kamalabari, on the northern bank of river Brahmaputra is clearly visible.

Massive land erosion started in Majuli during the monsoon in the year 2003. A Central Expert Team headed by Director, Flood Management, Central Water Commission visited vulnerable sites of Majuli Island in the month of June 2003 and recommended certain measures. The anti-erosion works carried out by Brahmaputra Board so far have yielded positive results. It may be stated that in the year 2007 the Sumoimari channel of Brahmaputra River, flowing along southern bank of Majuli Island from Dakhinpat to Kamalabari for an approximate length of 25 Km, carried a considerable discharge of Brahmaputra (40%-45% of total discharge of Brahmaputra). Use of RCC porcupine screens in Aphalamukh-Dakhinpat area i.e. at the mouth of the Sumoimari channel induced heavy siltation, as a result, gradually, flow in the channel got reduced substantially. Similarly, judicious laying of porcupine screens in the upstream at Tekeliphuta and downstream areas encouraged heavy siltation. As a result of above, the entire upper Majuli reach of Brahmaputra has seen no erosion during the monsoons of the years 2009 and 2010. This shows that the anti-erosion works carried out by Brahmaputra Board have brought about far-reaching consequences and changes in the river morphology and thereby these have considerable favourable impacts in river regime.

It may be worthwhile to mention that during the period from the year 1963 to the year 2004, there has been, year after year, loss of land mass of Majuli Island. Since 2004 no net loss of land mass of Majuli island has occurred. Erosion / Reclamation of land mass of Majuli Island during the years from 2004 to 2019 is analysed. Since the year 2004, with regular implementation of ant-erosion / bank protection measures, the total area of Majuli Island has increased. River bank line and main river channel on are

drawn on satellite images 1988 onwards. It is observed that the main channel was on south bank on southern side in the study reach till 1995. However, the main channel is divided into two halves, creating a new channel on northern side. These two channels are observed till 2010. Due to execution of work by Brahmaputra Board, the main channel is shifted to southern side.

3.3 River Sand Bar Analysis

River Bar dynamics relate to the morphologic behaviour of braided river and specially to the erosion and deposition processes. Planforms are characterized by numerous transient mid-channel bars and channels in a braided river. The planform changes rapidly and unpredictably in the case of a sand bed due to the relatively high energy and intense bedload transport condition, which accelerates instability especially for mid-channel bars (Egozi and Ashmore, 2009). These bars show various planforms, which seem to be stage-dependent and eventually construct a very wide range of alluvial planforms due to upstream and downstream erosion and sedimentation (Rth et al., 2011). To analysis the dynamics of the morphology such as large-scale sand bars, a time series satellite image analysis has been conducted. Six geo-referenced satellite images of 2015 to 2020 (image dated 15.02.2015, 05.02.2016, 09.02.2017, 22.01.2018, 16.02.2019, 13.02.2020) have been superimposed to assess sand bar movements over the years.

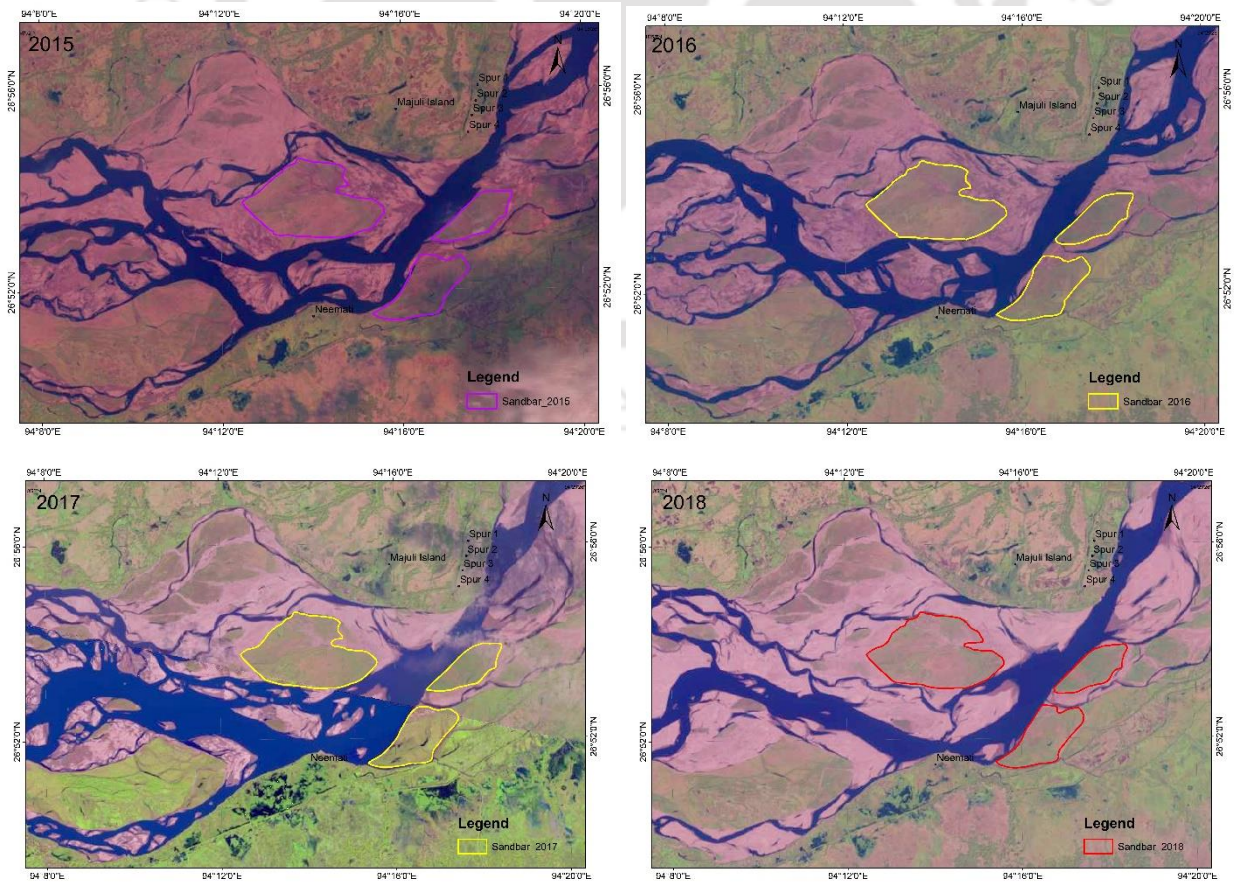

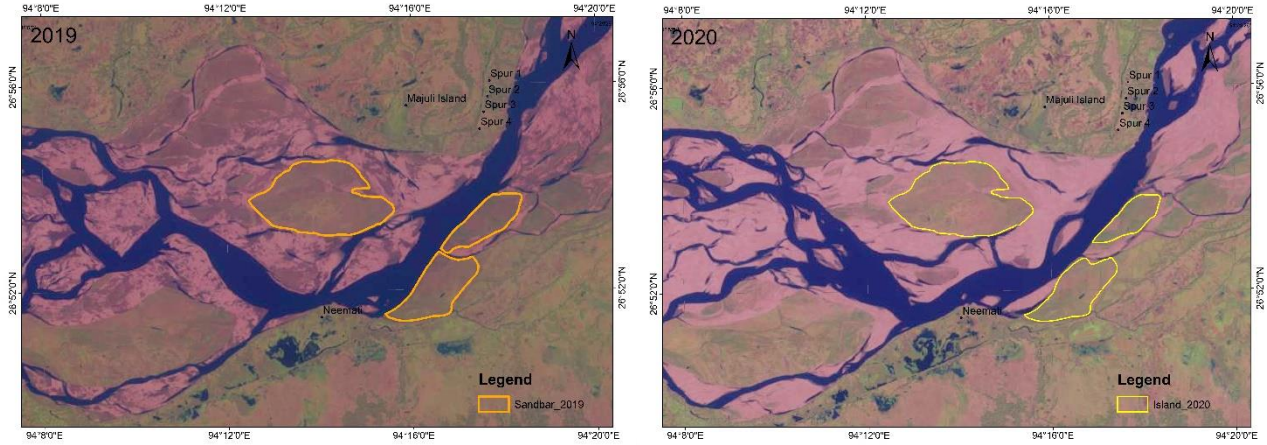

Figure 3.12 River Sand bar between Majuli and Nimati Ghat

The important sand bars in the study area are referred as sandbar-I, sandbar-II and sandbar-III as shown in Figure 3.12. Changes of these sand bars in each year were observed. It is found that sandbar-I is stable but erosion has been going on western side of the sand bar-II and sandbar-III. As earlier discussed, the construction of spurs at Majuli were done in 2010-2014, it is now clearly visible the water thrust increased in on western side of the sand bar-2 and sandbar-3 from 2015 onwards. This water thrust is finally creating erosion at NimatiGhat.

3.4 Soil Characteristic Study of River Brahmaputra

As the erosion has occurred more or less in entire stretch, soil samples are collected from river bed near bank in 19 locations. The locations for collection of soil sample are identified with in 50 km distance of separation. The locations from upstream to downstream of river Brahmaputra are Boginodi, Dibrugarh, Siyalmari, GunasingChuk, Majuli, ChayongChapori, Bordoloni, Na Bazar, Tezpur, BarbilGaon, Algachar, Chandrapur, Guwahati, Bhanganmari, BaghbarGaon, Chatpara, Aolatoli, Khodaidhila, Assameralga.

River bank erosion and soil parameters such as the Atterberg Limits, mechanical analysis, Maximum Dry Density (MDD), Optimum Moisture Content (OMC), specific gravity, and coefficient of permeability are co-related topics in river management. River bank erosion is the progressive removal of soil from riverbanks by flowing water, resulting in considerable land loss, structural damage, and ecological consequences. Water velocity, soil type, vegetation cover, and human activity are all factors that contribute to erosion. The Atterberg Limits identify the critical water concentrations of fine-grained soils, defining the boundaries between liquid, plastic, and solid states and providing information about soil susceptibility to erosion and deformation. Soils with High Plasticity (high LL and PL) can absorb more water and expand, thereby diminishing stability and

increasing erosion risk when saturated. In contrast, soils with limited flexibility may be more prone to cracking and erosion when dry. Determining the behaviour of soil under different moisture circumstances is crucial for developing efficient erosion management strategies and guaranteeing the stability of riverbanks, and this requires an understanding of the Atterberg Limits. Mechanical analysis, also known as particle size analysis, is the process of estimating the proportions of different particle sizes in a soil sample, which is commonly accomplished through screening and sedimentation. This examination aids in the classification of soil into four categories: gravel, sand, silt, and clay, each with its own set of physical qualities and behaviour under different conditions. Mechanical analysis is crucial in the context of river bank erosion because soil particle size and distribution have a substantial impact on erosion susceptibility. Engineers may project the potential for erosion and put into practice efficient erosion control measures, like choosing the right materials to protect riverbanks, by using the mechanical properties of soil. Strategies for soil conservation and sustainable riverbank management require an integration of knowledge about mechanical analysis and river bank erosion dynamics. Maximum Dry Density (MDD) refers to the highest density that a soil can achieve through compaction at its optimum moisture content. Understanding the MDD is crucial in the context of river bank erosion since it indicates how compact and erosion-resistant a soil is. Soils with higher MDD have stronger structural integrity and are less susceptible to water erosion. Soils with lower MDD, on the other hand, are more prone to erosion because they have less compaction and cohesiveness. Effective erosion control techniques must take the MDD into account in order to improve soil stability and prevent land deterioration along river banks. Integrating knowledge of river bank erosion dynamics with MDD aids in the development of effective soil conservation measures and ensures long-term riverbank management. Optimum Moisture Content (OMC) is a critical geotechnical engineering characteristic that relates to the moisture level at which soil achieves its maximum dry density when compacted. Understanding the OMC is critical in the context of river bank erosion, as soil that is either too dry or too saturated is more prone to erosion. Dry soil lacks cohesion, but very saturated soil loses strength and is readily washed away. As a result, regulating soil moisture content along riverbanks is critical to preventing erosion and preserving the land's stability and integrity. Integrating knowledge of river bank erosion with OMC improves soil and water conservation measures, resulting in strong riverbank stabilization. Specific gravity, defined as the ratio of the density of soil particles to the density of water, is an important quantity that influences soil behaviour under diverse conditions. Specific gravity is important in the context of river bank erosion because it reveals information about the mineral composition and density of the soil, which influences its stability and erosion resistance. Soils having a greater specific gravity usually have denser, more cohesive particles, making them

less prone to erosion. Soils with lower specific gravity, on the other hand, may be lighter and less stable, increasing their susceptibility to being carried away by running water. Understanding the specific gravity of soils along riverbanks aids in determining their erosion potential and developing appropriate erosion control measures. The coefficient of permeability, or hydraulic conductivity, measures how easily water moves through soil pores. Soils with high coefficients of permeability, such as sandy soils, allow water to flow through them fast, increasing the risk of erosion as water swiftly eliminates soil particles. Soils with low coefficients of permeability, such as clay, restrict water flow, lowering immediate erosion danger but potentially resulting in waterlogging and increasing pore pressure. Understanding the coefficient of permeability is critical for developing effective erosion control methods and anticipating riverbank behaviour under varied hydraulic circumstances. Integrating knowledge of river bank erosion and soil permeability aids in designing comprehensive land and water resource management plans that provide stability and sustainability in erosion-prone locations. Because erosion has occurred along the entire length of the Brahmaputra River in Assam, soil samples were taken from the riverbed near the bank at 19 locations. The soil sample collecting locations have been selected within a 50-kilometer range of each other. Boginodi, Dibrugarh, Siyalmari, GunasingChuk, Majuli, ChayongChapori, Bordoloni, Na Bazar, Tezpur, BarbilGaon, Algachar, Chandrapur, Guwahati, Bhanganmari, BaghbarGaon, Chatpara, Aolatoli, Khodaidhila, and Assameralga are the sites from upstream to downstream of the Brahmaputra. The grain size distribution, Atterberg's Limit, Maximum Dry Density (MDD), Optimum Moisture Content (OMC), specific gravity, and coefficient of permeability are all analysed, and each location's soil classification is calculated.

The test results of the soil samples which were collected from various sites of Brahmaputra River in Assam, during Brahmaputra Aamantran Abhijan as detailed below:

- **Classification of Soil**

  Mechanical Analysis was done for all the 19 (nineteen) samples. Out of these, 6 (six) samples fall under SP-SM group, 3 (three) samples fall under ML group, 4(four) samples fall under MI group, 6 (six) samples fall under SP group of Bureau of Indian Standards (BIS) Soil Classification system. The test results are appended in **Table No. 3.5**

- **Mechanical Analysis and Atterberg Limits**

  Results of Mechanical analysis and Atterberg limits are appended in **Table No. 3.6**

- **Standard Proctor Compaction**

  Standard Proctor Compaction test was conducted for all the 19 (nineteen) soil samples passing 4.75 mm Indian Standard (IS) sieve and the values are tabulated in **Table No. 3.7** The values of maximum dry density and optimum moisture content vary from 1.50 gm/cc to 1.69 gm/cc and 12.59% to 22.27% respectively.

- **Specific Gravity**

  The specific gravity of all the 19 (nineteen) soil samples are appended in **Table No. 3.7**

- **Laboratory Permeability**

  Falling head permeability test has been conducted on all the 19 (nineteen) soil samples. The test results are appended in **Table No. 3.8**

Table 3.5 Results of soil classification

Sample No	Site	Gravel %	Sand %	Silt %	Clay %	Finer %	D50	Silt factor	Cu	Cc	Liquid Limit	B.I.S. Soil Classification
Soil 1	Boginodi	0.00	94.20	5.78	0.01	5.79	0.14	0.66	1.92	0.99	-	SP-SM
Soil 2	Dibrugarh	0.00	84.40	15.09	0.51	15.60	0.08	0.50	-	-	32.24%	ML
Soil 3	Siyalmari	0.00	92.00	7.74	0.26	8.00	0.08	0.52	-	-	36.37%	MI
Soil 4	GunasingChuk	0.00	95.40	4.44	0.16	4.60	0.16	0.69	1.85	1.22	-	SP-SM
Soil 5	Majuli	0.00	81.20	16.92	1.88	18.80	0.08	0.51	-	-	35.88%	MI
Soil 6	ChayongChapori	0.00	83.00	15.11	1.89	17.00	0.08	0.50	-	-	29.28%	ML
Soil 7	Bordoloni	0.00	87.60	11.18	1.22	12.40	0.08	0.50	-	-	36.60%	MI
Soil 8	Na Bazar	0.00	85.20	4.38	0.41	4.79	0.14	0.65	2.12	0.97	-	SP-SM
Soil 9	Tezpur	0.00	96.20	3.47	0.33	3.80	0.17	0.72	1.65	1.29	-	SP
Soil 10	BarbilGaon	0.00	89.40	9.52	1.08	10.60	0.14	0.66	-	-	-	SP-SM
Soil 11	Algachar	0.00	96.20	3.47	0.33	3.80	0.17	0.73	1.59	1.11	-	SP
Soil 12	Chandrapur	0.00	84.80	13.65	1.55	15.20	0.08	0.50	-	-	36.48%	MI
Soil 13	Guwahati	0.00	95.00	4.49	0.51	5.00	0.17	0.72	1.66	1.37	-	SP
Soil 14	Bhanganmari	0.00	94.00	5.41	0.59	6.00	0.16	0.70	1.85	1.09	-	SP
Soil 15	BaghbarGaon	0.00	92.80	6.51	0.68	7.19	0.16	0.70	2.05	1.17	-	SP-SM
Soil 16	Chatpara	0.00	96.40	3.29	0.31	3.60	0.16	0.71	1.27	1.10	-	SP
Soil 17	Aolatoli	0.00	91.80	7.49	0.71	8.20	0.16	0.71	1.66	1.37	-	SP
Soil 18	Khodaidhila	0.00	81.60	17.30	1.09	18.39	0.08	0.52	-	-	35.33%	MI
Soil 19	Assameralga	0.00	95.60	4.11	0.29	4.40	0.12	0.61	1.69	1.05	-	SP-SM

Table 3.6 Results of Mechanical Analysis and Atterberg limits tests

Sl. No.	Location	Sample No.	Mechanical Analysis						Atterberg's Limit IS -0.425 mm sieve			B.I.S Soil Classification
			0.002 mm & less	0.002 to 0.075 mm	0.075 to 0.425 mm	0.425 to 2.0 mm	2.0 to 4.75 mm	4.75 mm & above	L.L	P. L	P. I	
1	Boginodi	Soil 1	0.02	6.75	93.19	0.04	0.00	0.00	-	-	0	SP-SM
2	Dibrugarh	Soil 2	1.36	40.17	58.43	0.04	0.00	0.00	32.24%	NP	0	ML
3	Siyalmari	Soil 3	1.21	35.44	63.35	0	0.00	0.00	36.37%	NP	0	MI
4	GunasingChuk	Soil 4	0.17	4.94	94.87	0.02	0.00	0.00	-	-	0	SP-SM
5	Majuli	Soil 5	3.48	31.33	65.19	0	0.00	0.00	35.88%	NP	0	MI
6	ChayongChapori	Soil 6	4.37	34.98	60.65	0	0.00	0.00	29.28%	NP	0	ML
7	Bordoloni	Soil 7	3.53	32.34	64.12	0.01	0.00	0.00	36.60%	NP	0	MI
8	Na Bazar	Soil 8	0.83	8.85	83.31	7.01	0.00	0.00	-	-	0	SP-SM
9	Tezpur	Soil 9	0.35	3.65	95.7	0.3	0.00	0.00	-	-	0	SP
10	BarbilGaon	Soil 10	1.11	9.9	88.73	0.26	0.00	0.00	-	-	0	SP-SM
11	Algachar	Soil 11	0.16	1.7	97.25	0.89	0.00	0.00	-	-	0	SP
12	Chandrapur	Soil 12	4.08	35.96	59.96	0	0.00	0.00	36.48%	NP	0	MI
13	Guwahati	Soil 13	0.24	2	97.57	0.19	0.00	0.00	-	-	0	SP
14	Bhanganmari	Soil 14	0.42	3.88	95.56	0.14	0.00	0.00	-	-	0	SP
15	BaghbarGaon	Soil 15	0.71	6.78	92.39	0.12	0.00	0.00	-	-	0	SP-SM
16	Chatpara	Soil 16	0.09	0.84	99.05	0.02	0.00	0.00	-	-	0	SP
17	Aolatoli	Soil 17	0.36	3.61	95.96	0.07	0.00	0.00	-	-	0	SP
18	Khodaidhila	Soil 18	2.04	31.99	65.95	0.02	0.00	0.00	35.33%	NP	0	MI
19	Assameralga	Soil 19	0.49	6.68	92.8	0.03	0.00	0.00	-		0	SP-SM

Table 3.7 Results of Proctor Compaction and Specific Gravity					
Sl No	Location	Sample No	Standard Proctor Compaction Test		Specific Gravity
			Max Dry Density (gm/cc)	Optimum Moisture Content (%)	
1	*2*	*3*	*4*	*5*	*6*
1	Boginodi	Soil 1	1.68	15.48	2.67
2	Dibrugarh	Soil 2	1.57	22.27	2.68
3	Siyalmari	Soil 3	1.5	22.2	2.61
4	Gunasing Chuk	Soil 4	1.64	17.38	2.73
5	Majuli	Soil 5	1.63	18.2	2.61
6	ChayongChapori	Soil 6	1.6	19.22	2.62
7	Bordoloni	Soil 7	1.58	17.99	2.56
8	Na Bazar	Soil 8	1.71	12.59	2.67
9	Tezpur	Soil 9	1.65	16.72	2.68
10	Barbil Gaon	Soil 10	1.68	16.02	2.61
11	Algachar	Soil 11	1.66	15.99	2.66
12	Chandrapur	Soil 12	1.6	15.93	2.65
13	Guwahati	Soil 13	1.67	13.08	2.68
14	Bhanganmari	Soil 14	1.62	15.57	2.73
15	Baghbar Gaon	Soil 15	1.69	14.29	2.72
16	Chatpara	Soil 16	1.58	18.15	2.7
17	Aolatoli	Soil 17	1.63	17.2	2.68
18	Khodaidhila	Soil 18	1.64	17.26	2.57
19	Assameralga	Soil 19	1.61	15.7	2.65

Table 3.8 Results of permeability test				
Sl. No	Location	Sample No.	Co-efficient of Permeability (cm/sec)	Remarks
1	Boginadi	Soil 1	0.00104403	Falling Head Test
2	Dibrugarh	Soil 2	0.00031582	
3	Siyalmari	Soil 3	0.00104403	
4	Gunasing Chuk	Soil 4	0.00190749	
5	Majuli	Soil 5	0.0006642	
6	ChayongChapori	Soil 6	0.00059129	
7	Bordoloni	Soil 7	0.00055496	
8	Na-Bazar	Soil 8	0.00160994	
9	Tezpur	Soil 9	0.00159937	
10	Barbil Gaon	Soil 10	0.00044975	
11	Algachar	Soil 11	0.00188263	
12	Chandrapur	Soil 12	0.00121427	
13	Guwahati	Soil 13	0.00080757	
14	Bhanganmari	Soil 14	0.00067082	
15	Baghbar Gaon	Soil 15	0.00101649	
16	Chatpara	Soil 16	0.00156782	
17	Aolatoli	Soil 17	0.00107761	
18	Khodaidhila	Soil 18	0.00109123	
19	Assameralga	Soil 19	0.0008478	

3.5 Discussion and Conclusion

In braided river systems, the dynamic interplay between bank soil and bank erosion intricately shapes the river's morphology dynamics. Bank soil, comprising a diverse amalgamation of sediment types ranging from coarse gravel to fine silt, forms the foundational material of the riverbanks. This composition is influenced by various geological factors, including the local substratum and sediment sources, as well as anthropogenic activities such as land use and engineering interventions. Conversely, bank erosion represents a dynamic process through which the banks of a braided river are continually shaped and reconfigured over time. This process is driven by a myriad of hydraulic and geomorphological factors, including channel migration, sediment transport dynamics, variations in flow regime, and seasonal fluctuations in water levels. Moreover, the transport of sediment associated with bank erosion plays a crucial role in the downstream transfer of nutrients, organic matter, and sedimentary substrates, influencing the geomorphic evolution of river corridors and the functioning of adjacent riparian ecosystems. In braided river systems, where sediment dynamics are inherently complex and spatially heterogeneous, the redistribution of sediment through bank erosion and sediment deposition drives the maintenance of channel morphology, sediment budgets, and the connectivity of fluvial habitats across the landscape. However, anthropogenic modifications to river systems, such as channelization, flow regulation, and land-use changes, can disrupt the natural balance between bank soil formation and bank erosion, leading to accelerated rates of bank instability, habitat degradation, and loss of ecosystem services. The complicated interplay between bank soil and bank erosion exerts profound influences on the sand bar dynamics and habitat diversity within braided river ecosystems. Conversely, bank erosion can alter the physical structure of the riverbanks, leading to habitat loss, bank collapse, and changes in channel morphology. These dynamic processes create a mosaic of habitats characterized by varying degrees of flow velocity, sediment composition, and vegetation cover, which in turn support a rich array of species adapted to different ecological niches. In summary, the intricate relationship between bank soil and bank erosion in braided river systems exemplifies the dynamic interplay between geomorphic processes, ecological dynamics, and human influences in shaping riverine landscapes. Understanding the mechanisms driving bank erosion and the factors influencing the stability of bank soil is essential for effective river management and conservation strategies aimed at preserving the integrity and resilience of braided river ecosystems in the face of ongoing environmental changes and anthropogenic pressures.

Accurate erosion mapping is crucial for river management, as it helps assess floodplain risks and predict the impacts of changes in flood patterns, bank stabilization, and land use. A study on the Ganga River upstream of the Farakka Barrage (Archana et al., 2012) identified increased meandering, higher sinuosity, and greater braidedness from 1955 to 2005, leading to significant agricultural land loss in Malda district, especially in the Manikchak and Kaliachak-II blocks. Factors such as soil stratification, sediment load, and the Farakka Barrage contribute to erosion, with leftward river bank shifting observed since 1973 (Mandal, 2017). In the Brahmaputra River, erosion causes stream pattern changes and land loss, with estimates ranging from 72.5 to 80 sq. km/year between 1997 and 2008 (Das et al., 2014). Majuli Island alone lost 2,745 hectares of land between 1991 and 1998 (Mani et al., 2003). Mitigation efforts, including rock armouring and the use of geosynthetics, have been implemented to address erosion (Sarma, 2013; Sarma, 2014; Maurya et al., 2022). GIS mapping is used to identify and forecast severe erosion areas, guiding local engineering departments in their interventions (Sarma & Dutta, 2016). After reviewing the published literature which was detailed in chapter 2, it is found that there is no such published paper where the river bank erosion is tried to co-relate with soil properties of river bank.

In this study it is found that river bank erosion in Brahmaputra has been occurred almost every location except few locations where rock-strata is available. The north and south bank line of entire stretch has been studied using GIS.

The GIS-based Brahmaputra River Morphology Study reveals significant left bank erosion in Assam, affecting Dibrugarh (68.43 sq. km), Kaziranga (32.11 sq. km), and vulnerable areas like Chandrapur and Barbilgaon (159.70 sq. km). Other impacted regions include Gunasing Chuk, Jorhat, Aolatoli, Baghbor Gaon, and Khodaldia, totalling 400.21 sq. km.

The Brahmaputra River, as it flows through the plains of Assam, exhibits braided channels due to its excessive sediment load. These braided channels are characterized by constant shifting and the formation of sand shoals. This phenomenon is influenced not only by the flood discharge of the Brahmaputra itself but also by the sediment discharge from its numerous tributaries. Over time, this process of channel shifting has been ongoing, shaping the landscape of the region. The river tends to shift laterally, a phenomenon particularly evident in changes to the outfalls of its various tributaries, especially along the south bank. Near their outfalls, these south bank tributaries typically flow parallel

to the Brahmaputra. The lateral movement of the river, predominantly in a southerly direction, results in the eastward shifting of the outfalls of these tributaries. This continual process of lateral movement and shifting of outfalls underscores the dynamic nature of the Brahmaputra River and its influence on the surrounding landscape in Assam.

The Brahmaputra River carries an excessive sediment load primarily due to frequent low-magnitude seismic disturbances and occasional devastating earthquakes in the North-Eastern Region, known for its geological instability. One such catastrophic event occurred on August 15, 1950, causing extensive devastation in Upper Assam, particularly in the Abor and Mishmi hills of Arunachal Pradesh, as well as parts of Lakhimpur and Sibsagar districts. The earthquake triggered large-scale landslides in the hills, leading to a massive influx of sediment and debris into the rivers. Consequently, the upper reaches of the Brahmaputra, along with the Subansiri, Dihang, Dibang, and Lohit rivers, experienced heavy siltation and obstruction. Although most of these temporary blockages burst within days, they caused significant floods and damage downstream in the plains.

As per a study, revealed significant changes in river morphology. The Brahmaputra showed siltation of 2.5 to 3 meters at Kobo, below the junction of the Dihang and Lohit, while Dibrugarh exhibited indications of 2 meters of silting. Furthermore, appreciably high low-water levels were observed upstream of Neamati and Disangmukh, indicating heavy siltation. The Dibang and its tributaries experienced extensive silting, with rapids disappearing and outfalls being blocked, disrupting the entire drainage system. Similar alterations were noted in the Dihang and its smaller tributaries, with significant silting observed below Pasighat. The Subansiri River channel remained relatively unaffected, except for a 3 to 3.5-meter siltation at Chauldhoghat, while the Ranganadi reported a 1-meter siltation. Despite the absence of similar accounts of earlier earthquakes, the report emphasized that seismic events severely disrupt the river's natural regime.

The catchment areas of Brahmautra river and its tributaries are delineated from freely available srtm data and compared with data available in various document/plan. The Brahmaputra River system commands a catchment area spanning 580,000 sq. km, making it one of the largest river basins in the region. Contributing to this vast network are numerous tributaries, each with its own significant catchment area. Notably, the Beki Manas Aie river boasts a catchment area of 43,497 sq. km, followed by the Subansiri (Dikrong) river with 37,000 sq. km and the Lohit River with 29,487 sq. km. Other

tributaries include the Barak (Main Stem) river with 26,193 sq. km, Kopili Kollang with 20,068 sq. km, and Sankosh-Raidak with 15,429 sq. km. Additionally, the Teesta River contributes with a catchment area of 12,165 sq. km, while the Dhansiri (South) and Jia Bharali (Kameng) rivers cover 10,305 and 10,289 sq. km, respectively. Further down the network, tributaries such as the Buridihing (Noa-Dehing), Torsa, and Imphal rivers exhibit catchment areas ranging from 8,730 to 7,970 sq. km. Other notable contributors include the Jaldaka, Dhaleshwari, Dikhow, Disang, Kulsi Deosila, Jinjiram, and Ranganadi rivers, each adding to the intricate hydrological landscape with catchment areas varying from 5,782 to 2,941 sq. km. It is observed that catchment areas of north bank tributaries surpass those of their counterparts on the south bank, with higher rainfall in the former leading to a greater discharge contribution to the main river. Secondly, from another the silt yield per square kilometre in north bank tributary catchments was found to be approximately 5 to 6 times higher than that of the south bank tributaries. Consequently, due to their larger catchment areas, the north bank tributaries are anticipated to contribute roughly eight to nine times more silt load compared to the south bank tributaries.

Deforestation and inadequate land management practices present significant challenges in the region, particularly in hilly areas where traditional shifting cultivation, known locally as jhumming, has been practiced by tribal communities for generations. While this method was suitable when populations were sparse and longer rotation periods were feasible, population growth has led to shorter rotation cycles, resulting in notable soil loss due to the removal of vegetation cover. The loss of soil carries two significant consequences: firstly, reduced soil capacity to retain rainfall exacerbates water runoff issues; and secondly, the substantial sediment and debris washed down from denuded catchments decrease river capacity while increasing discharge due to heightened runoff. Unregulated grazing further compounds soil erosion problems.

Despite abundant rainfall and adequate soil cover, hill slopes are typically well-forested. Along the foothills, a broad swath of forests and dense grass traditionally helped mitigate soil erosion. However, recent encroachment and deforestation in these areas have intensified soil erosion and sedimentation in tributaries, worsening environmental degradation and complicating water management and conservation efforts. Erosion issues, such as sheet erosion, rills, and gullies, are widespread in the plains as well. This problem is particularly pronounced on the north bank of the Brahmaputra, where the terrain slopes at a gradient of 1 to 5 percent towards the river from the foothills. Numerous small streams and

several large ones traverse this landscape. Given that the soil in this area comprises non-cohesive material with variable depths and long continuous slopes, erosion is extensive.

If the North-Eastern Region were not prone to seismic activity, the Brahmaputra River would have settled into a natural equilibrium capable of managing the annual sediment influx caused by heavy precipitation, steep hill slopes, and the friable nature of rocks. While these factors are relatively stable, deforestation and shifting cultivation can be gradually modified to mitigate their effects. However, earthquakes present a unique challenge. They are unpredictable and can abruptly introduce vast quantities of sediment into the river, as seen after the earthquakes of 1947 and 1950. The river attempts to adjust by pushing sediment downstream, leading to scouring of its bed, especially influenced by tributaries. Despite efforts, some heavier sediment fractions remain, causing the river to appear aggraded, particularly in its upper reaches. Sediment deposition from seismic events persists for decades, significantly affecting flood levels and necessitating careful consideration in the design of engineering structures, unless mitigated by embankments. Understanding the extent of increased water levels during floods is crucial for engineering works along the river.

Throughout its valley, the Brahmaputra River is joined by numerous north bank tributaries that carry excessive silt loads. Some of these tributaries form submarine deltas, which contribute to the southward shifting of the main river channel. This southward movement is especially noticeable in the upper reaches of the Brahmaputra. In the lower reaches of the river, below Guwahati, the Brahmaputra is confined between the inselbergs of the Garo-Khasi massif. In this area, the migration pattern of the river's bank line resembles the propagation of a low-amplitude wave. This pattern is characterized by a rising wave upstream on the north bank, which is matched by a falling wave downstream on the south bank. As a result of this migration pattern, many important villages along the riverbanks have experienced erosion. The continuous shifting of the river's course and the erosion of its banks have presented significant challenges to communities living in these areas, prompting the need for measures to manage and mitigate the impacts of river dynamics on settlements and infrastructure. In addition to its lateral movement, the Brahmaputra River intermittently erodes its banks, causing significant land loss annually. The extent of erosion in the valley fluctuates each year, influenced by flood severity. Following the major earthquake of 1950, erosion intensified due to the increased silt load from hillside landslides. This seismic event disrupted the river's flow regime, particularly in its upper reaches.

The narrowing points in the lower riverbed are a result of the Garo-Khasi massif's inselbergs, which restrict the river channel between them. However, in Upper Assam, these constriction points seem to arise from more resilient bank materials. At these nodes, the river's depth exceeds that of the wider reaches upstream and downstream, allowing for flood discharge accommodation. Upon exiting a nodal point, the river's hydraulic behaviour undergoes changes. There's a noticeable shift in velocity and silt distribution across its cross-section. Consequently, downstream from the node, the river deposits silt in the central portion, fostering the formation of side channels and braiding tendencies. This braiding phenomenon persists with multiple channels until reaching the subsequent nodal point downstream.

In this study, it is seen that major erosion has been occurred at average distance of 100 km whereas deposition has been occurred very less at left or south bank. The erosion is very high in compare to deposition on south bank. Similarly, erosion has been occurred at average distance 50 km whereas deposition is also occurred at average distance of 50 km in right or north bank. The location of erosion and deposition are not same and it is seen that erosion is higher than deposition on north bank. The erosion rate of south bank is more than 10 sq.km per year and erosion rate at north bank is less than 5 sq.km per year in last 40 years.

The grain size distribution, Atterberg's Limits, and soil classification across various riverbank locations in Assam reveal significant sediment variability. Boginodi stands out with the highest sand content (94.20%), while Majuli exhibits a higher silt and clay presence. Soils are classified into SP, SP-SM, ML, and MI groups, with distinct properties observed in Standard Proctor Compaction and Specific Gravity tests. Maximum dry densities range from 1.50 gm/cc to 1.69 gm/cc, and optimum moisture content varies between 12.59% and 22.27%. Coefficients of permeability indicate differences in soil permeability, ranging from 0.00031582 cm/sec to 0.00190749 cm/sec.

Within the braided river context, where multiple channels weave their way through bars of sediment, it is presumed, the composition and stability of bank soil play critical roles in determining the river's behaviour. The cohesion and permeability of bank soil affect its susceptibility to erosion, with softer, less consolidated materials being more prone to rapid degradation under the forces of flowing water. Moreover, the vegetation cover on the banks interacts with the bank soil, stabilizing it through root systems and mitigating erosion rates through the attenuation of flow velocities and the binding of sediments. In Brahmaputra River, characterized by complex channel networks and frequent changes in

channel morphology, bank erosion occurs not only along the main channel banks but also along the margins of secondary channels and bars. The lateral migration of channels, a common phenomenon in Brahmaputra River, leads to the progressive undermining and retreat of the adjacent banks, resulting in the lateral expansion of channels and the creation of new channels as the eroded sediment is redeposited downstream. High flow events, such as floods or sudden channel avulsions, can accelerate bank erosion rates by intensifying the erosive power of the water and mobilizing larger volumes of sediment. From soil characteristic study, it can be concluded that the bank erosion in large alluvial braided river is more dependent on flow pattern and direction in channels and it is not much dependent on bank soil properties where clay or rock is not available. To investigate hydraulic characteristic of the braided river and to suggest management measures for some specific problem areas, Mathematical and physical model study is carried out and presented in the subsequent chapters.

4.

Application of Mathematical Model for Simulating Flow in Braided River

4.1 Introduction

River bathymetry, velocity and morphology can be simulated through hydraulic river model. Saint-Venant equations are commonly used for this purpose. River geometry, flow boundary condition and coefficients are required to put as input information and water elevation and velocity are derived as output from the mathematical model which can be used to solve river engineering problems. The degree of flooding and erosion potential can be inferred from the computed depth of the water or the height of the water surface and from the velocity distribution. For the flow simulation and to have a fair idea about the flood inundation, digital elevation models (DEMs) are a crucial input to hydraulic models. Higher levels of uncertainty are present in coarser resolution DEMs, particularly when recording river-bed bathymetry. Many studies were carried out using freely available DEMs and utilizing the 1D and 2D HEC-RAS modelling techniques.

4.2 Development of Bathymetry

In the present study for preparation of DEM in HEC RAS 2D model, hydrographic survey data are used for the river portion. The hydrographic data used are elaborated in the following para. The Central Water Commission (CWC) though conducts periodic survey in river Brahmaputra, they do it in a coarser scale of around 10Km interval. The bathymetric survey carried out in this study is of finer resolution and the data for the available sections were checked with the CWC data. The data is converted into suitable format, i.e., in XYZ format where X, Y, Z are latitude, longitude and reduced level respectively. Interpolated elevation values are created in GIS platform for preparation of continuous surface of the surveyed area. This DEM is visualized in GIS and compared with ground data. As the cross-section survey is done @ 100 m centre to centre in central 3 km and @ 500 m centre to centre in remaining

portion, there is requirements of data in river bank, char area and area where there is sudden change in elevation. This data is logically interpolated and final DEM of the river portion is prepared. Shuttle Radar Topography Mission (SRTM) DEM is used for the area which is beyond river portion. SRTM data is not accurate but it helps in developing DEM in extended area.

This extended DEM is visualized in HEC RAS 2D software. Software like MIKE, FLOW2D, HEC RAS 2D, BRAHMA 2D are generally used for simulating river flow. All these software have their own advantages and disadvantages. Although BRAHMA model, developed by IIT Guwahati in collaboration with Brahmaputra Board has various advantage of simulating presence of turbulent structure, vegetation, porcupine etc. in the flow field through modification of governing equations, HEC RAS 2D is selected for these studies, because it is freely available and it has very user-friendly GIS tool named RAS Mapper. RAS Mapper has good modification and visualization tools. Also, the objective of the mathematical model study in this research is not to improve the mathematical model by modifying the governing equations or the solution technique, but to apply the model to understand flow pattern. The extended DEM is again overlayed with Google image and here again minor correction of DEM is done with RAS Mapper tool wherever required.

Computation grid of 30 m is formed around the study area except for the area where structure like bridge, abutments, spurs are there. 1.00 m grid is provided where such structures are there. Boundary condition is important factor for simulation of mathematical model study. Flow hydrograph, Stage hydrograph, Rating curve, Normal depth and precipitations are available for boundary condition in HEC RAS software. There are discharge sites at Pandu and Tezpur in river Brahmaputra. The data is confidential and is maintained by Central Water Commission, Government of India. The data were obtained for research project at NEHARI, Brahmaputra Board. The data is analysed and used for upstream boundary condition. The normal depth is used as downstream boundary condition. Mathematical Model Study is conducted in HEC RAS 2D for two reaches of river Brahmaputra with or without proposed dredging channel.

4.2 Survey in River Brahmaputra for the Model Study

The investigation into the typographical and hydrographical features of the Brahmaputra River necessitates the application of a comprehensive and multidisciplinary methodology, aiming to unravel

the intricate dynamics of this extensive watercourse. The exploration of typographical characteristics involves the utilization of terrestrial surveying techniques to meticulously chart the surrounding terrain, delineating elevation shifts, riverbanks, and noteworthy landmarks. This process employs precise data collection tools such as total stations or Global Positioning System (GPS) instruments. Additionally, aerial surveys and satellite imagery contribute essential insights for a more comprehensive understanding. On the hydrographical front, a systematic bathymetric survey is executed to gauge the river's depth and delineate the composition of the riverbed. Specialized sonar equipment, such as echosounders, facilitates the creation of intricate bathymetric maps. Hydrographic surveys utilizing Acoustic Doppler Current Profilers (ADCP) are deployed to scrutinize water flow patterns, velocity, and currents. Geotechnical surveys involve the extraction of soil samples from the riverbed to evaluate the stability of the riverbank. Concurrent environmental monitoring, encompassing ecological surveys, ensures a holistic comprehension of the Brahmaputra's ecosystem. The synthesis of these methodologies, complemented by remote sensing techniques and Geographic Information System (GIS) tools, yields a comprehensive dataset pivotal for judicious decision-making in the realms of infrastructure planning, environmental preservation, and sustainable river management.

4.2.1 Survey of River Brahmaputra in Guwahati Reach for the Model Study

Cross Section survey of river Brahmaputra in a reach of 25 km, from 15 km upstream to 10 km downstream of existing Saraighat Bridge at Guwahati was conducted with the expertise from Waves Tech India, New Delhi.

In order to create a digital elevation model of the reach, a survey is carried out to record the cross-section level and specifics along the river. The actions listed below formed part of the survey:

i) Using Geomax Differential Global Positioning System (DGPS), establish ground control points and GPS along the river.

ii) Level establishment with digital level.

iii) Surveying the riverbank's cross section and detailing the structures there in order to create a strip plan.

The most recent surveying equipment and techniques were used to perform the survey. For horizontal control points, Topcon Digital Levels were utilised, while Geomax DGPS was employed for cross-section and thorough surveys. Topcon Digital Levels were utilised for improved vertical accuracy. Table 4.1 shows the Co-ordinate of control of survey near Guwahati.

Table 4.1 Coordinate of control points for survey near Guwahati

Name	WGS84 Latitude	WGS84 Longitude	Elevation
GPS1	26°10'09.35115"N	91°40'20.55187"E	69.158
GPS2	26°10'17.70884"N	91°41'28.63784"E	52.488
GPS3	26°10'13.23432"N	91°42'53.07576"E	72.403
GPS4	26°10'44.78208"N	91°44'03.81642"E	48.779
GPS5	26°11'43.06493"N	91°45'21.58506"E	52.667
GPS6	26°12'04.05493"N	91°46'55.17032"E	73.893
GPS7	26°12'21.81197"N	91°48'22.26857"E	52.898
GPS8	26°10'00.80285"N	91°39'02.92054"E	47.379
GPS9	26°09'03.26636"N	91°38'06.11208"E	49.099
GPS10	26°08'43.03874"N	91°37'01.25719"E	48.169
GPS11	26°08'29.93463"N	91°35'33.99662"E	47.845

For the Topographic /Cross Section Survey, the Level has been carried out from the CWC Bench Mark (BM) and the details of the Bench mark are shown in Table 4.2.

Table 4. 2 Details of the Bench mark (near Guwahati)

Location	Latitude (N)	Longitude (E)	Elevation (m)
CWC BM	26° 10’ 10.20”	91° 40’ 7.85”	49.99

Figure 4.1 Photographs taken during bathymetry survey near Guwahati

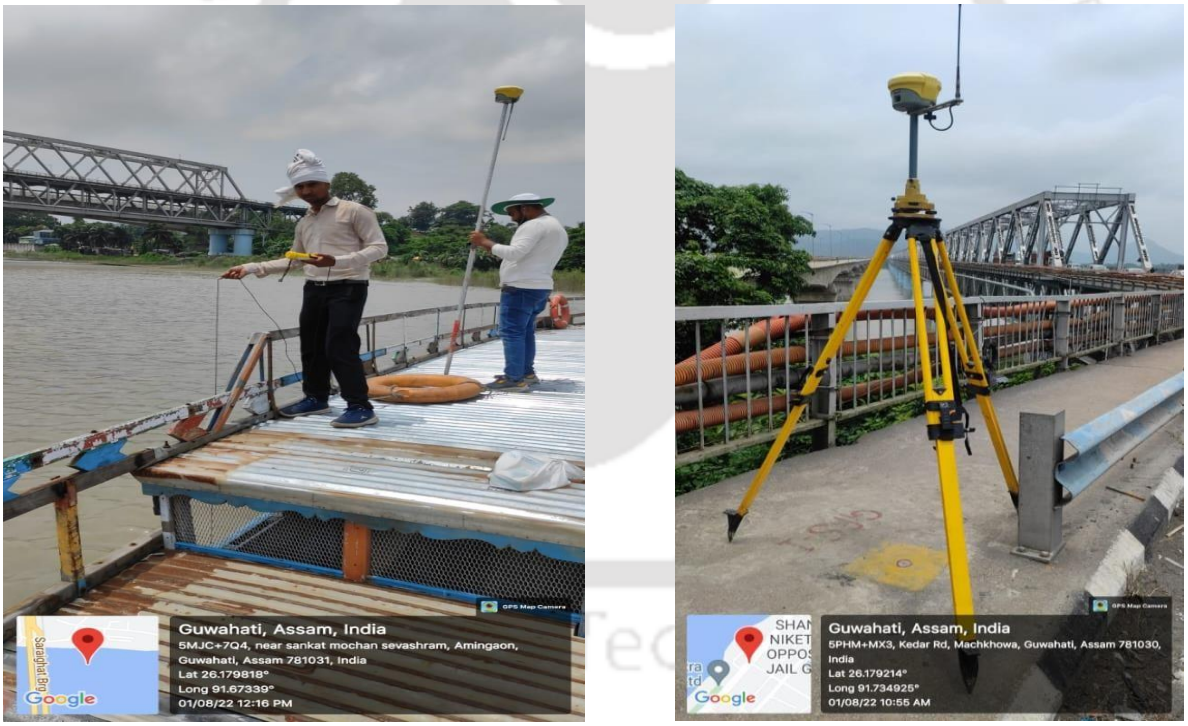

Figure 4.2 Photographs taken during bathymetry survey near Guwahati

A boat was engaged to survey the reach of Brahmaputra River with equipped machineries. Real Time Kinematics (RTK) with 20mm vertically & 10mm horizontally capability and Echo-Sounder were deployed. Echo- Sounder was used to obtain soundings on board the survey launches. A working frequency of 200 KHz was used for sounding operations. The digital output from the echo sounder was fed to the navigation data logging software for acquisition of survey data in real time. The performance of the echo sounder was found to be satisfactory during the entire duration of the survey. Figure 4.1 and Figure 4.2 shows photographs taken during bathymetry survey near Guwahati.

Co-ordinate and R.L. of points in the cross-section are taken once the Ground Control Points are finalised. Throughout this survey, all surface features along the river and 75 different cross-sections with spot levels at 50-meter intervals were determined using DGPS and depth sounders are shown in Figure 4.3.

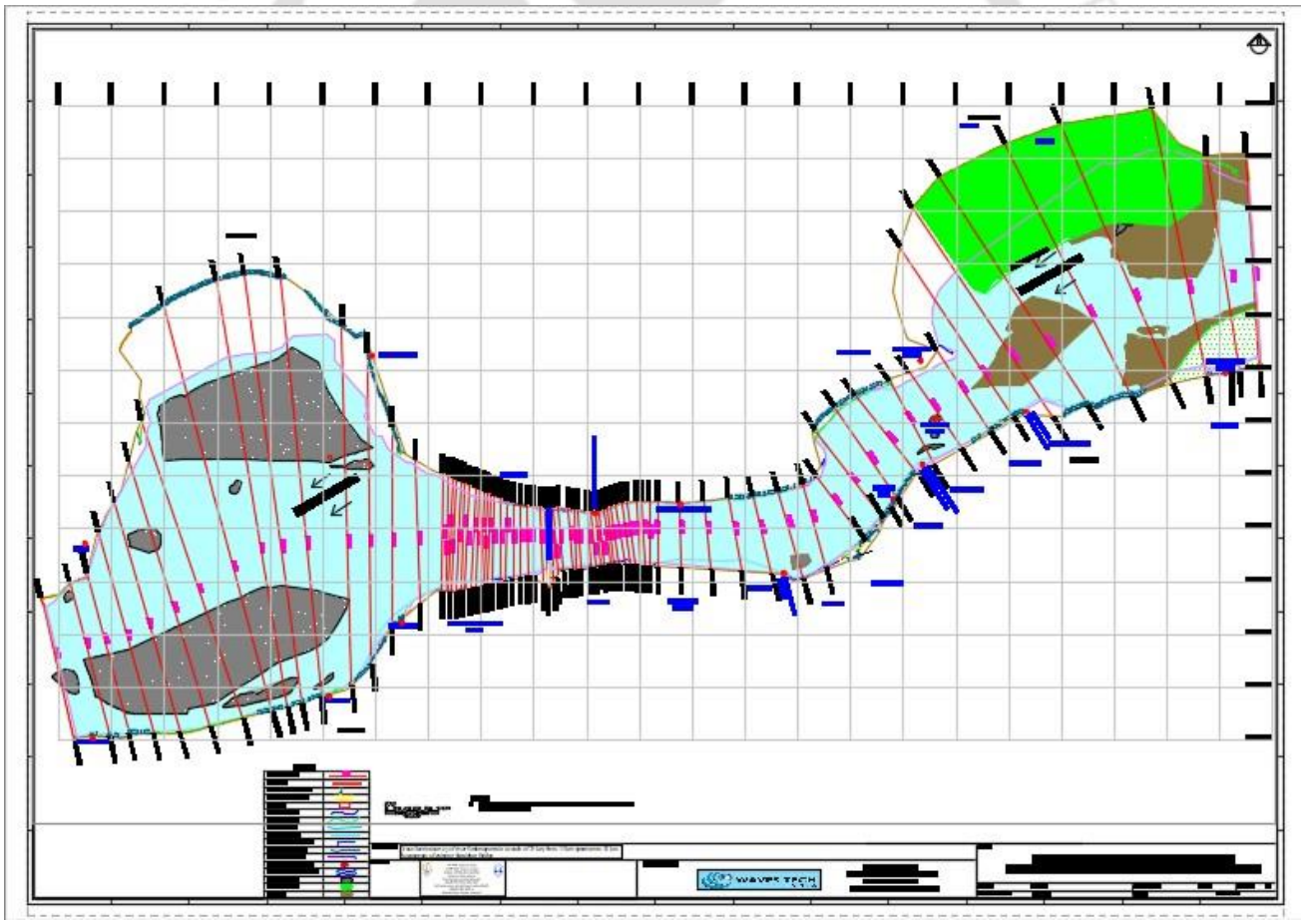

Figure 4.3 Cross Section for survey of river Brahmaputra near Guwahati

4.2.2 Survey Near Tezpur in River Brahmaputra for the Model Study

The Cross Section Survey has been carried out in the river Brahmaputra in a reach of 25 km, from 15 km upstream to 10 km downstream of Kaliabhomora Bridge near Tezpur along with Topography survey with the expertise from Precision Survey Consultancy, Kolkata. For the Topographic /Cross Section Survey, the Level has been carried out from the CWC Bench Mark (BM) and the details of the Bench mark are shown in Table 4.3.

Table 4.3 Details of the Bench mark (near Tezpur)

Location	Latitude (N)	Longitude (E)	Elevation (m)
CWC BM	26°36'41.67"	92°51'16.09"	71.600

Topographical Survey with DGPS: The Topographical Survey and spot levels were acquired through the use of GPS/RTK technology. The topography of the area and restricted visibility in the line of sight made it impossible to employ optical methods to determine spot levels. The GPS/RTK control was expanded in the GPS/RTK spot levelling procedure by employing the height and coordinates of the recovered geodetic station that was installed to different BM in the corresponding stretches. The spot levels of the rover sites were then determined using the Stop-Go technique using these BM as reference stations. Echotrac E-20 ECHO Sounder and Hypack navigation software were used during this survey. Table 4.3 shows the co-ordinate of control points for survey near Tezpur.

Table 4.4 Coordinate of control points for survey near Tezpur			
CP	Latitude	Longitude	Elevation
K-1	26°36'42.394"	92°51'09.801"	84.998
K-2	26°35'08.045"	92°51'43.93"	84.799
K-3	26°34'42.231"	92°53'10.581"	69.845
K-4	26°36'54.285"	92°56'08.679"	67.568
K-5	26°36'38.406"	92°55'50.789"	69.811
K-6	16°51'48.903"	145°12'17.5"	72.800
K-7	26°37'10.452"	92°57'10.369"	69.237
K-8	26°36'36.515"	92°59'44.705"	70.811
K-9	26°35'44.522"	92°59'24.263"	69.247
K-10	26°34'53.401"	93°00'31.595"	68.957
K-11	26°34'47.961"	92°51'16.638"	65.298
K-12	26°33'37.62"	92°50'43.905"	68.479
K-13	26°32'41.133"	92°48'16.601"	65.878
K-14	26°32'45.631"	92°47'39.769"	65.709
K-15	26°37'03.403"	92°50'39.043"	66.899
K-16	26°38'12.073"	92°49'23.976"	68.001
K-17	26°37'12.83"	92°49'23.492"	66.688
K-18	26°36'54.89"	92°48'45.053"	68.599
K-19	26°37'04.16"	92°48'17.777"	69.657
K-20	26°37'02.989"	92°47'11.891"	68.035
K-21	26°37'02.048"	92°46'11.444"	67.153
K-22	26°36'59.478"	92°45'39.618"	66.152

Topographical Survey with Lidar Drone:

Using a LIDAR drone, the forest area's topography has been surveyed. For the survey, Light Detection and Ranging (LiDAR) of Brand: SOUTH, Model: Z-Lab SZT-V100 is utilised. Drone operating at low altitudes is utilised to gather ground data with enough overlaps to create dense 3D point clouds. Using the data processing programme, the topographic data gathered during the fieldwork was processed and scrutinised. The steps and procedure involved in processing digital data are described in the flow chart in Figure 4.4. The Figure 4.5 shows the cross-section for survey near Tezpur and the Figure 4.6 shows the photographs during bathymetry survey near Tezpur.

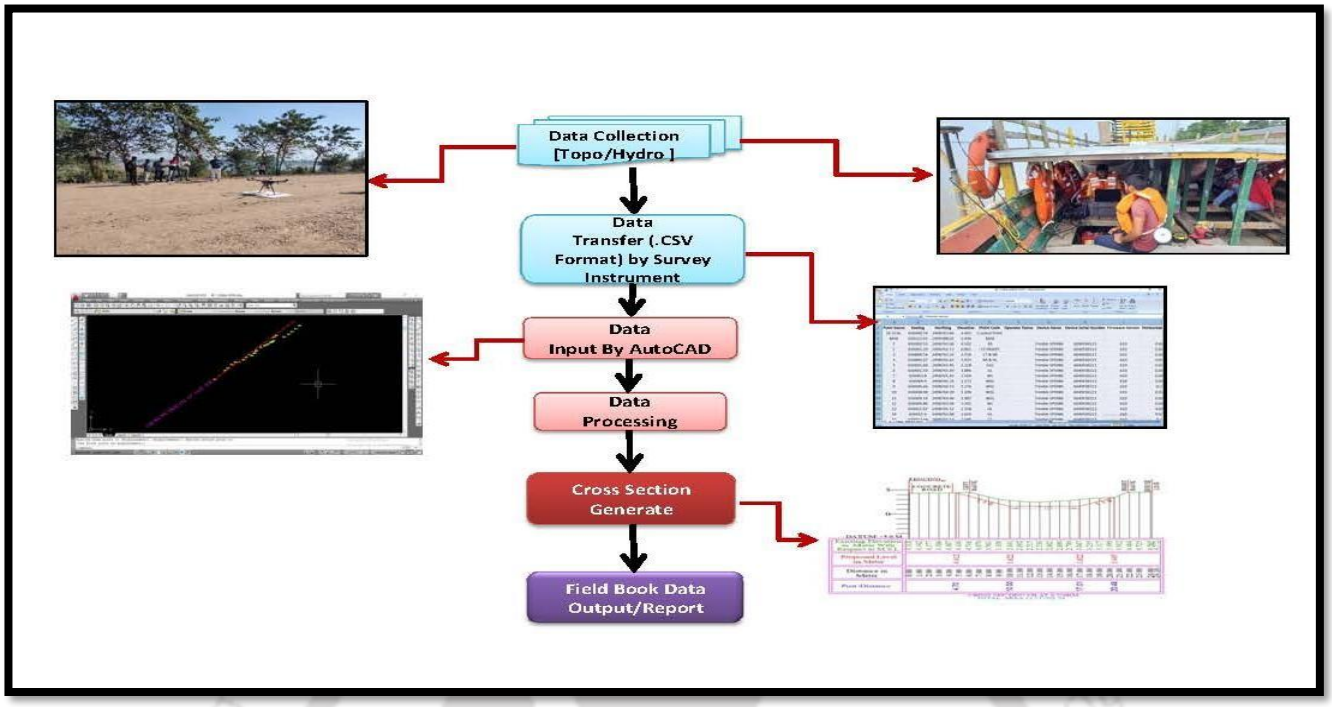

Figure 4.4 Flow chart for survey work at Tezpur

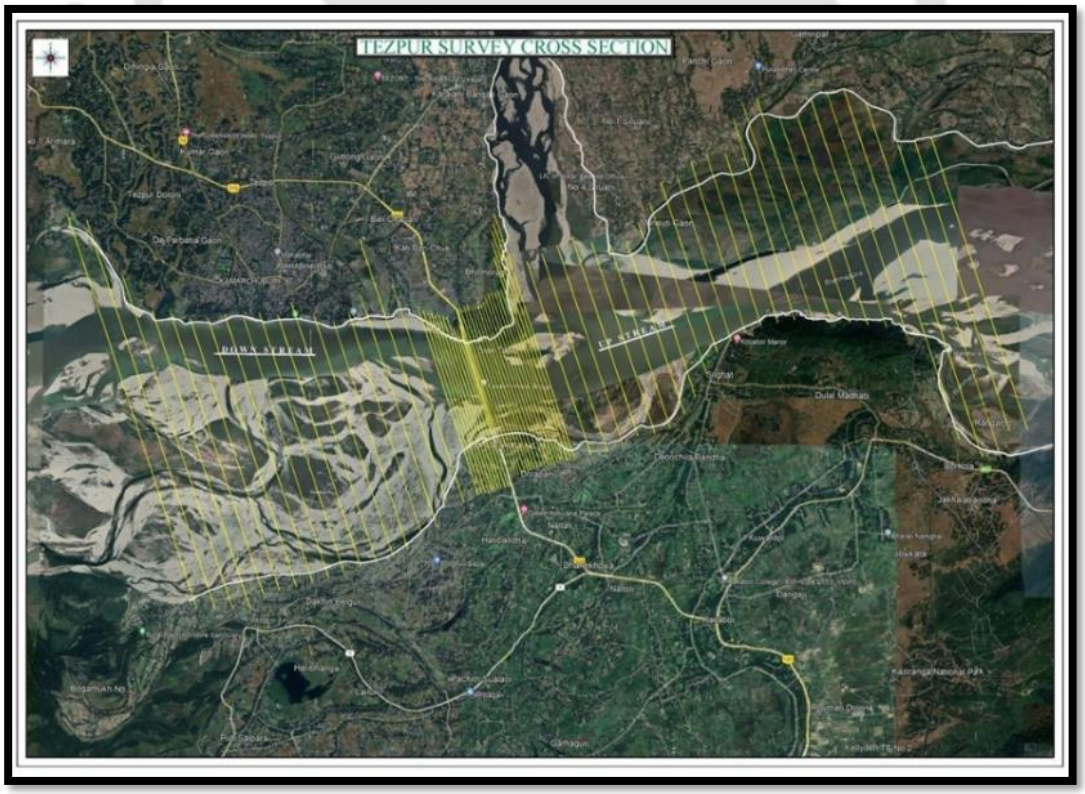

Figure 4.5 Cross-section for survey near Tezpur

Figure 4.6 Photographs taken during bathymetry survey near Tezpur

4.3 Hydrological Data Analysis

Hydrological statistical analysis of the data was carried using the Gumbel method, a pivotal tool in the domain of extreme value analysis, was introduced by Gumbel in 1941, giving rise to what is commonly referred to as Gumbel's distribution. This method involves scrutinizing extreme events, specifically focusing on the largest of the 365 daily flows within a dataset comprising annual flood flows as a series of maximum recorded values. Therefore, in light of the study's context and the conservative nature of Gumbel's method, it is judiciously selected for the determination of extreme values, forming an integral component of the analytical framework in this thesis.

Gumbel's Method –

The extreme value for a return period (T) can be obtained using the following equation.

$$x_T = \bar{x} + K \times Sdv \qquad (4.1)$$

Where,

x_T is the value of variate with a return period T

$\bar{x}$ is the mean of the variate

Sdv is the standard deviation of the sample

K is the frequency factor expressed as $K = (y - y_n)/S_n$

y is the reduced variate expressed as $ln\left\{ln\left[\frac{T}{(T-1)}\right]\right\}$

T is the return period

y_n is the Gumbel's reduced mean variable

S_n is the standard deviation

The regression equations proposed by Onen and Bagatur (2017) are used to obtain the value of y_n and S_n.

$$y_n = 0.5775 \times n^{(-0.66/n)}$$

$$S_n = 1.2811 \times n^{(-1.268/n)}$$

Where n is the amount of data.

4.3.1 Discharge and Water level estimation for Guwahati at different return periods.

The extreme value distribution is applied to obtain the annual maximum flow of the river Pandu gauging stations corresponding to different return periods. The annual maximum flow at the Pandu gauging station corresponding to different return periods is shown as per Table 4.4.

Table 4.5 Maximum flow corresponding to different return periods at Pandu

T	**Max Flow (m^3/sec)**
25	55122
50	59383
75	61859
100	63612

The 100-year flow of the river Brahmaputra at Pandu is 63,612 cumec. As per the information provided by the Water Resources Department of Govt. of Assam, the recorded maximum discharge of the Brahmaputra at Pandu near Guwahati is 72,779 cumec (on 23.08.62), and the minimum discharge is 1757 cumec (on 22.02.63).

The annual mean flow rate at the Pandu gauging station corresponding to different return periods is shown in Table 4.5. The 100-year annual mean flow rate of the river is 25874 cumec.

Table 4.6 Annual mean flow rate corresponding to different return periods at Pandu

T	**Annual mean flow rate (m^3/sec)**
25	22226
50	24057
75	25121
100	25874

As per a report published by Central Water Commission (CWC) and National Remote Sensing Centre (NRSC), the average annual discharge of the river Brahmaputra is 19,820 cumec. (Sarma, 2005) reported the mean annual discharge of the Brahmaputra at Pandu for 1955–1990 is 16,682.24 cumec. As per the information provided by the Water Resources Department of Govt. of Assam, the average annual discharge is about 20,000 cumec. Table 4.6 shows WL corresponding to different return period at Pandu.

Table 4.7 WL corresponding to different return periods at Pandu	
T	**WL (m)**
25	50.019
50	50.374
75	50.581
100	50.728

4.3.2 Discharge estimation for Tezpur at different return periods.

The extreme value distribution is applied to obtain the annual maximum flow of the river at Bhomoraguri gauging stations corresponding to different return periods. The annual maximum flow at the Bhomoraguri gauging station corresponding to different return periods is shown in Table 4.7

Table 4.8 Maximum flow corresponding to different return periods at Bhomoraguri	
T (Year)	Max Flow (m^3/sec)
25	55014
50	59585
75	62241
100	64122

The 100-year flow of the river Brahmaputra at Bhomoraguri is 64,122 cumec. As per the information shown on the website of the Water Resources Department of Govt. of Assam, the recorded maximum discharge of the Brahmaputra at Pandu near Guwahati is 72,779 cumec (on 23.08.62), and the minimum discharge is 1757 cumec (on 22.02.63).

The annual mean flow rate at the Bhomoraguri gauging station corresponding to different return periods is shown in Table 4.8. The 100-year annual mean flow rate of the river is 21835 cumec.

Table 4.9 Annual mean flow rate corresponding to different return periods at Bhomoraguri		
T	**KT**	**Rainfall**
25	2.776968	18647
50	3.500847	20247
75	3.921594	21176
100	4.219382	21835

4.4 Mathematical Model Application

HEC-RAS can perform 2D unsteady simulation using the continuity and momentum equations. For the incompressible flow, the unsteady differential form of the mass conservation equation can be written as

$$\frac{\partial H}{\partial t} + \nabla \cdot hV + q = 0 \quad (4.2)$$

Where, $V = (u, v)$ is the velocity vector, and the differential operator del (∇) is the vector of the partial derivative operator given by $\nabla = \left(\frac{\partial}{\partial x}, \frac{\partial}{\partial y}\right)$, $z(x, y)$ is the bottom surface elevation, $h(x, y, t)$ is the water depth, u, and v are the depth-averaged velocity component in x and y directions, respectively

The vector form of the momentum equation can be written as

$$\frac{\partial V}{\partial t} + V \cdot \nabla V = -g\nabla H + \vartheta_t \nabla^2 V - c_f V + f_k V \quad (4.3)$$

Where, ϑ_t is the horizontal eddy viscosity coefficient, c_f is the bottom friction coefficient, f is the Coriolis parameter, k is the unit vector in the vertical direction. Here every term of the momentum equation has a clear physical counterpart. The term from left to right are unsteady acceleration, convective acceleration, barotropic pressure term, eddy diffusion, bottom friction, and Coriolis term.

The development of computational mesh is an essential part of the mathematical modelling exercise to get accurate results. The mesh is important for modelling both the terrain as well as the water surface flowing over the terrain. Many 2D models use a single elevation for each cell, and finite element models use triangles as mesh shapes to represent the land surface. HEC-RAS, on the other hand, can have cells from three to eight sides, each cell having an elevation volume/area relationship, representing the details of the terrain. For making a proper computational mesh, it is ensured that the cell faces capture the high point of flow barriers considering the water surface slope. If the water surface slope varies rapidly in the domain, smaller cell sizes are recommended to capture the changing water surface and slope.

4.4.1 Development of Mathematical model for the reach in river Brahmaputra near Guwahati

The computational grid was generated for the near bank channel, and input/output to the computational domain from different sub-channels was decided based on the total flow considered for simulation, size of sub-channels, and shape of the bathymetry. The simulation started from an upstream section. The computational grid was generated to cover the entire width of the channel. A grid size of 30m is considered for the main river portion as well as for the floodplain. Figure 4.7 shows the computational grid used for the purpose.

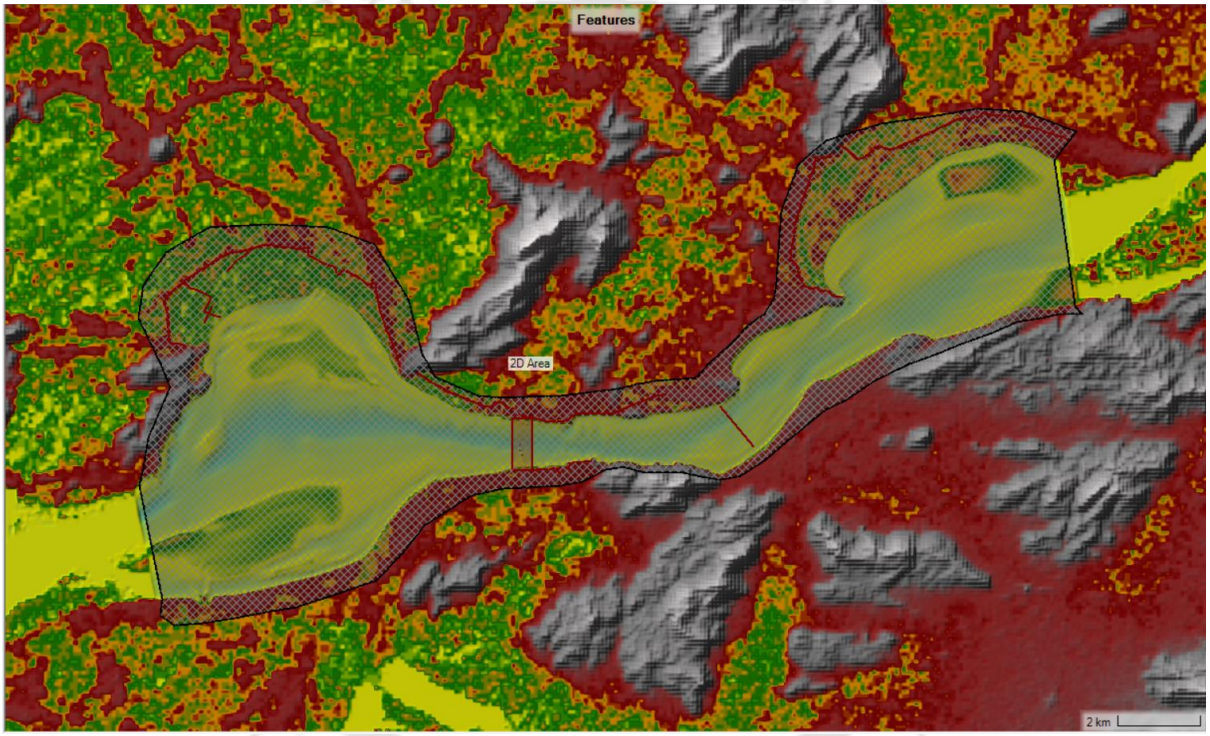

Figure 4.7 Mathematical Model in HEC RAS 2D for a reach near Guwahati

The model is calibrated and validated using the observed data recorded at the Pandu gauging station. One recorded event, as shown in Table 4.9 is considered for validation. The friction slopes downstream and Manning's n value for the river portion are adjusted by minimizing the difference between the simulated and observed water levels at Pandu. Figure 4.8, Figure 4.9, and Figure 4.10 show the steady state water surface elevation map, velocity map, and depth map of the river for 51319.000 m^3/sec. The simulated water level at Pandu is 49.07 m, and the recorded value is 49.14 m. The calibrated Manning's

n value for the river portion is 0.031, and the friction slope value is 0.00008. Manning's n value for the flood plain is 0.050.

Table 4.10 The recorded event at Pandu site considered for validation of the model			
Sl. No.	**Discharge (m^3/sec)**	**WL (m)**	**Date**
1	51319.000	49.14	30/07/84

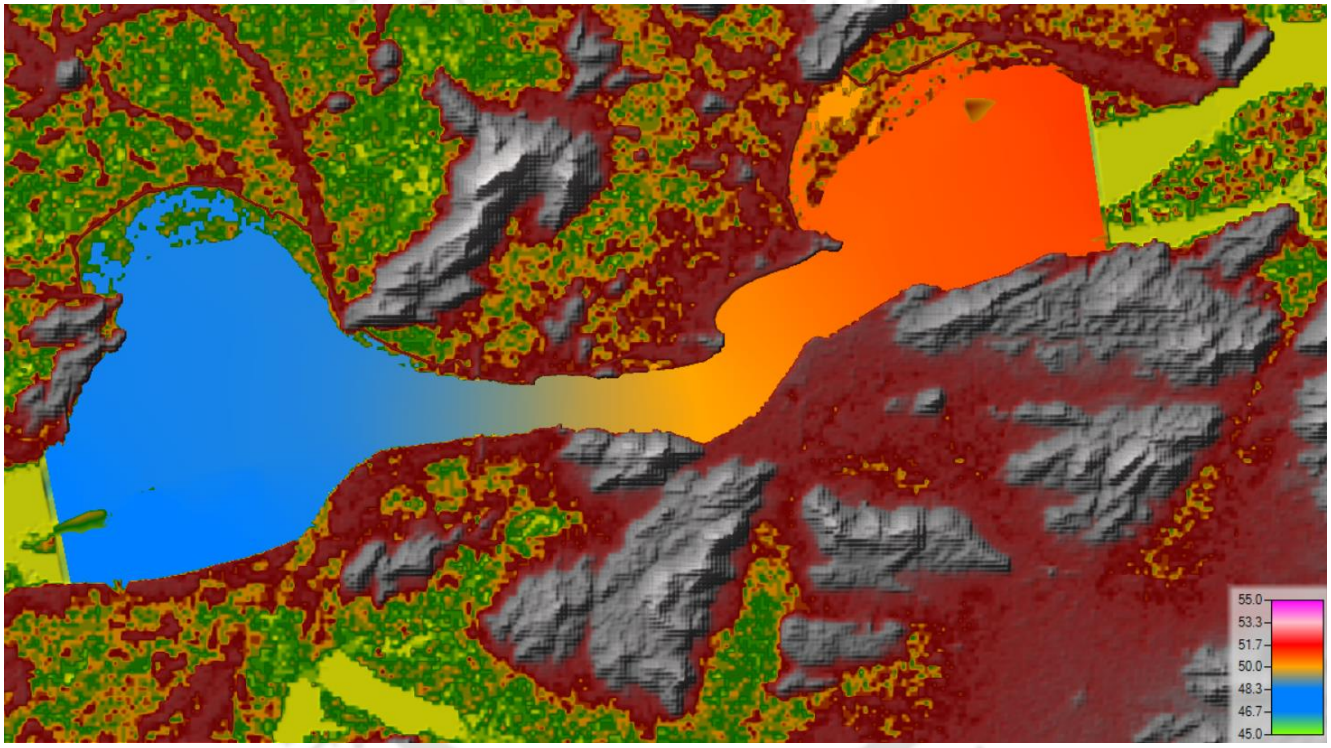

Figure 4.8 Water surface elevation map (For Q=51319.000 m3/sec)

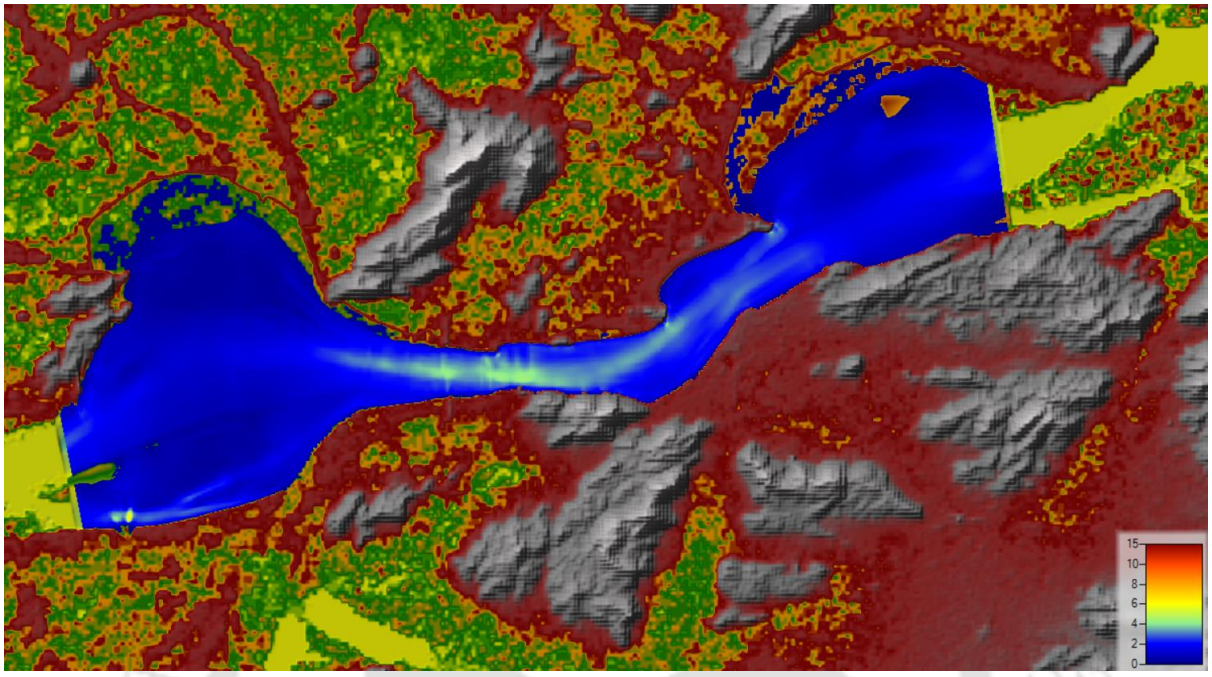

Figure 4.9 Velocity map (For Q=51319.000 m3/sec)

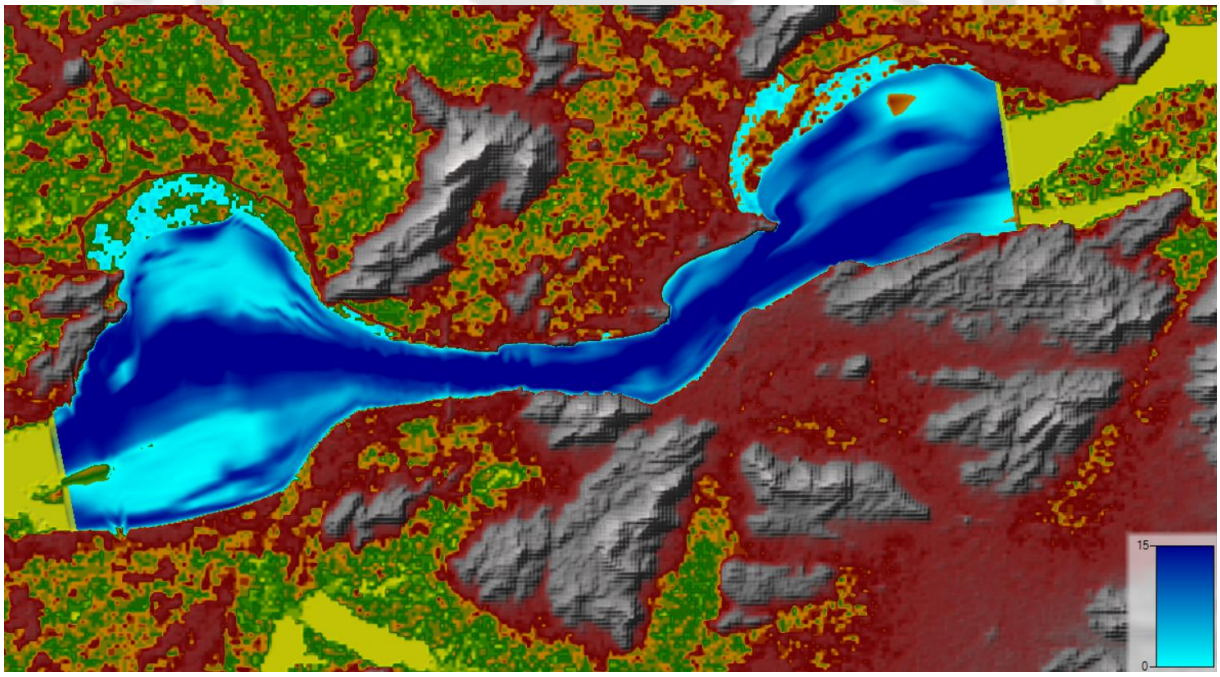

Figure 4.10 Depth map (For Q=51319.000 m3/sec)

4.4.2 Development of Mathematical model for the reach in river Brahmaputra near Tezpur

The computational grid was generated for the near bank channel, and input/output to the computational domain from different sub-channels was decided based on the total flow considered for simulation, size of sub-channels, and shape of the bathymetry. This was possible because the river flows with a major channel along the northern bank in its present form. The simulation started from an upstream section. The computational grid was generated to cover the entire width of the channel. A grid size of 30m is considered for the main river portion as well as for the floodplain.

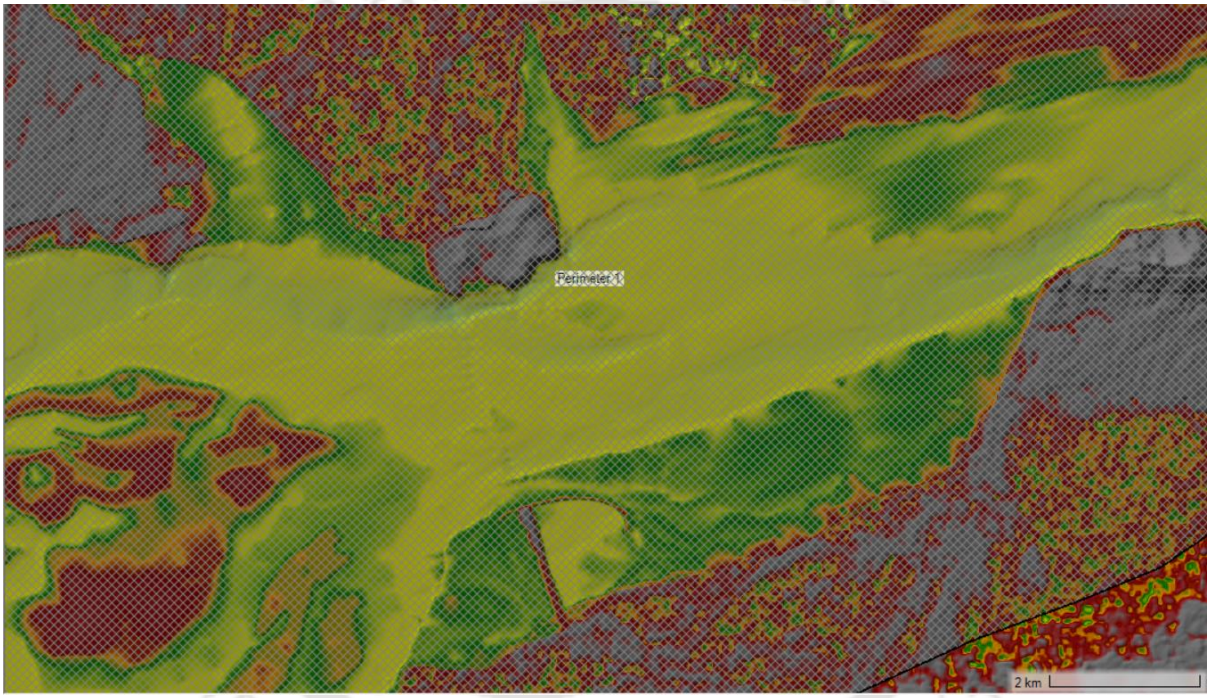

Figure 4.11 Mathematical Model in HEC RAS 2D for a reach near Tezpur

The model is calibrated and validated using the observed data recorded at the Bhomoraguri gauging station. The recorded event has been considered, as shown in Table 4.10. The friction slope at downstream and Manning's *n* value for the river portion are adjusted by minimizing the difference between the simulated and observed water levels at Bhomoraguri. Figure 4.11 shows the mathematical model in HEC RAS 2D for a reach near Tezpur. Figure 4.12, Figure 4.13, and Figure 4.14 shows the steady state water surface elevation map, velocity map, and depth map of the river for 50024.000 m^3/sec. The simulated water level at the Bhomoraguri bridge is 66.16 m, and the recorded value is 66.25 m. The

calibrated Manning's *n* value for the river portion is 0.03, and the friction slope value is 0.0001. Manning's *n* value for the flood plain is 0.06.

Table 4.11 The recorded events at Bhromaguri site considered for validation of the model			
Sl. No.	**Discharge (m^3/sec)**	**WL (m)**	**Date**
1	50024	66.25	21/07/2011

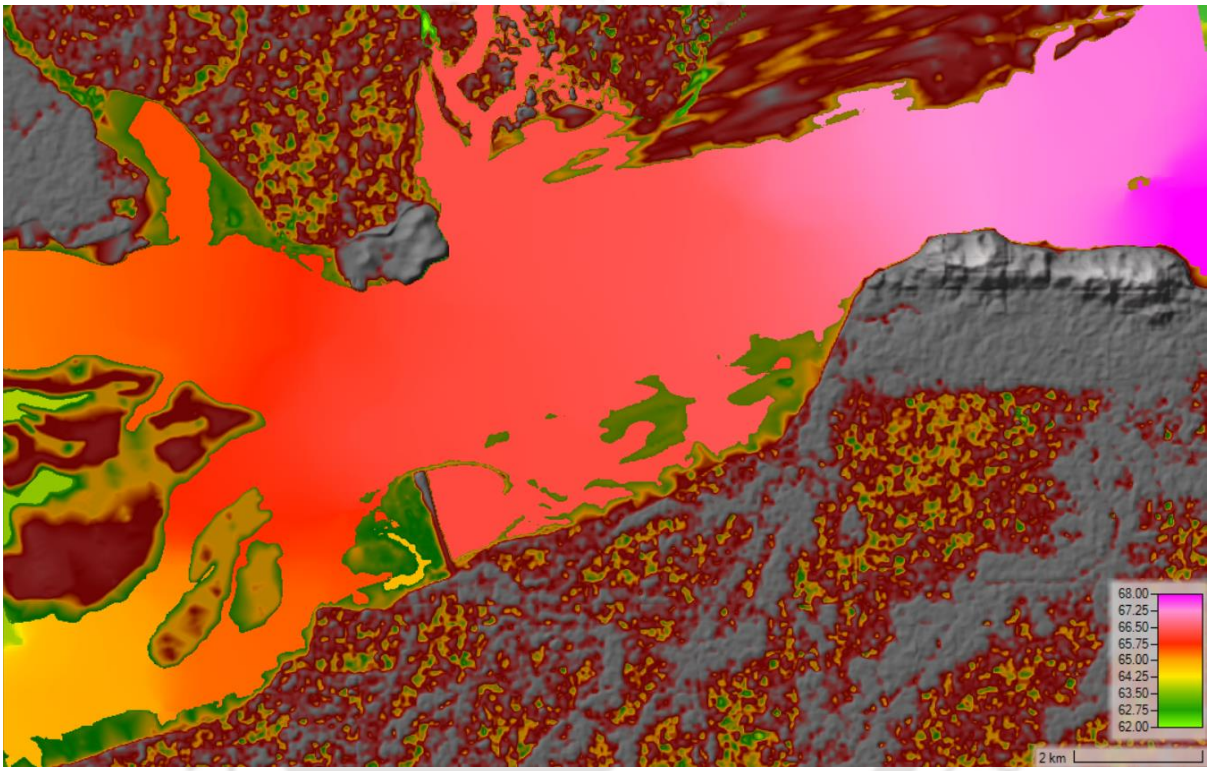

Figure 4.12 Water surface elevation map (For Q=50024 m3/sec)

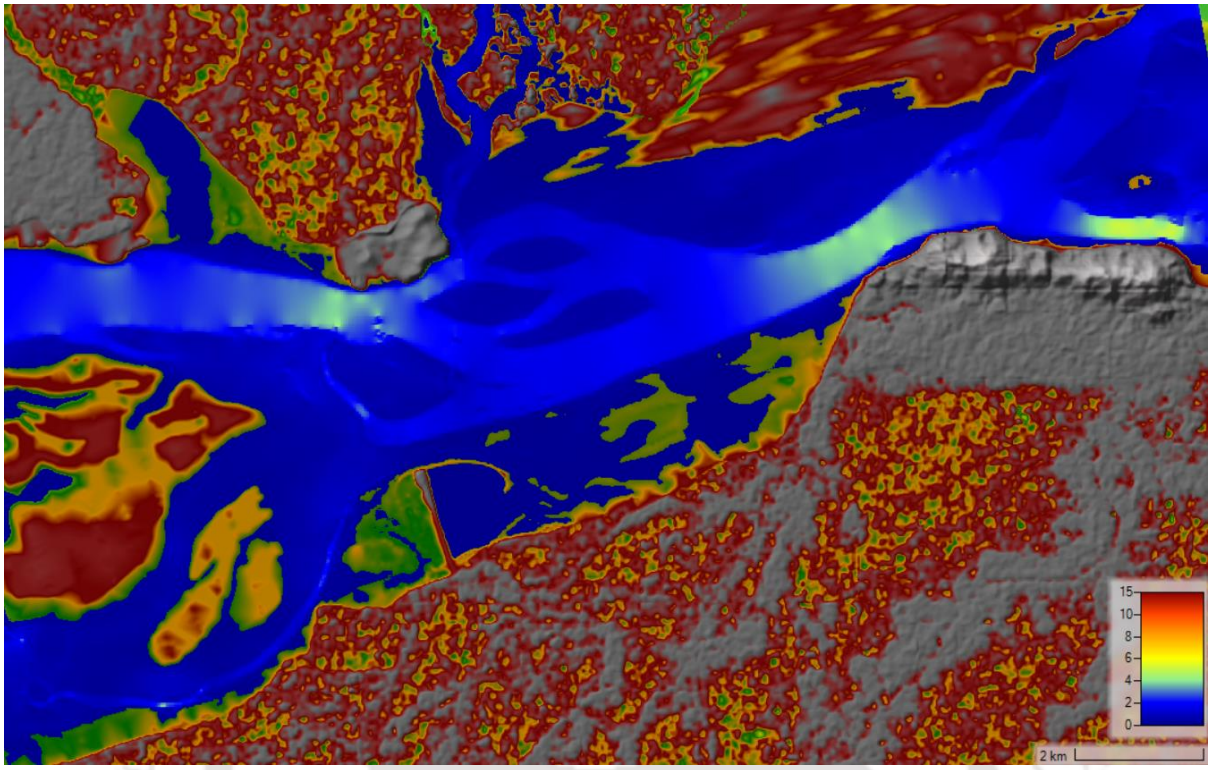

Figure 4.13 Velocity map (For Q=50024 m3/sec)

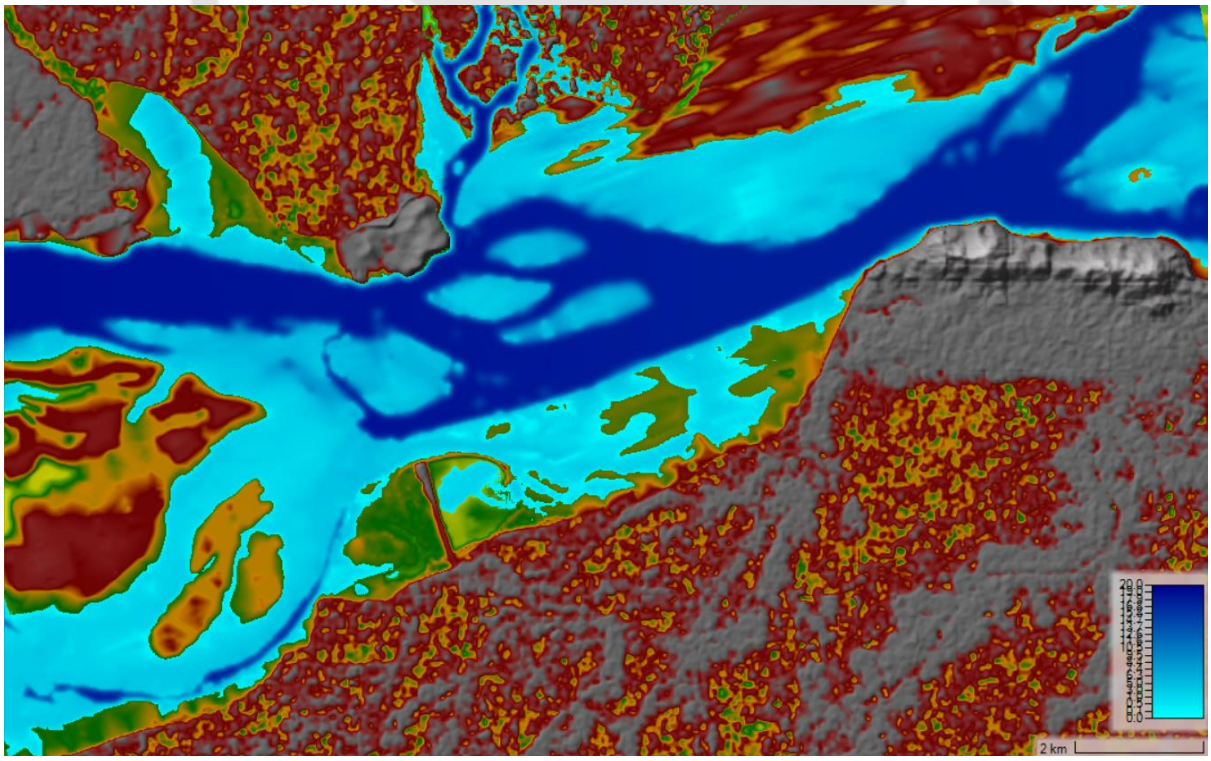

Figure 4.14 Depth map (For Q=50024 m3/sec)

4.5 Model Application for Creation of Dredging Channel and Discussions

The reach where Saraighat bridges were constructed near Guwahati, has constricted with rock out confining the river. The Brahmaputra River has minimum width at this bridge section. The river is widened just downstream of Saraighat bridge. The river is fanning out and has been eroding both North and South Bank. The Government of Assam has implemented anti-erosion work to save Palasbari Gumi area in south bank of river Brahmaputra under Assam integrated flood and River Bank Investment Program. Similarly, A project named 'Anti erosion measures to protect Sualkuchi town from the erosion of river Brahmaputra Ph-V (AS-122)' under Flood Management Programme (FMP) is executed. Another scheme (AS-91) under FMP named "Channelization of river Brahmaputra from downstream of Saraighat bridge is executed". There is still some Bank erosion problem in downstream of Saraighat bridge.

A channel is excavated from cross section number 4 to cross section number 18, covering a distance of 7 km and a width of 350 m. Studies have been done on how river flow changes in different discharges due to excavation of the channel. River flow velocities at different discharge are analysed from the bank to the dredging channel. It comes out that the dredging channel's creation has significantly decreased the flow rate at the bank. Figure 4.15 shows the study in HEC RAS 2D with proposed channel near Guwahati.

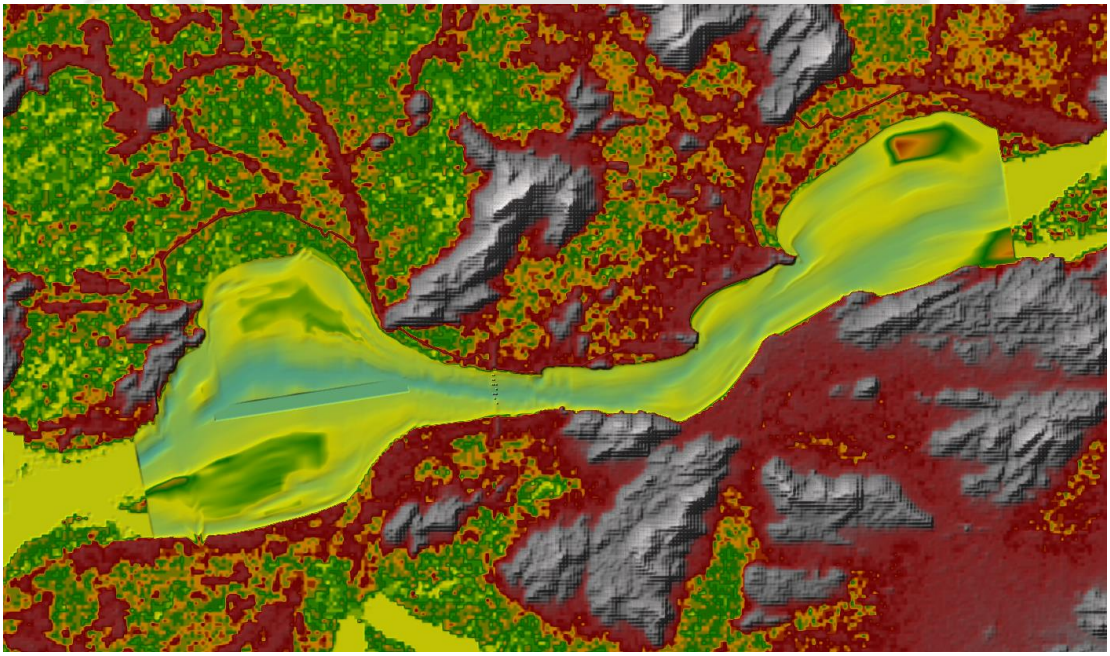

Figure 4.15 Study in HEC RAS 2D with proposed channel near Guwahati

The town of Tezpur is located on the stable north bank of the Brahmaputra River, directly downstream of the Kolia Bhomora bridge. But at South Bank, directly downstream of the bridge, there is a serious issue with river bank erosion. It has been observed that between 1998 and 2014, 1320.78 acres of land were lost due to erosion. Many initiatives were put in place by the Assam Government to safeguard the Bhurbandha location. Under the Flood Management Programme (FMP), a project titled "Protection of Bhurbandha and its adjoining area against the erosion of river Brahmaputra (AS-145)" was just finished in 2019. Building the land spur was the project's primary focus. However, river bank erosion continues to pose a threat to the Bhurbandha region.

A channel of water with a length of 5.5 km and a width of 450 m from cross section number 8 to cross section number 19 is dredged in a 2D mathematical model created in HEC RAS. Studies have been done on how river flow changes along cross section of river. River flow velocities are measured for discharges of 30,000, 40,000, and 50,000 cumec from the bank to the dredging channel. It becomes apparent that the dredging channel's excavation has significantly decreased the velocity at the bank. Figure 4.16 shows the study in HEC RAS 2D with proposed channel near Guwahati.

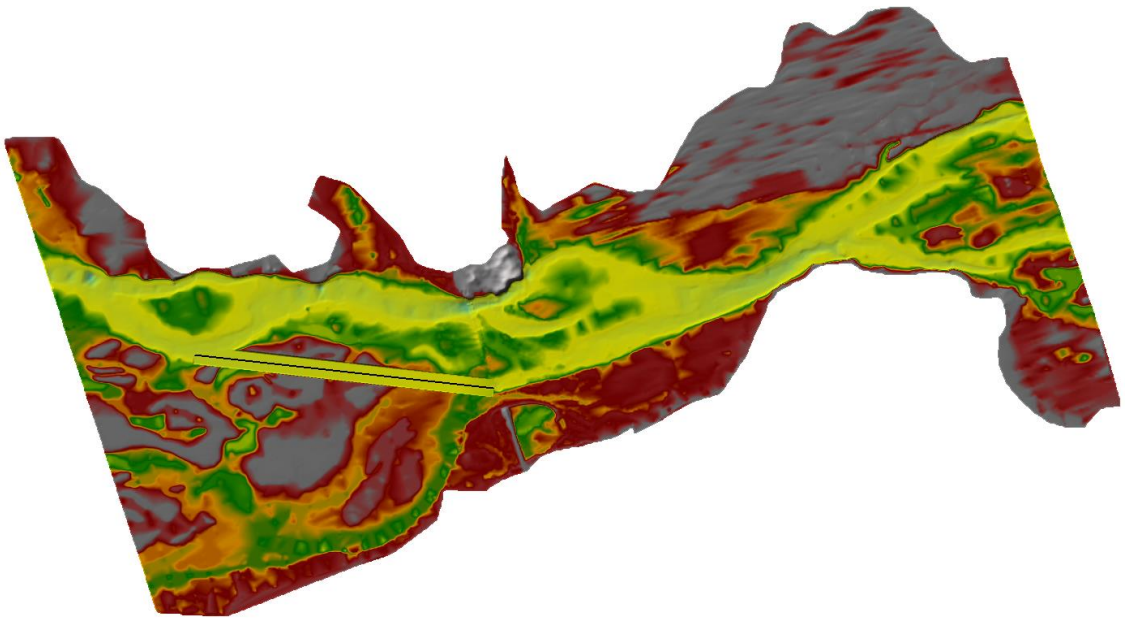

Figure 4.16 Study in HEC RAS 2D with proposed channel near Tezpur

This research undertook a detailed examination of the impacts of dredging on river systems, uncovering noteworthy findings across two crucial dimensions that play a pivotal role in bolstering river resilience and mitigating erosion risks. The first dimension of inquiry revolves around the substantial augmentation of flow capacity facilitated by dredging. This process involves deepening the river channel, providing it with the capability to efficiently manage increased water volumes during periods of heightened discharge. The outcome is a notable reduction in the likelihood of overbank flooding, as the dredged channel acts as a more effective pathway for water flow. This, in turn, mitigates the risk of bank erosion, a common consequence of excess water pressure. The net effect of dredging in this aspect is the establishment of heightened hydraulic stability within the river system, with a strengthened capacity to handle varying water flow conditions.

Moving on to the second integral aspect, the study delves into the considerable contribution of dredging towards the stabilization of channel geometry. This is achieved through the meticulous maintenance of a well-defined channel alignment. Dredging ensures the preservation of the river channel's intended depth, promoting smoother water flow and concurrently reducing erosive forces acting on the riverbanks. Furthermore, the deliberate preservation of a well-defined channel alignment plays a critical role in minimizing lateral migration of the channel, thereby significantly diminishing the associated risk of bank erosion. The findings underscore the pivotal role played by dredging in maintaining the structural integrity and stability of the river channel, with far-reaching implications for the prevention of erosion-related issues.

In amalgamating these two dimensions, the comprehensive interplay of dredging within river management emerges as a multifaceted and strategic intervention. Beyond the immediate hydraulic and geomorphic improvements, dredging incorporates critical measures to fortify riverbanks against potential erosive forces. This study, through its nuanced exploration, endeavours to contribute valuable insights into the intricate dynamics of dredging as a sustainable and effective practice in the realm of river systems management. This study carefully looked at how dredging affects rivers, and we discovered two important things. Firstly, dredging helps rivers handle more water during heavy rains by digging deeper into the riverbed. This prevents water from flooding over the riverbanks and reduces the risk of the banks getting washed away. Secondly, dredging stops the riverbed from building up bed sediments, which keeps the channel in good shape and prevents it from moving sideways. This also makes the water flow smoother. So, in simple terms, dredging makes rivers handle water better, keeps

their shape intact, and safeguards the banks from getting washed away. The Mathematical model study described in this chapter does not account for sediment transport processes, including bedload and suspended load transport. Hence, this limitation restricts their applicability in scenarios where sediment movement is a critical factor, such as in rivers and creating a dredging channel.

Rigid bed models overlook slope stability issues, especially side slope stability and the impact of bed materials on the slope stability of the channel. This limitation is crucial in dredging channel where understanding side slope stability is essential for effective implementation of dredging channel. Due to the absence of sediment transport considerations, this study cannot be used to accurately predict erosion and deposition patterns, limiting its usefulness in assessing changes to the dredging channel bed. Rigid bed models may be less sensitive to changes in flow conditions compared to mobile bed models. This reduced sensitivity can result in less accurate predictions of the system's response to variations in water velocity and discharge. Hence, in engineering projects related to riverbank erosion problem, rigid bed models may offer less comprehensive information for designing structures and interventions, as they do not account for the full range of hydraulic and sediment transport processes. Rigid bed models are less suitable for environments where sediment transport is a dominant factor, such as in large, braided rivers, where the movement of sediment is crucial for understanding channel dynamics.

In the current study, it is imperative to acknowledge certain limitations associated with the mobile bed simulation feature implemented in mathematical models for modelling rivers with sediment transport. One primary concern arises from the use of simplified sediment transport models inherent in mathematical model. While these models offer practical utility, their adequacy in capturing the intricate nature of sediment transport processes within real-world river systems is subject to scrutiny. Additionally, the assumption of steady flow conditions, a fundamental premise for mobile bed simulations, may not fully encapsulate the dynamic and unsteady aspects of sediment transport processes, particularly in the context of rivers undergoing rapid flow regime changes. Another significant limitation pertains to the reliance on accurate bed material data, as the availability and appropriateness of such data directly influence the reliability of the model predictions. As this current study delves into river modelling scenarios, it is essential to navigate these limitations judiciously, considering the necessity for reliable input data and the challenges associated with representing complex sediment transport phenomena.

4.6 Discussion and Conclusion

The comprehensive document titled "Understanding Dredging: Navigating Through Techniques, Environmental Concerns, and Applications" explores the evolution and significance of dredging across various industries, emphasizing objectives such as navigation enhancement, environmental remediation, and mining support (Dredging for Development, 1991). It highlights sustainable practices and the beneficial reuse of dredged materials for land reclamation and landscaping, alongside discussions on equipment types and operational constraints. In managing the Rhine River, projects like the Waal Project have addressed navigation and ecological concerns, emphasizing the importance of sustainable dredging strategies (Smedes et al., 2006). In Bangladesh, dredging plays a vital role in maintaining river navigability and supporting socio-economic development, with government plans focusing on river training and capital dredging (Sultana et al., 2017). Research on the Payra River reveals the environmental impacts of sand dredging and underscores the need for ongoing monitoring and regulated practices. Studies on the Jamuna River examine erosion-sedimentation dynamics and channel morphology changes due to dredging and river training efforts (Mossa and Chen, 2021). Additionally, the Apalachicola River case highlights the geomorphological changes and ecological impacts resulting from poor dredged material placement, stressing the importance of proper spoil management. The Pussur River study underscores challenges with siltation post-dredging and the need for sustainable sediment management practices (Valentine and Wilson, 2022). After reviewing the published literature which was detailed in chapter 2, it is found that there is no such published paper where the model study for dredging in river is done.

Therefore, utilizing HEC RAS, a mathematical model research was conducted to examine the hydraulic behaviour in the river. The study assisted in identifying the best dredging tactics by modelling different dredging scenarios. In order to support decision-making processes for dredging activity in the Brahmaputra River, the study supplied crucial information for creating efficient and sustainable dredging strategies. Bedload and suspended load transport are two sediment transport modes that could not possible to study in the mathematical model of River Brahmaputra. As a result, this restriction limits its applicability in situations where the movement of silt is crucial, like when forming a dredging channel. Because the dynamic interaction between water flow and sediment transport that leads to scour and deposition is not taken into consideration, the rigid bed models used in this study may yield less accurate estimates of scour or deposition in the channel. Rigid bed models disregard the channel's or

watercourse's natural evolution over time for the sake of a fixed, static bed morphology. Therefore, by ignoring the dynamic adaptations that take place in response to changes in flow conditions, sediment movement, and other factors, this study may oversimplify the behaviour of natural channels. Side slope stability and the effect of bed materials on the channel's slope stability are two slope stability issues that rigid bed models ignore. This restriction is significant for dredging channels since a thorough understanding of side slope stability is necessary for the efficient construction of the channel. The lack of sediment transport factors in this study limits its applicability in evaluating the dredging channel bed by making it impossible to forecast patterns of erosion and deposition. As a result, the HEC-RAS study's numerical findings are not presented or compared to those of the physical model study. Physical model studies with mobile beds were carried out in the aforementioned stretches of the Brahmaputra River to better understand the dynamics of the dredging channel's bed. Sand deposition was measured over time in the dredging channel to determine the sediment deposition rate. Also, velocities were compared before and after providing the dredging channel in the physical models.

5.

Study on Sustainability of Dredging Channel in River Brahmaputra in Physical Model

5.1 Introduction

A physical hydraulic model of a river is a scaled-down physical representation of a real river system used for studying and analysing various hydraulic and hydrodynamic aspects of the river's behaviour. This type of model is typically built in a laboratory setting and involves creating a scaled replica of the river channel, including its bed, banks, and surrounding features. Water is then pumped through the model to simulate the flow of the river under different conditions.

The primary purpose of a physical hydraulic model of a river is to better understand how water behaves in the river, especially in response to changes in flow rates, channel geometry, sediment transport, and other factors. Models can be used to assess the impact of constructing bridges, dams, or other structures on the river's flow patterns and sediment dynamics. Due to complexity of flow, sediment transport, erosion and siltation, bridge scour etc., physical modelling is considered as a reliable method to study these processes. Meeting the requirements for hydraulic similitude is a necessary condition to such model studies. This requires equating the ratio of appropriate pairs of forces in both scaled model and prototype that play significant roles in the physical processes.

Physical hydraulic models are mainly of two types:

a) Geometrically Similar Model

When utilising geometrically similar models, all dimensions are reduced to the same scale in any two-dimensional system. When conducting model experiments, one naturally wants to obtain quantitative results regarding flow conditions, velocity, acceleration of the flow force involved, etc. This can be

accomplished by operating the models in a way that yields a closed dynamic similarity, which is only achievable when geometrically similar models are utilised. Spillway model is an example of Geometrically similar model.

b) Distorted Model

The models wherein the vertical scale differs from horizontal scale and is always bigger. The distorted models are helpful for improving river training procedures determining bank erosion and safeguarding bridges over alluvial rivers. When exact similitude is no possible, distortion is allowed. Accuracy in vertical measurement will have to be compromised by using a small depth scale. Hydraulic forces are so greatly reduced when the prototype's dimensions are reduced that bed motions cannot be accurately simulated in the model unless very large models are employed, which is typically unfeasible due to cost, limited space, and water supply considerations. Typically, the scale must be distorted in order to provide sufficient bed movement. Vertically exaggerated models can be Rigid model or Moveable bed model.

Dynamic Similarity of Physical Model

The basic equation controlling all hydraulic parameters is Newton's Second Law of Motion. The dimensionless number known as Newton's Number can be used to represent this law.

Inertia force $F_i = M \times A$ (5.1)

Where F_i = inertia force

M = Mass

A= Acceleration

Writing $M = \rho L^3$

Where ρ is the density and L is leaner dimension

Hence $F_{ir} = \rho r L_r^3 \times L_r / T_r^2 = \rho r L_r^2 \times V_r^2$ (5.2)

The suffix to refer to the model prototype ratio

Thus $F_{ir} / \rho L_r^2 x V_r^2 = 1$ (5.3)

$F_i/\rho L^2 V^2$ is a dimensionless Number which is the ratio of Inertia force to resistive force and known as Newton Number.

For Hydraulic Models, $F_{ir} = F_{gr}$, where F_{gr} represents the ratio of the forces imposed on the liquid mass by gravity

$F_g = mg = W = \Upsilon L^3$ where $\Upsilon = \rho g$

Hence $F_{gr} = \Upsilon_r L_r^3$ (5.4)

But according to equation 5.3, $F_{ir} = \rho r L_r^2 x V_r^2$

Hence, $F_{ir}/F_{gr} = \rho r L_r^2 x V_r^2 / \Upsilon_r L_r^3 = 1$ (5.5)

Or, $\rho L_r^2 x V_r^2 / \rho_r g_r L_r^3 = V_r^2 / g_r L_r = 1$ (5.6)

Since $g_r = 1$ $V_r = L_r^{½}$

$L_r / T_r = L_r^{½}$

Or, $T_r = L_r^{½}$ (5.7)

The type of river for the experiments are to be conducted determines the scale to be used. In general, there may be two kinds: shallow and wide rivers or deep and narrow rivers. The former often transport "heavy loads" and have steep slopes in relation to their discharges. However, the later have high banks, which suggest a continuous flow, a small bed load and a significant amount of suspended silt charge. While determining scale ratios, it is necessary to take into account variations that exist between these extremes.

Longitudinal Scale is determined from considerations of discharge and space available. The scale selected should be such that the widths of channels are adequate to fit in the model area. Similarly for experiments to study structure for river training works, model discharges, corresponding to the design discharges in the prototype, with which study is to be carried out, should be available. From the following formula, the depth scale may be estimated:

Maning's Law: $V_r = 1/n_r D_r^{2/3} Sr^{½}$ (5.8)

Or $V_r = 1/n_r D_r^{2/3} D_r^{1/2} / L_r^{½}$ (5.9)

Or $V_r = 1/n_r D_r^{2/3} D_r^{1/2} / L_r^{½}$ (5.10)

If $n_r = 1$ & $V_r = D_r^{½}$

Hence $D_r^{½} = D_r^{2/3} D_r^{1/2} / L_r^{½}$ (5.11)

Hence $L_r^{½} = D_r^{2/3}$ (5.12)

Or $D_r = L_r^{¾}$ (5.13)

However, the depth scale should be fixed so that sufficient tractive force wds is available for the bed materials used in the model. Thus, the depth scale has to be fixed in conjunction with the slope scale; this aspect is described below. The scale should be determined in order to obtain a sufficiently high Reynolds' number and thus ensure turbulent flow in the model for the lowest discharge.

The Karman number: $R_k = K \sqrt{\frac{gRS}{U}}$

Where, $\sqrt{gRS}$ = shear velocity $= \sqrt{\tau_c}/p$

K = height of equivalent sand roughness, and V = kinematic viscosity, indicates the state of turbulence in the model. Its value should be greater than 50 to 60 for roughness of the sand grain- type, to ensure turbulent flow in the model.

The Lacey formulae $S = 0.542\ f^{5/3}/Q^{1/6}$ is sometimes used to determine slope scale. However, the formula takes in to account only the grade of the materials, but does not guarantee bed movement for the grade adopted. It does not, therefore, yield satisfactory results.

There are two broad types of rivers: wide, shallow and steep as against narrow and deep rivers. Vertical exaggeration of models of rivers in the first category is required to be greater than that of models of rivers in the second category, which have generally flatter slopes, to ensure proper depth and turbulence. However, a higher vertical exaggeration, accentuates the initially steep slopes of model of wide and shallow rivers, causing intense bed movement. On the contrary, the vertical exaggeration permissible in models of deep and narrow rivers is small; likewise, is the slope exaggeration (which equals in this case, the vertical exaggeration) which results in unsatisfactory bed movement.

Discharge Scale

Models are operated according to Froude's relationship; velocity scale = $(\text{depth scale})^{1/2}$, and hence the discharge scale equals $LD^{1.5}$

The discharge scale can also be derived from Manning's formula. If the cross-sections are shallow enough to permit substitution of depth for the hydraulic mean depth,

$$L^{1/2} \text{ X } d^{13/6}/n.$$

Another method is to adjust the discharge scale by trial and error. Water is introduced in to the model so as to reproduce certain known prototype gauges. The ratio of actual discharge of the prototype to the model discharge, capable of reproducing known prototype gauges, gives the discharge scale. However, the method is tentative.

Choice of Material

Sufficient bed movement is the criterion deciding the choice of materials, so that bed configuration is properly simulated. Bed materials should move in the model at the stage corresponding to which active bed movement exists in the prototype. Grade reduced to model dimensions would be excessively fine and float on the water surface due to surface tension. Moreover, fineness of grade brings in cohesiveness & higher velocities would be required to move such materials.

The relation between threshold velocities and material sizes are available. For material between 0.15 and 0.35 mm. in diameter, velocity required for movement is least. For finer materials, higher velocities are required. It is, therefore, desirable that material used in the model should fall within this range. Where velocities in models are not enough to move sand on bed, lighter materials are used as bed material. Pure saw dust, when used floats in water and to some extent, it can simulate suspended load. But as soon as it becomes wet, it slowly sinks forming in to a lump. This is due to the action of fungus. To prevent fungal action, the saw dust is treated with 1 per cent solution of copper sulphate which corrects this tendency. Coal dust from collieries is of an average specific gravity, of 1.4 to 1.5 and serves as an excellent bed material. The main objection against using coal dust is that it does not give a uniform size of material. Polystyrene is a by-product of synthetic rubber and of specific gravity 1.05 and is used in Europe. This material also is costly for a large-scale use. Plexiglas or plastic sand of specific gravity 1.18 is popular in Europe. Its cost prohibits its used on a large scale. Theoretically, the time scale is equal to $L/\sqrt{D}$. Model discharge stages are based on the nature of the hydrograph; duration of each run is determined according to the theoretical time scale and adjustments are made by trial and

error. Generally, low discharges have to be run in the model for a longer time and higher discharges for a shorter time than that worked out theoretically, so that scouring is not exaggerated and prototype conditions are reproduced in the model.

Determination of sand particle size for the physical model study:

Within the intricate process of determining channel "n" values, meticulous attention is warranted for two primary factors. Firstly, the characteristics of the materials forming the bed and banks of the channel play a pivotal role. Secondly, the channel's distinctive shape is a critical consideration. Cowan's devised methodology intricately assesses the impact of these factors on deriving the appropriate "n" value for a given channel.

The calculation of "n" involves a comprehensive breakdown:

1. "nb" (Base Value): This represents the fundamental value for a straight, uniform, and smooth channel within natural materials.
2. "n1" (Surface Irregularities Correction): A correction factor accounting for the influence of surface irregularities on the channel.
3. "n2" (Cross-Sectional Shape and Size): This value encapsulates the variations in both the shape and size of the channel's cross-section.
4. "n3" (Obstruction Impact): This factor incorporates the effects of obstructions within the channel.
5. "n4" (Vegetation and Flow Conditions): Addressing the impact of vegetation and the prevailing flow conditions on the channel.
6. "m" (Meandering Correction Factor): This correction factor accounts for the meandering tendencies of the channel.

   By comprehensively considering these components, the formula for "n" takes shape as follows:

   $n=(nb+n1+n2+n3+n4) \times m$

This thorough examination and breakdown of factors contribute to a nuanced understanding of the intricate dynamics influencing the determination of channel "n" values in the context of our sand particle size investigation for the physical model study.

The value of the hydraulic radius ratio (R_r) does not been any fixed relation to the length and depth scale but various with the shape of the cross-section. Then for any given reach, the "R_r" and the "L_r" are known and Manning's "Nr" can be compiled and applied to the prototype "n" to obtain the required value of "n" for the model.

Determination of "n" for model

$$V_r = \frac{1}{n_r} R^{2/3} S_r^{1/2} \quad (5.14)$$

$$S_r^{1/2} = \frac{n_r^2 \times V_r^2}{(R_r)\,4/3} \quad (5.15)$$

$$S_r = \frac{n_r^2 \times V_r^2}{(R_r)\,4/3} \quad (5.16)$$

Slope scale ratio (S_r) $= \frac{D_r}{L_r} = \frac{n_r^2 \times V_r^2}{(R_r)\,4/3}$ (5.17)

$$= \frac{D_r}{L_r} = \frac{n_r^2 \times D_r}{(R_r)\,4/3} \quad (5.18)$$

$$\therefore n_r^2 = \frac{(R_r)\,4/3 \times D_r}{D_r \times L_r} \quad (5.19)$$

$$n_r = \frac{(R_r)2/3}{(L_r)½} = \frac{(R_r)2/3}{(L_r)½} \quad (5.20)$$

$$\therefore n_m = n_p \times \frac{(R_r)2/3}{(L_r)1/2} \quad (5.21)$$

n_m = Roughness Co-efficient in model

n_p = Roughness Co- efficient in prototype

Where, $V_r = \sqrt{D_r}$

(Velocity scale $= \sqrt{D_r}$)

$\therefore V_r^2 = D_r$

and $R_r \approx D_r$

$$n_r = \frac{n_m}{n_p}$$

$$\therefore n_m = n_r \times n_p \quad (5.22)$$

The calculation of mobile bed design for incipient motion involves determining the critical shear stress or critical velocity required to initiate sediment transport in a river or water channel. Incipient motion is the point at which the forces applied by flowing water are just sufficient to move sediment particles

from the bed. The Shields criterion is commonly used for calculating the critical shear stress for incipient motion. The Shields parameter (also known as the dimensionless shear stress) is expressed as:

$$\tau*=(\rho s-\rho)gD\tau \quad (5.23)$$

where:

- $\tau*$ is the Shields parameter (dimensionless shear stress),
- τ is the shear stress exerted by the flow on the bed,
- ρs is the density of sediment particles,
- ρ is the density of water,
- g is the acceleration due to gravity,
- D is the median particle diameter of the sediment.

The Shields parameter at incipient motion, denoted as τc, is the critical value that initiates sediment transport. This critical value is typically determined experimentally for different sediment types and conditions.

The Shields criterion is a fundamental concept used to predict the onset of sediment motion in a flow. The graphical representation of the Shields criterion features the Shields parameter (τ*) on the y-axis and the ratio of shear stress to particle weight on the x-axis. This visual presentation illustrates the relationship between flow dynamics and sediment properties. To apply the criterion, one must first determine the properties of the sediment, such as the density of sediment particles (ρs) and the median particle diameter (D). Next, calculate the shear stress (τ) exerted by the flow on the bed, which is influenced by flow conditions, channel geometry, and water velocity distribution. Then, calculate the Shields parameter (τ*) using the formula: τ* = τ / ((ρs - ρ) * g * D), where τ is the shear stress, ρs is the sediment density, ρ is the fluid density, g is the acceleration due to gravity, and D is the median particle diameter. Finally, compare the calculated Shields parameter (τ*) with the critical Shields parameter (τc) for incipient motion. If τ* exceeds τc, sediment transport is likely to occur, indicating that the flow has the potential to mobilize sediment particles. This comparison is essential for understanding sediment transport dynamics in natural and engineered water systems.

Requirements of Field Data for River Model Experiments:

Central Board of Irrigation and Power published Requirements of Field Data for River Model Experiments in the publication No. 204 named River Behaviour Management and Training.

The requirement of data for conducting model study are as follows:

1. Report including details of the problem, its history and probable, previous remedial measures, Photos depicting behaviour of the river during floods, Geotechnical description etc.
2. Survey Data including Index plan, Survey plan, Cross-section at suitable intervals, Plan showing contours or spot level over the spill area with contour interval varying from 0.3 m in case of flat terrain to 1.5 m for steep country, details of existing and proposed structures like bridges, dams, weirs, barrages, spurs, revetments. Latitudes and longitudes should be market also on this plan.
3. Hydraulic Data including Daily gauge and discharge data at all existing sites for one or more flood seasons. Data of existing discharge site for preparation of gauge discharge curve. If no discharge site exists, it should be established.
4. Geo-technical Data including grain size distribution and mean diameter of bed and bank material. Suspended silt Samples should be collected at medium and high flood stages at 0.5 or 0.6 depth.
5. Other Data including calculation regarding afflux, waterway design, designed maximum flood, maximum scour, detailed drawings of piers, abutments, etc, and their foundations and detailed designs and drawings of guide bunds in case of constricted bridges.

5.2 Laboratory Setup and Equipment used for study

All pertinent laboratory examinations were executed within Model Tray at the North Eastern Hydraulic and Allied Research Institute (NEHARI). Within an 80m X 45m model tray, a dynamic riverbed model was meticulously developed. The upstream discharge for the model was induced through a twin rectangular weir, with the flow meticulously regulated by control gates. A pump with a maximum capacity of 20 cusecs facilitated the water supply to the weirs. The system allowed for water recirculation through interconnected canals and tanks strategically positioned along the periphery of the model trays. Figure 5.1 shows an aerial view of hydraulic model tray and Figure 5.2 shows twin rectangular weir at hydraulic laboratory.

Figure 5.1 An Aerial View of Hydraulic Models Tray

Figure 5.2 Twin rectangular weir at Hydraulic Laboratory

Measurement of Velocity

Current Meter

A device known as a current meter is employed to gauge the speed of water currents in rivers, oceans, and other water bodies. In NEHARI's Hydraulic Laboratory, there is a mechanical current meter in place.

Mechanical current meters typically comprise a rotor or impeller immersed in the water flow. As water flows past this rotor, it induces its rotation. The rate at which the rotor spins correspond directly to the speed of the water current. The meter is adjusted to convert the rotational speed of the rotor into a velocity measurement. For assessing discharge in laboratory and river models, NEHARI possesses an OTT C2 small current meter. This meter has the capability to mechanically measure dependable flow velocities ranging from 0.025 to 5m/s with an accuracy level of ±2%. Figure 5.3 shows a photograph of propeller type velocity meter. Figure 5.3 shows the photograph of propeller type velocity meter.

Figure 5.3 Photo of Propeller type Velocity Meter

Acoustic Doppler Velocity Meter

An Acoustic Doppler Velocity meter (ADV) stands as a specialized tool employed for gauging water velocity within rivers, oceans, and various aquatic settings. It relies on Doppler shift principles for precisely ascertaining water current velocities. The primary aim of ADVs is to deliver finely detailed velocity measurements at specific points. ADV devices come with several benefits, including their ability to provide high-resolution readings, disturb the water flow minimally, and capture intricate variations in velocity. Researchers, environmental monitors, and hydrology investigators routinely make use of ADVs to gain deeper insights into fluid dynamics. Figure 5.4 shows the photograph of Acoustic Doppler Velocity meter (ADV).

Figure 5.4 Photo of Acoustic Doppler Velocity meter (ADV)

Gauge Measurement

A gauge scale is mounted via fixed bar of channel section to measure the water surface elevation of model accurately. Reading from gauge scale can be converted to prototype (real) water surface elevation using vertical scale of model adopted. Figure 5.5 shows the photograph of gauge scale.

Figure 5.5 Photo of Gauge Scale

5.2.1 Development of Physical Model of River Brahmaputra in Reach near Guwahati

A movable bed physical hydraulic model of river Brahmaputra was constructed in Model tray -I of NEHARI, adopting a section of 25km stretch of river Brahmaputra i.e., 15km upstream and 10km downstream of existing Saraighat bridge section thus producing 75 cross-sections. Figure 5.6 shows the plan of model survey data

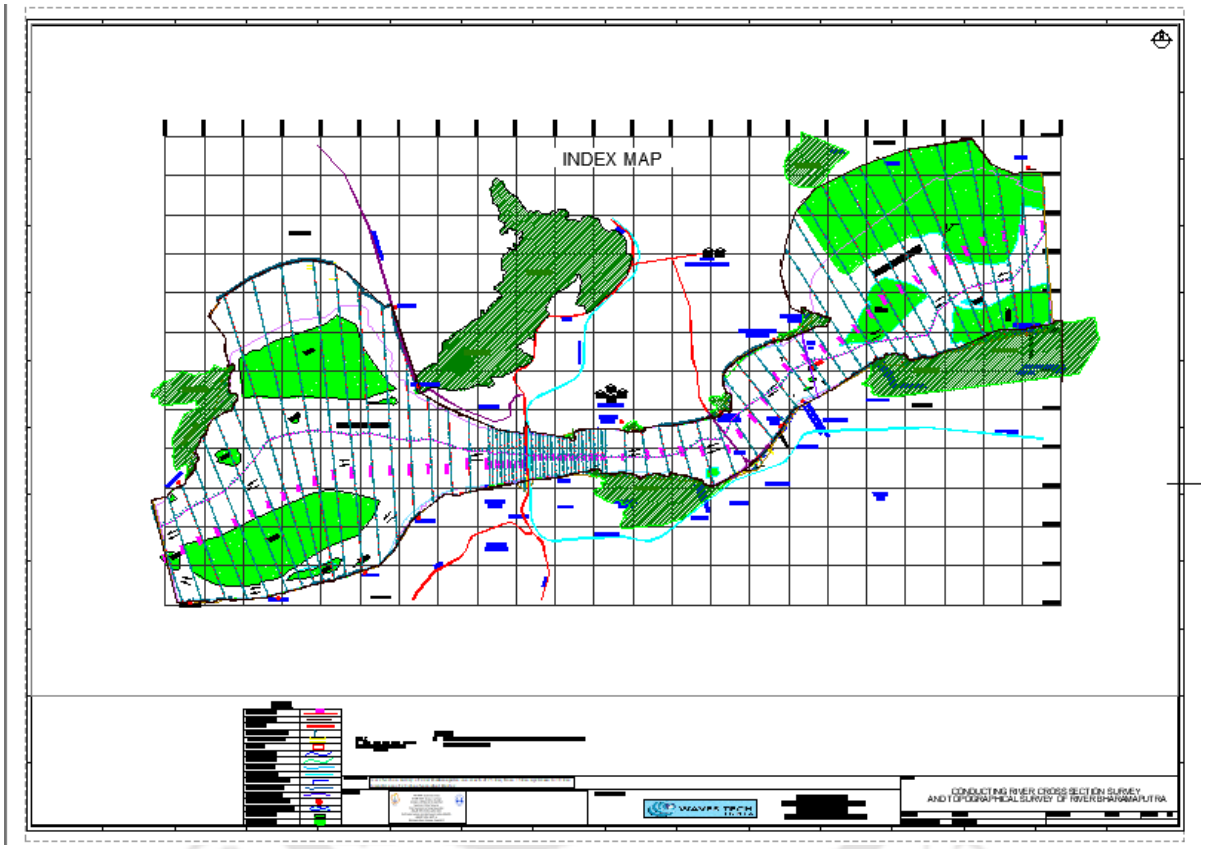

Figure 5.6 Plan of Model Survey Data

The cross-section data available through river Bathymetric survey is then plotted by adopting a suitable scale in physical hydraulic model tray i.e. in a lab-controlled environment. The sand of riverbed is then moulded appropriately at every cross-section to reflect real-world profile of riverbed of prototype. Figure 5.7 shows the plan of model prior to run i.e. at dry state and Figure 5.8 shows a photo of the model at the run.

Figure 5.7 A Photo of Model prior to run (Dry State)

Figure 5.8 A Photo of Model at the Run

Froude number similarity was used to design the model and distorted model was adopted due to a large aspect ratio of width and depth of flow.

Generally, open channel flows are modelled based on Froude number similitude, since gravitational forces are the predominant driving forces

$$Froudian\ Model\ Similarity \quad \left(\frac{v}{\sqrt{gy}}\right) Model = \left(\frac{v}{\sqrt{gy}}\right) Prototype \tag{5.24}$$

A total length of 25 km of the Brahmaputra River from 15km upstream of the Saraighat bridge to 10 km downstream was modelled. Piers of existing and the proposed bridge were produced in the model. Figure 5.9 shows the plan of the model tray in Auto-CAD.

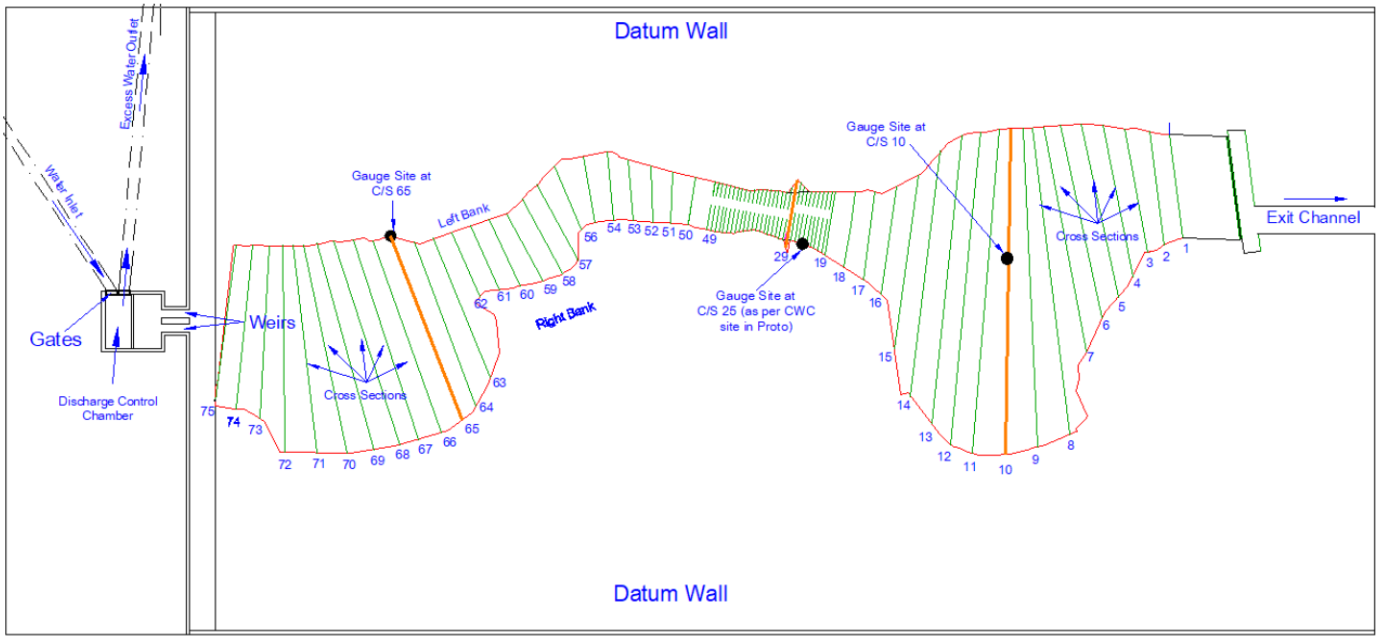

Figure 5.9 Plan of model tray Auto-CAD

Table 5.1 Model parameters of Physical Model of River Brahmaputra in Reach near Guwahati		
Sr. No.	**Model Parameter**	**Values**
1.	Horizontal Scale (Xr)	1: 350
2.	Vertical Scale (Zr)	1: 70
3.	Velocity Scale	$1: 70^{0.5} = 1: 8.366$
4.	Discharge Scale	$1: 350*70*70^{0.5} = 1:204981.70$
5.	Distorted Ratio	350/70 = 5.00
6.	Hydraulic Time Scale	$Xr/Zr^{0.5} = 1: 41.86$

Table 5.1 shows the model parameters of physical model of river Brahmaputra in reach near Guwahati. Model scales are selected such that model size is appropriate and ensuring that the model Reynolds number is large enough to make the flow turbulent and possibly fully rough at the smallest test flows.

Modelling

Riverbed in Model

A movable bed river model is a type of physical hydraulic model that specifically focuses on simulating the movement of sediment (sand, gravel, etc.) within a river system. In natural rivers, sediment transport plays a crucial role in shaping the river channel, influencing erosion and deposition patterns, and affecting the overall morphology of the riverbed and banks. A movable bed river model is designed to replicate these sediment transport processes in a controlled laboratory environment. The model can be used to study how changes in flow velocity and direction lead to scour (erosion of the bed) at specific locations, such as around bridge piers or bends in the river. A movable riverbed was designed in the physical hydraulic model using shields graph and Shield's Criteria for incipient motion for designing model. D_{50} of sand in prototype from laboratory analysis of soil sample at NEHARI = 0.168mm. Figure 5.10 shows the soil grading curve for prototype riverbed.

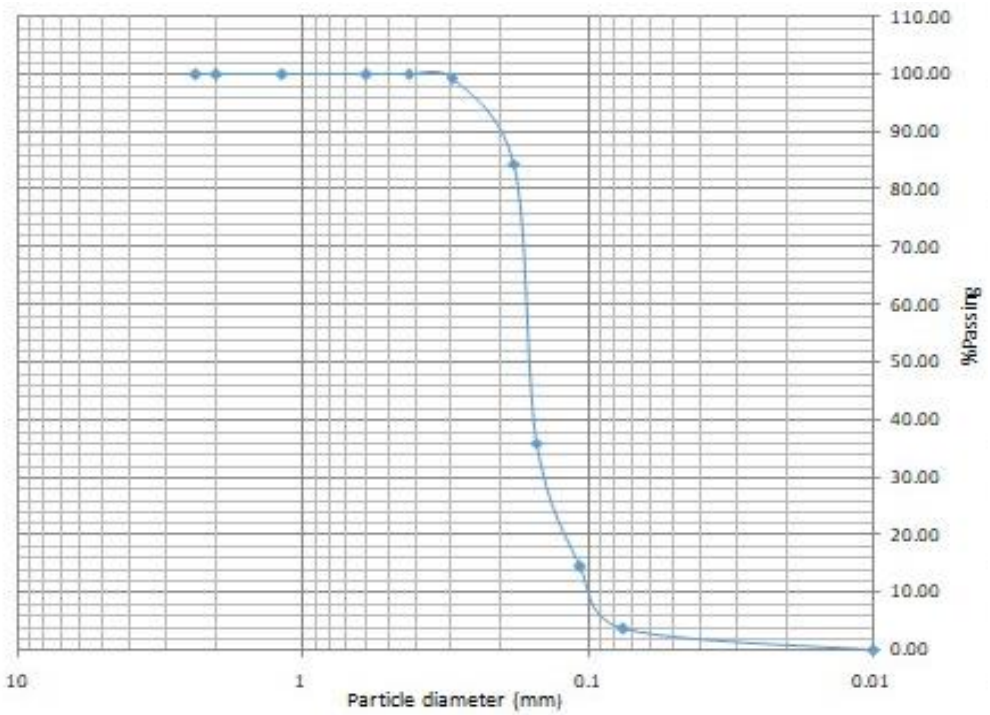

Figure 5.10 Soil Grading Curve for Prototype Riverbed.

Following Parameters Corresponding to Prototype in Bridge Section are calculated based upon mathematical model analysis -

1. Hydraulic Radius R = A/P = 8.98m

2. Reynolds no. of prototype Flow = 6.05 X 107 hence flow is sufficiently turbulent.

3. Prototype Tractive Stress = 94.34 N/m2

4. Shear Velocity u*= 0.378 m/s

5. Grain Reynolds no. Re* = 60.56

Following Parameters Corresponding to Model based upon scale conversion are Calculated-

1. Velocity in Model = 6.74/8.366 = 0.805 m/s

2. Model hydraulic radius (Mean Depth) (m) ~ Calculated using Manning Velocity equation = 0.11939m

3. Shear Velocity = 0.079 m/s

5. Model Tractive Stress = 6.27 N/m2

6. Reynolds No. of Model flow = 9.63 x 104 (Sufficiently Turbulent)

Movable bed design:

Using Shield's Criteria for incipient motion for designing model. Figure 5.11 shows the shield incipient motion graph.

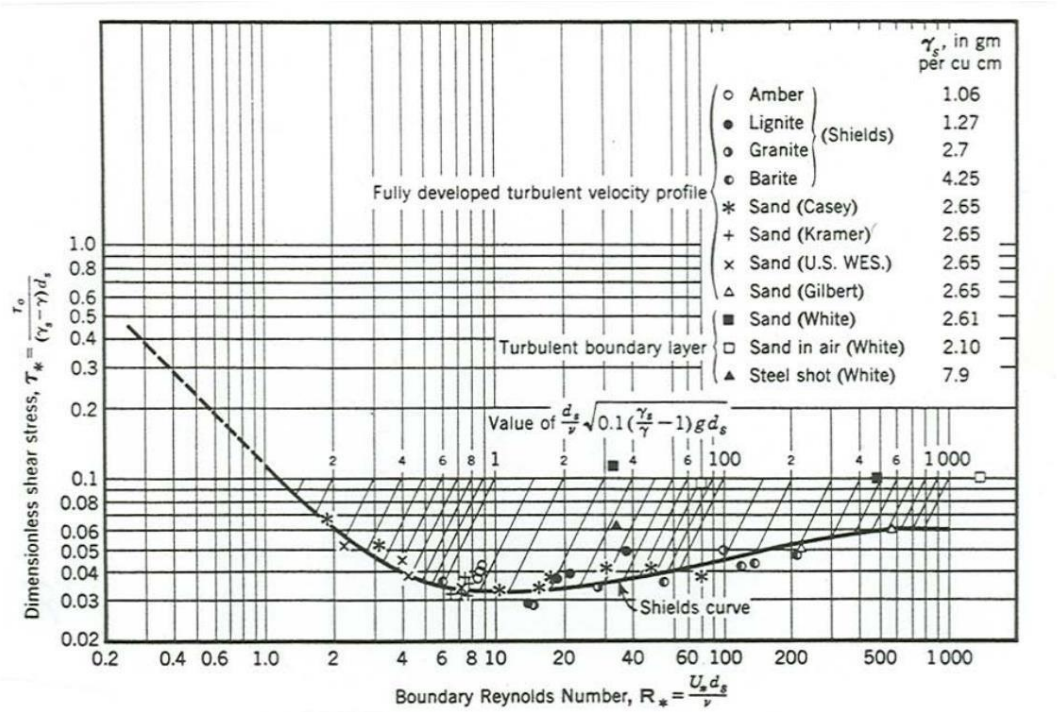

Figure 5.11 Shield Incipient Motion Graph.

A Brief description of Graph-

Region below the Shield's Curve shows no incipient motion occurs in particle of riverbed, while points lying above the curve shows the occurrence of incipient motion.

Dimensionless Shear Stress used for Shield's design is given as-

$$\Theta = \tau^* = \tau o / (ys\text{-}yw)\, d_{50} \qquad (5.25)$$

Where, τo is tractive stress, it can be seen since in our prototype (in Saraighat stretch of River Brahmaputra) Re* = 60.56 hence Dimensionless shear Stress that lies on shield's curve is approximately 0.04, hence tractive stress corresponding to this dimensionless shear stress can be called as Critical Tractive Stress.

Critical tractive Stress in Prototype = 0.1056N/m2, now since Tractive stress in Prototype = 94.34 N/m2 > Critical tractive Stress in Prototype = 0.1056 N/m2, hence incipient motion occurs in prototype.

Movable bed design for Physical Hydraulic Model: -

Let us assume a Dimensionless Shear Stress greater than already present in prototype (0.04), let us assume this to be 0.06, now since critical tractive stress increases as dimensionless shear stress increases hence it can be said a safety is adopted in design consideration.

Therefore, for available grain sizes of sand particle to be used in our model, critical shear stress can be calculated using equation: -

$$\Theta = \tau^* = \tau c / (y - yw)\, d_{50} \qquad (5.26)$$

Where $\Theta = 0.06$ is adopted for design consideration Using $\Theta = 0.06$, gives us freedom to use $2 < Re^* < 400$, since as evident using shield's curve this is domain for incipient motion.

Let us consider different D_{50} and calculate critical shear stress corresponding to $\Theta = 0.06$

D_{50} in Model riverbed (mm)	Critical tractive stress corresponding to $\Theta = 0.06$
0.10	0.099 N/m2
0.15	0.1485 N/m2
0.20	0.198 N/m2
0.25	0.2475 N/m2
0.30	0.297 N/m2
0.35	0.3465 N/m2

Now Since, Model Tractive Stress τo = 6.27 N/m2

It can be seen that all particle 0.10 mm < d50 < 0.35 mm satisfy, criteria for incipient motion to occur (τc < τo) and appropriate factor of safety is being provided corresponding to all these diameter range for bed movement to occur. Figure 5.12 shows soil grading curve of model sand.

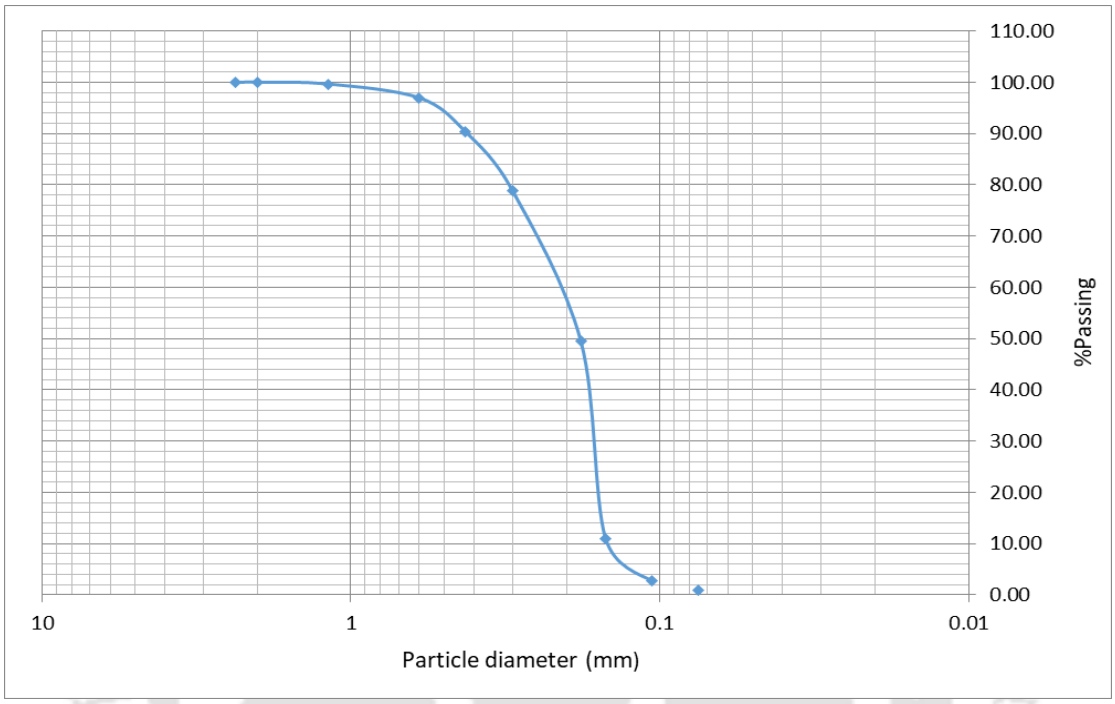

Figure 5.12 Soil Grading Curve of Model Sand

A Stage-discharge curve of river Brahmaputra for Pandu-GDS site was plotted using data received from CWC. Water level of the station at different discharges were obtained form that curve. Physical model was run at constant (steady) discharge and water level corresponding to discharge obtained through G-D curve, were maintained in model by regulating downstream shutter gates. Since Pandu-GDS site lies adjacent to C/s no. 25 of study, hence a gauge was installed at C/s no. 25 of model for validation purpose i.e.to satisfy boundary conditions and additional gauges were installed at C/s no.11 and 62 for satisfactory validation. Flow was said to be stabilized if, at known constant discharge and corresponding gauge at C/s 25, expected water levels are recorded in model at C/s no. 62 and 11 i.e., upstream, and downstream of bridge. These cross-sections are shown in Figure 5.9.

The gauge reading was stabilized after seven cycles of run and re-moulding. The water level as observed in model was found in agreement with prototype. Hence the area of interest was said to be reproduced fully. Figure 5.13 shows Gauge – Discharge Curve for Pandu GDS.

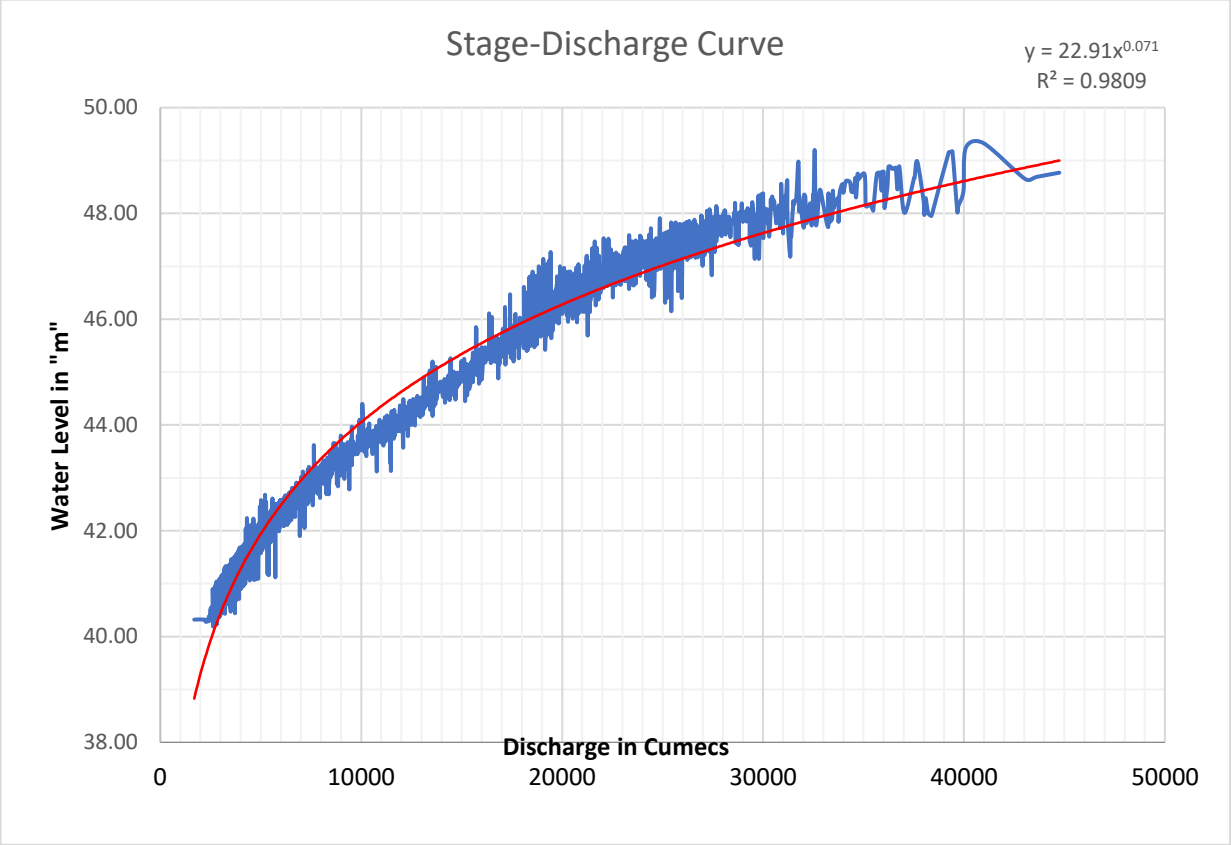

Figure 5.13 Gauge – Discharge Curve for Pandu GDS

5.2.2 Development of Physical Model Study of River Brahmaputra in Reach near Tezpur

In the case of Tezpur stretch of the Brahmaputra River, at NEHARI a movable bed physical hydraulic model was constructed in Model Tray-II. This model replicated a 25km section of the river, including 15km upstream and 10km downstream of the existing Kaliabhomora Bridge, resulting in 75 cross-sectional representations. Figure 5.14 shows the plan of model survey data.

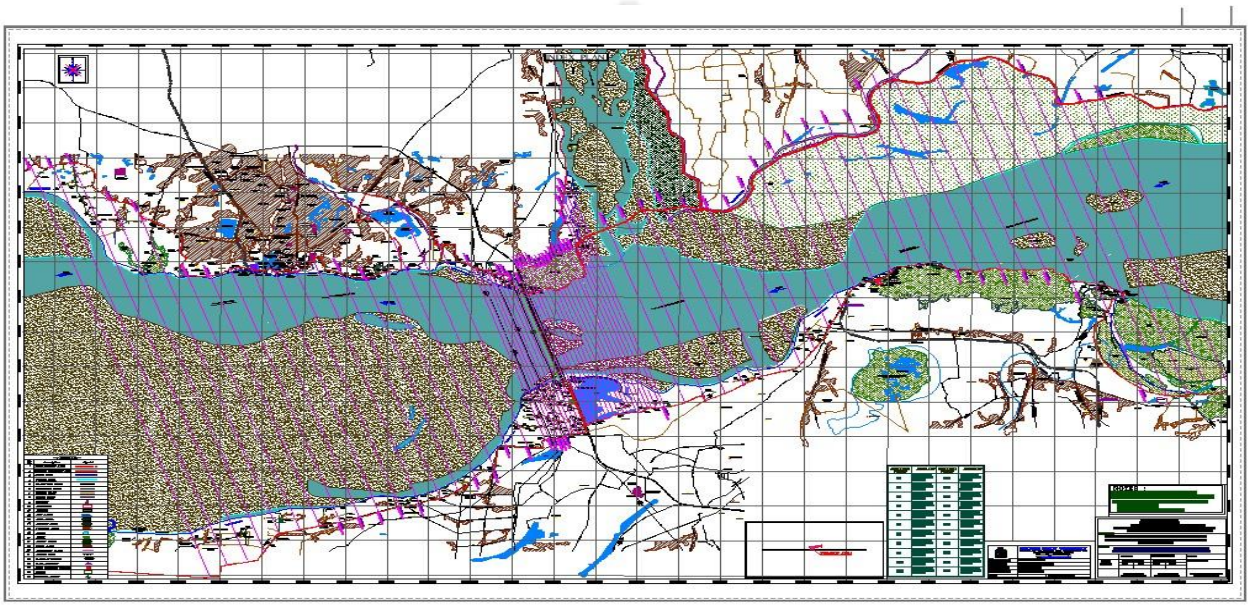

Figure 5.14 Plan of Model Survey Data

The river's cross-sectional data collected during the Bathymetric survey is subsequently represented on a physical hydraulic model tray in a controlled laboratory setting, using an appropriate scale.

Next, the riverbed sand is shaped to match the actual riverbed's profile at each cross-section, closely mimicking the real-world conditions of the prototype river.

Figure 5.15 A Photo of Model Tray during Run

To design the model, Froude number similarity was employed, and a distorted model was chosen because of the significant difference in the width and depth of the flow. Typically, open channel flows are modelled with Froude number similitude as gravitational forces are the dominant driving forces in these situations. Figure 5.15 shows a photo of model tray during run

Finally, a total length of 25 km of the Brahmaputra River from 15km upstream of the Kaliabhomora bridge to 10 km downstream was modelled. Piers of existing and the proposed bridge were produced in the model. Figure 5.16 shows the plan of model tray in Auto-CAD.

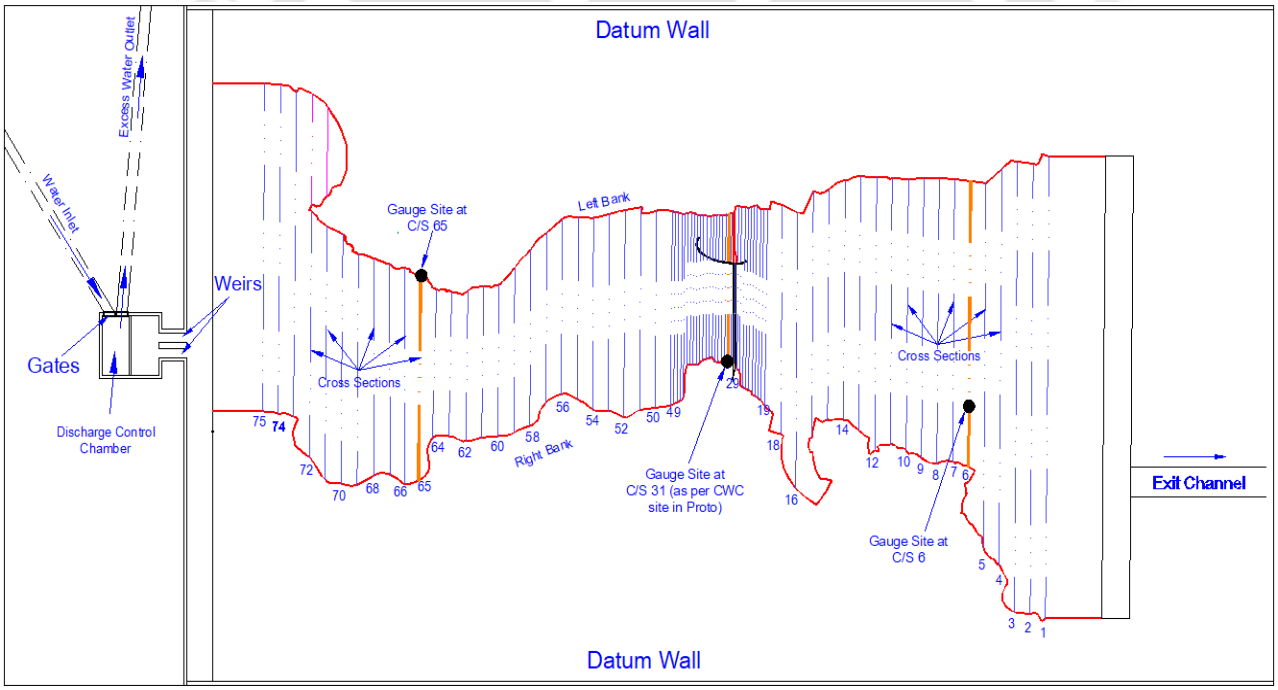

Figure 5.16 Plan of Model Tray Auto-CAD

Table 5.2 shows the model parameters of physical model of river Brahmaputra in reach near Tezpur

Table 5.2 Model Parameters of Physical Model of River Brahmaputra in Reach near Tezpur

Sr. No.	Model Parameter	Values
1.	Horizontal Scale (Xr)	1: 450
2.	Vertical Scale (Zr)	1: 90
3.	Velocity Scale	$1 : 90^{0.5} = 1 : 9.49$
4.	Discharge Scale	$1 : 450*90*90^{0.5} = 1 : 384216.74$
5.	Distorted Ratio	450/90 = 5.00
6.	Hydraulic Time Scale	$Xr/Zr^{0.5}$= 1: 47.43

Modelling Riverbed in Model

A movable bed river model is a type of physical hydraulic model that specifically focuses on simulating the movement of sediment (sand, gravel, etc.) within a river system. In natural rivers, sediment transport plays a crucial role in shaping the river channel, influencing erosion and deposition patterns, and affecting the overall morphology of the riverbed and banks. A movable bed river model is designed to replicate these sediment transport processes in a controlled laboratory environment. The model can be used to study how flow velocity and direction changes lead to scour (erosion of the bed) at specific locations, such as around bridge piers or bends in the river. A movable riverbed was designed in the physical hydraulic model using a shield graph and Shield's Criteria for incipient motion for designing the model. D_{50} of sand in prototype from laboratory analysis of soil sample at NEHARI = 0.125mm. Figure 5.17 shows soil grading curve for prototype river bank.

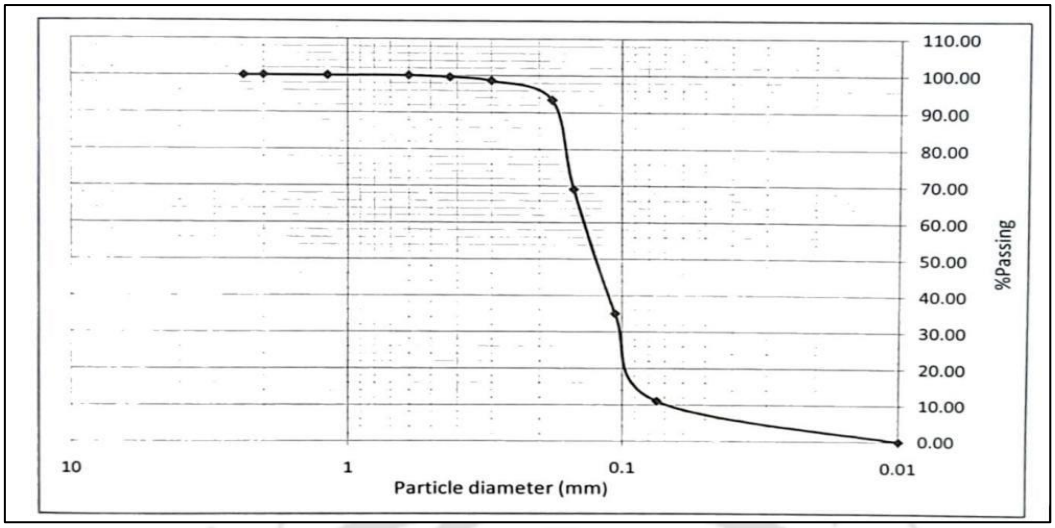

Figure 5.17 Soil Grading Curve for Prototype River bank

The following Parameters corresponding to the Prototype in the Bridge Section are calculated based on mathematical model analysis -

1. Hydraulic Radius R = A/P = 7.22m
2. Reynolds no. of prototype Flow = 1.68 X 10^7 hence flow is sufficiently turbulent.
3. Prototype Tractive Stress = 10.62 N/m^2
4. Shear Velocity u^*= 0.103 m/s
5. Grain Reynolds no. Re* = 12.88

The following Parameters Corresponding to the Model based on scale conversion are calculated-

1. Velocity in Model = 2.91/9.48 = 0.307 m/s
2. Model Hydraulic radius (Mean depth) (m) ~ Calculated using Mannings Velocity equation = 0.131 m
3. Shear Velocity = 0.031 m/s
4. Model Tractive Stress = 0.963 N/m^2
5. Reynolds No. of Model flow = 4.02 x 10^5 (Sufficiently Turbulent)

Movable bed design

Using Shield's Criteria for incipient motion for designing model as shown in Figure 5.18.

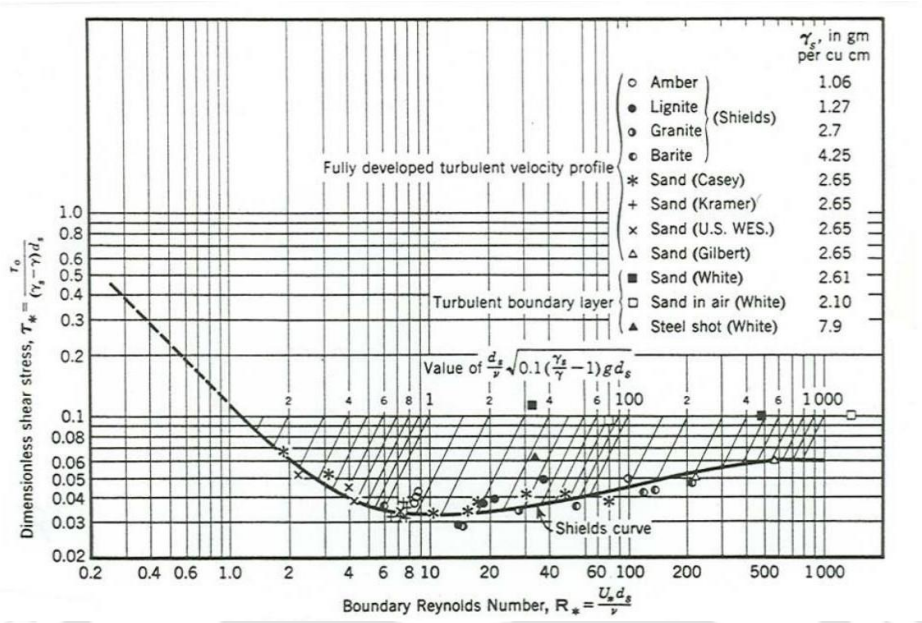

Figure 5.18 Shield Incipient Motion Graph.

A Brief description of Graph-

Region below the Shield's Curve shows no incipient motion occurs in particle of river bed, while points lying above the curve shows the occurrence of incipient motion.

Dimensionless Shear Stress used for Shield's design is given as-

$\Theta = \tau^* = \tau o / (ys-yw)\, d_{50}$ (5.27)

Where, τo is tractive stress, it can be seen since in our prototype (in Kaliabhomora stretch of River Brahmaputra) Re* = 12.88 hence Dimensionless shear Stress that lies on shield's curve is approximately 0.035, hence tractive stress corresponding to this dimensionless shear stress can be called as Critical Tractive Stress.

Critical tractive Stress in Prototype = 0.0708N/m2, now since Tractive stress in Prototype = 10.62 N/m2 > Critical tractive Stress in Prototype = 0.0708 N/m2, hence incipient motion occurs in the prototype.

Movable bed design for Physical Hydraulic Model:

Let us assume a Dimensionless Shear Stress greater than already present in the prototype (0.04), let us assume this to be 0.06, since critical tractive stress increases as dimensionless shear stress increases hence it can be said a safety is adopted in design consideration.

Therefore, for available grain sizes of sand particles to be used in our model, critical shear stress can be calculated using the equation:

$$\Theta = \tau^* = \tau c / (y - yw)\, d_{50} \qquad (5.28)$$

Where $\Theta = 0.06$ is adopted for design consideration

Using $\Theta = 0.06$ gives us the freedom to use $2 < Re^* < 400$ since as evident using the shield's curve this is the domain for incipient motion.

Let us consider different d50 and calculate critical shear stress corresponding to $\Theta = 0.06$

D50 in Model riverbed	Critical tractive stress
0.10	0.099 N/m^2
0.15	0.1485 N/m^2
0.20	0.198 N/m^2
0.25	0.2475 N/m^2
0.30	0.297 N/m^2
0.35	0.3465 N/m^2

Now Since, Model Tractive Stress $\tau o = 0.963$ N/m2 (5.29)

All particle 0.10 mm $< d_{50} <$ 0.35 mm satisfy, criteria for incipient motion to occur ($\tau c < \tau o$) and appropriate factor of safety is being provided corresponding to all these diameter range for bed movement to occur.

Soil grading curve of model sand is shown in Figure 5.19.

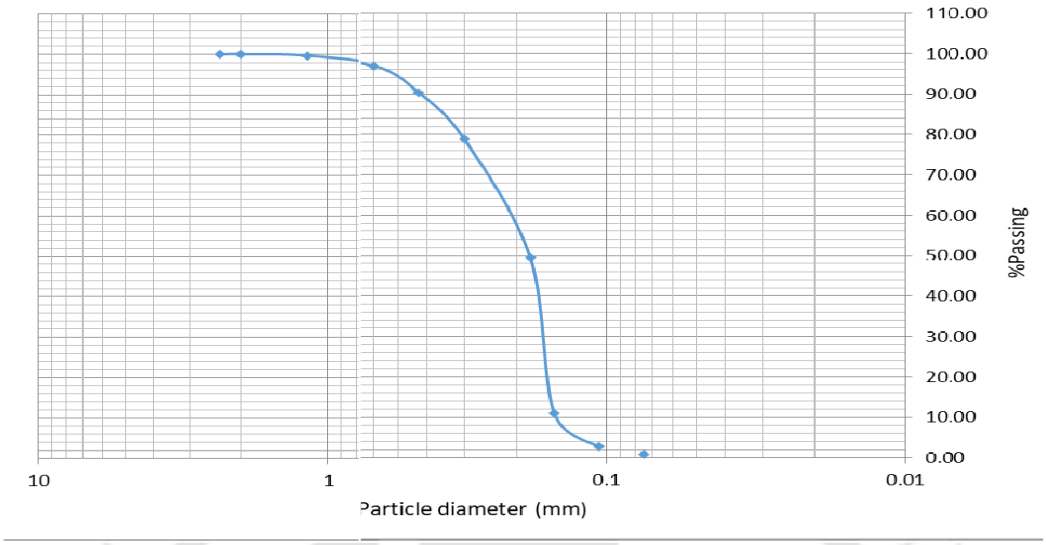

Figure 5.19 Soil Grading curve of model sand

Calibration of Model

In the physical model, a constant (steady) discharge was maintained, and the corresponding water levels from the data of Central Water Commission (CWC) were replicated by adjusting downstream shutter gates. Because the Bhomoraguri-GDS site is adjacent to C/S no. 32 in the study area, a gauge was installed at this location in the model to validate and satisfy boundary conditions. Flow stability was confirmed when the expected water levels, consistent with the known constant discharge and the gauge at c/s 32 were recorded. The cross-section is shown in Figure 5.16.

It took seven cycles of running the model and adjusting achieve stable gauge readings. The water levels observed in the model matched those in the real world, indicating a successful reproduction of the area of interest. Additionally, verification from GIS data has confirmed that this critical section's flow characteristics have remained constant over a long period, emphasizing the necessity of studying only this critical section. Hence, a critical section consisting of 10 piers starting from the right bank (Tezpur side) of the kaliabhomora bridge (Pier No. 25) till the pier number 16 have been studied for the purpose.

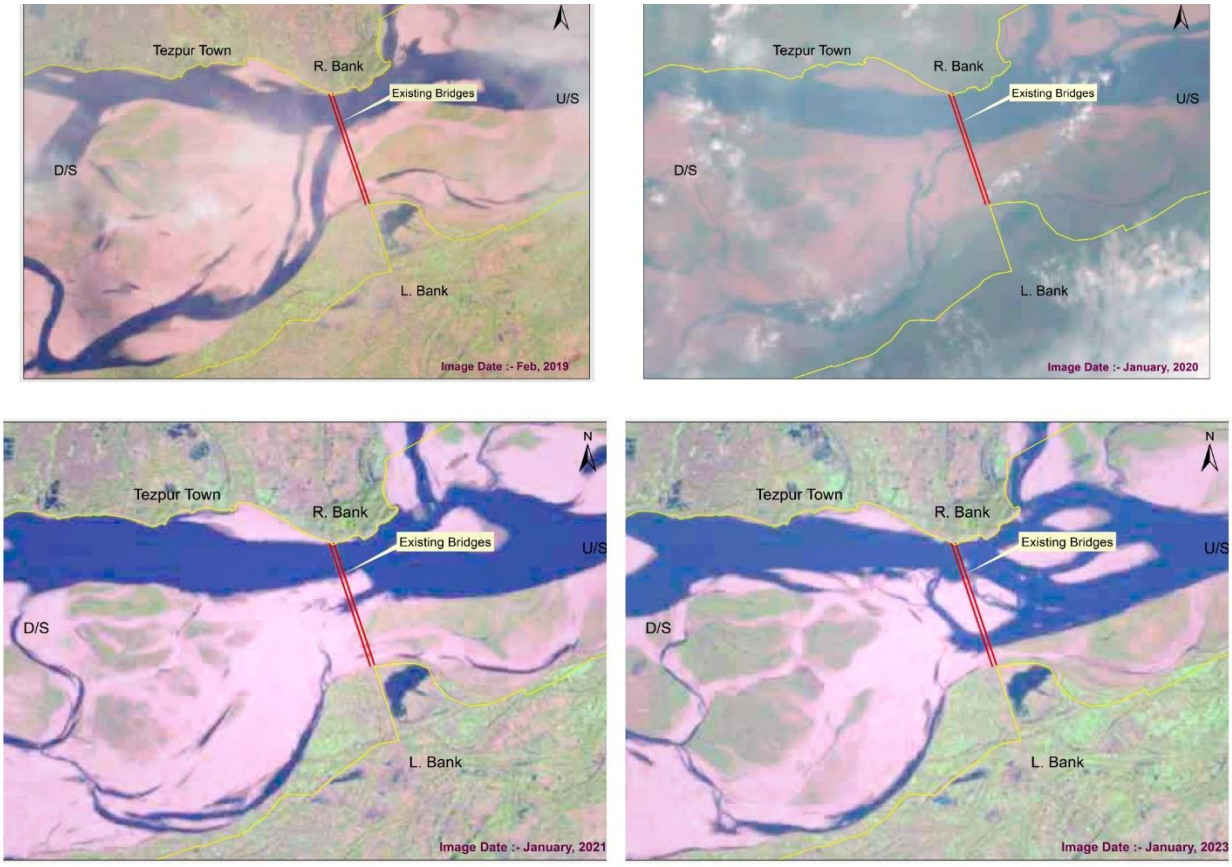

Figure 5.20 Satellite Images of the Study Area for various years

It is evident from the images obtained by satellite imagery for the study area in four different years (2019, 2020, 2021, 2023 as shown in Figure 5.20) that the flow of water predominantly occurs along the right bank of the Kaliabhomora Bridge stretch. This underscores the critical nature of this area, necessitating a focused study within this stretch.

5.3 Dredging channel at River Brahmaputra

The creation of a dredging channel for the river Brahmaputra is a visionary initiative designed to optimize water flow, alleviate sedimentation concerns, and enhance navigational capabilities along the river. This comprehensive project involves the precise excavation and removal of accumulated sediments, crafting a well-defined pathway that not only facilitates smoother transportation but also plays a pivotal role in environmental sustainability. By strategically reducing bank velocities of flow, the dredging channel contributes to the prevention of flood erosion, a critical aspect in safeguarding the riverbanks and adjacent areas. Employing state-of-the-art dredging technologies and adhering to

stringent environmental regulations, this initiative not only revitalizes the waterway for economic activities but also ensures minimal ecological impact, fostering a balanced coexistence between human interventions and the river's natural dynamics. The creation of this dredging channel for the river Brahmaputra stands as a testament to the commitment to sustainable development and the preservation of the region's environmental integrity.

5.3.1 Physical Model Analysis of proposed dredging Channel near Guwahati in river Brahmaputra

A channel is dredged in physical model for a river length of 7 km and river width of 350 m from cross section number 4 to cross section number 18. The effects of river flow in various discharges have been studied. The velocities of river flow from bank to proposed channel are measured for discharge 30000, 40000 and 50,000 cumec. It is found that velocity at bank is considerably reduced due to construction of dredging channel. However, siltation is observed in the dredging channel. The deposition of sand is measured with time in cross section number 6, 11, 15. The readings and observations from three cross sections are obtained and shown as per Figure 5.21, Figure 5.22 & Figure 5.23 respectively.

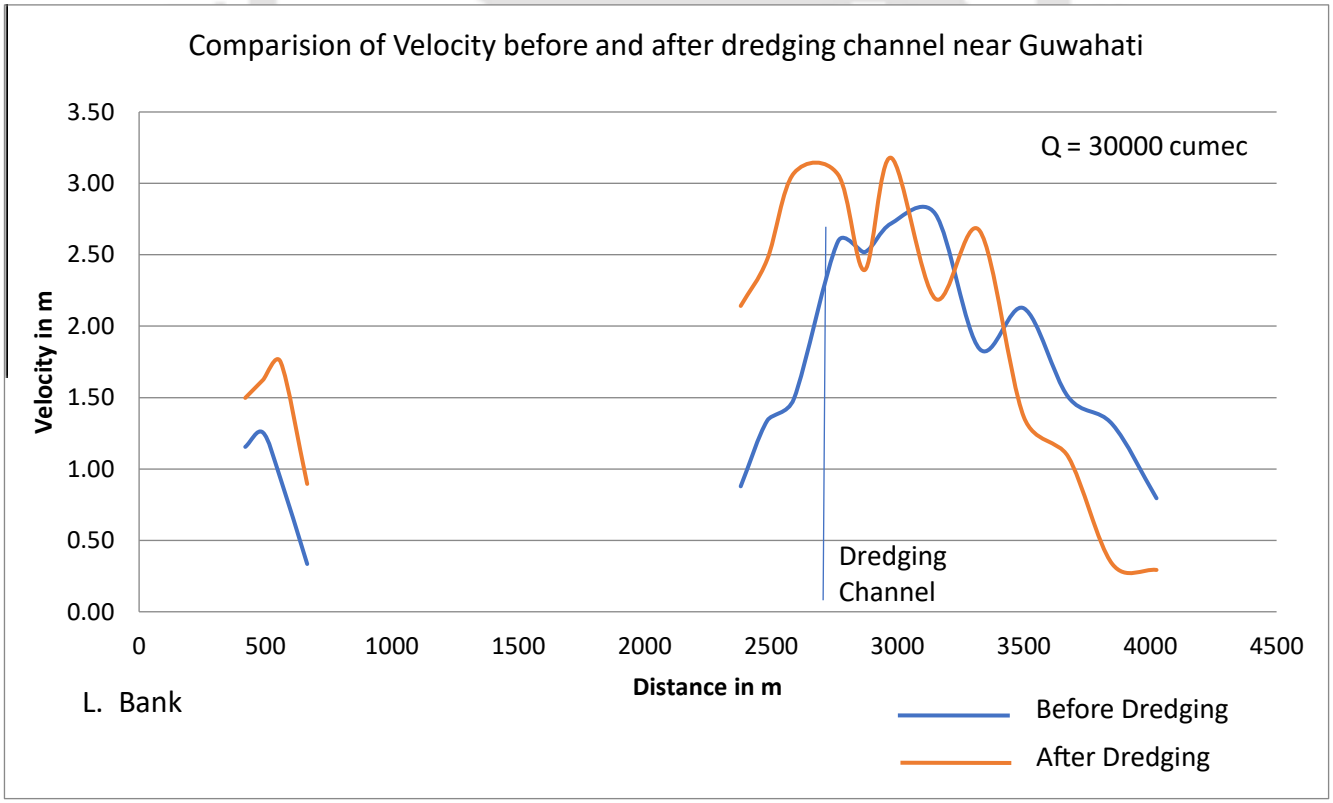

Figure 5.21 Comparison of Velocity at 30000 cumec before and after dredging channel near Guwahati

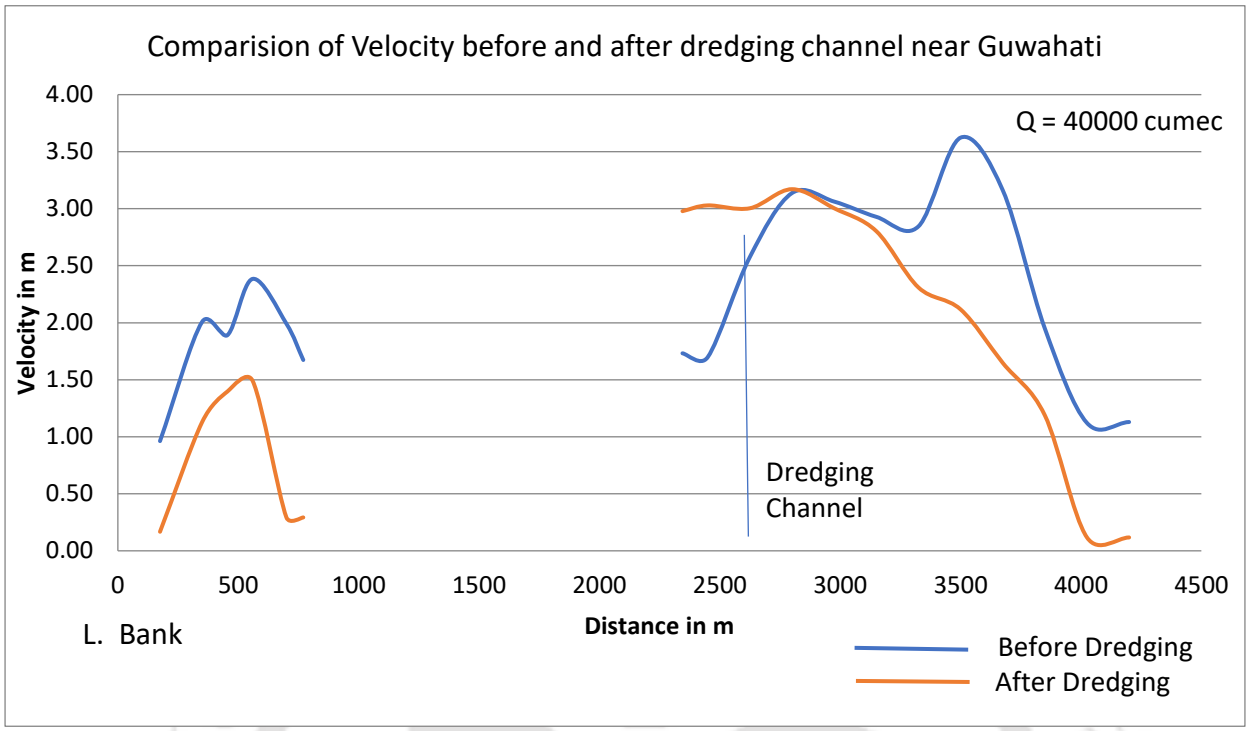

Figure 5.22 Comparison of Velocity at 40000 cumec before and after dredging channel near Guwahati

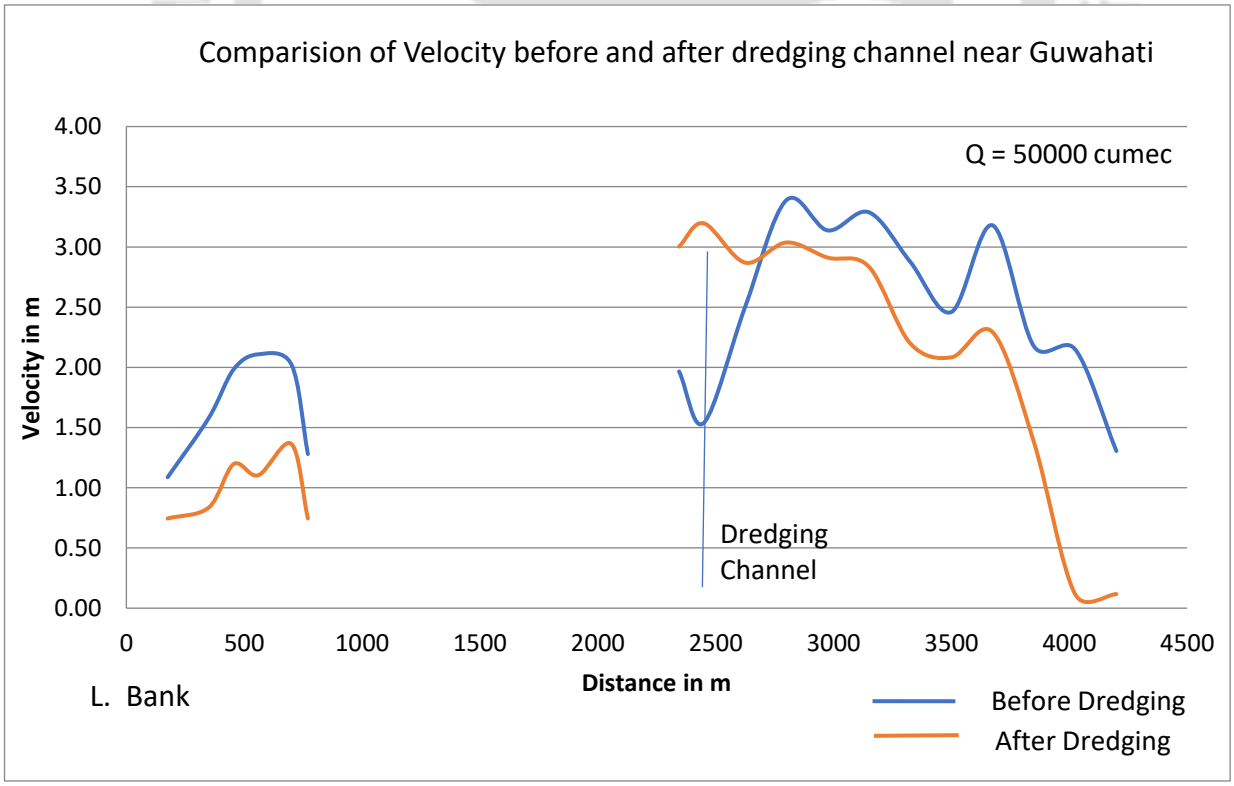

Figure 5.23 Comparison of Velocity at 50000 cumec before and after dredging channel near Guwahati

Table 5.5 shows the changes in bed of proposed dredging channel in model study

Table 5.3 Changes in Bed of Proposed Dredging Channel in Model Study

CS. No	RL of River Bed as per Survey (m)	RL of Proposed Channel Bed (m)	Dredging (m)	RL of bed after Run (m)	Balance Dredging after Run (m)	Deposition (m)
CS 18	35.20	35.20	0.00			
CS 17	36.66	34.94	1.72			
CS 16	38.35	34.67	3.68			
CS 15	37.07	34.41	2.66	36.70	0.37	2.29
CS 14	37.40	34.15	3.25			
CS 13	37.90	33.89	4.01			
CS 12	37.28	33.62	3.66			
CS 11	40.28	33.36	6.92	35.46	4.82	2.10
CS 10	39.68	33.10	6.58			
CS 9	40.01	32.83	7.18			
CS 8	39.43	32.57	6.86			
CS 7	36.44	32.31	4.13			
CS 6	35.40	32.05	3.35	31.63	3.78	-0.42
CS 5	32.12	31.78	0.34			
CS 4	31.52	31.52	0.00			

Figure 5.24 shows a photo of physical model showing cross-section near Guwahati

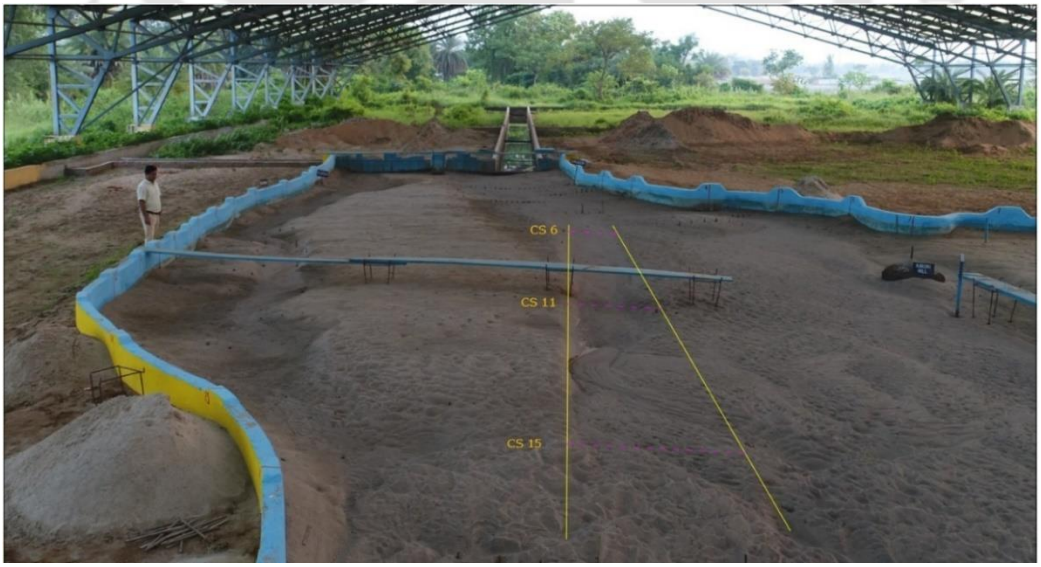

Figure 5.24 Photo of Physical Model showing cross section near Guwahati

Observation and Calculation for Deposition at CS-15 in Proposed Dredging Channel near Guwahati

Model Run Time (min)	Prototype Run Time (Time Scale 41.86)	Prototype Run Time (hrs)	Prototype Run time (Days)	Deposition in Model (cm)	Deposition in Proto (m)	Time Reqd. (days) for Deposition of 1 m
0	0	0	0.0	0.00	0.00	
30	1255.80	21	0.9	1.97	1.38	0.63
60	2511.60	42	1.7	2.47	1.73	2.49
90	3767.40	63	2.6	2.77	1.94	4.15
120	5023.20	84	3.5	2.98	2.09	5.93
240	10046.40	167	7.0	3.10	2.17	41.53
360	15069.60	251	10.5	3.21	2.25	45.30
540	22604.40	377	15.7	3.24	2.27	249.17
720	30139.20	502	20.9	3.27	2.29	249.17

Avg. time Reqd. for deposition of 1 m in last two model Run = 249.17

Balance depth of channel = 0.37 m

Time Reqd. for deposition in the balance depth = 92.2 days

Figure 5.25 shows the deposition with respect to time in cross-section no 15 Near Guwahati.

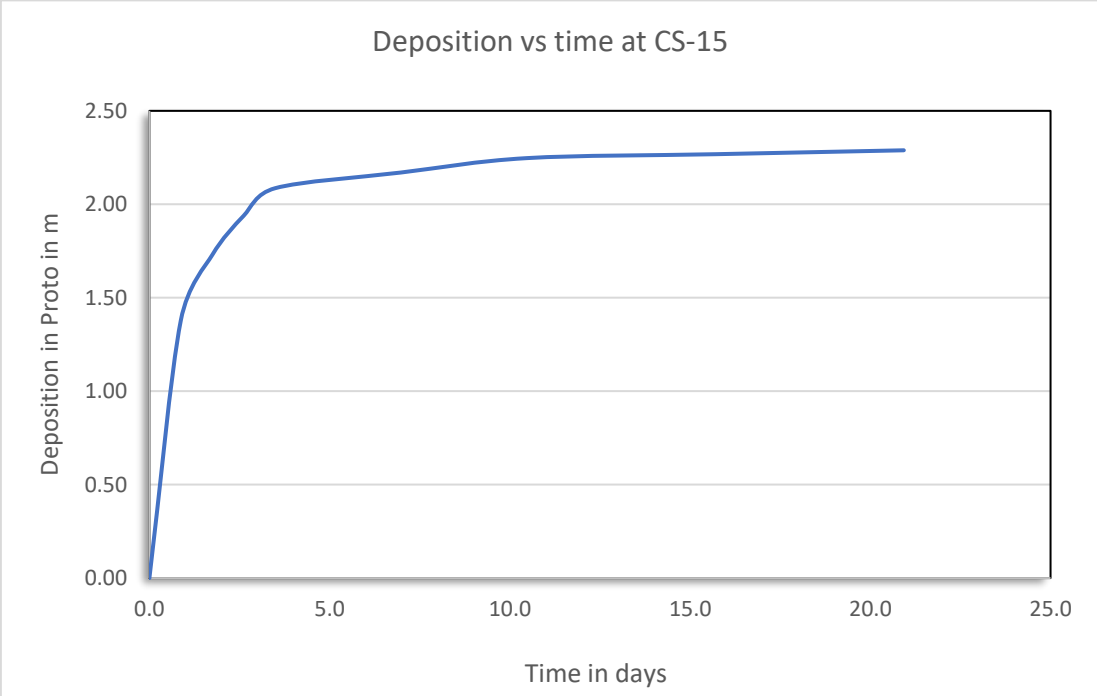

Figure 5.25 Deposition with respect to time in cross-section no. 15 Near Guwahati.

Observation and Calculation for Deposition at CS-11 in Proposed Dredging Channel near Guwahati

Model Run Time (min)	Prototype Run Time (Time Scale 41.86)	Prototype Run Time (hrs)	Prototype Run time (Days)	Deposition in Model (cm)	Deposition in Proto (m)	Deposition Rate in (m)	Time Reqd. (days) for Deposition of 1 m
0	0	0	0	0	0		
30	1255.80	20.93	0.87	1.6	1.12	0.05351	0.78
60	2511.60	41.86	1.74	2	1.4	0.01338	3.11
90	3767.40	62.79	2.62	2.2	1.54	0.00669	6.23
120	5023.20	83.72	3.49	2.4	1.68	0.00669	6.23
240	10046.40	167.44	6.98	2.6	1.82	0.00167	24.92
360	15069.60	251.16	10.47	2.78	1.946	0.00151	27.69
540	22604.40	376.74	15.70	2.9	2.03	0.00067	62.29
720	30139.20	502.32	20.93	3	2.1	0.00056	74.75

Avg. time Reqd. for deposition of 1 m in last two model Run = 68.52

Balance depth of channel = 4.82 m

Time Reqd. for deposition in the balance depth = 330.5 days

Figure 5.26 shows the deposition with respect to time in cross-section no. 11 Near Guwahati

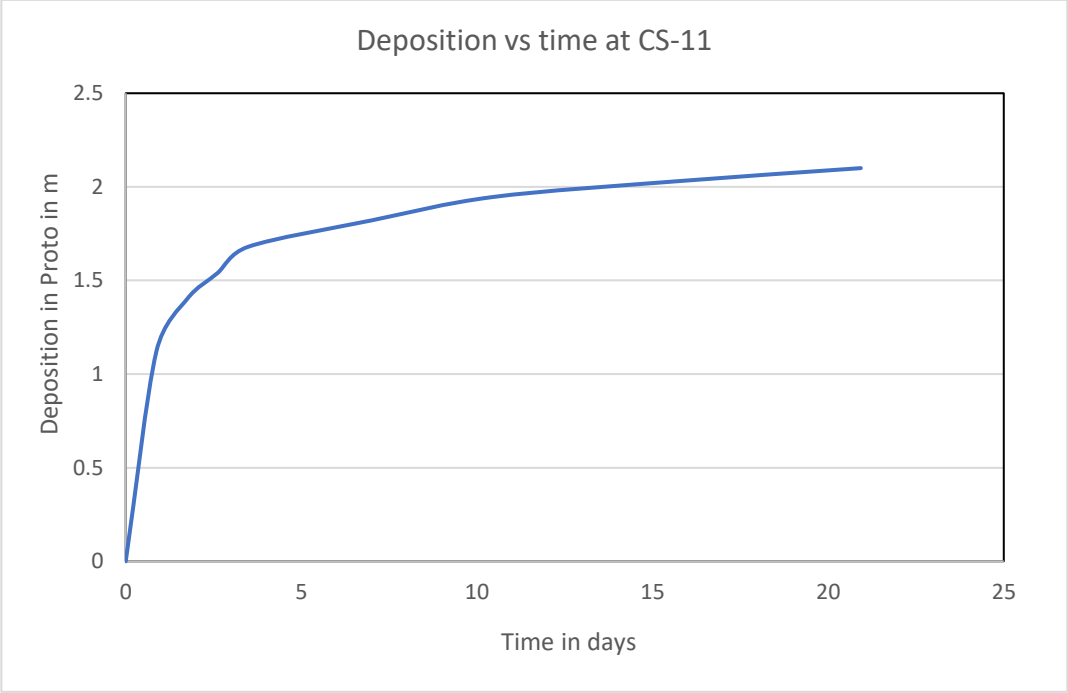

Figure 5.26 Deposition with respect to time in cross-section no. 11 Near Guwahati.

5.3.2 Physical Model Analysis of Proposed Dredging Channel near Tezpur in River Brahmaputra

The north bank of river Brahmaputra just downstream of Kolia Bhomora bridge is stable where is the Tezpur town is situated. But there is vast river bank erosion problem at South Bank just downstream of bridge. It is reported, an area of 1320.78 ha has been eroded from 1998 to 2014. The Government of Assam implemented a lot of schemes to save the Bhurbandha area. A project named 'Protection of Bhurbandha and its adjoining area against the erosion of river Brahmaputra (AS-145)' under Flood Management Programme (FMP) is recently completed in 2019. The main component of the project was construction of land spur. However, the Bhurbandha area is still under continuous threat of river bank erosion. A channel is dredged in physical model for a river length of 5.5 km and river with of 450 m from cross section number 8 to cross section number 19. The effects of river flow in various discharges have been studied. The velocities of river flow from bank to proposed channel are measured for discharge 30000, 40000 and 50,000 cumec. It is found that velocity at bank is considerably reduced due to construction of dredging channel. However, siltation is observed in the dredging channel. The deposition of sand is measured with time in cross section number 10, 15, 18. The readings and observations from three cross sections are shown in Figure 5.27, Figure 5.28 and Figure 5.29.

Velocity Comparison between Before and After Dredging of channel

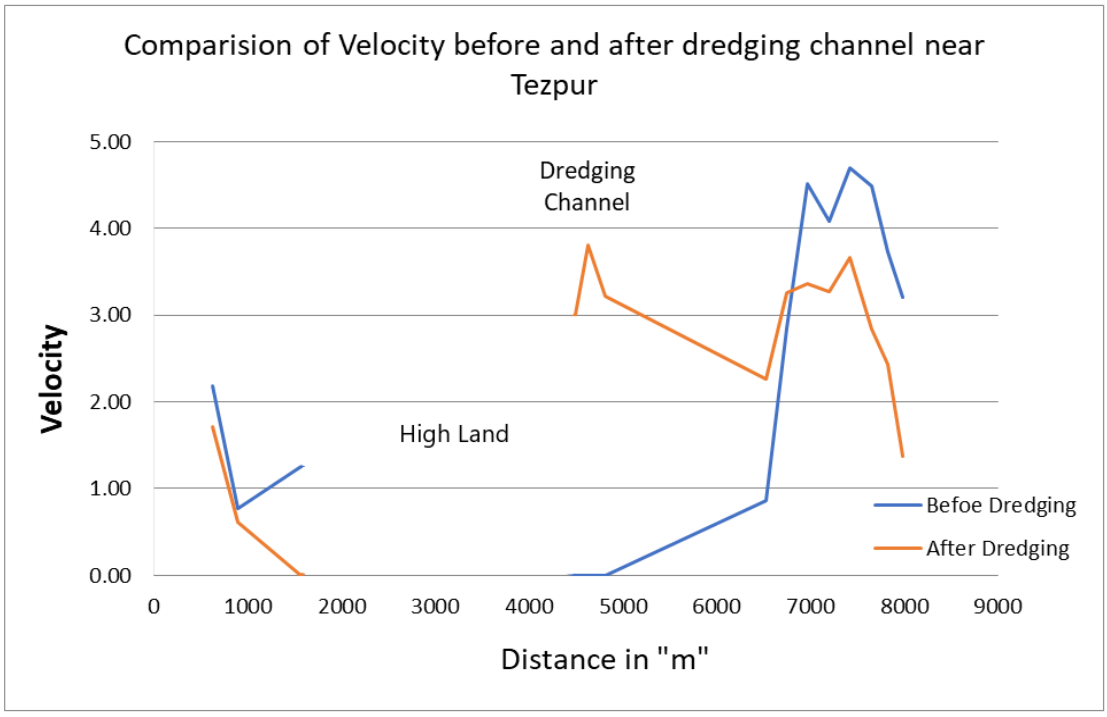

Figure 5.27 Comparison of Velocity at 30000 cumec before and after dredging channel near Tezpur

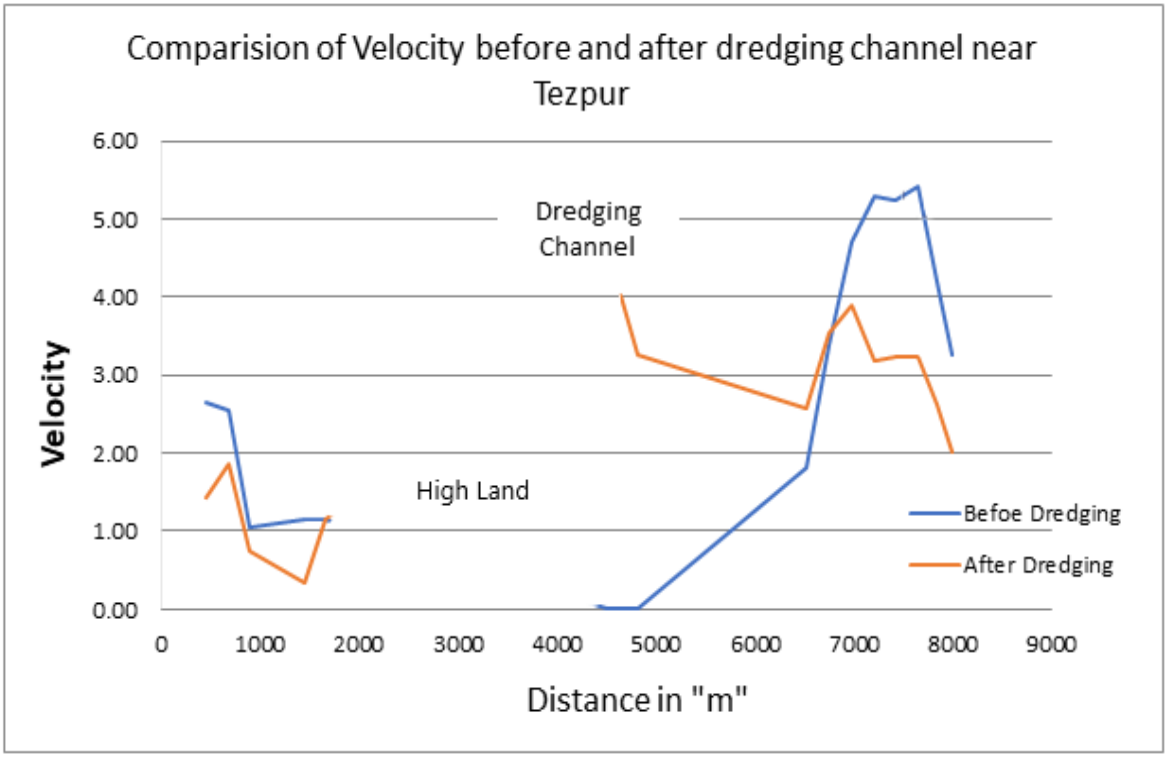

Figure 5.28 Comparison of Velocity at 40000 cumec before and after dredging channel near Tezpur

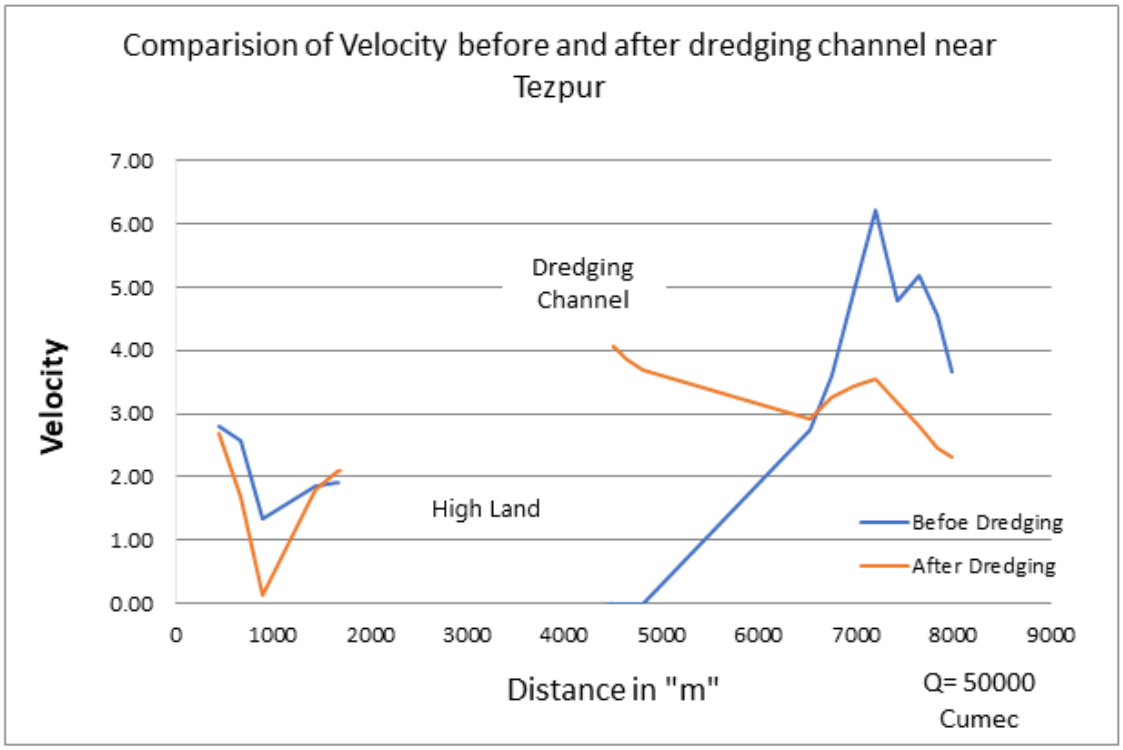

Figure 5.29 Comparison of Velocity at 50000 cumec before and after dredging channel near Tezpur

Table 5.4 shows the changes in bed of proposed dredging channel in model study

Table 5.4 Changes in Bed of Proposed Dredging Channel in Model Study

CS. No	RL of River Bed as per Survey (m)	RL of Proposed Channel Bed (m)	Dredging (m)	RL of bed after Run in (m)	Balance Dredging after Run (m)	Deposition (m)
CS 19	61.28	61.28	0.00			
CS 18	64.35	60.50	3.85	62.62	1.73	2.12
CS 17	64.75	59.73	5.02			
CS 16	66.39	58.95	7.44			
CS 15	67.59	58.17	9.42	60.19	7.40	2.02
CS 14	66.37	57.39	8.97			
CS 13	66.45	56.62	9.83			
CS 12	65.94	55.84	10.10			
CS 11	64.15	55.06	9.09			
CS 10	66.47	54.28	12.18	56.14	10.33	1.86
CS 9	56.92	53.51	3.42			
CS 8	53.36	52.73	0.63			

Figure 5.30 shows a photo of the physical model showing cross-section near Tezpur

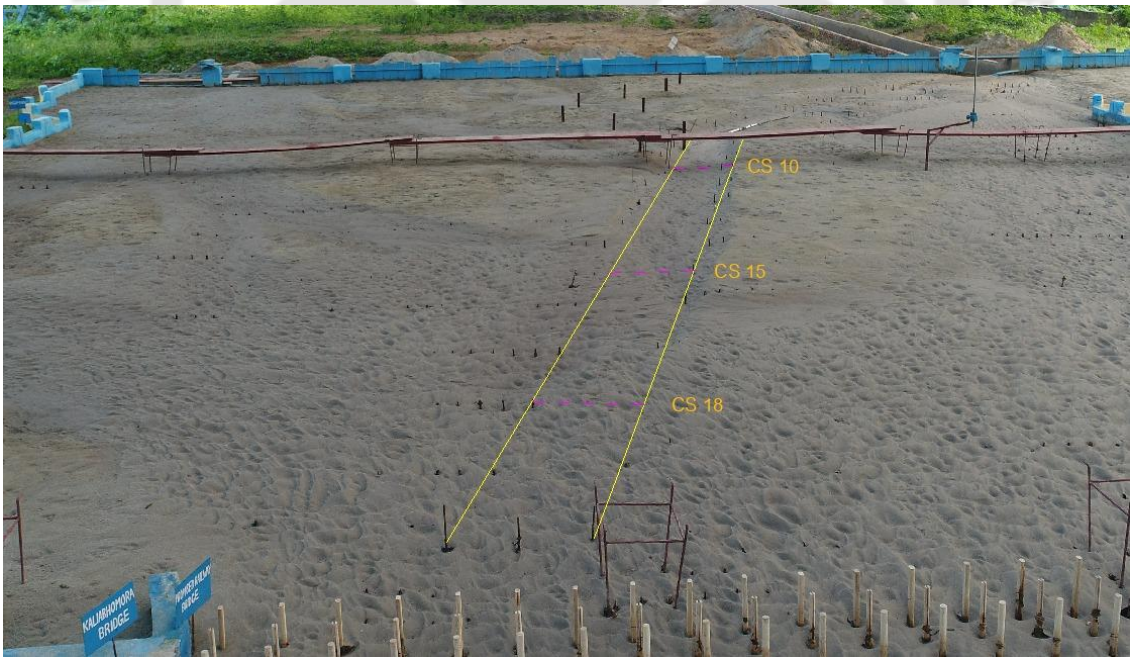

Figure 5.30 Photo of Physical Model showing cross-section near Tezpur

Observation and Calculation Deposition at CS-18 in Proposed Dredging Channel near Tezpur

Model Run Time (min)	Prototype Run Time (Time Scale 47.43)	Prototype Run Time (hrs)	Prototype Run time (Days)	Deposition in Model (cm)	Deposition in Proto (m)	Time Reqd. (days) for Deposition of 1 m
0	0	0.00	0.00	0.00	0	
30	1422.9	23.72	0.99	1.20	1.08	0.91
60	2845.8	47.43	1.98	1.70	1.53	2.20
90	4268.7	71.15	2.96	1.95	1.755	4.39
120	5691.6	94.86	3.95	2.10	1.89	7.32
240	11383.2	189.72	7.91	2.21	1.989	39.92
360	17074.8	284.58	11.86	2.29	2.061	54.90
540	25612.2	426.87	17.79	2.35	2.115	109.79
720	34149.6	569.16	23.72	2.40	2.16	131.75

Avg. time Reqd. for deposition of 1 m in last two model Run = 120.77

Balance depth of canal below danger level (65.23m) = 2.61 m

Time Reqd. for deposition in the balance depth = 315.21 days

Figure 5.31 shows the deposition with respect to time in cross-section no 18 Near Tezpur.

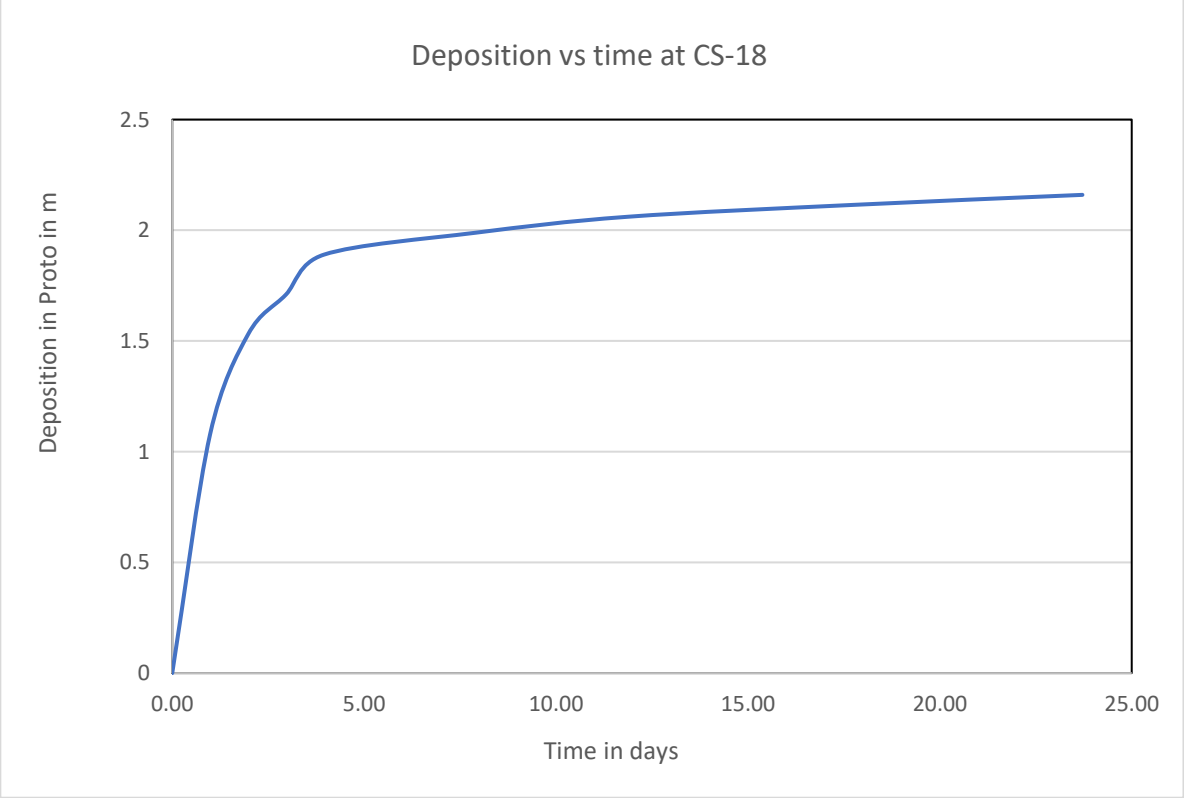

Figure 5.31 Deposition with respect to time in cross-section no. 18 Near Tezpur.

Observation and Calculation Deposition at CS-15 in Proposed Dredging Channel near Tezpur

Model Run Time (min)	Prototype Run Time (Time Scale 47.43)	Prototype Run Time (hrs)	Prototype Run time (Days)	Deposition in Model (cm)	Deposition in Proto (m)	Time Reqd. (days) for Deposition of 1 m
0	0	0	0	0	0	
30	1422.9	23.715	1.0	1	0.9	1.10
60	2845.8	47.43	2.0	1.4	1.26	2.74
90	4268.7	71.145	3.0	1.7	1.53	3.66
120	5691.6	94.86	4.0	1.9	1.71	5.49
240	11383.2	189.72	7.9	2.06	1.854	27.45
360	17074.8	284.58	11.9	2.14	1.926	54.90
540	25612.2	426.87	17.8	2.23	2.007	73.19
720	34149.6	569.16	23.7	2.30	2.07	94.11

Avg. time Reqd. for deposition of 1 m in last two model Run = 83.65

Balance depth of canal below danger level (65.23m) = 5.04 m

Time Reqd. for deposition in the balance depth = 421.6 days

Figure 5.32 shows the deposition with respect to time in cross-section no 15 Near Tezpur.

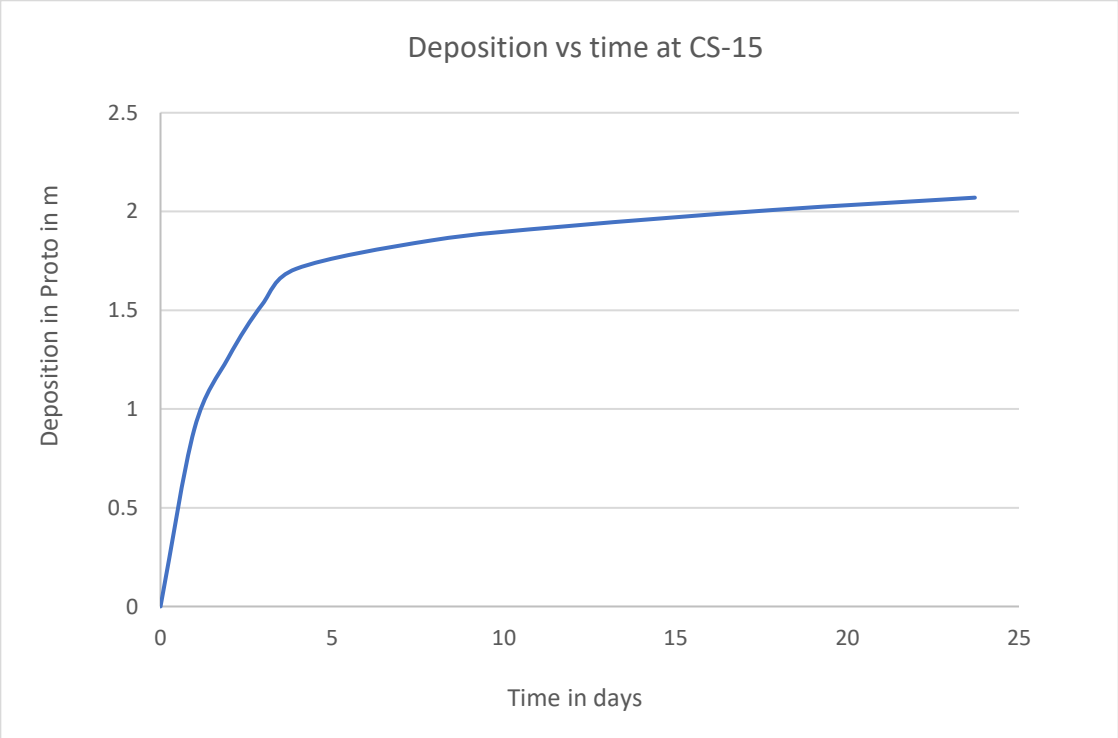

Figure 5.32 Deposition with respect to time in cross-section no. 15 Near Tezpur.

Observation and Calculation Deposition at CS-10 in Proposed Dredging Channel near Tezpur

Model Run Time (min)	Prototype Run Time (Time Scale 47.43)	Prototype Run Time (hrs)	Prototype Run time (Days)	Deposition in Model (cm)	Deposition in Proto (m)	Time Reqd. (days) for Deposition of 1 m
0	0	0	0	0.00	0.00	
30	1422.9	23.715	0.99	0.90	0.81	1.22
60	2845.8	47.43	1.98	1.40	1.26	2.20
90	4268.7	71.145	2.96	1.50	1.35	10.98
120	5691.6	94.86	3.95	1.60	1.44	10.98
240	11383.2	189.72	7.91	1.81	1.63	20.91
360	17074.8	284.58	11.86	1.90	1.71	48.80
540	25612.2	426.87	17.79	2.01	1.81	59.89
720	34149.6	569.16	23.72	2.10	1.89	73.19

Avg. time Reqd. for deposition of 1 m in last two model Run = 66.54

Balance depth of canal below danger level (65.23m) = 9.09 m

Time Reqd. for deposition in the balance depth = 604.9 days

Figure 5.33 shows the deposition with respect to time in cross-section no 10 Near Tezpur.

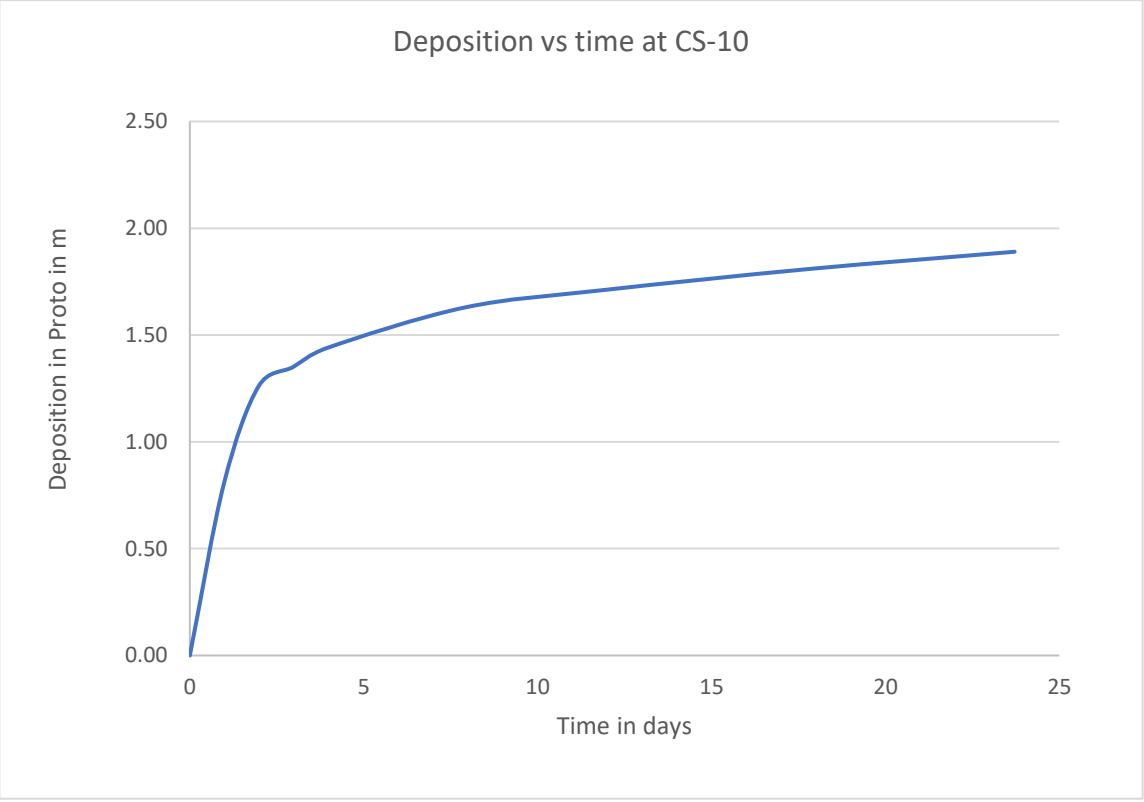

Figure 5.33 Deposition with respect to time in cross-section no. 10 Near Tezpur.

5.4 Study of Scour Hole of Bridges in Physical Model of River Brahmaputra

There are several methods for computing scour depth:

1. For the prototype, you can estimate scour based on what is observed in the model using the vertical scale. However, when calculating scour depth for the prototype using the vertical scale derived from Froude number similarity, the result is often very shallow scour. This occurs because the scour around the bridge piers is primarily influenced by the flow's jet action rather than gravitational forces.

2. The scour depth can also be calculated for the prototype by scaling the observed scour depth in the model using scour depth equations.

3. Another approach involves using flow parameters obtained from physical model studies, such as determining unit discharge through model experiments and then calculating bridge scour using the Lacey equation.

Calculation of Scour Depth by Lacey Formula

Lacey's method is commonly used in India for estimating the scour depth around bridge piers placed in alluvial rivers. This method is recommended for design by the Indian Road Congress and Indian Railways (IRC: 5-2015 / IRC: 78-2014). According to Lacey's formula

Scour depth $D_s = 1.35 \times \left(\frac{q^2}{f}\right)^{1/3}$ (5.30)

Where D_s if the scour depth (m), q is the discharge per unit width (cumec/m), and f is Lacey's silt factor.

The silt factor (f) is determined by using the expression, $f=1.76*\sqrt{d_m}$ (5.31)

d_m is the mean diameter of the bed material (mm)

Maximum Depth of Scour for Design of Foundation

The maximum depth of scour below the Highest Flood Level (HFL) for the design of piers (D_{sp}) and abutments (D_{sa}), having individual foundations without any floor protection are as follows:

In the vicinity of pier: $D_{sp} = 2D_s$ (5.32)

Soil Characterization

The soil testing report is used in this study.

Lacey's silt factor is found as, f = 1.76* $f\sqrt{0.160}$ =0.704. It is assumed that the soil parameters are not changing with depth, as the soil condition below the bed level is not known.

Calculation of Scour Depth by Lacey Formula at Guwahati and Tezpur Bridge are shown in Table 5.5 and Table 5.6

Table 5.5 Scour depth calculation		
Actual waterway of the river	1045.40	m
Q for scour ($Q = 1.1Q_{100}$)	69973.20	m^3/sec
Silt factor	0.70	
Discharge per unit width (cumec/m)	66.93	m^2/sec
Normal Scour (m, below HFL)	25.02	m
Maximum Scour under Pier (m, below HFL)	50.03	m

Table 5.6 Scour Depth Calculation Considering the Flow Concentration Through the Primary Channels		
Length of the bridge in which there is a concentration of flow	1538.00	m
Q for scour ($Q = 1.1Q_{100}$)	70534.00	m^3/sec
Silt factor	0.60	
Discharge per unit width (cumec/m)	45.86	m^2/sec
Mean Scour (m, below HFL)	20.51	m
Maximum Scour under Pier (m, below HFL)	41.03	m
HFL	67.50	m
RL (m) of the scoured bed below the pier	26.46	m

However, it has been observed from the bathymetric data that the flow of the river generally takes place through two channels, not through the entire width of the river. The scour depth value will be highly underestimated if the discharge per unit width is calculated using the available width of the channel. As such, the scour depth of calculated considering the width of the channel through which the flow generally takes place. Table 5.5 shows the scour depth calculation considering the flow concentration through the primary channels. The mean scour depth, in this case, is 20.51 m.

As per the CWC guidelines, if the width of the river is more than Lecey's waterway, the scour depth is to be calculated using the following formula.

Mean Scour depth $D_s = 0.473 \times \left(\frac{Q}{f}\right)^{1/3}$ (5.33)

In this case, the mean scour depth will be 23.18 m.

Observation of scour depth at piers in model

Melville and Sutherland (1988) proposed a method for estimating the scour at bridge piers, which is completely based on the analysis of the laboratory data. Their equation for scour depth below the bed, Ds is,

Ds/b = K1.Kd.Ky.K∞.Ks (5.34)

Where the K's are expressions that describe the influence of each parameter in the above equation. K1=flow intensity; Kd=sediment size; Ky=flow depth; K∞ =angle of attack; Ks= pier shape; b=projected pier width with respect to the direction of the flow.

Equation (5.34) in terms of the ratio between prototype and model can be written as:

$$(Ds)p/(Ds)m = bp/bm \quad (5.35)$$

Where subscript 'p' and 'm' indicate prototype and model, respectively.

(Ds)p = (Ds)m x (bp/bm) = (Ds)m.(Xr) = 450 X (Ds)m

Table 5.7 shows the observed scour depth at various piers in model for Guwahati area.

Table 5.7 Observed scour depth at various piers in model for Guwahati area.		
Pier Number	**Observed Scour at Bridge below bed level.**	
	MODEL (cm)	**PROTO (m)**
1.	6.00	21.00
2.	3.80	13.30
3.	5.20	18.20
4.	5.60	19.60
5.	8.20	28.70
6.	9.60	33.60
7.	9.10	31.85
8.	5.60	19.60
9.	8.50	29.75
10.	9.00	31.50
11.	2.60	9.10

Table 5.8 shows the observed scour depth at various piers in model for Tezpur area.

Table 5.8 Observed scour depth at various piers in model for Tezpur area.		
Pier Number	**Observed Scour at Proposed Rail Bridge Below Bed Level**	
	MODEL (cm)	**PROTO(m)**
16.	3.3	14.8
17.	4.1	18.4
18.	6.2	27.9
19.	5.1	22.9
20.	5.6	25.2
21.	8.6	38.7
22.	4.2	18.9
23.	2.7	12.1
24.	5.7	25.6
25.	7.85	35.3
26.	11.9	53.5

The scour depths are measured in the physical model for bridges in river Brahmaputra at Guwahati & Tezpur. The major scour depths at pier are scaled up using Melville & Sutherland equation and compare with the computed scour depth by Lacey's formula. It is found that maximum measured scour depth is just within the calculated scour depth. Therefore, it may be concluded that Melville & Sutherland equation can be used for physical model study for river Brahmaputra.

Observation for influence of scour hole at piers in model

As per a study conducted by (Singh et. al., 2020) the scouring effect of the existing bridge on its downstream side is 3.5D, and the scour effect for the proposed bridge on its upstream side is 2.5D, where D is the diameter of the well of the bridge. Figure 5.34 shows the empirical scour width.

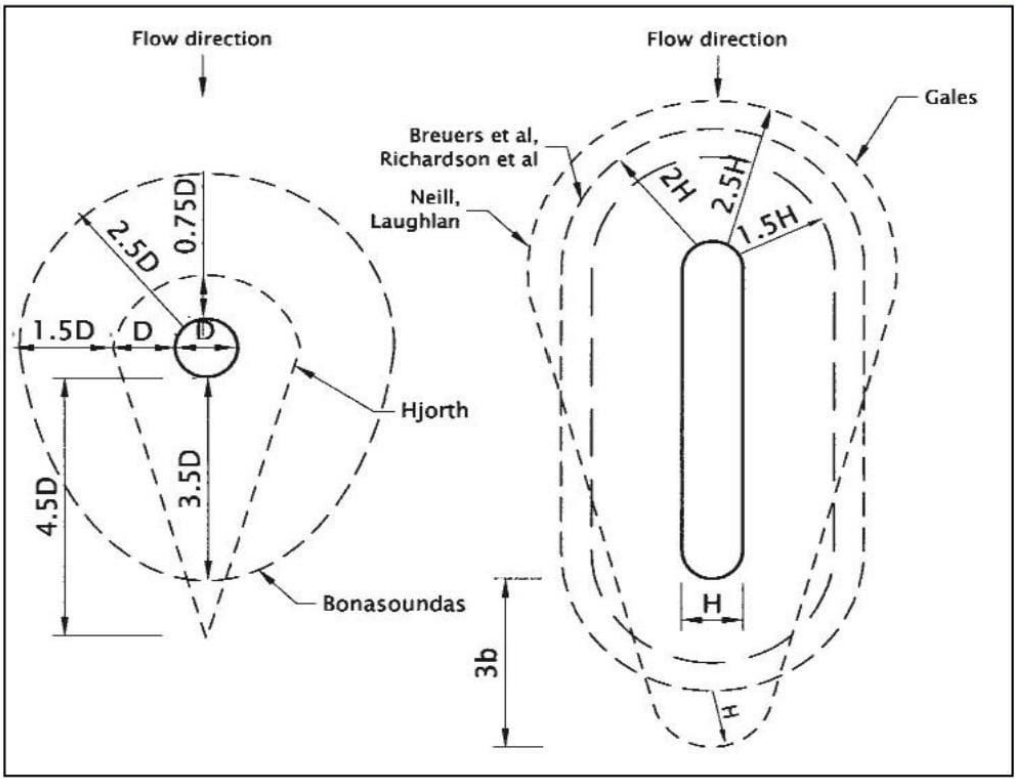

Figure 5.34 Empirical Scour Width (After Singh et al. (2020))

Figure 5.35 shows a photograph of scour hole around pier no. 5 of bridge near Guwahati and Figure 5.36 shows a photograph of scour hole around pier no. 19 of bridge near Tezpur.

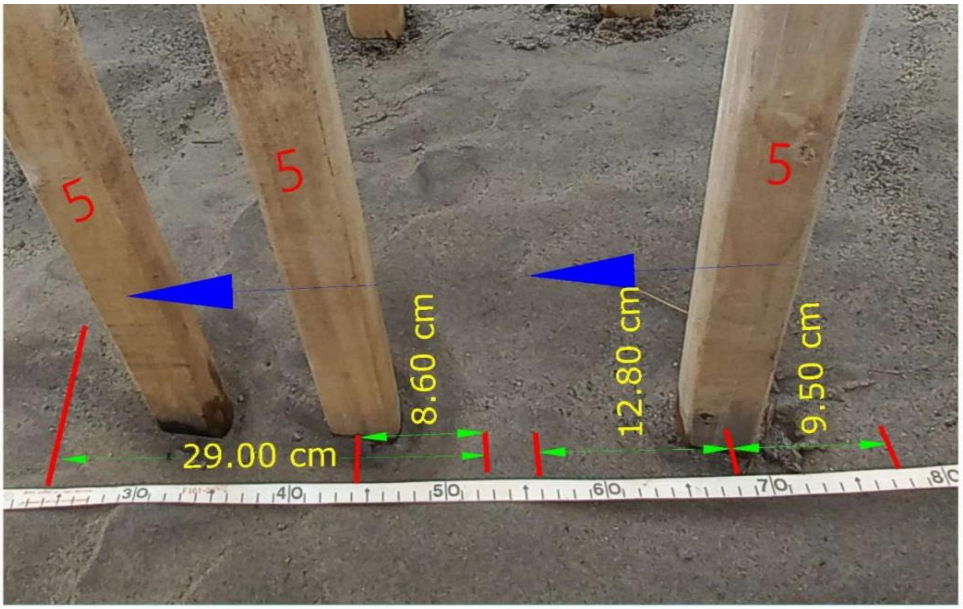

Figure 5.35 Photo of scour hole around pier no. 5 of bridge near Guwahati

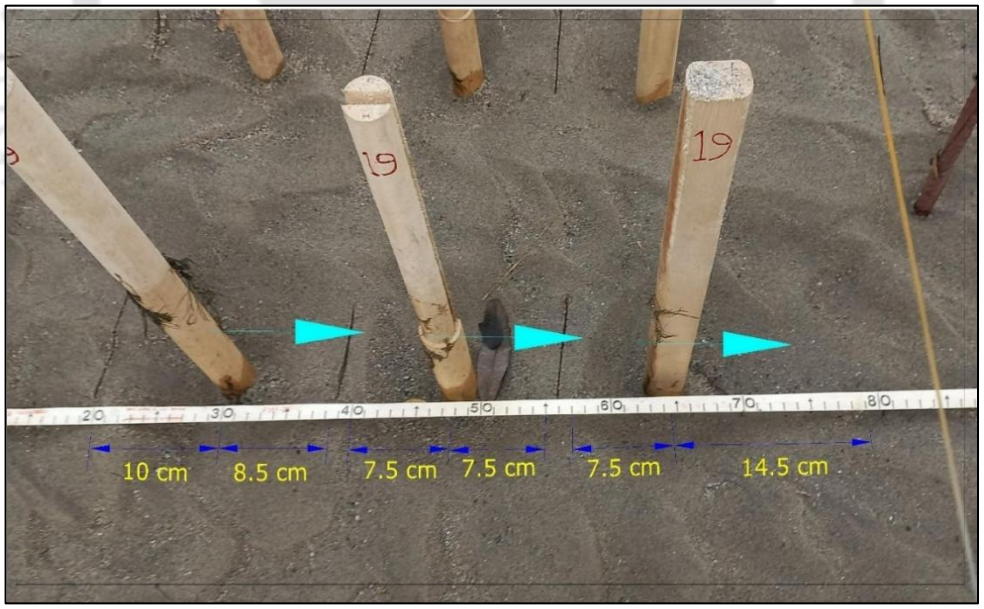

Figure 5.36 Photo of scour hole around pier no. 19 of bridge near Tezpur

The distances for scour effect are also measured for upstream and downstream of physical model of these two Bridges. The measured distances are scaled up by using horizontal ratio and compared with the competed scour hole influenced distance by the formula given by Singh et. al (2020). It is found that measured distances are at par with the computed distance. Therefore, it may be concluded that the formula given by Singh et. al is applicable for river Brahmaputra

5.5 Discussion and Conclusion

Hydraulic and geometric scaled models are vital for studying river management and hydraulic structures, allowing for reasonable relaxation in grain Reynolds numbers (Ashworth et al., 1994). Dynamic similarity is determined by key force ratios like Froude, Reynolds, and Euler numbers (Taylor & Heller, 2011). Physical model analysis provides reliable engineering solutions but must be executed accurately and followed by post-construction management for sustainability (Islam, 2008). Despite the long history of hydraulic modelling, complete downsizing of all essential parameters is challenging (Taylor & Heller, 2011). The challenges posed by scale effects in physical models can be mitigated through inspectional analysis, dimensional analysis, and calibration with prototype data (De, 2021). The use of physical models has proven effective in solving hydraulic issues that defy analytical solutions, as demonstrated by various studies. For example, a distorted hydraulic model was used to study flow diversion with spurs in the Kosi River, improving flood protection by deflecting flow away from vulnerable embankments (Burele et al., 2012). Similarly, an undistorted movable-bed model was used to study sediment flow and erosion in the Old Rhine, highlighting the need to enhance physical modelling capabilities to manage climate change impacts (El et al., 2013; Baynes et al., 2018). Physical models also help optimize hydraulic designs, such as the Pump Sump Model for vortex issues and the Spillway Dam model for safety validation (Firdaus Zulkefly et al., 2019). Studies on the Kosi River and the Sabarmati River have shown that physical models, when combined with numerical models like HEC-RAS, provide valuable insights into hydraulic performance and safety measures (Burele et al., 2018; Khan & Mujumdar, 2021). After reviewing the published literature which was detailed in chapter 2, it is found that there is no such published paper where the physical model study for dredging in river is done. Therefore, physical model study of Proposed Dredging Channel near Guwahati and Tezpur are done.

Discussion and Conclusion on physical model study of Proposed Dredging Channel near Guwahati

In the model study of the proposed dredging channel, observations reveal significant alterations in the bed profiles across various survey points (CS) along the channel. Beginning with CS 18, the riverbed remains unchanged with no dredging required. As we progress downstream, the dredging needs become evident. At CS 17, a dredging depth of 1.72 meters is indicated, followed by deeper dredging requirements at CS 16, where a depth of 3.68 meters is necessary to align with the proposed channel bed. The most substantial dredging requirement is observed at CS 11, where a significant depth of 6.92 meters is essential to match the proposed channel bed. Conversely, at CS 6, a slight elevation in the bed is recorded, necessitating a reduction in the proposed dredging depth by 0.42

meters. Notably, deposition is recorded at CS 15 and CS 11, indicating sediment accumulation of 0.37 meters and 4.82 meters, respectively.

These observations underscore the dynamic nature of the channel bed, highlighting the necessity for precise dredging operations to achieve the desired channel configuration and mitigate the impacts of sediment deposition. Additionally, careful monitoring and management strategies are crucial to maintaining optimal navigational conditions within the dredging channel. The observations from both CS-15 and CS-11 in the proposed dredging channel near Saraighat indicate a progressive pattern of sediment deposition over time. In CS-15, prototype runtimes range from 0 to 20.9 days, correlating with deposition depths of 0 to 2.29 meters. Meanwhile, in CS-11, prototype runtimes vary from 0 to 20.93 days, with deposition depths ranging from 0 to 2.1 meters. While the deposition rates fluctuate, with CS-15 showing an average of 249.17 days for the deposition of 1 meter and CS-11 averaging 68.52 days, both locations demonstrate ongoing sedimentation processes. Considering the remaining depths of the canal, recorded at 0.37 meters for CS-15 and 4.82 meters for CS-11, estimated deposition times of 92.2 days and 330.5 days, respectively, are projected for these segments.

Discussion and Conclusion on physical model study of Proposed Dredging Channel near Tezpur

Following the physical model study of the proposed dredging channel, notable changes in the bed profiles are observed across various survey points (CS) along the channel. At CS 19, no dredging is required, as the riverbed aligns perfectly with the proposed channel bed. However, significant dredging is necessary at subsequent survey points to achieve alignment. At CS 18, dredging of 3.85 meters is needed, resulting in a post-run bed level of 62.62 meters. Similarly, at CS 15, a substantial dredging depth of 9.42 meters is required, resulting in a post-run bed level of 60.19 meters. Conversely, deposition is recorded at CS 18 and CS 15, indicating sediment accumulation of 1.73 meters and 7.40 meters, respectively. Further downstream, at CS 10, dredging of 12.18 meters is necessary, leading to a post-run bed level of 56.14 meters. Notably, deposition is also observed at CS 10, indicating sediment accumulation of 10.33 meters. These findings underscore the dynamic nature of the channel bed and the necessity for precise dredging operations to achieve the desired channel configuration. Additionally, careful monitoring and management strategies are crucial to addressing sediment deposition and maintaining optimal conditions within the dredging channel.

The observations and calculations from CS-18, CS-15, and CS-10 in the proposed dredging channel near Tezpur provide crucial insights into the sedimentation dynamics and the associated challenges

of constructing a channel in a braided river system. At CS-18, it's evident that as the prototype run time increases, there's a steady deposition of sediment within the channel. This deposition progresses from 1.08 meters at 0.99 days to 2.16 meters at 23.72 days, indicating a substantial accumulation over time. The average time required for the deposition of 1 meter in the last two model runs stands at 120.77 days. With a balance depth of the channel below the danger level at 2.61 meters, there's an estimated time of 315.21 days required for further deposition, highlighting the challenges of maintaining desirable depths in the face of sediment accumulation. Similarly, at CS-15, sediment deposition is observed to increase over time, with an average time of 83.65 days required for the deposition of 1 meter in the last two model runs. The balance depth of the channel below the danger level is recorded at 5.04 meters, indicating a significant need for dredging to maintain required conditions. The estimated time required for deposition in this segment is 421.6 days, underscoring the ongoing challenges of sedimentation in the braided river environment. At CS-10, the observations reveal a similar trend of sediment accumulation, with an average time of 66.54 days required for the deposition of 1 meter in the last two model runs. With a balance depth of the channel below the danger level recorded at 9.09 meters, the estimated time required for further deposition is 604.9 days, emphasizing the substantial dredging requirements necessary to ensure navigational safety.

These findings underscore the dynamic and evolving nature of sedimentation within the channel prototype, suggesting the necessity for possible maintenance work before making decisions regarding construction or maintenance activities within the dredging channel. Above studies are conducted considering 50,000 cumec steady discharge in each case. However, actual discharge in river is unsteady. The study can be improved considering unsteady flow in future. Overall, these observations highlight the complex and ongoing challenges associated with constructing and maintaining a dredging channel in a braided river system. Effective management strategies and continuous monitoring are essential to address sedimentation issues and maintain required depths. From the above studies, it can be concluded that constructing a dredging channel in a braided river presents a host of challenges stemming from the dynamic nature of such watercourses. One of the primary issues faced during construction is the constant need to navigate and adapt to changes in channel morphology caused by sediment deposition and erosion. This necessitates frequent dredging to maintain desirable depths, which can be costly and resource-intensive. Additionally, the presence of multiple channels and shifting sandbars complicates the identification of the optimal alignment for the dredging channel, requiring thorough hydrological studies and ongoing monitoring. Furthermore, environmental concerns such as habitat disruption and sediment release during dredging operations must be carefully managed to mitigate adverse impacts on aquatic ecosystems.

Overall, construction of dredging channel in a braided river demands a holistic approach that integrates engineering expertise with stewardship to ensure the long-term sustainability and effectiveness of the dredging channel.

6.

Need and Scope of Using Porcupine Screen and Dredging Independently or in Combination.

6.1 Study on use of Porcupine Screen Along with Proposed Dredging Channel for a Reach in River Brahmaputra near Majuli.

In the realm of riverine ecosystems, braided rivers stand as dynamic and intricate landscapes characterized by the presence of multiple interconnected channels and shifting bars or islands. The ever-changing nature of braided rivers makes them susceptible to erosion, necessitating effective erosion control measures to maintain the stability and ecological health of these unique environments. Among the arsenal of erosion control techniques, the porcupine screen, also referred to as a porcupine mat or erosion control mat, emerges as a valuable tool. This article explores the application of porcupine screens as anti-erosion measures in braided rivers, elucidating their role in stabilizing riverbanks, promoting vegetation growth, influencing channel morphology, protecting floodplains, enhancing habitats, reducing sediment transport, and ensuring long-term effectiveness.

Riverbanks, susceptible to the erosive forces of flowing water, demand strategic interventions to prevent erosion and maintain stability. Porcupine screens prove instrumental in achieving this by providing a physical barrier that reinforces riverbanks against the erosive impacts of the water. Installation along riverbanks and on bars within the braided river, these screens act as a stabilizing force, securing the soil and preventing it from being dislodged during periods of high flow. The intertwining structure of the porcupine mat creates a stable surface conducive to the establishment of vegetation. This dual function, combining erosion control with vegetation support, renders porcupine screens an effective anti-erosion measure for riverbanks in braided rivers. Braided rivers exhibit a unique morphology with multiple channels weaving through the landscape. These channels are separated by bars or islands, contributing to the dynamic nature of the river system. Porcupine screens can be strategically placed to guide the flow within these channels, influencing the natural morphological changes that are characteristic of braided rivers. By encouraging the formation of desirable channel patterns, porcupine screens play a role in maintaining a more stable and

sustainable river system. This aspect of their application aligns with the dynamic nature of braided rivers, offering a way to manage and guide the morphological evolution of the channels.

During high-flow events, braided rivers are prone to scouring of floodplains and riverbanks, posing a threat to both the stability of the ecosystem and adjacent human infrastructure. Porcupine screens act as a protective layer, absorbing the energy of the flowing water and reducing the potential for scouring. By stabilizing the floodplains, these screens contribute to the preservation of the natural habitat and prevent the erosion-induced alteration of the landscape. The protective function of porcupine screens becomes crucial in mitigating the impact of extreme events, ensuring the resilience of the braided river system.

Porcupine screens extend their influence beyond erosion control and stability—they play a pivotal role in enhancing habitats within the braided river ecosystem. The stabilized environment created by these screens contributes to the creation of a more favourable habitat for aquatic and riparian species. Riverbanks protected by porcupine screens provide conducive conditions for the establishment of vegetation, creating niches for various species. The enhanced habitat quality supports biodiversity, contributing to the overall ecological health of the braided river system. In this way, porcupine screens act as guardians of the intricate web of life within the riverine environment. Sediment transport is a defining characteristic of braided rivers, with the continuous movement of sediments shaping the dynamic landscape. However, excessive sediment transport can lead to downstream issues, affecting water quality and ecosystems. Porcupine screens play a crucial role in managing sediment transport by trapping and stabilizing sediments. Positioned strategically, these screens reduce the export of sediment downstream, minimizing the potential impact on water quality and downstream ecosystems. The ability of porcupine screens to balance the natural sediment transport dynamics of braided rivers makes them valuable tools in preserving the delicate ecological balance. Durability is a key attribute of effective erosion control measures, especially in environments as dynamic as braided rivers. Porcupine screens are designed to withstand the erosive forces of flowing water, ensuring their long-term effectiveness. Constructed from durable materials, these screens provide a resilient barrier against erosion, maintaining their structural integrity over time. The durability of porcupine screens enhances their reliability as a sustainable erosion control solution, offering long-term protection to riverbanks and contributing to the overall stability of the braided river system.

In conclusion, porcupine screens emerge as multifaceted tools in the realm of anti-erosion measures for braided rivers. Their ability to stabilize riverbanks, promote vegetation growth, influence channel

morphology, protect floodplains, enhance habitats, reduce sediment transport, and ensure long-term effectiveness positions them as valuable assets in the management of these dynamic environments. The intertwining structure of porcupine screens provides a physical barrier that not only combats erosion but also facilitates the establishment of vegetation, contributing to the overall ecological health of braided rivers. As custodians of river stability and biodiversity, porcupine screens offer a comprehensive approach to erosion control in braided rivers, aligning with the intricate and dynamic nature of these unique ecosystems.

Therefore, it is proposed to conduct physical model study of an important reach of river Brahmaputra using porcupine screen along with proposed dredging channel. A channel is proposed to be dredged in the area of study with widths varying from 100 m to 400 m with an idea to divert the flow of the river away. Porcupine screens are also proposed to lay upstream of the channel to divert the river flow towards the dredged channel. The effects of river flow in various scenarios i.e. considering varying widths and discharges will be studied. Figure 6. 1 shows the methodology used to propose and finalise the dredging channel.

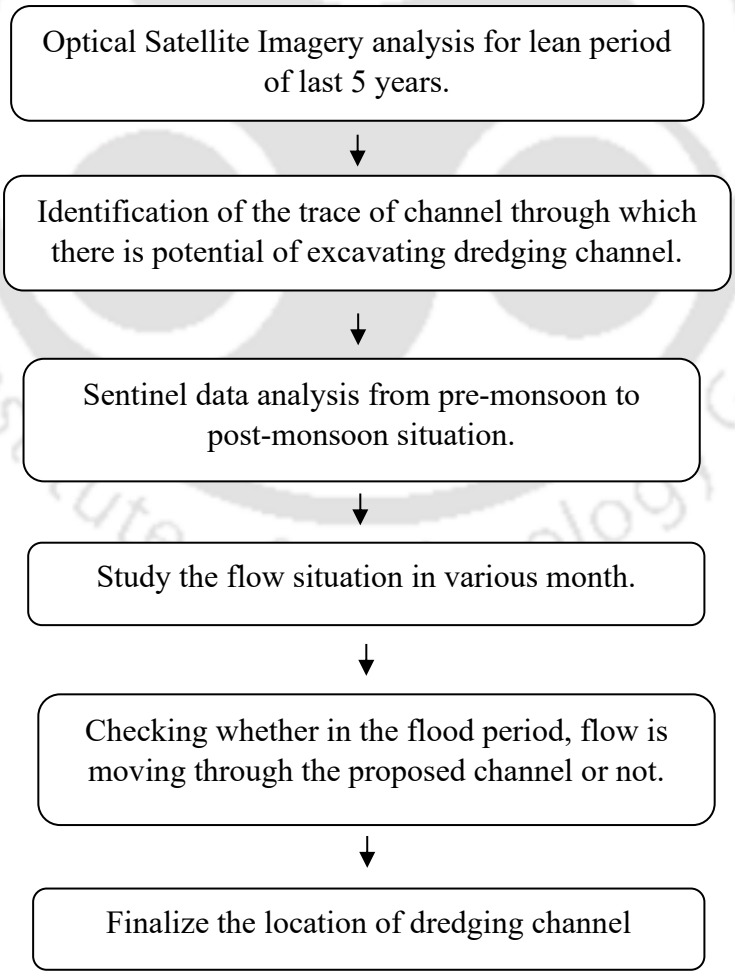

Figure 6. 1 Methodology used to propose and finalise the dredging channel

Preliminary Alignment of Dredging Channel Considering River Sand Bar Dynamics.

River Bar dynamics relate to the morphologic behaviour of braided river and specially to the erosion and deposition processes. Planforms are characterized by numerous transient mid-channel bars and channels in a braided river. The planform changes rapidly and unpredictably in the case of a sand bed due to the relatively high energy and intense bedload transport condition, which accelerates instability especially for mid-channel bars (Egozi and Ashmore, 2009). These bars show various planforms, which seem to be stage-dependent and eventually construct a very wide range of alluvial planforms due to upstream and downstream erosion and sedimentation (Ashworth et al., 1994). To analysis the dynamics of the morphology such as large-scale sand bars, a time series satellite image analysis has been conducted. Six geo-referenced satellite images of 2015 to 2020 (the satellite images are dated - 15.02.2015, 05.02.2016, 09.02.2017, 22.01.2018, 16.02.2019, 13.02.2020) have been superimposed to assess sand bar movements over the years. It is found that Sand Bar – I, is stable but Sand Bar – II & III are eroded. Therefore, dredging alignment may be done as shown in Figure 6.2.

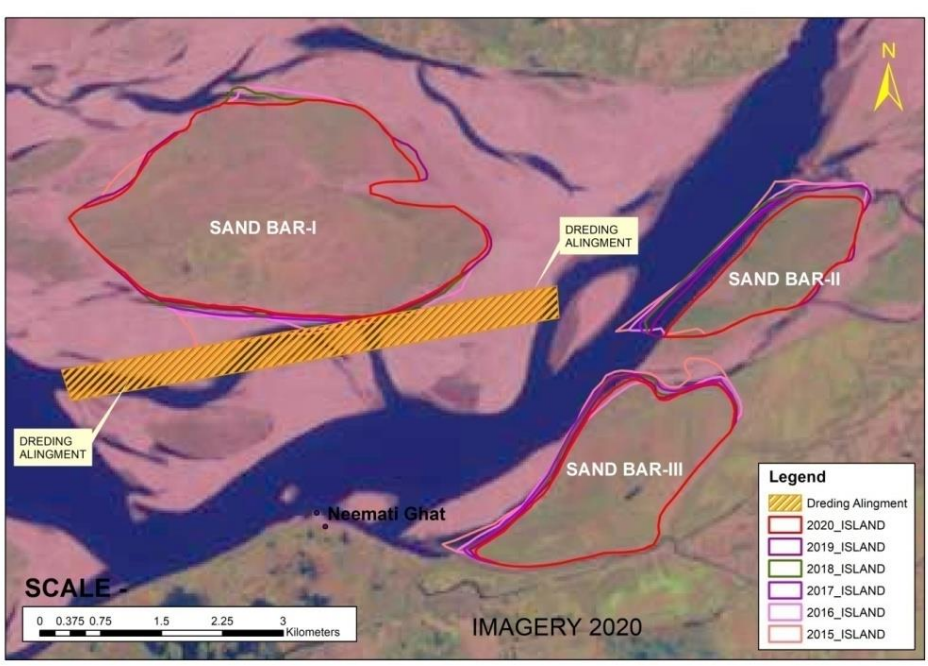

Figure 6. 2 Preliminary dredging alignment near Majuli

Radar Data Analysis for Proposed Dredging Channel:

Optical sensors used in Landsat series are affected by the cloud cover. In Brahmaputra basin average cloud is more than 50% for the month from April to November in a year, which limits the use of optical sensors in this area significantly. Synthetic Aperture Radar (SAR) has the advantage of operating at wavelengths not impeded by cloud cover or a lack of illumination and can acquire data

over a site during day or night time under all weather conditions. The first methods and algorithms used to detect floods with SAR were introduced in the early 1980s and have been developed since then (Tavus et al., 2018).

C-band sensor of Sentinel-1 SAR data is freely available. There are two satellites namely Sentinel-1A and Sentinel-1B carrying radar sensor and both of them operating in the same orbit. European Space Agency launched Sentinel-1A and Sentinel-1B in 2014 and 2016, respectively. The Sentinel-1 mission includes C-band imaging operating in four exclusive imaging modes with different resolution (down to 5 m) and coverage (up to 400 km). (https://sentinel.esa.int/). Other SAR imagery is not freely available; these include: Radarsat-2, TerraSAR-X, and Cosmo-SkyMed.

In this study, river channel maps are generated from April to November of the year using Sentinel-1 data. For this purpose, the study has been carried out in three main stages; i) Processing of Sentinel 1 data, ii) Mapping procedure, and iii) Creation of KML file and Evaluation of the vector files. SAR data from Sentinel-1, was downloaded after registration at the Sentinels Scientific Data Hub. In this Data Hub, a search option becomes available which is used to specify the data need such as region of interest, product type, sensor mode, sensing period, among others. In this case, Level-1 Ground Range Detected (GRD) Sentinel-1 data is used which incorporates already some basic pre-processing. The Sentinel-1 sensors have 4 different modes with different resolutions, extents, polarizations and incidence angles: Strip map (SM), Interferometric Wide Area (IW), Extra Wide (EW) and Wave (WV). The IW area mode has been used. This mode is the main acquisition mode over land and has single and dual polarizations (VV: vertical transmitting- vertical receiving; and VH: vertical transmitting- horizontal receiving) (Cazals et al., 2016). VV polarized images are considered more adequate for flood and water bodies detection than VH in several previous studies (Twele et al., 2016). For this reason, VV polarized images have been used in this study. The flow chart of the methodology used here is shown in Figure 6.3.

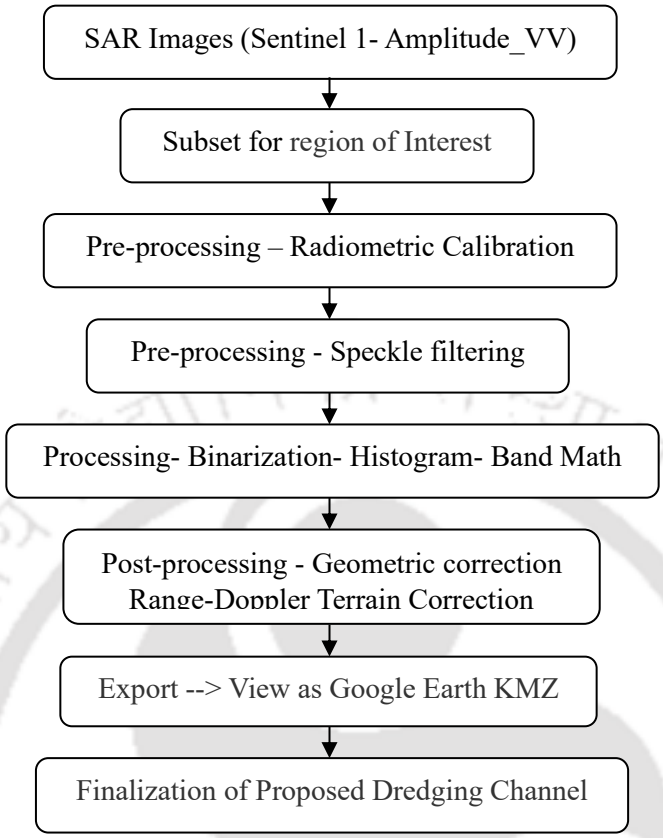

Figure 6.3 Flowchart of the methodology

The images were processed with the free software SNAP (Sentinel Application Platform) Tool [http://step.esa.int], created by ESA for the analysis of the data captured by Sentinel satellites. One Sentinel 1 imagery for every month from April'2020 to September'2020 was used to finalized the proposed dredging channel. After cropping area of study in these images, pre-processing like radiometric calibration, speckle filtering was done. The last step in image processing is to perform terrain correction. This primarily eliminates distortions due to changes in topography and incidence angle with the ground from the nadir. The geometric calibration used in this study was Range Doppler terrain Correction and the Digital Elevation Model (DEM) –SRTM-3Sec. The UN-SPIDER Recommended the Practice for radar-based flood mapping [https://www.un-spider.org/]. Finally, the KMZ and Vectors file are generated after analysing with this practice.

Finalization of Possible Dredging Channel after Sentinel 1 Data Analysis

The resulting river channel maps in vector format of the study area is shown figure below. The location of proposed dredging channel was initially fixed based on non-monsoon satellite image of

Landsat series. This location is checked in these river channel vector maps. It is found that the proposed location works as main branch channel in monsoon season. Therefore, the proposed location is finalized for dredging after analysis of sentinel 1 data. Figure 6.4 shows the river channel maps of the study area from April, 2020 to September, 2020

Vector files after analysis Sentinel 1 Data of different months

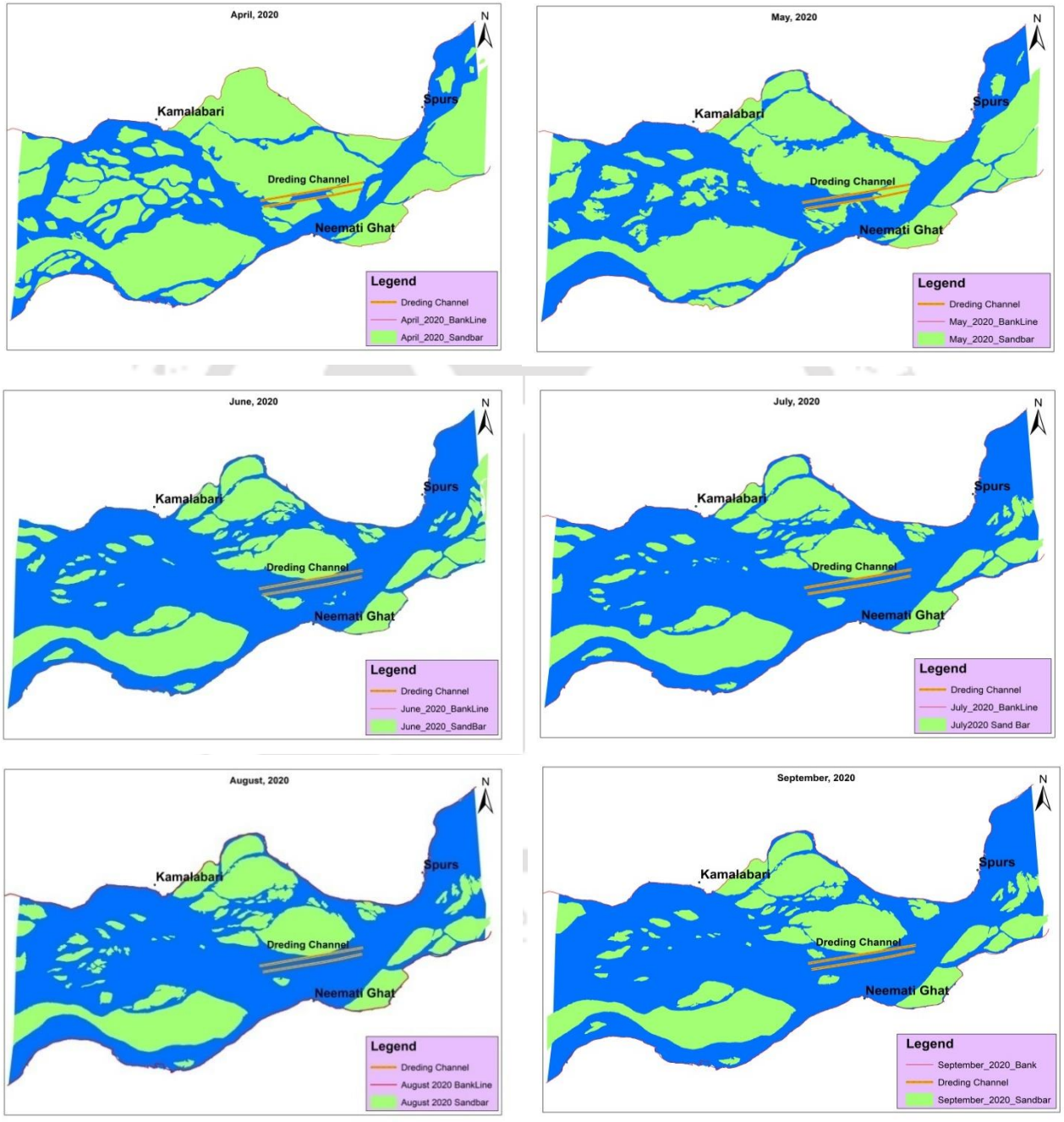

Figure 6.4 River channel maps of the study area from April, 2020 to September, 2020.

6.2 Survey Data for the Model Study:

i. Survey plan of post flood 2018 at a scale 1:50000, covering the entire reach of Majuli Island (55 km). This reach from conjunction of Brahmaputra and Dikhow River up to conjunction of Brahmaputra and Subansiri River.

ii. 56 nos. Cross sections of river Brahmaputra between existing embankment/road at 1 km interval on either side of bank is shown in Figure 6.5 and Figure 6.6 shows area of Physical Model Study. Cross-Sections of River Brahmaputra used in Physical Model Study are shown in Figure 6.6.

iii. Index plan of river Brahmaputra (covering entire Majuli Island) showing river training works on and around the reach (post flood 2018)

iv. Cross-section data of river of Brahmaputra through Nimati Ghat for the year 2014, 2016, 2018 & 2019.

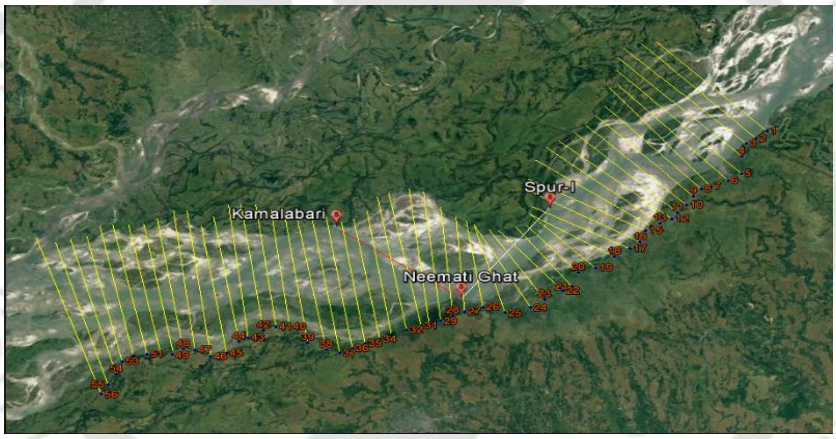

Figure 6.5 Image showing 56 nos. Cross sections for Bathymetry Survey

Figure 6.6 Image showing area of Physical Model Study

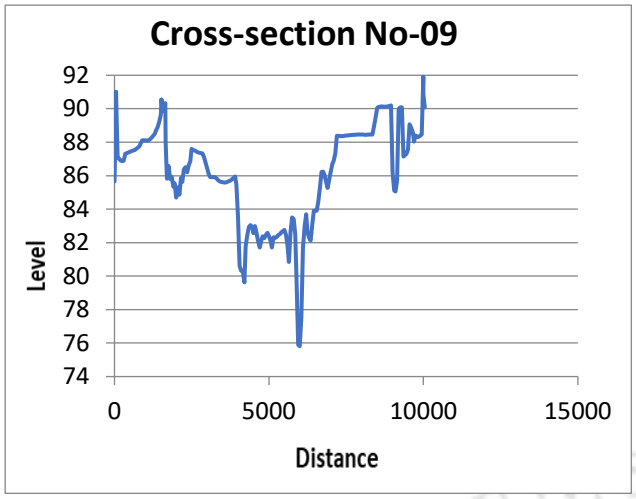
Cross-section No-09
Level
92
90
88
86
84
82
80
78
76
74
0
5000
10000
15000
Distance

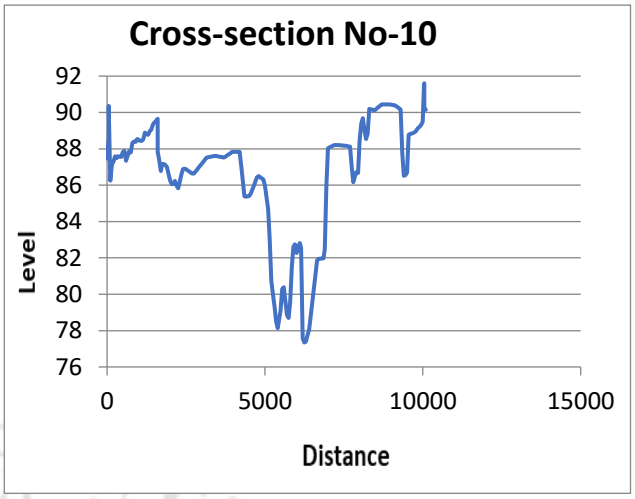
Cross-section No-10
Level
92
90
88
86
84
82
80
78
76
0
5000
10000
15000
Distance

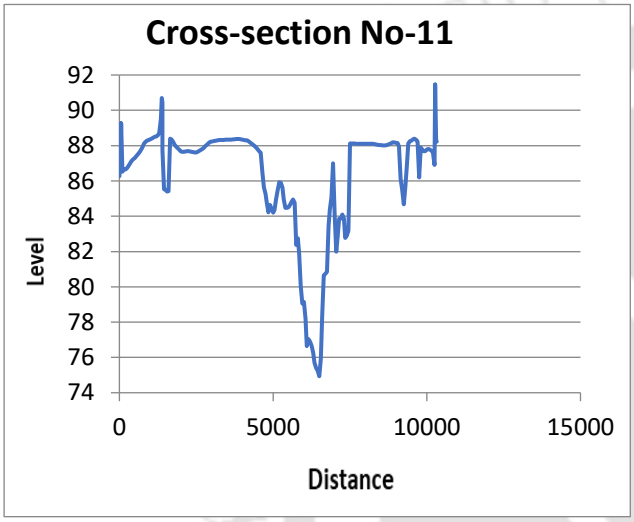
Cross-section No-11
Level
92
90
88
86
84
82
80
78
76
74
0
5000
10000
15000
Distance

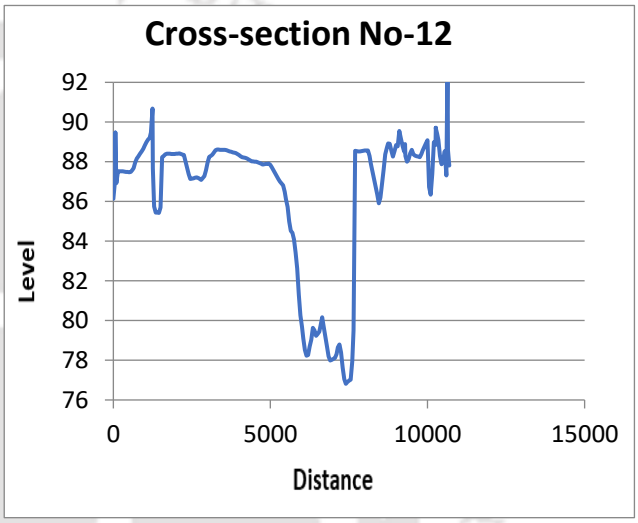
Cross-section No-12
Level
92
90
88
86
84
82
80
78
76
0
5000
10000
15000
Distance

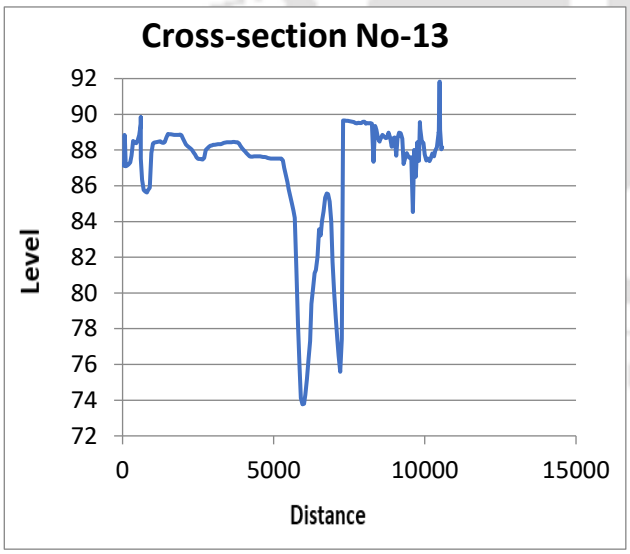
Cross-section No-13
Level
92
90
88
86
84
82
80
78
76
74
72
0
5000
10000
15000
Distance

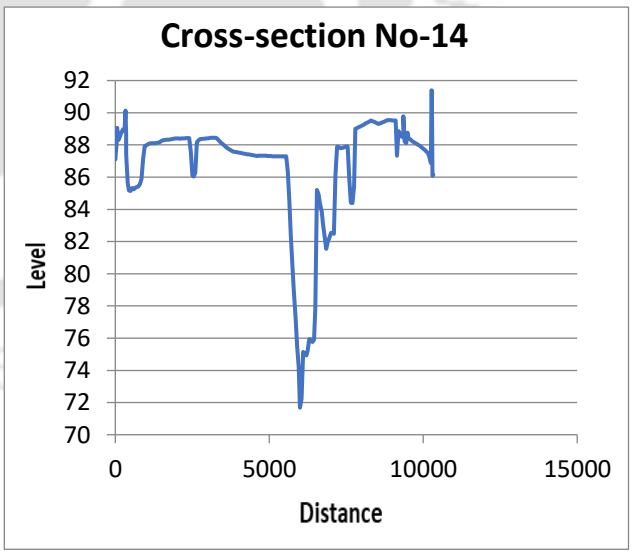
Cross-section No-14
Level
92
90
88
86
84
82
80
78
76
74
72
70
0
5000
10000
15000
Distance

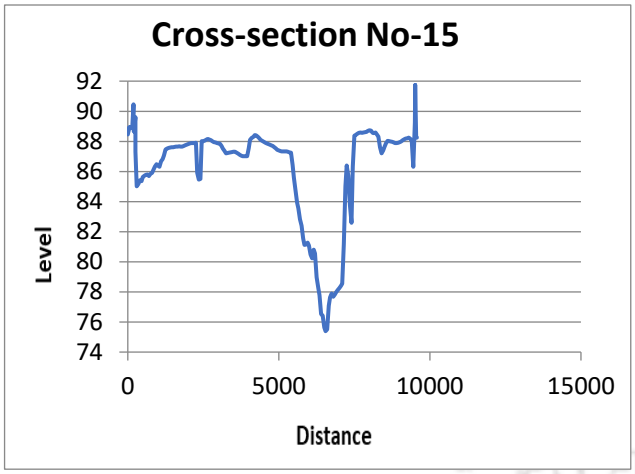
Cross-section No-15
Level
92
90
88
86
84
82
80
78
76
74
0
5000
10000
15000
Distance

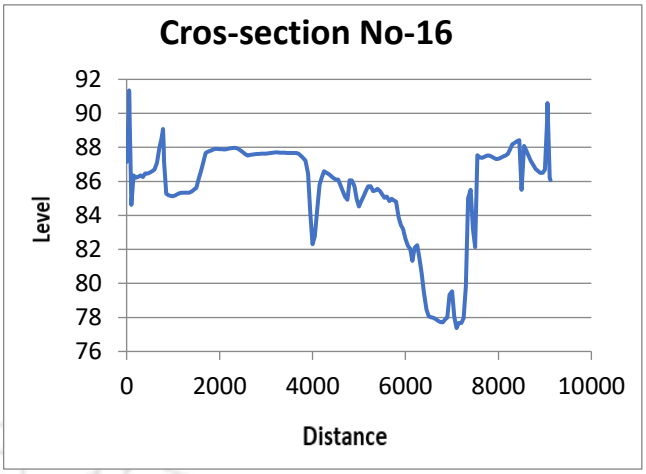
Cros-section No-16
Level
92
90
88
86
84
82
80
78
76
0
2000
4000
6000
8000
10000
Distance

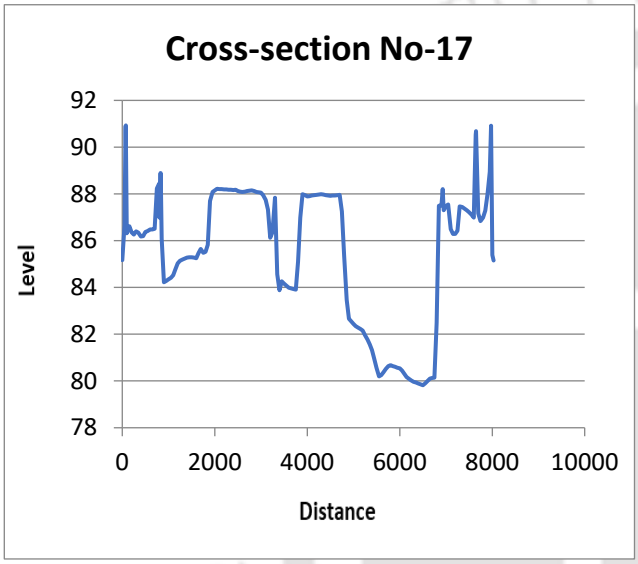
Cross-section No-17
Level
92
90
88
86
84
82
80
78
0
2000
4000
6000
8000
10000
Distance

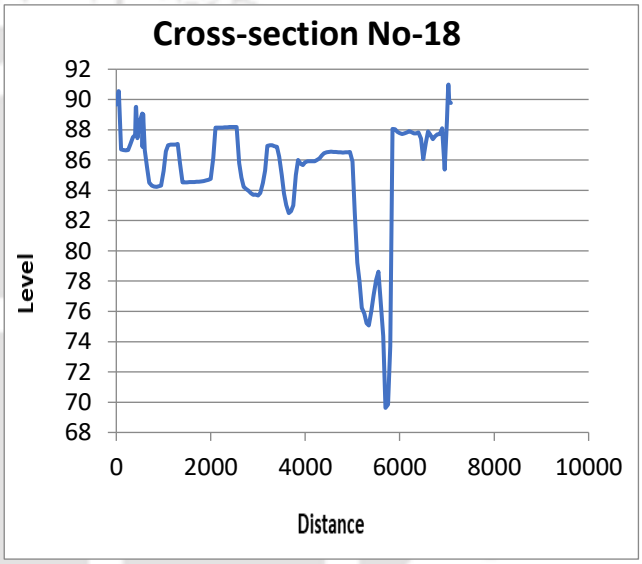
Cross-section No-18
Level
92
90
88
86
84
82
80
78
76
74
72
70
68
0
2000
4000
6000
8000
10000
Distance

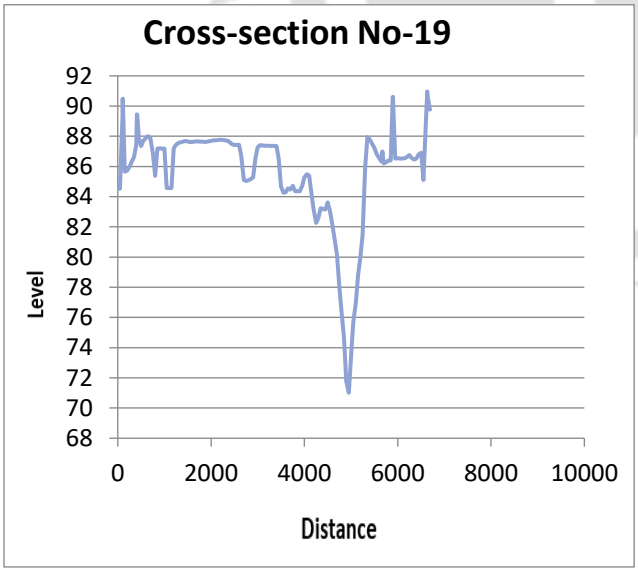
Cross-section No-19
Level
92
90
88
86
84
82
80
78
76
74
72
70
68
0
2000
4000
6000
8000
10000
Distance

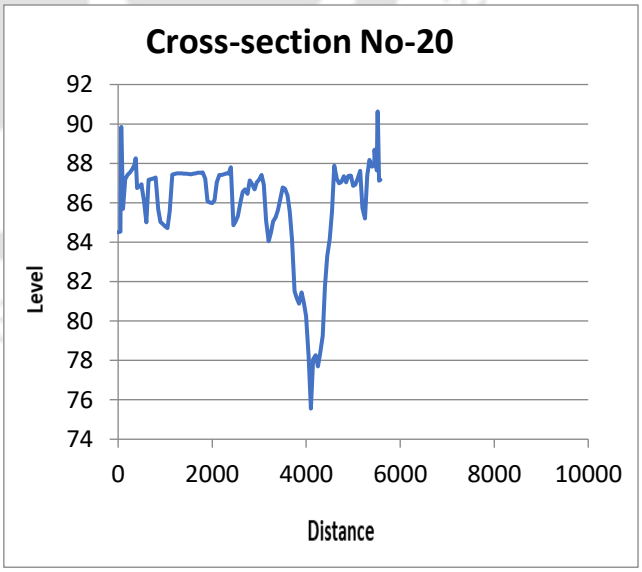
Cross-section No-20
Level
92
90
88
86
84
82
80
78
76
74
0
2000
4000
6000
8000
10000
Distance

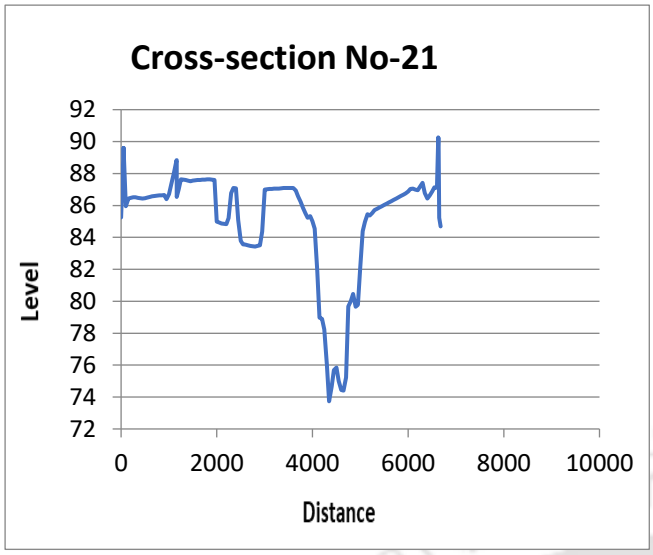
Cross-section No-21
Level
92
90
88
86
84
82
80
78
76
74
72
0
2000
4000
6000
8000
10000
Distance

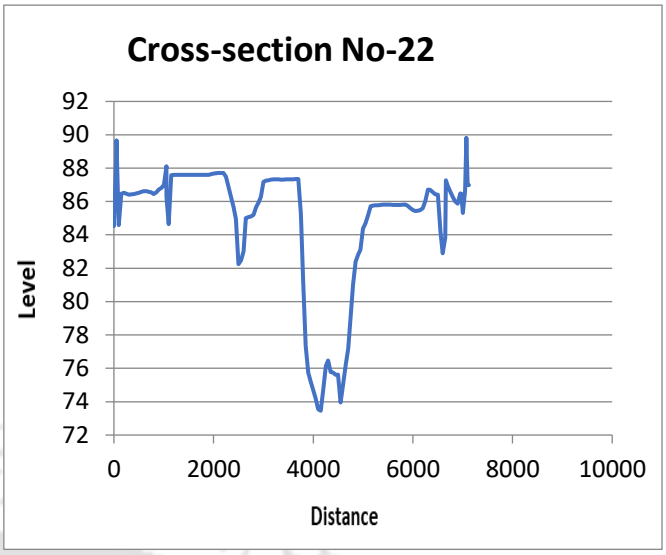
Cross-section No-22
Level
92
90
88
86
84
82
80
78
76
74
72
0
2000
4000
6000
8000
10000
Distance

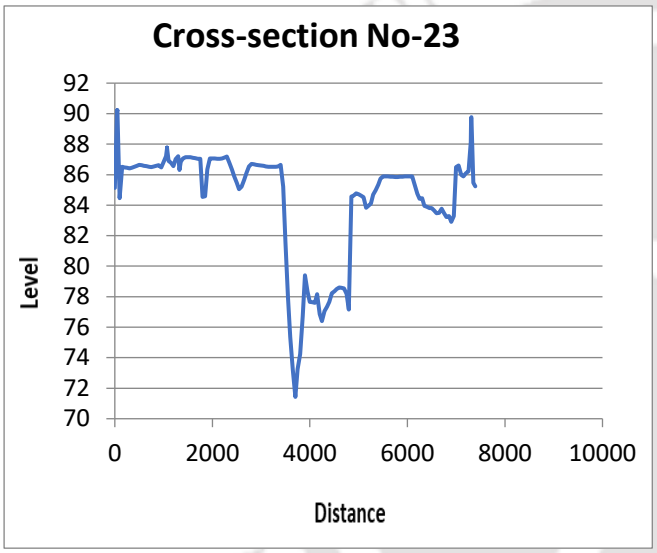
Cross-section No-23
Level
92
90
88
86
84
82
80
78
76
74
72
70
0
2000
4000
6000
8000
10000
Distance

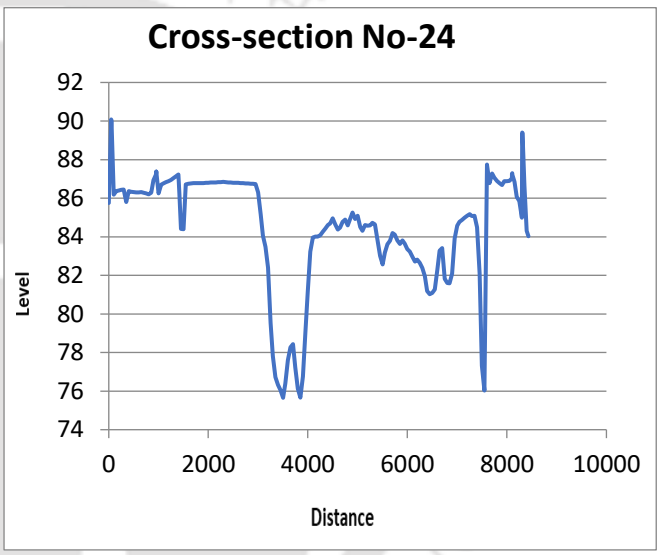
Cross-section No-24
Level
92
90
88
86
84
82
80
78
76
74
0
2000
4000
6000
8000
10000
Distance

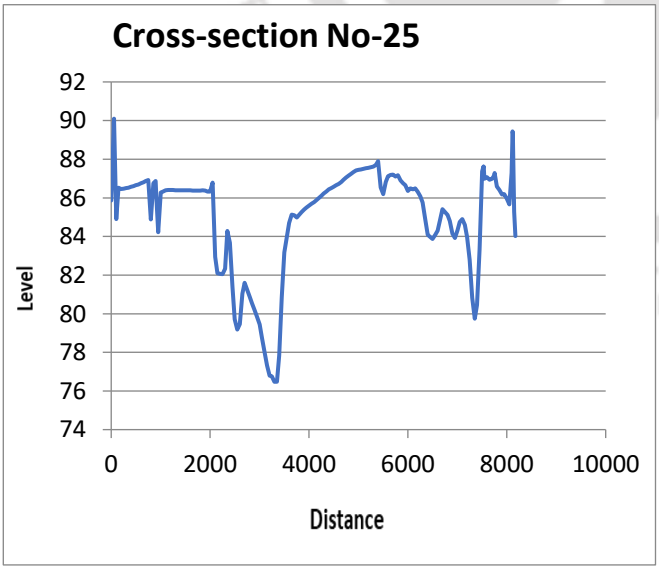
Cross-section No-25
Level
92
90
88
86
84
82
80
78
76
74
0
2000
4000
6000
8000
10000
Distance

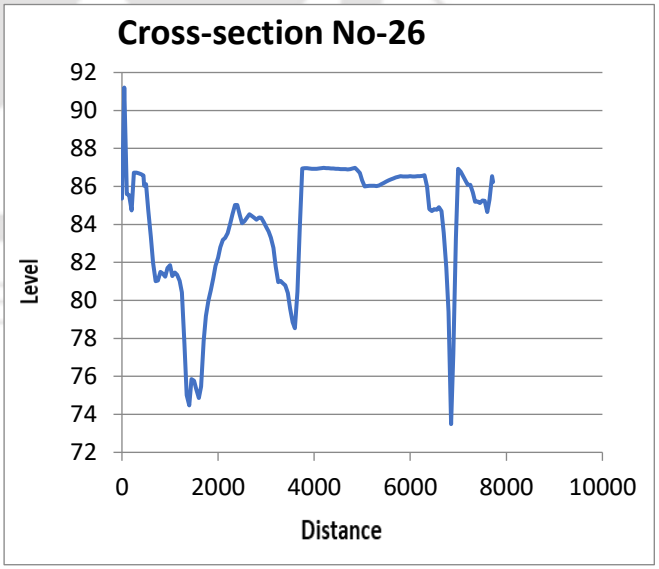
Cross-section No-26
Level
92
90
88
86
84
82
80
78
76
74
72
0
2000
4000
6000
8000
10000
Distance

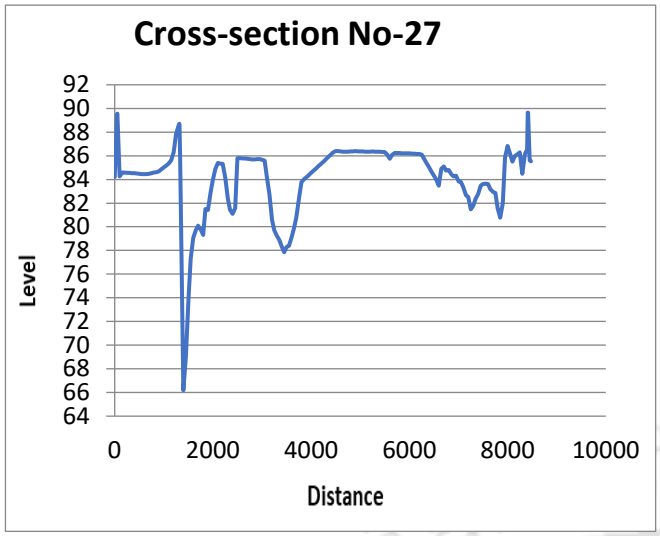
Cross-section No-27
Level
92
90
88
86
84
82
80
78
76
74
72
70
68
66
64
0
2000
4000
6000
8000
10000
Distance

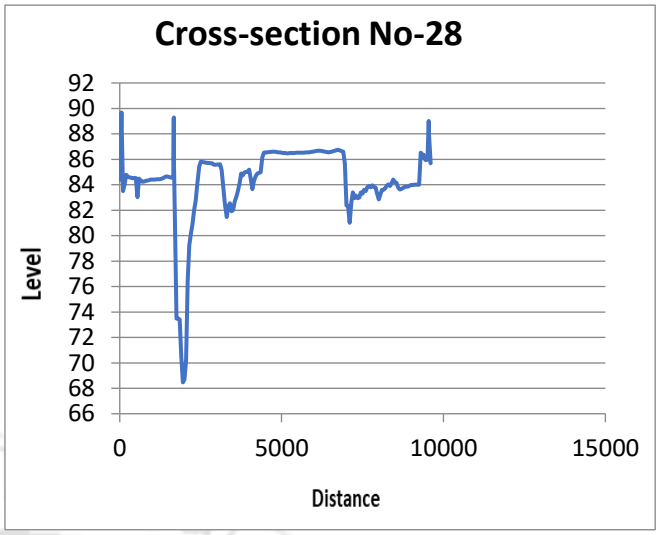
Cross-section No-28
Level
92
90
88
86
84
82
80
78
76
74
72
70
68
66
0
5000
10000
15000
Distance

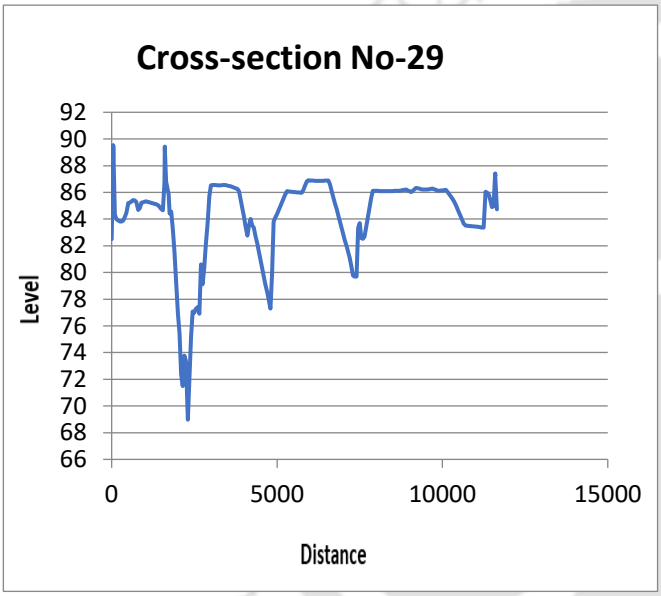
Cross-section No-29
Level
92
90
88
86
84
82
80
78
76
74
72
70
68
66
0
5000
10000
15000
Distance

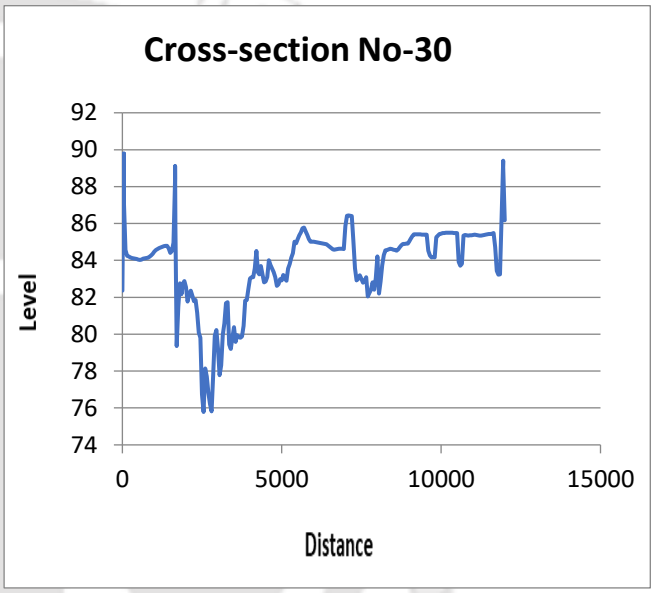
Cross-section No-30
Level
92
90
88
86
84
82
80
78
76
74
0
5000
10000
15000
Distance

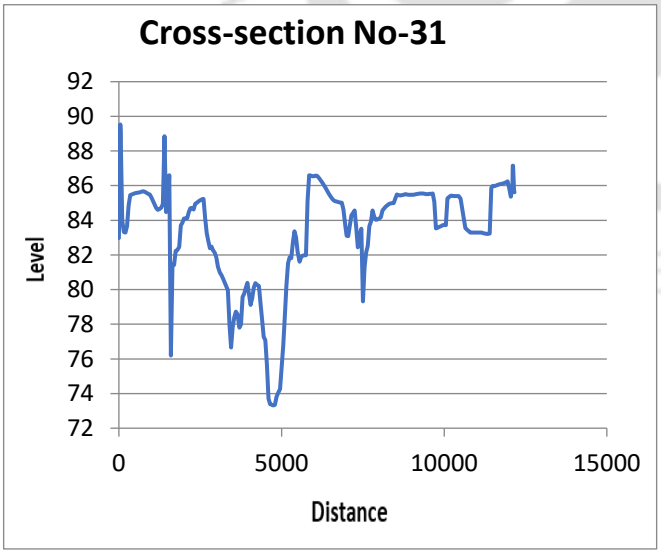
Cross-section No-31
Level
92
90
88
86
84
82
80
78
76
74
72
0
5000
10000
15000
Distance

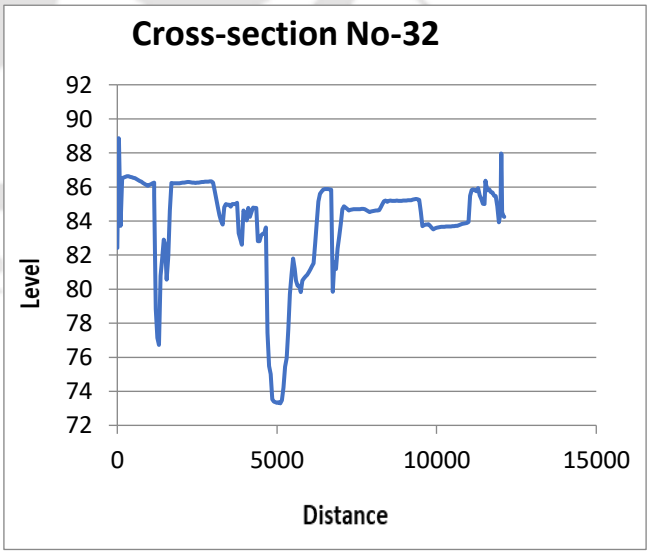
Cross-section No-32
Level
92
90
88
86
84
82
80
78
76
74
72
0
5000
10000
15000
Distance

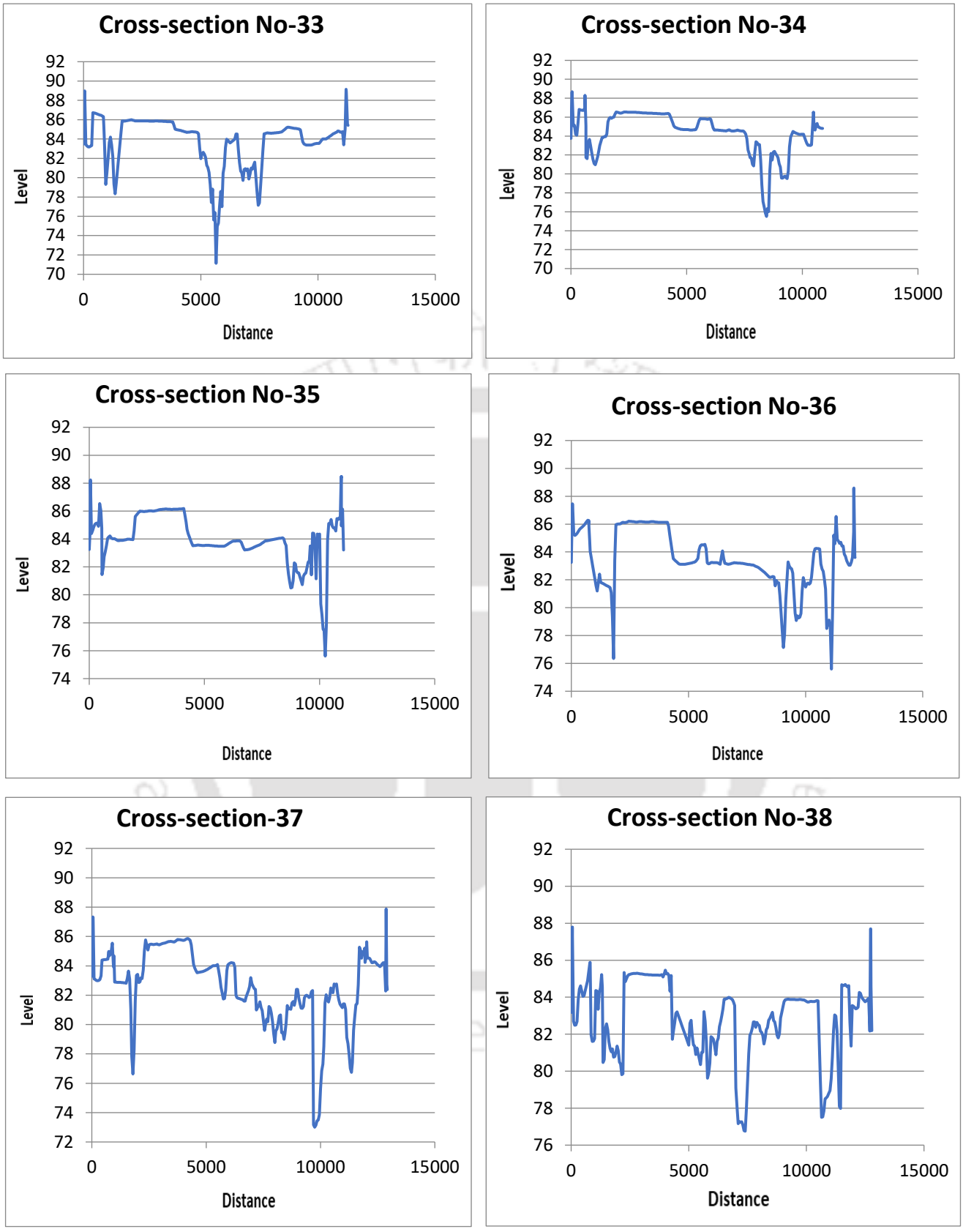

Figure 6.7 Cross-Sections of River Brahmaputra used in Physical Model Study

6.3 Hydrological Data for the Model Study:

Gauge and Discharge data

a. The daily gauge, discharge, data of river Brahmaputra at Bessamara site from 1976 to 1998 Also, there was a Gauge Discharge Silt Site at Bessamara maintained by Water Resources Department, Government of Assam. Observation of the Bessamara G/D/S station was taken on daily basis from the year 1976 to 1998. Data collection in the site was stopped from 1998 onwards. Discharge data at Bessamara for the period from 1976 to 1998 are taken into consideration for hydrological analyses. Some extreme data are not considered for this study. Monthly Maximum, Minimum and Average Water Level of river Brahmaputra at Bessamara is shown in Table 6.1.

Table 6.1 Monthly Maximum, Minimum and Average Water Level of river Brahmaputra at Bessamara

Sl. No.	Year	Month	Maximum Water Level	Minimum Water Level	Average Water Level
1	1976	January	82.90	82.58	82.72
		February	82.94	82.49	82.60
		March	83.92	83.02	83.43
		April	84.51	82.72	83.81
		May	84.94	83.30	83.96
		June	87.22	84.66	85.43
		July	86.44	84.54	85.54
		August	86.07	84.86	85.55
		September	85.46	84.44	85.00
		October	84.90	83.94	84.20
		November	84.03	83.77	83.90
		December	83.88	83.33	83.51
2	1977	January	83.37	83.22	83.30
		February	84.12	83.02	83.33
		March	84.87	83.50	84.01
		April	85.83	84.31	84.94
		May	85.83	84.36	84.95
		June	86.02	85.14	85.69
		July	86.52	85.69	86.10
		August	86.96	85.59	86.05
		September	85.84	84.81	85.20
		October	85.59	83.27	84.04
		November	83.52	82.18	82.75
		December	82.49	81.85	82.08
3	1978	January	81.89	81.72	81.79
		February	82.96	81.73	81.88

		March	82.39	81.90	82.08
		April	84.21	82.24	83.21
		May	85.48	83.81	84.33
		June	87.28	84.88	85.63
		July	86.88	85.28	85.74
		August			
		September			
		October			
		November			
		December			
4	1979	January	81.60	81.24	81.38
		February	81.54	81.16	81.28
		March	82.46	81.31	81.70
		April	83.50	82.09	82.94
		May	85.75	83.34	84.41
		June	86.40	84.20	84.95
		July	87.15	85.65	86.30
		August	86.55	85.29	86.08
		September	86.92	84.87	86.05
		October	87.21	84.11	85.46
		November	84.06	82.81	83.35
		December	83.14	82.21	82.58
5	1980	January	82.36	81.90	82.04
		February	82.46	81.92	82.13
		March	83.97	82.36	82.88
		April			
		May	85.83	84.16	84.64
		June	86.90	82.90	85.61
		July	87.23	86.12	86.49
		August	87.27	85.91	86.53
		September	85.80	85.07	85.42
		October	85.33	83.05	84.12
		November			
		December			
6	1981	January	80.96	80.71	80.84
		February	81.96	80.02	80.95
		March	82.69	81.06	81.97
		April	83.66	81.86	82.77
		May	85.22	82.77	83.77
		June	87.02	84.04	84.92
		July	86.55	85.76	86.15
		August	86.47	85.62	85.98
		September	85.95	83.98	85.16
		October	85.66	82.58	83.67
		November	82.84	81.37	81.95
		December	81.65	80.71	81.08

7	1982	January	80.69	80.36	80.50
		February	80.75	80.35	80.46
		March	81.91	80.54	80.98
		April	83.87	81.59	82.82
		May	85.48	83.39	84.01
		June	86.62	83.73	85.42
		July	86.94	85.76	86.23
		August	86.24	84.61	85.21
		September	86.94	84.41	85.45
		October	85.54	82.43	83.48
		November	82.34	81.43	81.81
		December	81.36	80.72	80.98
8	1983	January	80.73	80.24	80.44
		February	80.75	80.38	80.61
		March	82.63	80.58	81.25
		April	83.46	81.33	82.43
		May	85.29	82.93	84.16
		June	86.58	84.56	85.68
		July	86.78	85.79	86.34
		August	86.80	85.07	85.68
		September	86.91	85.36	86.06
		October	86.06	82.94	84.23
		November	82.84	81.46	82.04
		December	81.44	80.84	81.08
9	1984	January	80.96	80.61	80.75
		February	80.82	80.48	80.58
		March	82.17	80.51	81.16
		April	84.94	81.15	83.31
		May	86.45	83.25	84.50
		June	86.94	84.75	85.90
		July			
		August			
		September			
		October			
		November			
		December			
10	1989	January			
		February			
		March	81.94	81.10	81.36
		April	84.71	81.75	82.75
		May	85.06	83.29	84.01
		June	86.27	84.61	85.19
		July	87.36	85.29	86.16
		August	86.14	84.90	85.20
		September	86.21	85.06	85.51
		October	85.92	83.60	84.71

		November	83.53	82.14	82.88
		December	82.13	81.39	81.66
11	1990	January	81.39	80.00	81.06
		February	82.01	81.17	81.52
		March	82.63	81.20	81.52
		April	84.19	81.95	83.18
		May	84.95	83.06	83.99
		June	87.22	84.51	85.80
		July	86.93	85.56	86.22
		August	86.12	85.28	85.62
		September	86.61	84.94	85.52
		October	86.32	83.61	85.20
		November			
		December	85.58	81.15	81.57
12	1991	January	81.13	80.80	80.92
		February	80.89	80.72	80.79
		March	82.59	80.94	81.86
		April	84.72	80.86	83.04
		May	86.15	82.47	84.54
		June	86.54	84.16	85.60
		July	86.46	85.64	86.02
		August	86.58	85.53	86.12
		September	86.12	85.14	85.57
		October	85.21	83.85	84.28
		November	83.29	82.38	82.78
		December	82.30	81.72	81.96
13	1992	January	81.76	81.28	81.49
		February	81.88	81.46	81.73
		March	83.85	81.00	81.90
		April	84.67	82.24	83.41
		May	87.15	83.11	83.75
		June	86.50	83.55	84.38
		July	86.48	85.24	85.72
		August	85.94	84.75	85.29
		September	85.66	83.94	84.89
		October	84.59	83.15	83.82
		November	82.94	82.02	81.79
		December	81.99	81.62	81.79
14	1993	January	82.54	81.41	81.64
		February	82.85	81.35	81.86
		March	82.92	81.59	81.94
		April	83.57	81.24	82.46
		May	85.86	83.44	84.44
		June	86.50	84.25	85.55
		July	87.57	85.40	86.05
		August	86.83	85.66	86.40

		September	86.38	84.67	85.31
		October	85.85	83.13	84.27
		November	85.95	81.06	82.45
		December	82.27	81.09	81.43
15	1994	January	81.22	80.77	80.93
		February	81.11	80.77	80.92
		March	84.31	80.78	81.69
		April	84.52	82.40	83.26
		May	85.82	82.75	84.15
		June	86.91	85.10	85.89
		July	89.06	84.47	85.51
		August	85.70	85.02	85.41
		September	85.55	84.53	84.99
		October	85.23	82.89	84.08
		November	82.91	81.86	82.33
		December	82.47	81.34	81.63
16	1995	January	81.34	81.00	81.21
		February	81.98	80.95	81.16
		March	82.33	81.19	81.50
		April	83.86	81.75	82.53
		May	86.76	83.80	85.26
		June	87.21	85.15	86.00
		July	87.88	85.06	86.41
		August	86.94	85.00	85.66
		September	87.02	84.84	85.46
		October	86.89	83.00	84.63
		November	82.92	82.10	82.50
		December	82.05	81.45	81.71
17	1996	January			
		February			
		March			
		April			
		May			
		June	85.82	84.21	85.30
		July			
		August			
		September	85.82	84.47	85.12
		October	85.69	82.04	82.71
		November	84.57	82.04	82.71
		December	81.99	81.22	81.57

Table 6.2 shows the yearly maximum water level of Brahmaputra River at Bessamara

Table 6.2 Yearly Maximum Water Level of Brahmaputra River at Bessamara

Year	Maximum WL
1976	87.22
1977	86.96
1978	87.28
1979	87.21
1980	87.27
1981	87.02
1982	86.94
1983	86.91
1984	86.94
1989	87.36
1990	87.22
1991	86.58
1992	87.15
1993	87.57
1994	89.06
1995	87.88
1996	85.82

Figure 6.8 shows the Maximum WL for the period 1976 to 1996 at Bessamara

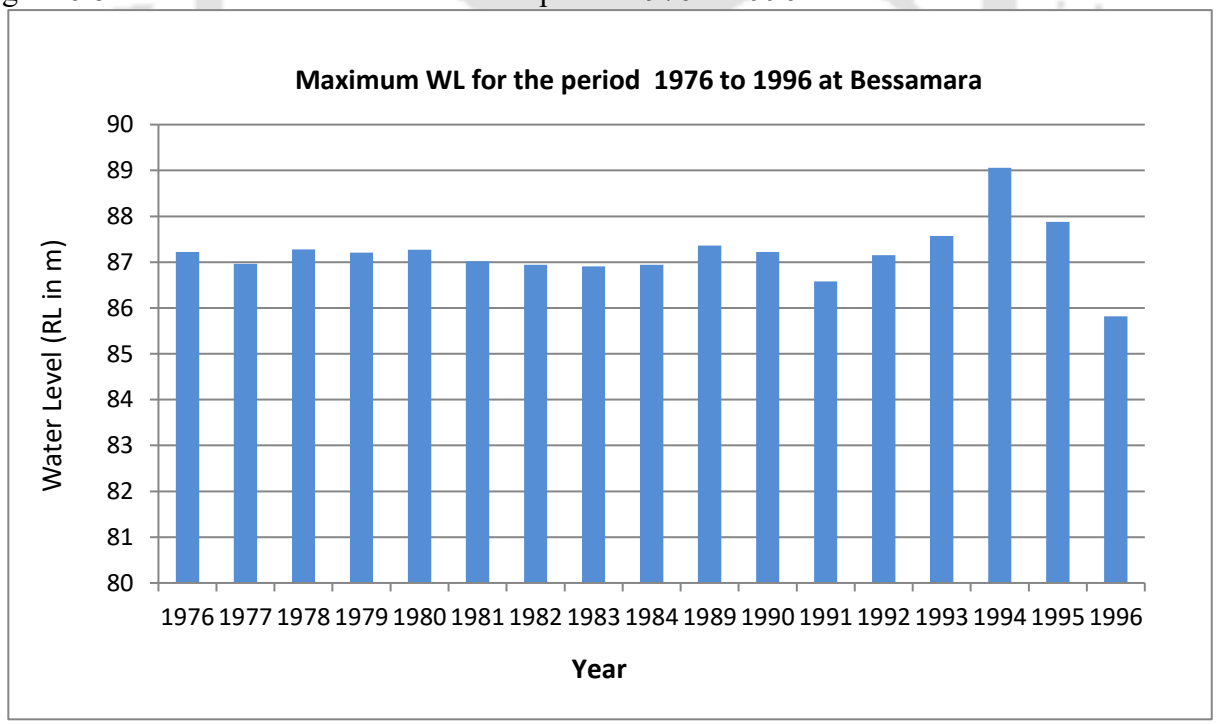

Figure 6.8 Maximum WL for the period 1976 to 1996 at Bessamara

Table 6.3 shows the monthly maximum, minimum and average water level of Brahmaputra River at Bessamara from 1976 to 1993

Table 6.3 Monthly Maximum, Minimum and Average Water Level of Brahmaputra River at Bessamara from 1976 to 1993			
Month	Maximum WL	Minimum WL	Average WL
January	83.37	80.00	81.40
February	84.12	80.02	81.45
March	84.87	80.51	81.95
April	85.83	80.86	83.12
May	87.15	82.47	84.30
June	87.28	82.90	85.47
July	89.06	84.47	86.07
August	87.27	84.61	85.77
September	87.02	83.94	85.38
October	87.21	82.04	84.19
November	85.95	81.06	82.43
December	85.58	80.71	81.76

Figure 6.9 shows the water level for the period 1976 to 1996 at Bessamara

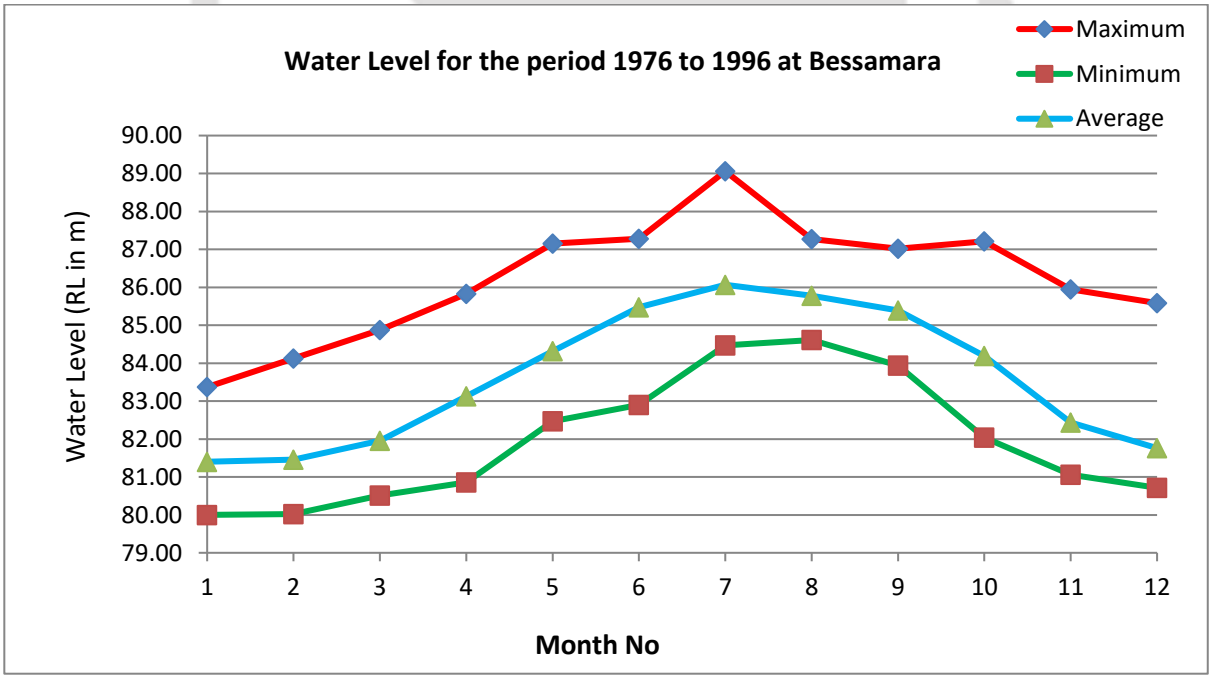

Figure 6.9 Water Level for the period 1976 to 1996 at Bessamara

Monthly Maximum, Minimum and Average Discharge Data of river Brahmaputra at Bessamara is shown in Table 6.4.

Table 6.4 Monthly Maximum, Minimum and Average Discharge Data of river Brahmaputra at Bessamara

Sl. No.	Year	Month	Maximum Discharge	Minimum Discharge	Average Discharge
1	1976	January	2525.33	1807.71	2094.00
		February	2756.61	1586.48	2320.87
		March	4685.60	2791.93	3917.03
		April	5347.03	4333.06	4847.50
		May	6118.11	4673.00	5269.14
		June	18926.11	6237.11	11228.51
		July	17779.96	10342.20	14703.42
		August	16021.48	10657.97	12919.15
		September	13699.36	9092.76	10860.91
		October	10646.71	7759.84	9076.74
		November	8471.97	6951.89	7536.74
		December	7079.98	5072.92	6244.84
2	1977	January	5351.50	3968.88	4451.84
		February	5180.16	2912.49	3838.35
		March	4960.41	3251.95	3859.63
		April	8039.15	4196.58	5974.49
		May	11311.95	6087.20	8725.73
		June	19502.22	15155.38	17398.89
		July	29258.42	15099.17	20068.88
		August	26021.55	12243.31	18827.46
		September	19002.65	11238.47	14754.79
		October	19717.19	5908.46	10404.81
		November	5446.33	2750.33	3997.06
		December	3310.92	1939.50	2507.67
3	1978	January	2106.04	1809.33	1919.09
		February	2273.55	1738.15	1954.91
		March	2957.80	1917.02	2384.78
		April	6719.21	3628.10	4853.72
		May	10517.60	5073.73	7095.78
		June	28022.40	8720.67	14588.28
		July	19445.51	14758.56	17601.76
		August			
		September			
		October			
		November			
		December			
4	1979	January	2586.31	1417.94	2093.41

		February	2228.03	1250.32	1572.40
		March	4352.91	1745.34	2395.74
		April	7504.19	3454.35	5821.21
		May	13297.05	7227.25	8841.69
		June	16413.82	7937.19	9810.11
		July	29450.00	13862.16	19647.66
		August	18980.29	11102.18	15682.60
		September	24557.00	10957.52	15851.89
		October	25275.32	2662.80	14049.97
		November	7896.29	3817.16	5422.58
		December	4647.62	2614.11	3533.68
5	1980	January	2831.52	1350.12	1934.35
		February	2971.27	1355.95	1802.95
		March	5705.64	2526.58	4232.05
		April			
		May	10605.27	8140.03	9319.08
		June	23999.20	8086.61	14294.26
		July	29617.00	15528.40	20328.30
		August	29709.93	11231.98	20371.10
		September	14892.58	12514.63	13767.51
		October	13179.13	5462.08	9695.16
		November			
		December			
6	1981	January	1745.49	1001.28	1299.41
		February	3357.50	1441.49	1782.57
		March	3848.58	1966.31	2489.66
		April	5791.36	2320.38	4533.79
		May	12751.78	4058.88	7970.05
		June	27844.48	9368.84	13451.22
		July	14568.50	10950.00	12549.17
		August	20245.50	10240.29	16990.99
		September	16962.63	11382.90	14045.28
		October	19530.24	9331.84	12491.05
		November	9770.49	4125.05	7318.70
		December	4045.72	1897.12	3176.65
7	1982	January	1858.05	1412.45	1652.21
		February	1707.65	1374.80	1526.04
		March	2714.45	1044.55	1848.47
		April	5754.51	2526.92	4499.00
		May	12482.86	5314.65	7585.14
		June	26871.12	8537.89	13184.89
		July	27869.50	15203.10	18528.46
		August	17096.74	14047.00	15389.59
		September	27939.00	14653.04	17444.56
		October	16278.36	13158.75	14620.67
		November	11041.00	3169.13	7633.60

		December	5280.05	2369.08	3553.28
8	1983	January	2666.34	1033.88	1608.04
		February	2076.14	1433.64	1769.24
		March	2810.19	1631.51	2131.85
		April	4426.51	2343.36	3457.99
		May	14140.82	3794.42	7681.54
		June	19678.84	10627.84	15229.41
		July	29288.52	16006.92	19907.47
		August	28952.00	15906.27	16926.24
		September	17490.69	16433.32	16870.89
		October	14704.08	6318.01	8315.87
		November	9158.70	5134.00	5895.21
		December	5002.12	2202.65	3531.58
9	1984	January	2839.61	2005.51	2416.31
		February	2703.04	1693.69	1942.49
		March	3261.67	1862.63	2484.74
		April	5290.20	2928.76	4318.61
		May	15721.71	4843.49	8606.94
		June	25291.81	11845.83	16700.97
		July			
		August			
		September			
		October			
		November			
		December			
10	1989	January			
		February			
		March	2618.49	1928.00	2130.55
		April	3312.67	1201.37	2176.95
		May	6750.09	2556.91	3893.60
		June	18818.45	4662.55	8764.89
		July	39091.36	18729.58	23921.36
		August	19084.47	16411.24	17219.79
		September	19181.02	7634.68	11744.97
		October	8451.34	4492.86	6981.74
		November	4321.53	2067.08	2760.31
		December	2180.17	2017.44	2045.86
11	1990	January	3134.73	2046.42	2136.64
		February	3011.68	2344.20	2696.51
		March	3678.66	2430.86	2904.27
		April	3873.89	2918.28	3448.62
		May	7541.64	3607.31	4614.75
		June	36088.15	12852.00	20275.56
		July	31646.40	12852.00	20275.56
		August	17817.36	11958.71	14575.80
		September	21858.71	15644.80	17597.64

		October	19039.38	13576.75	17501.40
		November			
		December	2843.60	2203.55	2502.65
12	1991	January	2246.10	2042.28	2134.66
		February	2304.61	2038.02	2120.39
		March	2543.70	2220.81	2315.70
		April	3957.98	2255.27	3308.48
		May	7492.81	3245.71	5487.08
		June	18870.11	6267.54	11936.64
		July	21551.76	16530.22	19296.02
		August	18733.51	15525.06	17519.06
		September	17460.50	15332.89	16576.46
		October	16739.18	7958.10	14270.44
		November	9373.43	3404.19	4494.86
		December	3477.25	2007.66	3195.93
13	1992	January	2858.04	2351.71	2557.13
		February	2370.08	2234.98	2290.56
		March	10044.20	2233.81	4135.13
		April	11620.86	7212.09	9324.72
		May	13952.37	10504.75	11747.92
		June	19165.95	11747.96	13932.04
		July	18602.81	16338.38	17827.93
		August	18194.79	15350.88	16468.84
		September	16818.46	14041.66	15699.01
		October	15482.26	11229.77	13209.63
		November	10941.93	6008.75	7721.33
		December	5940.13	4149.24	5206.65
14	1993	January	4838.49	3011.54	3886.88
		February	5152.82	2615.26	3314.24
		March	4218.71	2326.26	2707.22
		April	5957.35	3304.52	4435.63
		May	12433.64	6575.89	11029.35
		June	13987.62	11208.13	12970.43
		July	32660.71	10117.63	22456.34
		August	31617.52	13419.84	23775.79
		September	19623.31	15544.75	17145.87
		October	17472.10	9440.53	12943.46
		November	9286.74	8242.60	8657.28
		December	8332.58	7231.94	7645.41
15	1994	January	7137.25	6200.74	6594.23
		February	6200.74	4439.48	5037.11
		March	11202.99	4544.31	6139.13
		April	13354.62	7129.37	8961.11
		May	14933.77	8542.26	10111.32
		June			
		July			

		August			
		September			
		October			
		November			
		December			
16	1995	January			
		February			
		March			
		April			
		May			
		June			
		July			
		August			
		September			
		October			
		November			
		December			
17	1996	January			
		February			
		March			
		April			
		May			
		June	31536.00	11433.77	19884.82
		July			
		August			
		September	16355.91	13977.78	15210.61
		October	14004.44	1619.70	9739.66
		November	6598.54	4302.24	9343.70
		December	5878.51	4455.30	5037.95

Table 6.5 shows the yearly maximum discharge data of Brahmaputra River at Bessamara

Table 6.5 Yearly Maximum Discharge Data of Brahmaputra River at Bessamara	
Year	Maximum Discharge (cumec)
1976	18926.11
1977	29258.42
1978	28022.40
1979	29450.00
1980	29709.93
1981	27844.48
1982	27939.00
1983	29288.52
1984	25291.81
1989	39091.36
1990	36088.15
1991	21551.76
1992	19165.95
1993	32660.71

Figure 6.10 shows the Maximum Discharge for the period 1976 to 1993 at Bessamara

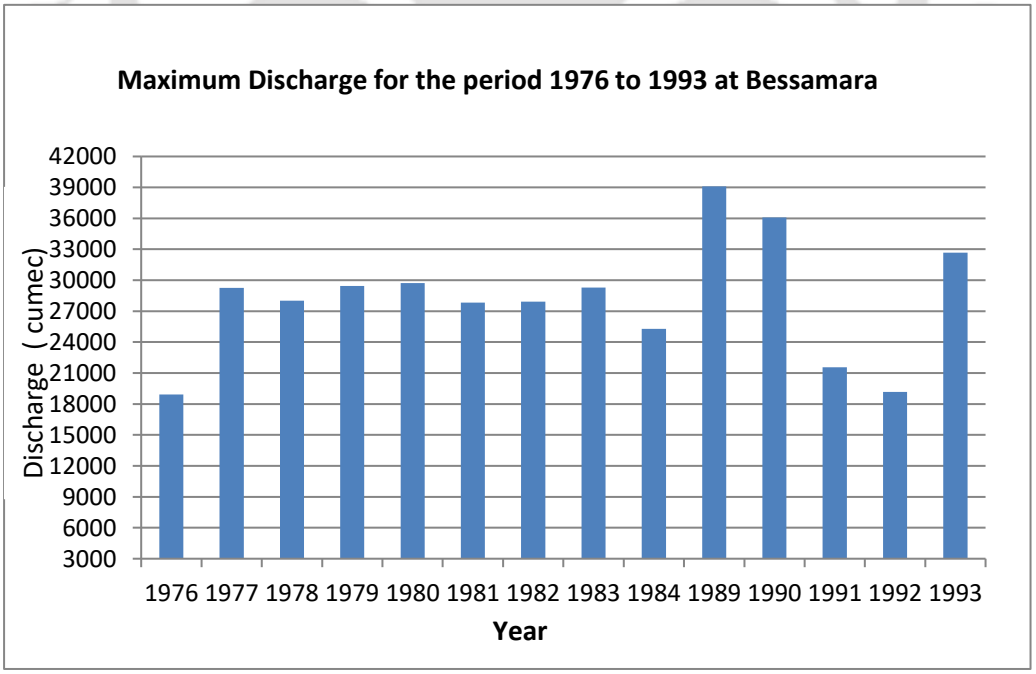

Figure 6.10 Maximum Discharge for the period 1976 to 1993 at Bessamara

The Table 6.6 shows monthly maximum, minimum and average discharge data of Brahmaputra River at Bessamara from 1976 to 1993.

Table 6.6 Monthly Maximum, Minimum and Average Discharge Data of Brahmaputra River at Bessamara from 1976 to 1993			
Month	Maximum Discharge	Minimum Discharge (cumec)	Average Discharge
January	5351.50	1001.28	2321.84
February	5180.16	1250.32	2225.50
March	10044.20	1044.55	2852.63
April	11620.86	1201.37	4692.36
May	15721.71	2556.91	7704.84
June	36088.15	4662.55	13840.44
July	39091.36	10117.63	19008.64
August	31617.52	10240.29	17222.20
September	27939.00	7634.68	13290.20
October	25275.32	2662.80	11227.44
November	11041.00	2067.08	6143.77
December	8332.58	1897.12	3922.20

Figure 6.11 shows the Maximum Discharge for the period 1976 to 1993 at Bessamara

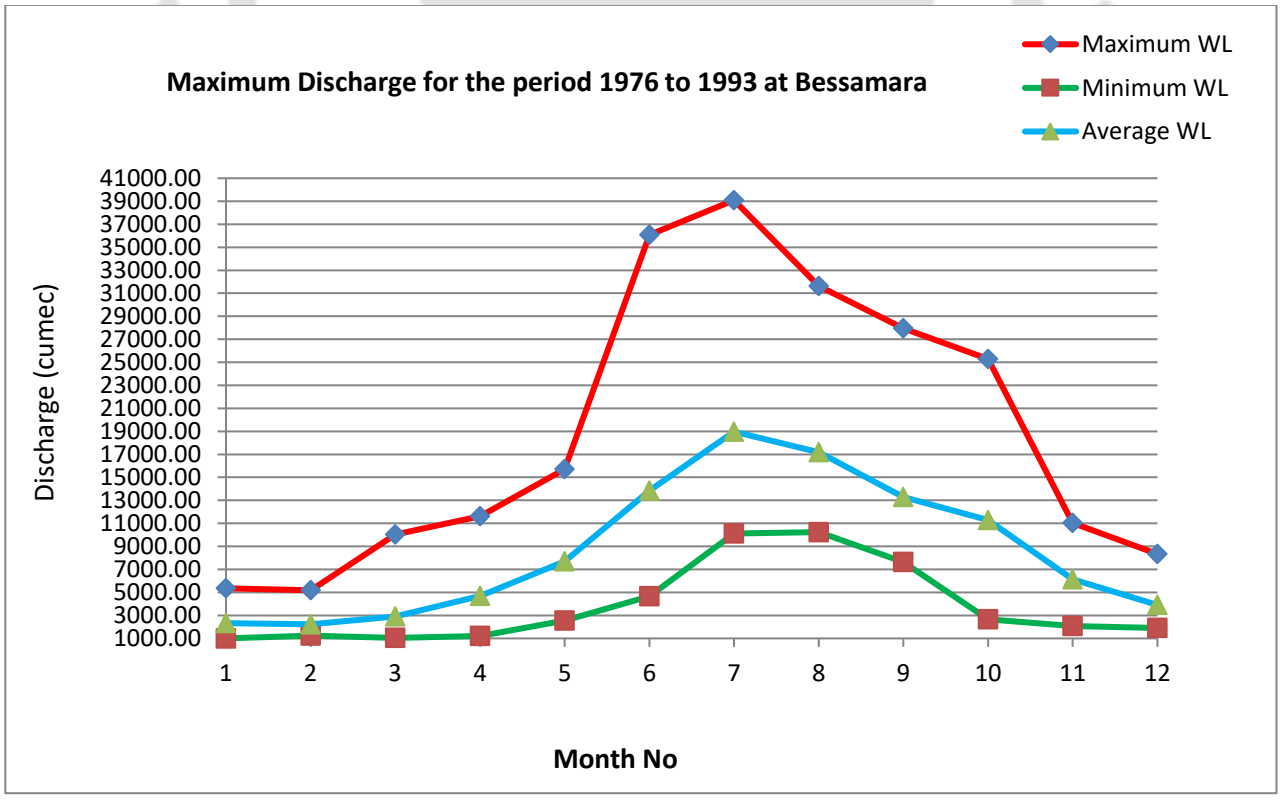

Figure 6.11 Maximum Discharge for the period 1976 to 1993 at Bessamara

Rating Curve of Bessamara Site is shown in Figure 6.12

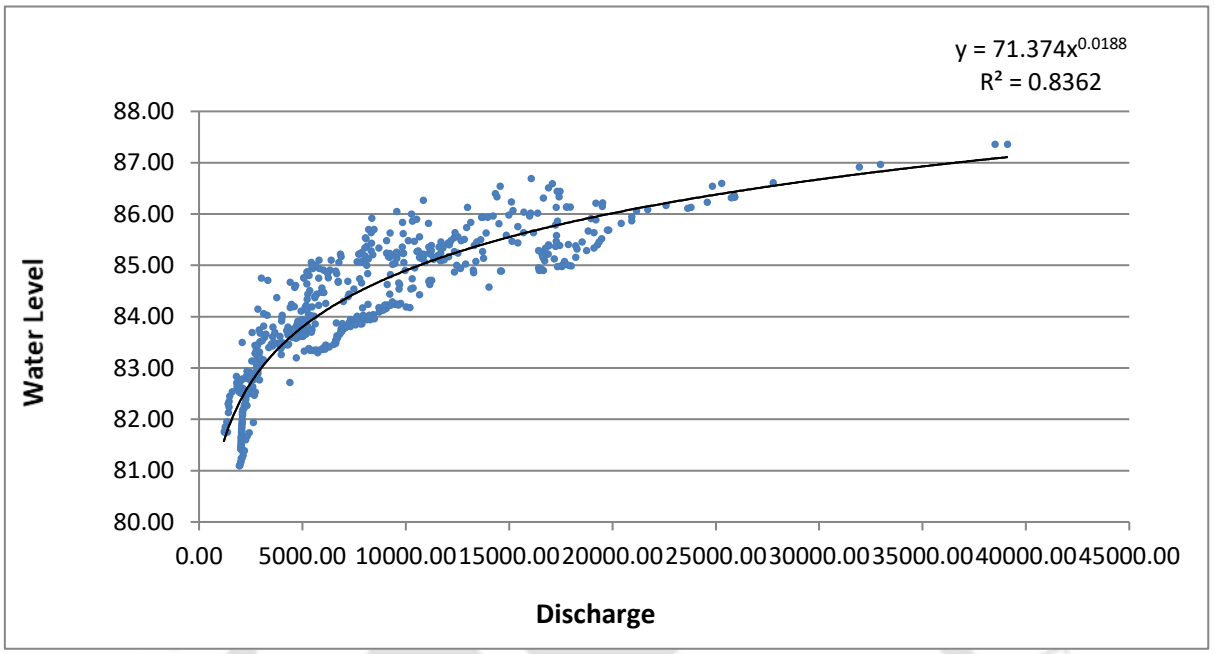

Figure 6.12 Rating Curve of Bessamara Site

FLOOD FREQUENCY ANALYSIS

RIVER: Brahmaputra
Site: Bessamara
Unit: CUMEC

LOG-PEARSON TYPE III

YEAR	PEAK CUMEC	REARRANGED PEAK	Y=LN(Q)	(Y-YAVG)	(Y-YAVG)^2	(Y-YAVG)^3		RANK
1976	18926.11	39091.36	10.5737	0.3481	0.1211	0.0422		1
1977	29258.42	36088.15	10.4937	0.2681	0.0719	0.0193		2
1978	28022.40	32660.71	10.3939	0.1683	0.0283	0.0048		3
1979	29450.00	29709.93	10.2992	0.0736	0.0054	0.0004		4
1980	29709.93	29450.00	10.2904	0.0648	0.0042	0.0003		5
1981	27844.48	29288.52	10.2850	0.0593	0.0035	0.0002		6
1982	27939.00	29258.42	10.2839	0.0583	0.0034	0.0002		7
1983	29288.52	28022.40	10.2408	0.0152	0.0002	0.0000		8
1984	25291.81	27939.00	10.2378	0.0122	0.0001	0.0000		9
1989	39091.36	27844.48	10.2344	0.0088	0.0001	0.0000		10
1990	36088.15	25291.81	10.1382	-0.0874	0.0076	-0.0007		11
1991	21551.76	21551.76	9.9782	-0.2474	0.0612	-0.0151		12
1992	19165.95	19165.95	9.8609	-0.3647	0.1330	-0.0485		13
1993	32660.71	18926.11	9.8483	-0.3773	0.1424	-0.0537		14
		YAVG =	10.2256021		0.582576248	-0.050739024	N=	14

STD. DEV = 0.211692129
SKEW COF = -0.479989144

RETURN PERIOD (YEAR)	K	DISCHARGE CUMEC
2	0.053303792	27914.07
5	0.853920157	33069.62
10	1.243106376	35909.53
25	1.636407838	39027.30
50	1.878763872	41081.85
100	2.0890099	42951.59
1000	2.639747459	48262.78
10000	3.051617296	52659.69

FLOOD FREQUENCY ANALYSIS

GUMBEL'S E.V. DISTRIBUTION

RIVER: Brahmaputra Site: Bessamara

YEAR	PEAK CUMEC	REARRANGED PEAK Q	RANK M	RETURN PERIOD T=N+1/M	QAVG-Q	(QAVG-Q)^2 x 10^4		REDUCED VARIATE
1976	18926.11	39091.36	1	15	-10927.88857	11941.87486		1
1977	29258.42	36088.15	2	8	-7924.678571	6280.053046		2
1978	28022.40	32660.71	3	5	-4497.238571	2022.515477		3
1979	29450.00	29709.93	4	4	-1546.458571	239.1534113		4
1980	29709.93	29450.00	5	3	-1286.528571	165.5155765		5
1981	27844.48	29288.52	6	3	-1125.048571	126.5734288		6
1982	27939.00	29258.42	7	2	-1094.948571	119.8912374		7
1983	29288.52	28022.40	8	2	141.0714286	1.990114796		8
1984	25291.81	27939.00	9	2	224.4714286	5.038742224		9
1989	39091.36	27844.48	10	2	318.9914286	10.17555315		10
1990	36088.15	25291.81	11	1	2871.661429	824.643936		11
1991	21551.76	21551.76	12	1	6611.711429	4371.472801		12
1992	19165.95	19165.95	13	1	8997.521429	8095.539186		13
1993	32660.71	18926.11	14	1	9237.361429	8532.884616		14
	QAVG =	28163.47143	14		SUM OF =	42737.32199		
			N=		(QAVG-Q)^2	X 10^4		

STD. DEV= 5733.66053

CO. VAR = 0.203585007

RETURN PERIOD (YEAR)	DISCHARGE CUMEC
2	27221.591
5	32288.596
10	35643.394
20	38861.397
25	39882.190
50	43026.771
100	46148.133
1000	56462.089
10000	66757.847

U = 25583.08915

ALFA = 4470.516774

Table 6.7 shows the yearly maximum, minimum discharge data of Brahmaputra River at Bessamara

Table 6.7 Yearly Maximum, Minimum Discharge Data of Brahmaputra River at Bessamara

Year	Maximum Discharge	Date	Minimum Discharge	Date	Remarks
1976	18926.11	14.06.76	1586.48	03.02.76	1119.77 cumec lowest discharge observed on 28.12.80
1977	26021.55	28.08.77	1939.50	27.12.77	
1978	28022.40	24.06.78	1812.54	19.01.78	
1979	29719.69	07.10.79	1250.59	14.02.79	
1980	29709.93	17.08.80	1119.77	28.12.80	
1981	28101.63	04.07.81	1897.12	31.12.81	
1982	27939.00	16.09.82	1374.80	04.02.82	
1983	28952.00	01.08.83	2202.65	26.12.83	
1984	29224.82	10.07.84	1693.69	20.02.84	51384.96 cumec highest discharge observed on 13.08.87
1985	31591.48	25.07.85	1501.84	31.01.85	
1986	26716.20	16.09.86	1373.62	01.02.86	
1987	51384.96	13.08.87	2226.62	25.01.87	
1988	-	-	-	-	
1989	39091.36	03.07.89	1201.37	12.04.89	
1990	36088.15	09.06.90	2046.42	28.01.90	
1991	39182.65	18.06.91	2038.02	05.02.91	
1992	33259.00	27.06.92	2233.00	05.03.92	
1993	32660.71	04.07.93	2326.26	12.03.93	
1994	-	-	-	-	
1995	-	-	-	-	
1996	-	-	-	-	
1997	38277.94	10.07.97	2014.08	31.12.97	
1998	38213.78	04.09.98	-	-	

B. Gauge data at Nimati Ghat

There is Gauge station at Nimati Ghat maintained by CWC. Hourly Gauge data from 2014 to 2019 is studied. Figure 6.13 shows the yearly maximum water level of Brahmaputra River at Nimati Ghat.

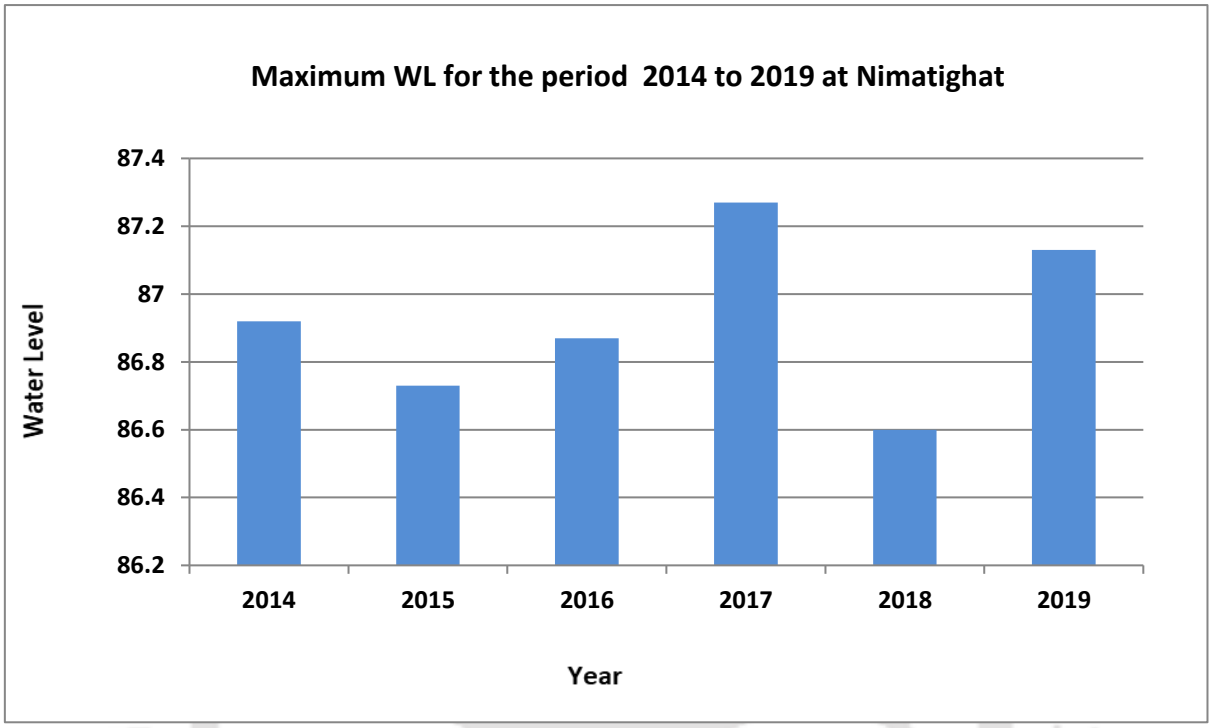

Figure 6.13 Yearly Maximum Water Level of Brahmaputra River at Nimati Ghat

Figure 6.14 shows the monthly maximum, minimum and average water level of Brahmaputra River at Nimati Ghat from 2014 to 2019.

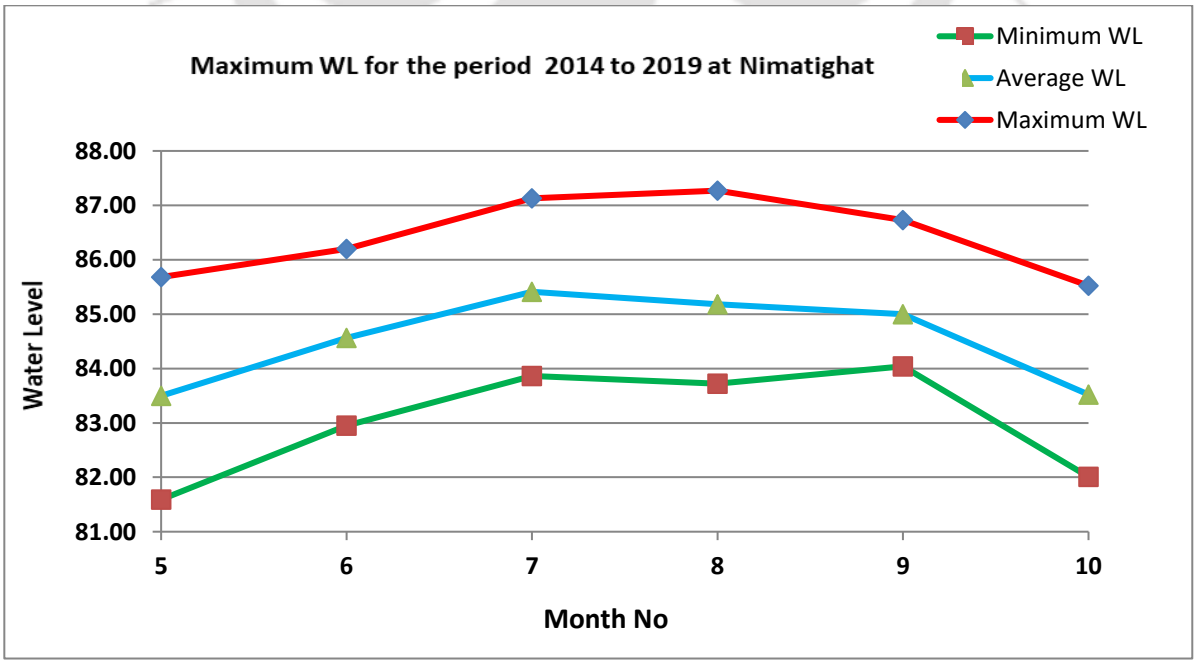

Figure 6.14 Monthly Maximum, Minimum and Average Water Level of Brahmaputra River at Nimati Ghat from 2014 to 2019

C. Gauge data at Kamalabari

There is Gauge station at Kamalabari. Daily Gauge data from 2008, 2009 & 2011 to 2020 is studied. Monthly Maximum, Minimum and Average Water Level of Brahmaputra River at Kamalabari is shown in Table 6.8.

Table 6.8 Monthly Maximum, Minimum and Average Water Level of Brahmaputra River at Kamalabari

Sl. No.	Year	Month	Maximum Water Level	Minimum Water Level	Average Water Level
1	2008	May	82.68	81.54	82.11
		June	83.00	80.10	82.06
		July	84.95	82.30	83.98
		August	85.41	82.64	84.33
		September	85.19	82.54	83.81
		October	82.14	81.24	81.86
2	2009	May	81.57	80.67	81.21
		June	83.52	81.16	81.91
		July	84.97	81.23	83.63
		August	84.90	81.23	84.01
		September	84.96	81.23	83.70
		October	83.66	81.99	82.60
3	2011	May	82.20	80.53	81.06
		June	82.80	80.93	82.19
		July	83.53	80.80	82.15
		August	86.60	84.20	85.66
		September	84.36	82.63	83.00
		October	83.49	81.74	82.68
4	2012	May	84.95	83.22	83.86
		June	86.84	83.87	84.95
		July	87.71	86.60	87.12
		August	85.38	84.07	84.65
		September	85.94	83.04	84.64
		October	85.88	83.06	84.17
5	2013	May	84.13	83.39	83.77
		June	85.59	82.67	83.87
		July	85.60	82.60	83.74
		August	86.97		85.38
		September	85.17		82.73
		October	83.43	82.60	82.88
6	2014	May	84.45	82.85	83.51
		June	84.92	83.22	83.94
		July	85.51	83.22	83.94
		August	86.29	84.25	85.00
		September	84.73	82.94	83.94
		October	83.79	82.72	83.00

7	2015	May	81.93	80.76	81.31
		June	83.26	81.03	82.13
		July	84.98	83.18	84.20
		August	86.00	82.52	84.18
8	2016	May	84.92	83.26	83.61
		June	85.67	83.38	84.24
		July	86.37	84.76	85.40
		August	84.65	83.54	84.29
		September	85.22	83.54	84.20
		October	84.99	83.07	83.80
		November	82.92	82.92	82.98
9	2017	May	83.55	82.92	83.19
		June	84.72	82.86	83.60
		July	86.07	84.00	84.80
		August	86.72	84.03	84.67
		September	85.28	83.60	84.20
		October	84.72	83.47	83.80
10	2018	May	83.55	80.67	81.57
		June	83.05	81.08	81.60
		July	84.54	83.41	83.86
		August	84.26	83.39	83.81
		September	84.95	83.00	83.82
		October	82.86	82.42	82.74
11	2019	May	83.37	81.42	82.19
		June	84.90	83.20	84.06
		July	84.95	82.24	83.90
		August	84.59	83.13	83.90
		September	85.10	83.00	84.01
		October	83.51	81.27	82.28
12	2020	May	83.97	81.12	82.49
		June	85.31	83.22	84.27
		July	85.51	83.58	84.48
		August	85.33	83.85	84.48
		September	84.11	83.69	83.86
		October			

Table 6.9 shows the yearly maximum water level of Brahmaputra River at Kamalabari

Table 6.9 Yearly Maximum Water Level of Brahmaputra River at Kamalabari	
Year	Maximum WL
2008	85.41
2009	84.97
2011	86.60
2012	87.71
2013	86.97
2014	86.29
2015	86.00
2016	86.37
2017	86.72
2018	84.95
2019	85.10
2020	85.51

Maximum Water Level for the period 2008 to 2020 at Kamalabari is shown in Figure 6.15

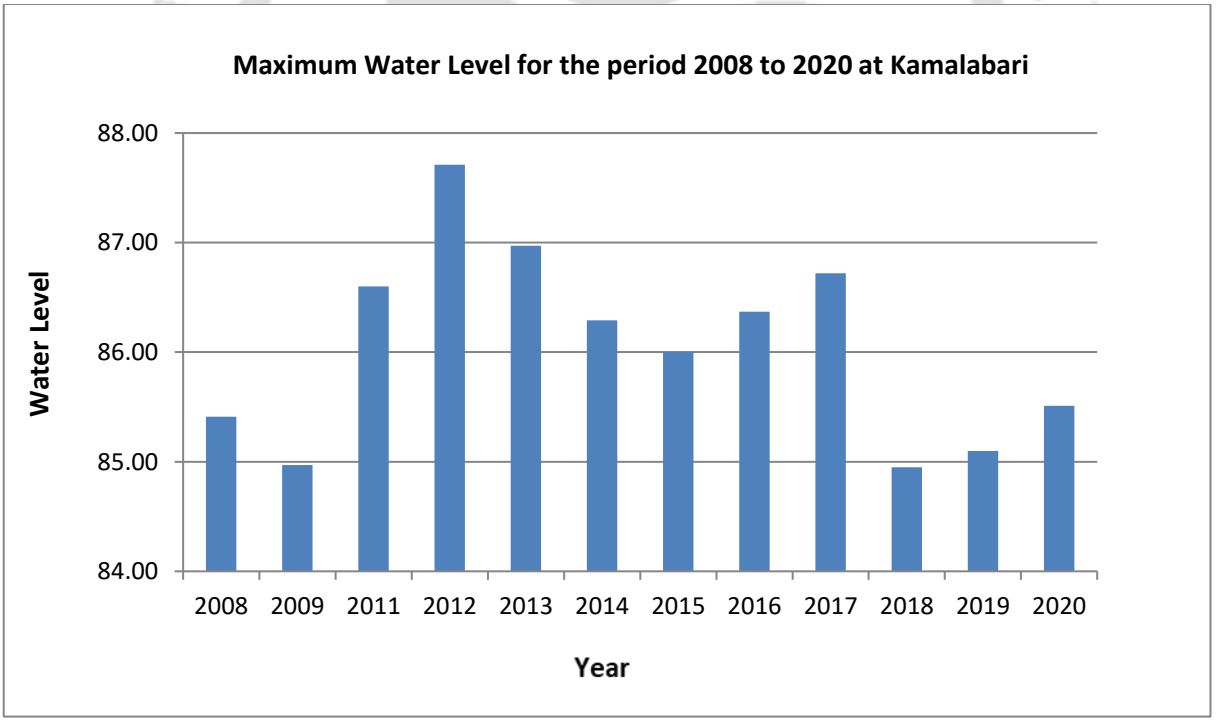

Figure 6.15 Maximum Water Level for the period 2008 to 2020 at Kamalabari

Monthly Maximum, Minimum and Average Water Level of Brahmaputra River at Kamalabari from 2014 to 2019 is shown in Table 6.10

Table 6.10 Monthly Maximum, Minimum and Average Water Level of Brahmaputra River at Kamalabari from 2014 to 2019

Month	Maximum WL	Minimum WL	Average WL
May	84.95	80.53	82.49
June	86.84	80.10	83.23
July	87.71	80.80	84.27
August	86.97	81.23	84.53
September	85.94	81.23	83.79
October	85.88	81.24	83.10

Maximum Water Level for the period 2008 to 2020 at Kamalabari is shown in Figure 6.16

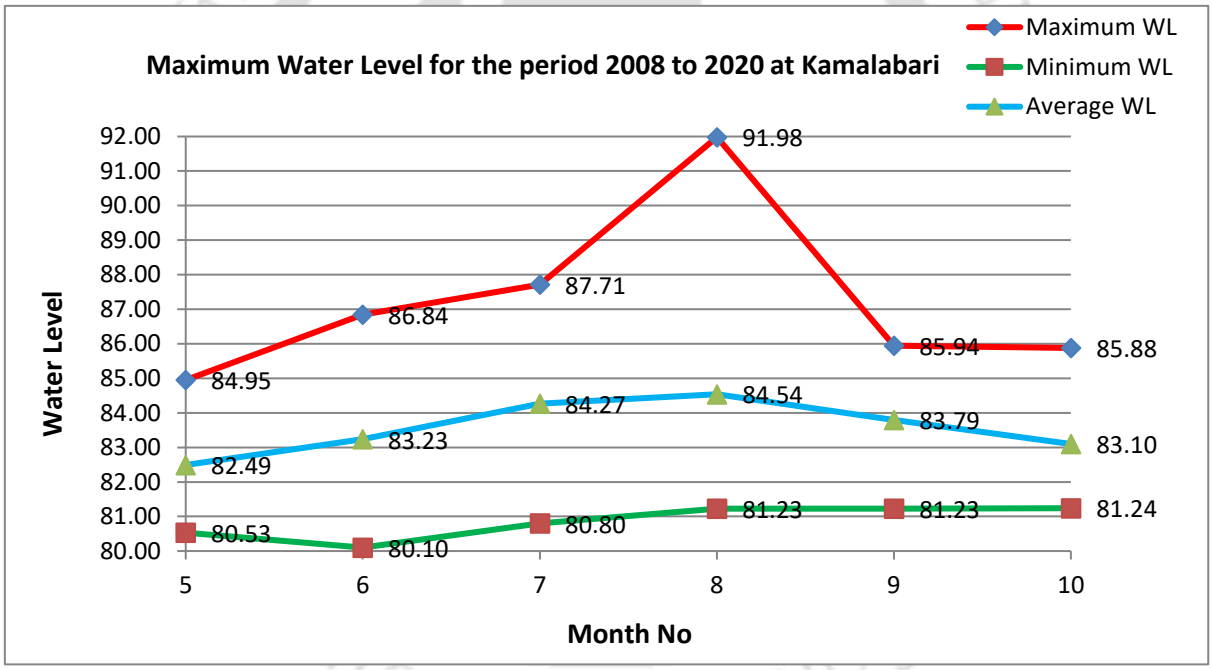

Figure 6.16 Maximum Water Level for the period 2008 to 2020 at Kamalabari

6.4 Design of Scale as per Froudian Similitude:

$F_r = \frac{V}{\sqrt{gd}}$ or $V_r = \sqrt{D_r} = \sqrt{67} = 8.185$

Horizontal scale L_r= 1:500 Vertical exaggeration VE

Vertical scale ratio D_r= 1:67 $= \frac{500}{67} = 7.46$

= Slope exaggeration

Which implies that model bed slope is 7.46 times skipper than proto slope.

Time water wave $t_r = 1:\frac{L}{\sqrt{D}} = 1: \frac{500}{\sqrt{67}} = 1:61.08$

Velocity Scale

U = 1: $\sqrt{D}$ = 1:8.185 implies that model velocity is 8.185 less than prototype velocity

∴ Prototype velocity = Model velocity X 8.185

Discharge Scale q = 1: L_r x D_rx $\sqrt{D_r}$

= 1: 500 x 67x$\sqrt{67}$

= 1: 2,74,209.3

= 1: 2,74,210

Which implies that Model Discharge = Prototype Discharge/ q

For Prototype q = 60,000m^3/sec

Model q $= \frac{60,000}{2,74,209.3}$

= 0.02188 m^3/sec

Water circulation discharge at NEHARI is sufficient

Forces/ Stress = 1: L x D^2

= 1:500 x 67^2

= 1:22,44500

Let us take discharge of Bessamora DDS site

Max^m Q = 60,000 m^3/sec

Water surface slope 1:7500

WL at Bessamara = 88.67 m

Deepest bed well = 70.69 m

Flow depth = 17.98 ≈ 18 m

As per present cross-sectionMax^m Water depth = 19.731 m

(in cross-section no. 27)

Tractive force=τ_{proto} = γds γ=Specific wtof water in kg/m^3

= 1000 X 18 X 1/7500 d=Depth of flow in m

= 2.4 kg/m^2 S =Slope (Water surface)

=1:7500

If Scale (L) =1:500

(D) =1:67

τ_{scale} $= d_s S = d_s \frac{d_s}{L_s} = \frac{d_s^2}{L_s} = \frac{67 \text{ X } 67}{500} = 8.98$

$\tau_{model} \approx \frac{\tau_{proto}}{\tau_{scale}} = \frac{2.4}{8.98} = 0.27 \text{ kg/m}^2$

$\tau_{model} \approx 3.06 = \frac{0.27}{0.088} = 3.06\ \tau_c$ (for Q = 60,000m^3/sec

For D_{50} 0.33mm dia sand

Critical tractive force τ_c= 0.088 kg/m^2

Hence $\tau_{model} > \tau_c$, 0.27> 0.088 ok

Depth$= \frac{1800}{67}$ = 26.86 cm = Depth of water in model

Checking for lower discharge

Say Q proto = 15,000m^3/sec

Deepest bed level = 71m & Water Level = 82m

∴flow depth = Water Level- Deepest bed level

= 82-71= 11m

Tractive force = τ_{proto} = γds

= 1000 X 11X $\frac{1}{7500} = \frac{110}{75}$

$\tau_{proto} = \frac{110}{75} = 1.467$ kg/m^2

$\tau_{scale} = \frac{ds^2}{Ls} = \frac{67 \text{ X } 67}{500} = 8.98$

$\tau_{model} = \frac{\tau_{proto}}{\tau_{scale}} = \frac{1.467}{8.98} = 0.163$ kg/m^2

τ_c = 0.088

$\tau_{model} > \tau_c$

∴ $\frac{\tau_m}{\tau_c} = \frac{0.163}{0.088} = 1.85$ ok

Flow depth = $\frac{1100}{67} = 16.42$ cm

Velocity at Q, 15,000m^3/sec

V_{proto} = 2.00m/sec

∴ Average velocity = 2.00 X 0.85

= 1.7m/sec

$V_{model} = \frac{1.7}{\sqrt{67}} = \frac{1.7}{8.18}$ Velocity, scale = $\sqrt{D}$

= 0.20m/sec = $\sqrt{67}$

= 20.78cm/sec

Checking of tractive force for incipient motion

Prototype tractive force

Cross-section No	Channel	Q= A X V (m^3/sec)	Area (A) m^2	Wetted perimeter (P)m	R = $\frac{A}{P}$ (m)	v(m/sec)	Tractive force τ = wRS (kg/m^2)
16	1	1100	1394	885	1.58	0.782	
	2	23442	15524	3696	4.20	1.51	0.56
26	1	23251	14704	3234	4.54	1.58	0.61
	2	3008	2262	644	3.51	1.33	

Main Channel is considered for design of scale ratio, regime and sediment transport scale etc.

(i) For medium sand critical tractive force

τ_c =0.18N/m^2

n = 0.02

v = 0.50 m/sec

From shield diagram, considering sand dia. to be used in model d_{50} = 0.30 mm

For d_{50} = 0.30 mm τ_o=0.19N/m^2

$\tau_c = \frac{\tau_o}{g}$ g = 9.81 m/s^2

$= \frac{0.19}{9.81}$ = 0.0194 kg/m^2

3 times of τ_c = τ_cx3 = 0.0194 x 3 = 0.058 kg/m^2

(ii) Mayer Peter Muller equation

τ_c= 0.078 d = 0.078 x $\frac{0.30}{1000}$ (6.1)

= 0.014 kg/m^2

(iii) By ASCE Manual No- 54

τ_c= 0.018lb/ft^2

$= \frac{0.018 \times 10.76}{2.2}$ = 0.088/m^2

6.5 UAV Study on Physical Model of River Brahmaputra

Figure 6.17 shows A photo during use of Unmanned Aerial Vehicle (UAV) to generate digital surface models (DSMs) of model bed.

Figure 6.17 A photo during use of UAV to generate Digital Surface Models (DSMs) of model bed

UAV/drone is flown over a sample area of the physical model, the images are taken so that Digital Surface Model (DSM) can be generated in that area. The images are imported to the Pix4D software and point cloud is generated in the software using the GCPs. DSM and orthomosaic images are generated using this point cloud. Digital Surface Model (DSM) and orthomosaic images are generated before and after dredging in the physical model of Majuli reach in river Brahmaputra. The images generated before and after dredging are compared and it is observed that the difference can be visualized clearly. The DSMs are imported to ArcGIS software and contour maps are generated with 1cm and 1mm contour interval. Now, with this concept, we can study the effect of dredging in river Brahmaputra by physical model study.

Figure 6.18 shows the UAV Ortho-mosaic image and DSM of Model area before dredging and Figure 6.19 shows the UAV ortho-mosaic image and DSM of Model area after dredging

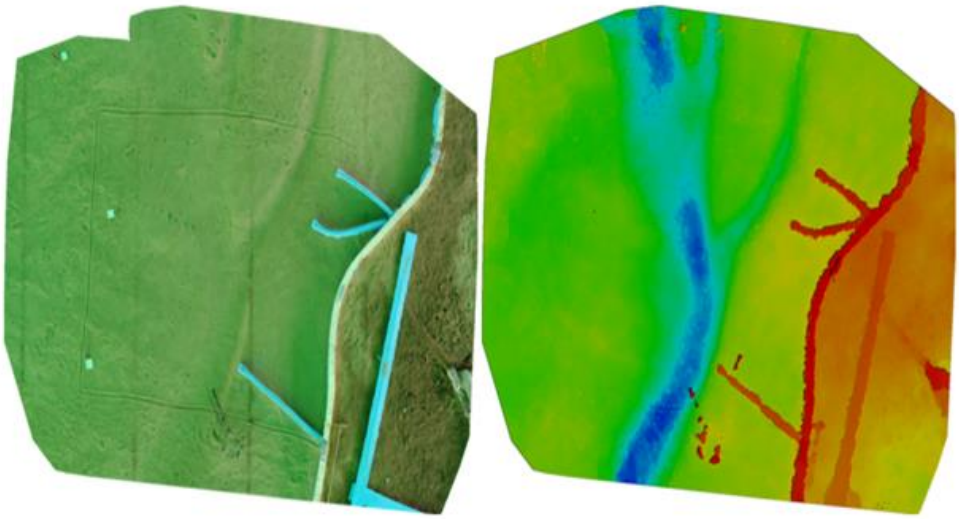

Figure 6.18 UAV ortho-mosaic image and DSM of Model area before dredging

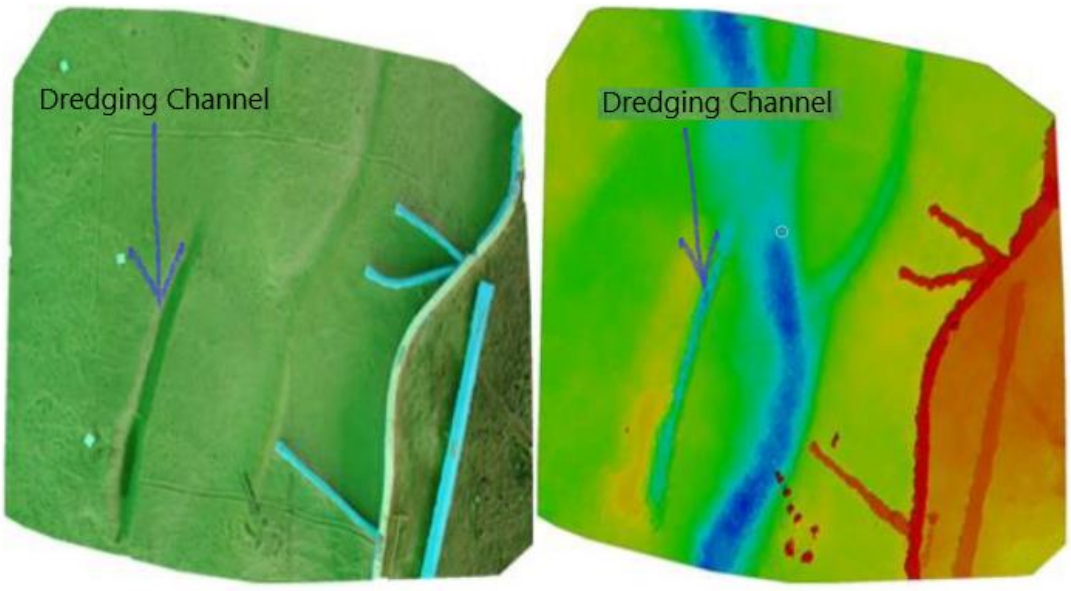

Figure 6.19 UAV ortho-mosaic image and DSM of Model area after dredging

6.6 Observation of Depth and Velocity in the Present Physical Model Study

The area of concern i.e. Nimatighat is located on the left bank of river Brahmaputra. Nimatighat is an important river port which connects Majuli Island with Jorhat District. Nimatighat is around 20 km from Jorhat Town and is considered one of the major lifelines for inhabitants of Majuli Island. The Brahmaputra River is obliquely hitting the river bank at Nimatighat and a major portion of the bank has already eroded by the river. This erosion poses a serious threat to the District Administration. Various efforts have been undertaken by concerned organizations to control the erosion from time to time. Accordingly, a physical model study of this reach has been conducted to study the effects of the river flow towards Nimatighat in order to find an amicable solution to control the erosion at Nimatighat area. The critical reaches of Majuli Island have been moulded for the x-sections starting from x-section 9 to 39 in the physical model. The area of study i.e. Nimatighat in the south bank, lies near 3 (three) x-sections i.e. x-section 25, 26 and 27 in the physical model.

A channel has been dredged in the area of study with widths varying from 100 m to 400 m with an idea to divert the flow of the river away from Nimatighat. Porcupine screens were also laid upstream of the area of study to divert the river flow towards the dredged channel. The readings and observations for different discharges and channel widths (both without and with porcupine screens) are obtained from the 3 (three) x-sections i.e. x-section 25, 26 and 27 in the physical model. The effects of river flow in various scenarios i.e. considering varying widths and discharges have been studied and are being presented hereunder in Table 1. Discharges to the tune of 10,000 cumecs to 30,000 cumecs for each channel width of 100 m, 200 m, 300 m and 400 m have been physically regulated and laid in the model to study the effects.

Table 6.11 Velocities before and after dredging without porcupine.										
Scenarios Average of 10,000; 20,000; and 30,000 cumecs	**Location**	**Velocity before dredging**				**Velocity after dredging (Without Porcupine)**				**% Change in Av. velocity**
		CS25	**CS26**	**CS27**	**Avg.**	**CS25**	**CS26**	**CS27**	**Avg.**	
Scenario - 1 (@ 100 m channel)	Left Bank	0.180	0.155	0.250	0.195	0.118	0.130	0.217	0.155	-20.76%
	Dredged Channel	0.065	0.098	0.200	0.121	0.303	0.268	0.242	0.271	124.26%
Scenario - 2 (@ 200 m channel)	Left Bank	0.180	0.155	0.250	0.195	0.092	0.106	0.186	0.128	-34.53%
	Dredged Channel	0.065	0.098	0.200	0.121	0.319	0.276	0.259	0.285	135.75%
Scenario - 3 (@ 300 m channel)	Left Bank	0.180	0.155	0.250	0.195	0.017	0.090	0.226	0.111	-43.17%
	Dredged Channel	0.065	0.098	0.200	0.121	0.311	0.295	0.265	0.290	140.07%
Scenario - 4 (@ 400 m channel)	Left Bank	0.180	0.155	0.250	0.195	0.000	0.096	0.223	0.106	-45.62%
	Dredged Channel	0.065	0.098	0.200	0.121	0.331	0.254	0.268	0.284	135.11%

The following can be observed from the aforesaid Table 6.11: -

(1) In respect of Scenario 1, for dredging channel width of 100 m, it can be observed that average velocity on the left bank (i.e. towards Nimatighat) has decreased by 20.76 % and average velocity in the dredged channel has increased from 0.121 m/s to 0.271 m/s which is by 124.26%.

(2) In respect of Scenario 2, for dredging channel width of 200 m, it can be observed that average velocity on the left bank (i.e. towards Nimatighat) has decreased by 34.53 % and average velocity in the dredged channel has increased from 0.121 m/s to 0.285 m/s, i.e. by 135.75 %, which is a higher than Scenario 1.

(3) In respect of Scenario 3, for dredging channel width of 300 m, it can be observed that average velocity on the left bank (i.e. towards Nimatighat) has decreased by 43.17 %. The average velocity in the dredged channel has increased from 0.121 m/s to 0.290 m/s, i.e. by 140.07 %, which is also the highest observed average velocity in comparison to all other scenarios.

(4) In respect of Scenario 4, for dredging channel width of 400 m, it can be observed that average velocity on the left bank (i.e. towards Nimatighat) has decreased by 45.62 % which is somewhat higher than Scenario 3. The average velocity in the dredged channel has increased from 0.121 m/s to 0.284 m/s, i.e. by 135.11 %, which lower in comparison to Scenario 3.

Velocity of flow hitting the river bank is more or less directly proportional to the quantum of erosion of the bank i.e. more velocity towards the bank means higher likelihood of erosion of the river bank or vice versa. Now, from the above scenarios, it can be observed that the velocity of flow towards

the bank of concern i.e. Nimatighat has decreased for all scenarios and river flow has been diverted towards the dredged channel. From above comparison, it is eminent that Scenario 3 and Scenario 4 is more or less alike. As dredging of a 400 m channel would have a higher financial involvement, Scenario 3 with dredged channel width of 300 m seems to be the better alternative which will have a lower financial involvement. To take the study further, permeable porcupine screens have also been laid in the physical model at upstream of Nimatighat to study the effects of the river flow. The various scenarios in the range of 10,000 cumecs to 30,000 cumecs for each channel width of 100 m, 200 m, 300 m and 400 m has been physically regulated and laid in the model to study the effects which are tabulated in Table 2 below.

Table 6.12 Velocities before and after dredging with porcupine

Scenarios Average of 10,000; 20,000; and 30,000 cumecs	**Location**	**Velocity before dredging**				**Velocity after dredging (With Porcupine)**				**% Change in Av. velocity**
		CS25	**CS26**	**CS27**	**Avg.**	**CS25**	**CS26**	**CS27**	**Avg.**	
Scenario - 5 (@ 100 m channel)	Left Bank	0.180	0.155	0.250	0.195	0.093	0.115	0.212	0.140	-28.38%
	Dredged Channel	0.065	0.098	0.200	0.121	0.318	0.287	0.285	0.297	145.40%
Scenario - 6 (@ 200 m channel)	Left Bank	0.180	0.155	0.250	0.195	0.068	0.099	0.168	0.112	-42.83%
	Dredged Channel	0.065	0.098	0.200	0.121	0.349	0.289	0.281	0.306	153.40%
Scenario - 7 (@ 300 m channel)	Left Bank	0.180	0.155	0.250	0.195	0.017	0.064	0.209	0.096	-50.63%
	Dredged Channel	0.065	0.098	0.200	0.121	0.368	0.285	0.285	0.312	158.46%
Scenario - 8 (@ 400 m channel)	Left Bank	0.180	0.155	0.250	0.195	0.000	0.061	0.211	0.091	-53.47%
	Dredged Channel	0.065	0.098	0.200	0.121	0.374	0.261	0.280	0.305	152.39%

The following can be observed from the aforesaid Table 6.12: -

(1) In respect of Scenario 5, for dredging channel width of 100 m, it can be observed that average velocity on the left bank (i.e. towards Nimatighat) has decreased by 28.38 % and average velocity in the dredged channel has increased from 0.121 m/s to 0.297 m/s which is by 145.40 %.

(2) In respect of Scenario 6, for dredging channel width of 200 m, it can be observed that average velocity on the left bank (i.e. towards Nimatighat) has decreased by 42.83 % and

average velocity in the dredged channel has increased from 0.121 m/s to 0.306 m/s, i.e. by 153.40 %, which is higher than Scenario 5.

(3) In respect of Scenario 7, for dredging channel width of 300 m, it can be observed that average velocity on the left bank (i.e. towards Nimatighat) has decreased by 50.63 %. The average velocity in the dredged channel has increased from 0.121 m/s to 0.312 m/s, i.e. by 158.46 %, which is also the highest observed average velocity in comparison to all other scenarios.

(4) In respect of Scenario 8, for dredging channel width of 400 m, it can be observed that average velocity on the left bank (i.e. towards Nimatighat) has decreased by 53.47 % which is somewhat higher than Scenario 7. The average velocity in the dredged channel has increased from 0.121 m/s to 0.305 m/s, i.e. by 152.39 %, which lower in comparison to Scenario 8.

Velocity of flow hitting the river bank is more or less directly proportional to the quantum of erosion of the bank i.e. more velocity towards the bank means higher likelihood of erosion of the river bank or vice versa. Now, from the above scenarios, it can be observed that the velocity of flow towards the bank of concern i.e. Nimatighat has decreased for all scenarios and river flow has been diverted towards the dredged channel. From above comparison, it is eminent that the maximum flow has been diverted towards the dredged channel in Scenario 7 and the flow towards Nimatighat has been reduced the highest in Scenario 8. It may also be observed that the difference of flow towards Nimatighat for both Scenario 7 and Scenario 8 is nominal. As dredging of a 400 m channel would have a higher financial involvement, Scenario 3 with dredged channel width of 300 m seems to be the better alternative which will have a lower financial involvement.

Lastly, if we compare Scenario 3 and Scenario 7 (comparison of velocity in dredged channel without porcupine and with porcupine), it can be observed that the flow towards Nimatighat has decreased from 0.111 m/s to 0.096 m/s which is 13.11 % and velocity of flow has increased in the dredged channel from 0.290 m/s to 0.312 m/s which is 7.66 %. Therefore, it can be observed that Scenario 7, wherein porcupine screens have been used as an intervention seems to be better proposition than Scenario 3. Besides, RCC porcupine screens is a widely adopted intervention method for river training works in the Brahmaputra River valley which can be easily undertaken for diverting the river flow as in this case of Scenario 7. In respect of the Scenario 7, the mammoth task in hand will be the volume of work and cost involved in dredging a channel of width 300 m across the river to divert the river flow. However, the task is not an impossible one and can be accomplished with the new age technologies and skilled workmanship. Dredging is the major component of the work and

involves a high cost. The porcupine screens will be the ancillary component of the work and will involve a minimum cost in comparison the major work of dredging.

In order to save the Nimatighat area of Jorhat Town for the greater benefit of the people, dredging a channel of to divert the flow can be an option that needs to be explored and adopted.

6.7 Study on use of Porcupine Screen as Anti-Erosion Measure for a Critical Location in River Brahmaputra near Majuli.

There was erosion problem in the area downstream of Chinatoli Chapori and upstream of Salmara of Majuli in 2022.Brahmaputra Board proposed to lay 3 nos of RCC Porcupine Screen of variable length at the mouth of the channel at spacing of 100 m c/c as per site condition with 5 rows in bottom layer. The number of layers was decided as per depth of flow at points of x-section limited to the 50% of depth of flow. The length of the screens was decided as 200m, 300m and 400m in river and 20m at bank. Physical model study is conducted for above arrangement of porcupine screen. Velocities are measured downstream of porcupine screen and analyzed. It is found velocity is decreased just downstream of porcupine screen. Field study is done during and after execution of screens in actual location and it is found that siltation is occurred as desired. Figure 6.20 shows the erosion problem near Salmara, Majuli

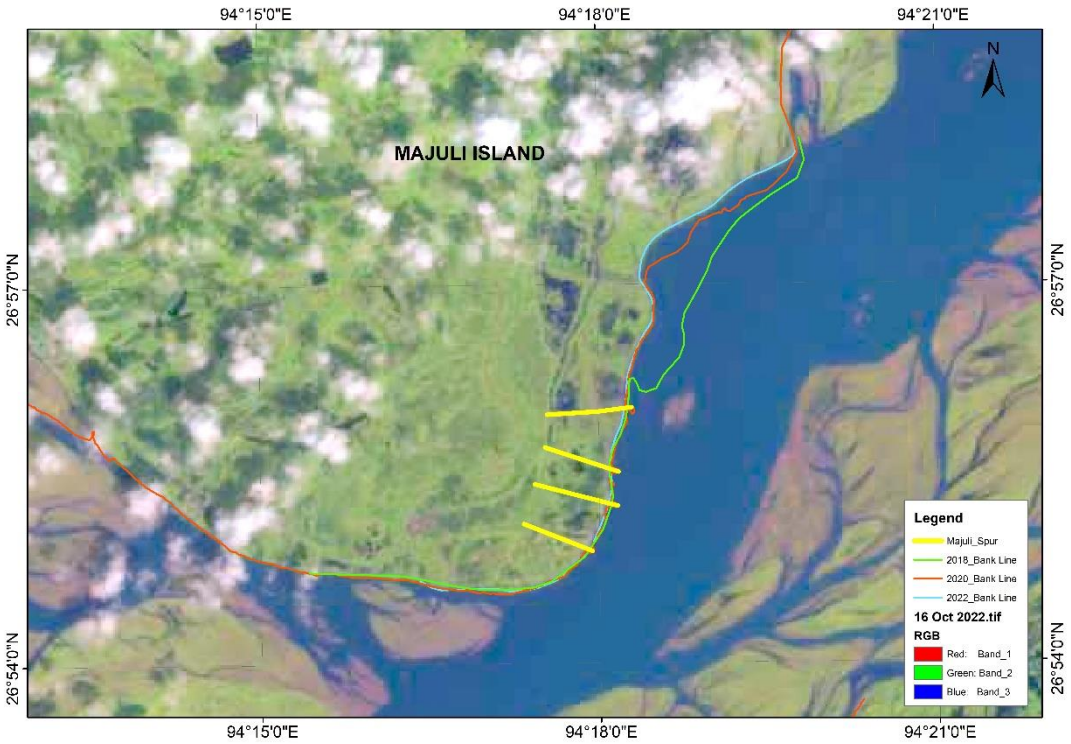

Figure 6.20 Erosion problem near Salmara, Majuli

Figure 6.21, 6.22 and 6.23 shows the Velocity distribution from model study for Salmara reach at 20000 cumec, 30000 cumec and 40000 cumec respectively.

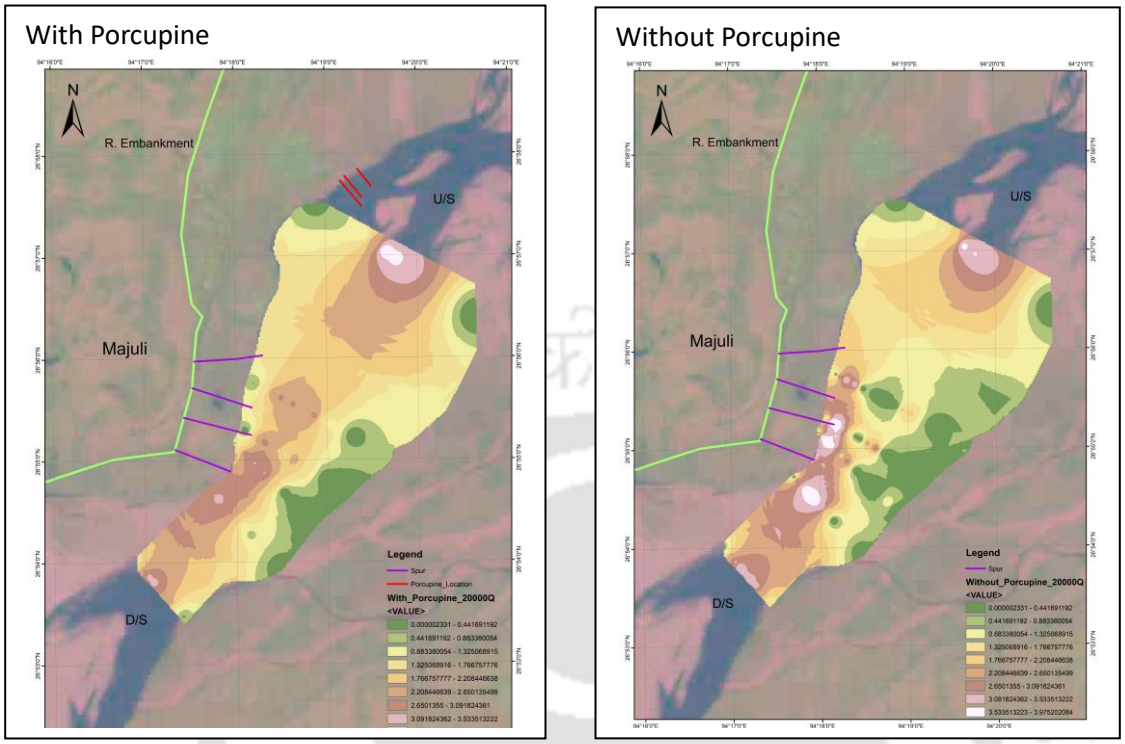

Figure 6.21 Velocity distribution from model study for Salmara reach (at 20000 cumec)

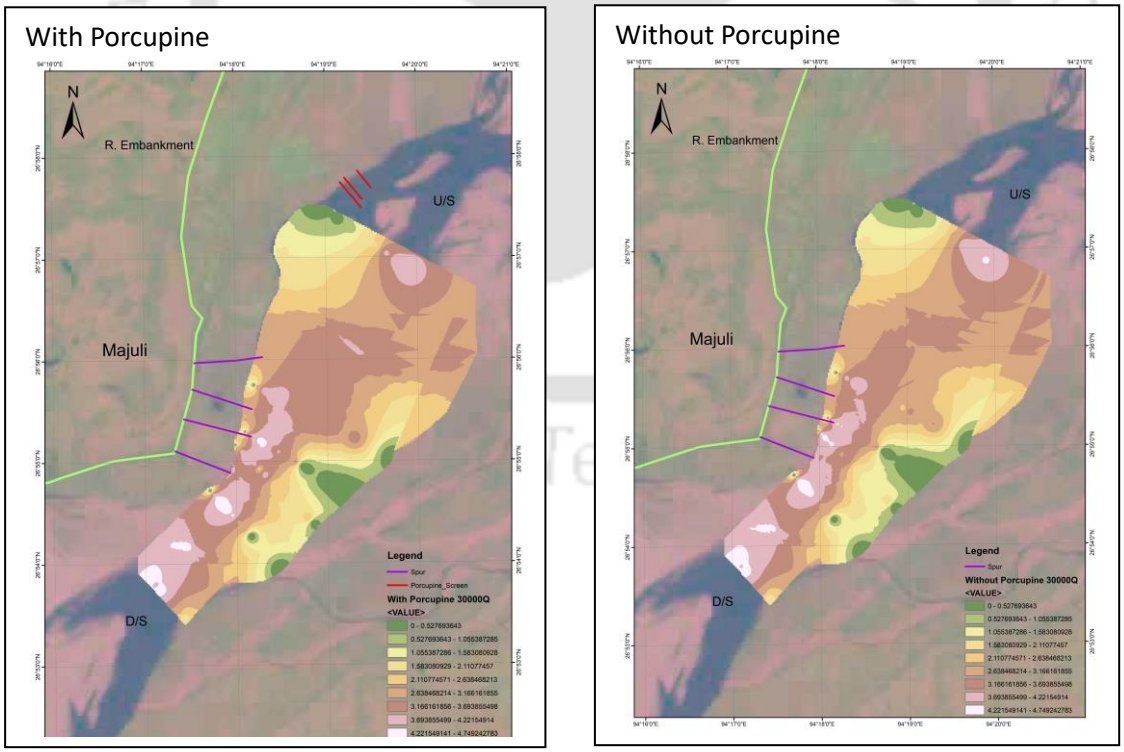

Figure 6.22 Velocity distribution from model study for Salmara reach (at 30000 cumec)

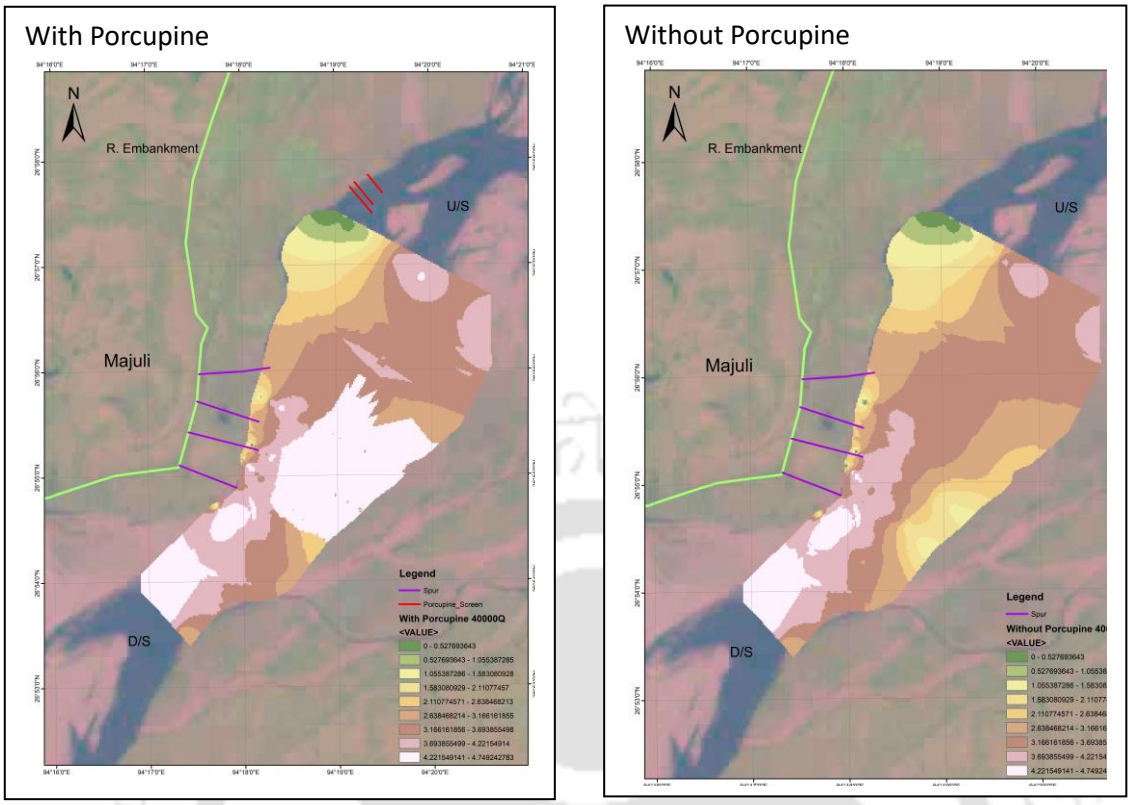

Figure 6.23 Velocity distribution from model study for Salmara reach (at 40000 cumec)

A physical model study is conducted for a solution of bank erosion problem near Salmara in Majuli. Velocities are observed in physical model before and after laying scaled down porcupine screens. The best alignment for porcupine screens is finalized after observation of velocities in required location where deposition of sediment was expected. The porcupine screens are laid in actual field and observed deposition of sediment as required. It is concluded that the physical model study is an important tool in planning for solution of bank erosion problem in critical reaches of braided river

6.8 Discussion and Conclusion

Discussion and Conclusion for Physical Model Study for a reach in river Brahmaputra near Majuli at North Bank and Nemati Ghat at South Bank

The construction of a dredging channel near Majuli in the Brahmaputra River demands a meticulous assessment of various scenarios and considerations to determine the optimal solution. Two analyses, one without porcupine structures and the other with, shed light on the impact of dredging on flow velocities, crucial for informed decision-making in this endeavour. In the first analysis, where dredging is conducted without porcupine structures, significant improvements in flow dynamics are observed across all scenarios. For instance, in Scenario 1 with a 100-meter channel width, there's a notable 124.26% increase in average velocity post-dredging, indicating enhanced water flow

efficiency. Similarly, in Scenario 4 with a 400-meter channel width, there's a substantial 135.11% surge in average velocity post-dredging, demonstrating the effectiveness of dredging in mitigating sedimentation and facilitating smoother navigation. Conversely, the second analysis incorporates porcupine structures into the dredging process, moderating the increase in velocity while still providing significant enhancements. In Scenario 5, for instance, with a 100-meter channel width, the average velocity increases by 145.40%, showcasing the combined effect of dredging and porcupine structures in improving flow dynamics.

The choice between dredging methods depends on several factors, including the desired level of flow enhancement and environmental considerations. While dredging without porcupine structures yields higher percentage increases in average velocities, indicating more pronounced improvements in flow efficiency, the addition of porcupine structures offers a balanced approach, addressing concerns related to sediment management and ecological preservation. Therefore, for the construction of a dredging channel near Majuli, a hybrid approach that combines dredging with carefully designed porcupine structures emerges as the best solution. This approach ensures not only significant improvements in flow dynamics but also the preservation of the delicate ecological balance of the Brahmaputra River ecosystem.

The implementation of such a hybrid approach requires meticulous planning and execution, taking into account factors such as channel width, sedimentation rates, and ecological sensitivity. Furthermore, ongoing monitoring and assessment are essential to gauge the effectiveness of the dredging channel and make necessary adjustments to optimize its performance while minimizing environmental impact. Additionally, stakeholder engagement and community involvement are crucial to ensuring the project's success and garnering support from local communities who rely on the river for their livelihoods. In conclusion, the construction of a dredging channel near Majuli in the Brahmaputra River necessitates a thoughtful and integrated approach that balances the need for flow enhancement with environmental conservation. By combining dredging with porcupine structures, it's possible to achieve significant improvements in flow dynamics while mitigating adverse environmental effects. With careful planning, execution, and stakeholder engagement, such a project has the potential to enhance navigation, mitigate flood risks, and preserve the ecological integrity of the Brahmaputra River ecosystem for generations to come.

Discussion and Conclusion for Physical Model Study to use Porcupine Screen as Anti-Erosion Measure for a Critical Location at Salmara, Majuli

Based on the observed velocities at different flow rates (20,000 cumecs, 30,000 cumecs, and 40,000 cumecs), the following conclusions can be drawn:

1. Effect of Porcupines on Velocity Distribution:

Porcupines, when placed near the right bank, exhibit a notable impact on velocity distribution across the cross-section. Near the right bank, where erosion is typically a concern, the velocity is consistently decreased with the presence of porcupine screens. This indicates a successful reduction in flow velocity near the bank, which can help mitigate erosion issues. Conversely, as the distance from the right bank increases, velocity tends to be higher. This suggests that porcupine screens do not impede overall flow but rather redistribute it, potentially reducing erosive forces near vulnerable areas.

2. Impact on Spur Region:

In the spur region, where flow dynamics are crucial for stabilizing the bank, porcupine screens demonstrate consistent effectiveness in reducing velocity near the bank. This reduction in velocity near the bank indicates a potential for decreased erosive forces, contributing to the stability of the spur region. Similarly, as observed in other sections, velocity tends to be higher as the distance from the bank increases, suggesting a redistribution rather than a blockage of flow.

3. Overall Effectiveness:

Across different flow rates, the effectiveness of porcupine screens in reducing velocity near vulnerable areas remains consistent. This suggests that porcupine screens could be a reliable solution for bank erosion problems across a range of flow conditions. However, further studies may be needed to assess long-term durability, maintenance requirements, and potential ecological impacts of implementing porcupine screens in riverbank stabilization projects.

5. Considerations for Future Research:

While the observations provide valuable insights into the immediate effects of porcupine screens on velocity distribution and vortex formation, additional research is needed to explore their long-term

effectiveness. Furthermore, computational modelling and field experiments can help refine the design and placement of porcupine screens for optimal erosion control.

In conclusion, the observations from the porcupine screen placement experiments indicate a promising solution for mitigating bank erosion problems. By strategically reducing flow velocity near vulnerable areas such as the right bank and spur regions, porcupine screens have demonstrated their effectiveness in redistributing flow dynamics to reduce erosive forces. Additionally, the formation of vortices near the right bank suggests additional benefits for erosion control. Further research and field trials may provide valuable insights into optimizing porcupine screen placement and maximizing their effectiveness in riverbank stabilization efforts.

7.

Sediment Transport Study for Proposed Dredging Channel of River Brahmaputra

7.1 Introduction

River morphology and river channel changes are closely related to the sediment transport. Sediment transport is the rate at which the sediment is moved (m^3/s). For a fluid to begin transporting sediment that is currently at rest on a surface, the boundary (or bed) shear stress exerted by the fluid must exceed the critical shear stress for the initiation of motion of grains at the bed. This is typically represented by a comparison between a dimensionless shear stress and a dimensionless critical shear stress. The non-dimensionalization is in order to compare the driving forces of particle motion (shear stress) to the resisting forces that would make it stationary (particle density and size). This dimensionless shear stress, is called the Shields parameter. Only one size of particle is considered in Shields equation. However, river beds are often formed by a mixture of sediment of various sizes. In case of partial motion where only a part of the sediment mixture moves, the river bed becomes enriched in large gravel as the smaller sediments are washed away. The smaller sediments present under this layer of large gravel have a lower possibility of movement and total sediment transport decreases. This is called armouring effect. Other forms of armouring of sediment or decreasing rates of sediment erosion can be caused by carpets of microbial mats, under conditions of high organic loading. The Shields diagram empirically shows how the dimensionless critical shear stress (i.e. the dimensionless shear stress required for the initiation of motion) is a function of a particular form of the particle Reynolds number, or Reynolds number related to the particle.

Bed load

It is that part of the load moving near the bed by rolling, saltation or sliding. Bed load leads to ripple and dune formation. Ripples are of smaller particles and Dunes can be of very large particles. Ripples and Dunes move downstream.

Suspended load

This part of the load moves in suspension. At this stage ripples and dunes will tend to wash out. Clays and finer particles will not have a bed load stage and will be less likely to form bed forms.

Classification of sediment load

Bed material load/ bed sediment load

Sediment (sand and gravel) that resides in the bed but goes into transport during high flow events (e.g., floods) consists of bed load and the proportion of the suspended load that are generally found in the bed sediments. Bed material load is correlated with the water discharge

Wash load

The finest portion of the sediment, generally silt and clay that is washed out through the channel with an insignificant amount of it being found in the bed. The discharge of wash load depends primarily on the rate of supply and generally correlated to the flow characteristics. It remains in suspension even during low flow events in a river.

Dissolved load

The invisible load of dissolved ions (Ca, Mg, K, HCO_3)

Different sediment transport formulae developed based on three different approaches

Shear stress approach

Power approach

Parametric approach

Sediment transport formulae are also classified according to their applicability into

Bed load formulae

Suspended load formulae and

Bed material load formulae

Classification of sediment transport formulae based different approaches

Shear stress approach

1) DuBoys formula
2) Shield's formula
3) Einstein bed load function
4) Meyer-Peter-Muller formula
5) Einstein-Brown formula
6) Parker et al formula for gravels

Power approach

1) Engelund-Hansen formula
2) Ackers-White formula
3) Yang formula

Bed material load formulae

1) Engelund-Hansen formula
2) Ackers-White formula
3) Yang formula
4) Colby relation

The amount of silt entering the Brahmaputra River from its principal points of origin has been determined, and the results indicate that the Yarlung-Tsangpo Gorge (45%), the Himalayan Mountains (40%), and the rest like Mishmi Hills, Indo-Burman Ranges, and Shillong Plateau account for the of the sediment entering the River (Wasson et al., 2022). The Brahmaputra River's current movement of sediment encounters with inconsistency (Fischer et al., 2017). The average yearly load of sediment for the hydrological year 2021 and the bank full discharge are predicted to be 257 and 314 Mt/year, respectively. The historically measured sediment load in the Brahmaputra is 400 Mt/year (Pareta, 2021). The average yearly amount of sediment at Bahadurabad is expected to rise by 27% in 2020 (Haque et al., 2021). The Great Earthquake generated enormous landslides in the Himalayan region that resulted in 45 billion cubic metres of silt in 1950 (Pareta and Pareta,

2023). The richness of particles in suspension is 5–10 times that of bed sediments in terms of heavy metal (El et al., 2014).

The Old Rhine's non-uniform sediment flow, river erosion, and bank failure were studied using an undistorted, movable-bed physical model. The model was created to test different technical solutions to improve sediment movement through bank erosion rather than for quantitative analyses of the river bed morphology. The Old Rhine's non-uniform sediment flow, river erosion, and bank failure were studied using an undistorted, movable-bed physical model. The Froude number, Colebrooke White equation relationship, and bank stability coefficient were used to create the model as precisely as physical limitations would allow. In order to prevent the production of ripples and significant distortion of the critical Shields number, this specific scaling strategy relaxes the requirement for similar Shields and particle Reynolds values for each grain size class that makes up the bank material. To maintain the mass density and internal friction angle between the model and the prototype, sand was kept as the model bank material. The most significant ones result from the relaxation of the Shields number and the cohesive characteristics of the model material. The model grain sizes used to replicate the prototype material are slightly coarser than they should be since the Shields number was not followed. These bigger grains (by as much as 40%) and the material's cohesiveness, which makes the model bank more stable than the prototype bank, may cause the degraded volumes to be underestimated. The creation of ripples, which may boost bed load transmission but cannot be duplicated in the model, and, to a lesser extent, vegetation roots, may somewhat offset the scale impacts. Physical models offer understanding of the pertinent processes and recommendations on the optimum technical solution for a given objective despite inevitable scale effects (El et al., 2014).

Using movable bed model studies, the consequences of offshore dredging at Chang-Hwa reclamation area in Taiwan were examined. The current scale law is a helpful tool for real-world applications. The following test cases were conducted: (1) tests for timing; (2) tests for changes in the sea bottom under current conditions; (3) tests for changes in the sea bottom after dredging at -15m water depth; and (4) testing of countermeasures for coast protection after dredging. The factor that has the greatest impact on where erosion occurs has been identified. Groin construction techniques were thought to lessen beach erosion. It was established that the suggested groynes do a good job of preventing erosion along the shore (Chang, 2018).

A movable bed model was made in a lab flume to simulate a mixed load sand-bed stream. In order to reproduce bedload and suspended sediment transfer as well as downstream and transverse

sediment fluxes at ratios that were comparable to those at the field site, sediment transport models were developed. In this study, a method for scaling the sediment dynamics of a stream with a sand bed in a 1:16 laboratory model was provided. The smaller coal flakes interfered with the bed profiler device and occasionally impeded measuring of the bed. The apricot pips were adequate, but after a few months of use, they began to disintegrate. If price is not a concern, plastic media would be preferable to both of these materials because it would prevent the aforementioned issues (Gorrick and Rodríguez, 2014).

At a pilot location in the Old Rhine, a trained river, five series of mobile bed reduced-scale physical model tests were conducted to evaluate the likelihood that groyne modification would cause bank erosion. The bank material's grain size distribution was recreated using a combination of four sand grainsizes, and the model was constructed at a 1:40 undistorted scale. The Shields parameter was not preserved because to scaling constraints, but the initial grain motion was accurately reflected. When the bank protection was removed, it was discovered that the groynes that were already there weren't strong enough to prevent bank erosion. A new configuration was made with two longer, taller island groynes that sped up bank-side flow and increased bed load conveyance. This solution is effective in causing bank erosion, with a consistent pattern of erosion and deposition, according to a series of studies with constant model flow rates between 0.0395 and 0.311 m3/s) and flood hydrograph tests. The resulting bank erosion was also discovered to be self-stabilizing, and the lateral adjustment of the bank was discovered to be sufficiently stable to not provide a threat to the nearby Grand Canal d'Alsace shipping canal. By changing existing groynes to encourage bank erosion, the study's findings suggest a novel way to prevent sediment feeding in trained rivers (Die moran et al., 2013).

PVC powder used to study sediment transport and deposition in tidal beel in reinforced concrete flume. Constant inflow discharge 125l/min and sediment of 80um and 1.75 gm/cc density was supplied. Outflow discharge was varied in Case 1 and Sediment Concentration in Case 2, keeping other variable constant in either of cases. Sediment Concentration was measured using Turbidimeter at various points in Cross-section. When higher outflow discharge is allowed to flow from side basin higher sediment is transported towards it and lesser sediment on the course of river.it is obvious that increase in concentration at inlet will surely increase concentration at side basin and outlet. Moreover with increase in outflow discharge towards side basin, sediment transportation and deposition also increases (Talchabhadel and Nakagawa, 2016).

7.2 Scaling of Sediment Size and Rate for the Physical Model Study

In this research, Froudian Similarity is being used to design the settling velocity of suspended bed particles in a movable bed physical model of distorted scale of Horizontal 1:500 and Vertical 1:67.

An artificial dredging channel is constructed at physical model of dimension 12m which in prototype measures 6km spanning from Lat- 26°53'7.45"N, Long- 94°15'38.65"E to Lat - 26°53'18.61"N, Long - 94°11'57.11"E. The width of channel is 250m. Figure 7.1 shows the location of dredging channel for model study.

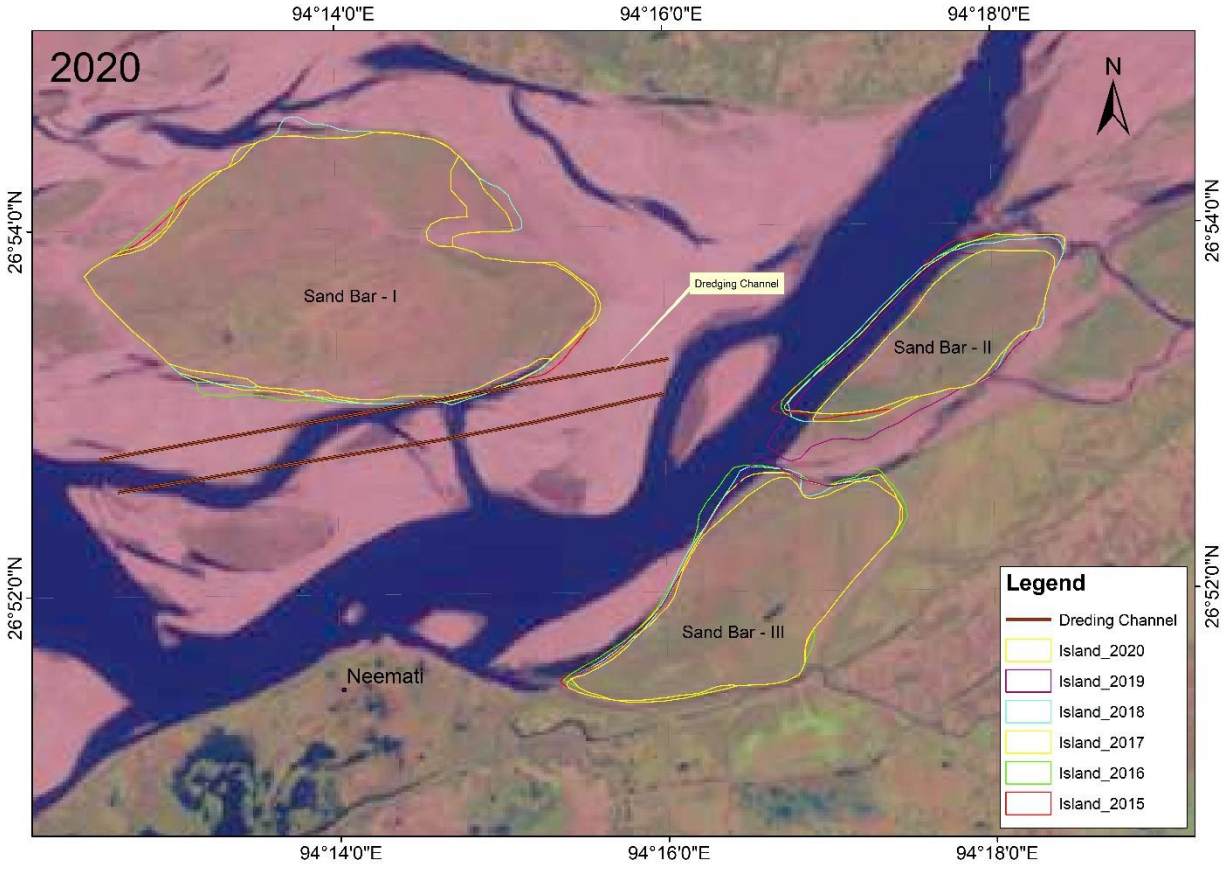

Figure 7.1 Location of Dredging Channel for Model Study

Figure 7.2 Construction of Dredging Channel in Physical Model

Figure 7.2 shows the construction of dredging channel in physical model

The movable bed in physical model is designed as per shields criteria of movable bed design and artificial sediments are further injected at upstream of channel to study settling characteristics of suspended particles in channel.

Suspended particle was designed considering settling velocity similarity exists between model and prototype.

Similarity between the settling velocity of model and prototype:

According to stokes equation, settling velocity of suspended particle is given as -

$$V = \frac{1}{18} x \frac{(\rho - \rho_o)g}{\eta_0} x D^2$$

Where V is the settling velocity
ρ is Particle density
ρ_o is Solvent density
η_0 is solvent viscosity

D is the diameter of particle

Now since settling velocity similarity between prototype and model is being considered, the above equation in terms of dimensional similarity can be written as-

$$\frac{Vsproto}{Vsmodel} = \frac{(2.65-1)gd^2/18\mu}{(G-1)gd^2/18\mu}$$

$Vs_r = (G\text{-}1)\ {}_rd_{50}^2$, $Vs_r = (Z_r)^{0.5}$

Hence,

$Vs = g(G\text{-}1)d^2/18u$

Now since settling velocity of model should be $Z_r^{0.5}$ less than prototype.

For this present physical model, settling velocity is $(67)^{0.5}$ times less.

Hence, this model as per settling velocity criteria:

The properties of prototype sand are G=2.65 and d_{50}=0.19mm

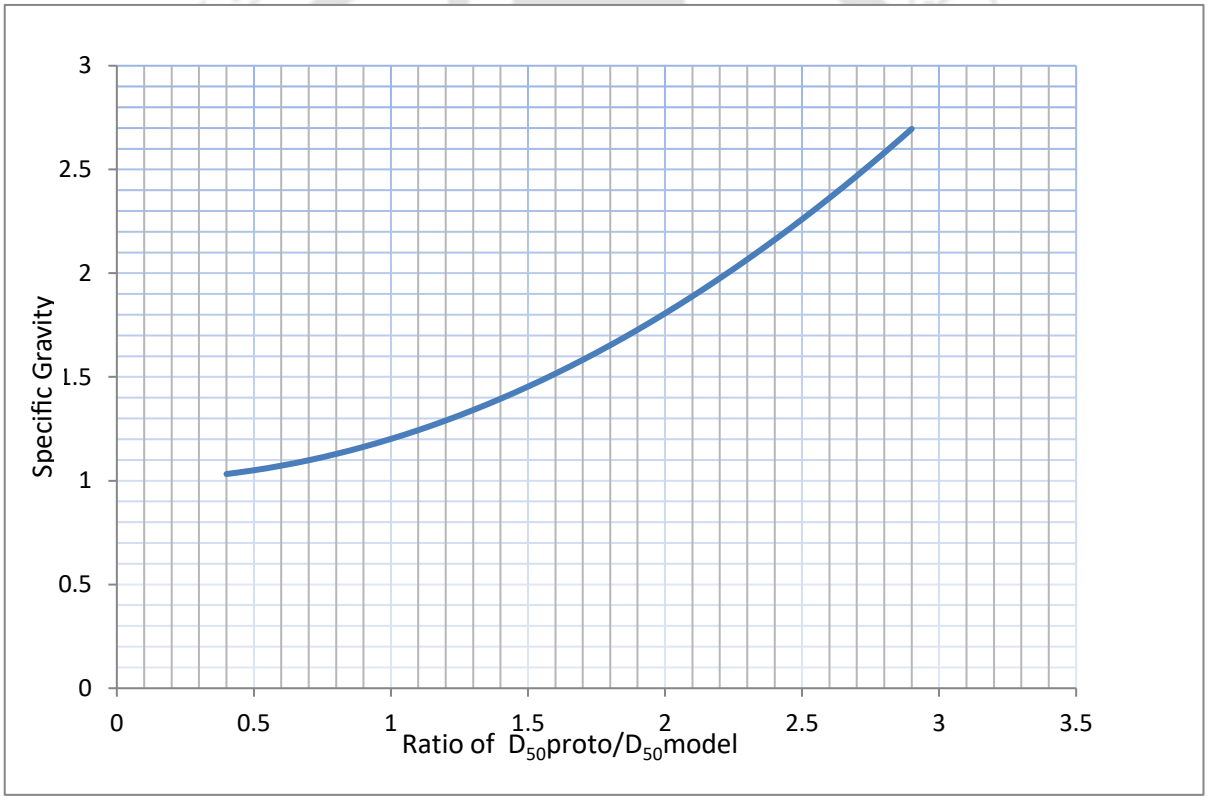

Figure 7.3 Graph for specific gravity vs D_{50}Proto/D_{50}Model

Figure 7.3 shows the graph for specific gravity vs D_{50}Proto/D_{50}Model

Assuming ratio of average diameter size to be 1.26 (D_{proto}/D_{model})

The particle specific gravity required comes out to be

$67^{0.5}=(2.65\text{-}1)d_r^2/(G\text{-}1)$ where d_r is 1.26 , then G=1.32 .

Hence, the required particle of specific gravity is 1.32.

After checking of properties of various materials for suspended sediment in model, PVC powder is selected and the characteristics of PVC Powder are mentioned below.

Specific Gravity (Calculated by pycnometer in Non polarising liquid Kerosene)	1.32
D_{50} (obtained from sieve analysis)	0.15

Sediment is injected as per scaling the prototype sediment load (Kg/s) in Majuli island reach, for which past data is obtained from CWC and other government bodies.

Average Annual prototype Sediment load as per CWC data = 35910312 tonnes/year

Discharge Scale=274209 ($500*67*67^{0.5}$)

Hence Average load to be applied at Model = 35910312 X 10^3 (kg/year) / 274209 = 130959.6 kg/year

Since at Prototype Discharge 20000 cumec, discharge in model is 0.0729 m^3/s and discharge in artificial channel is 0.0331 m^3/s (Discharge Observation at Model).

Hence,

Sediment load to be applied at channel =130959.6 * 0.0331/0.0729

= 59641.43 kg/year

= 6.80kg/hr

= 6.80*1000000/3600 mg/sec

Average Parts per Million (PPM) concentration in mg/l at given discharge of 0.0331 m^3/s = 0.0331 *1000 lit/sec in artificial channel (6.80*1000/(0.0331*3600)) =57.13 mg/l (PPM).

Similarly in monsoon load of 82351754 tonnes/year, parts per million concentrations of sediment to be applied at channel comes out to be 92.16 mg/l at prototype discharge of 30000 cumecs.

Hence concentration of 50PPM and 90PPM is chosen to be poured upstream at varying discharge levels. Concentration when multiplied with discharge provides the sediment load in model channel which can be used to calculate sediment load at prototype channel and river.

Keeping 50PPM concentration in upstream discharge is varied and then process is repeated for 90PPM concentration.

Amount of suspended particle (kg) injected at each concentration and discharge is noted for each run and then after each run for a given concentration and discharge, channel is dried up and particles that are sedimented are collected and are placed in soil laboratory for sieve analysis.

Sieve size greater than 0.180 contained only sand of movable bed, while sieve less than 0.180mm contained mix of both PVC and Sand.

Hence sample from sieve less than 0.180mm is collected and amount of PVC and sand in representative sample is noted via water column analysis of sample.

From this amount of PVC and sand being sedimented at every concentration and corresponding discharge is noted.

7.3 Observation of Sedimentation in the Proposed Dredging Channel in the Physical Model

Table 7.1 shows reading for 50 PPM suspended sediments and Table 7.2 shows reading for 90 PPM suspended sediments.

Table 7.1 Reading for 50 PPM Suspended Sediments

Discharge	Wt. of Sand +Wt. of PVC in Sieve	Height of PVC	Height of Sand	Wt. of PVC in 200gm sample	Wt. of Sand in 200gm sample	Total Wt. of PVC (gms)	Wt. of Sand (gms)	Total Sand Collected from Channel (gms)
20000	200	4.00	4.10	65.41	134.59	306.11	629.89	3324.89
10000	200	6.50	2.21	118.87	81.13	1325.35	904.65	2383.65
30000	200	1.10	4.90	20.11	179.89	289.05	2584.95	7938.9

Table 7.2 Reading for 90 PPM Suspended Sediments

Discharge	Wt. of Sand +Wt. of PVC in Sieve	Height of PVC	Height of Sand	Wt. of PVC in 200gm sample	Wt. of Sand in 200gm sample	Total Wt. of PVC	Wt. of Sand (gms)	Total Sand Collected from Channel (gms)
20000	200	6.90	2.10	124.15	75.85	1868.40	1141.60	5765.60
10000	200	10.80	0.20	192.83	7.17	3981.96	148.04	1891.04
30000	200	1.80	4.40	33.86	166.14	298.27	1463.73	11052.83

Keeping same concentration, observations at different discharges.

Figure 7.4 shows the Observation at 50 PPM Suspended Sediment and Figure 7.5 shows Observation at 90 PPM Suspended Sediment

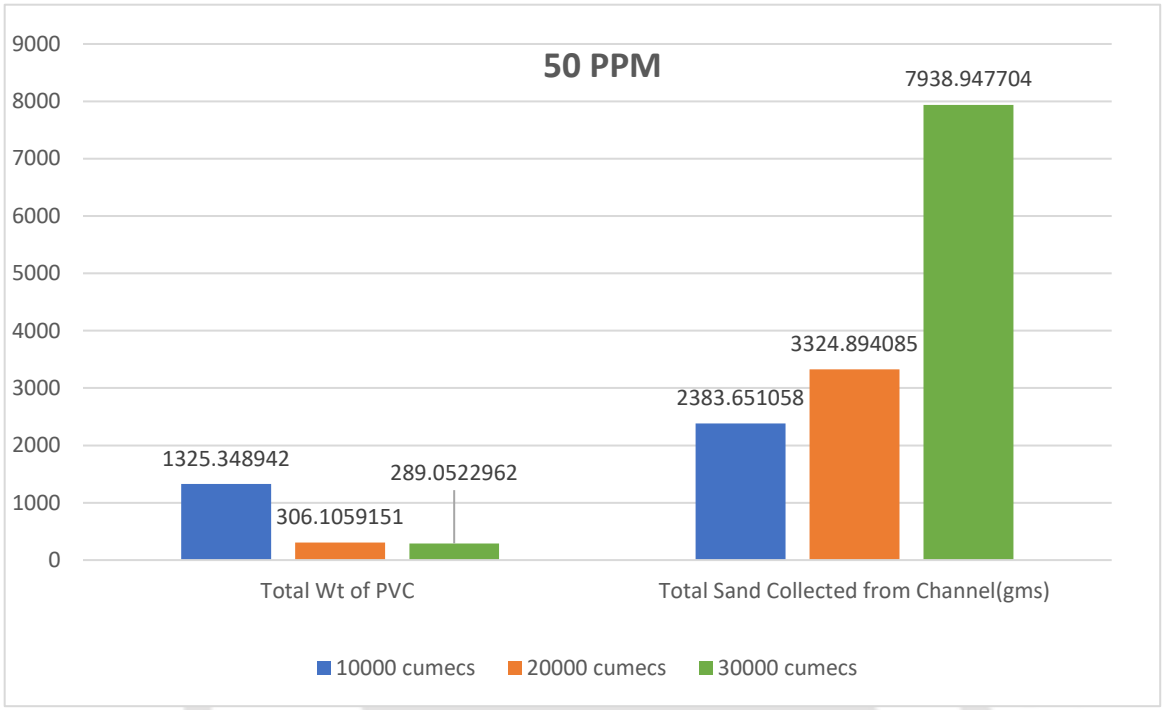

Figure 7.4 Observation at 50 PPM Suspended Sediment

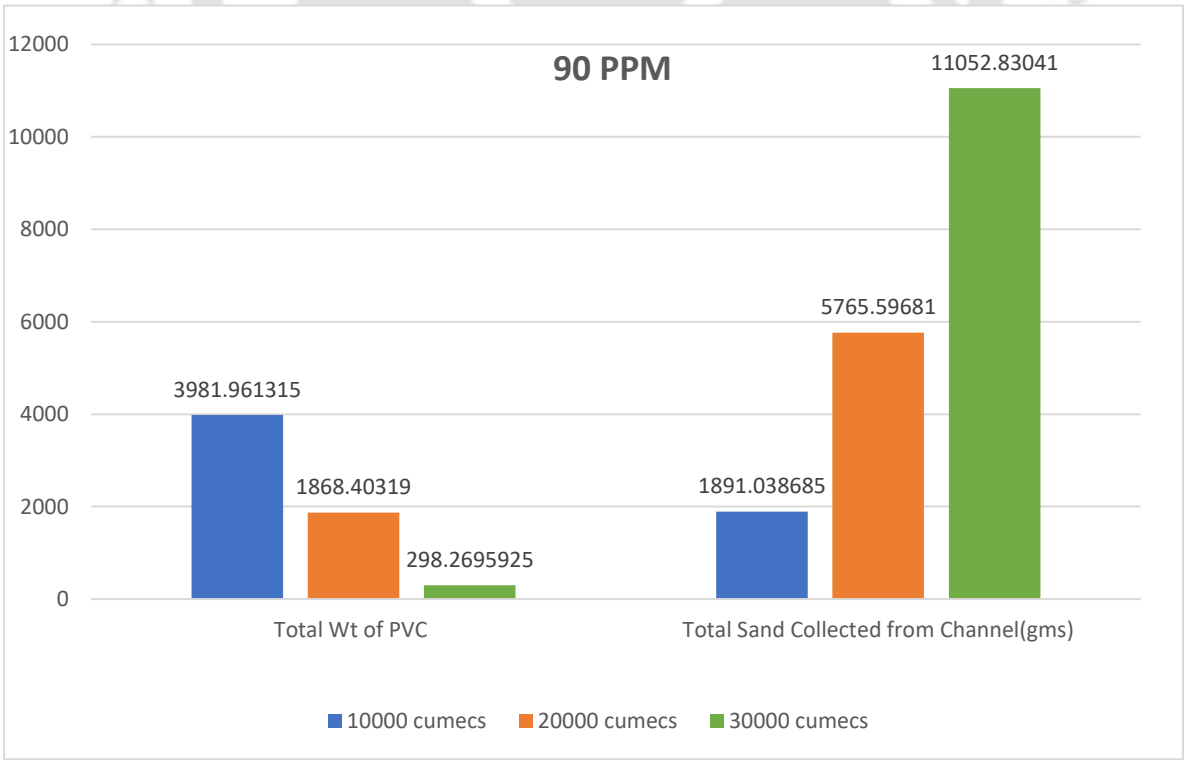

Figure 7.5 Observation at 90 PPM Suspended Sediment

Figure 7.6 shows the Sediment in percentage Flushed out of Channel at 50 PPM and Figure 7.7 shows the Sediment in percentage Flushed out of Channel at 90 PPM

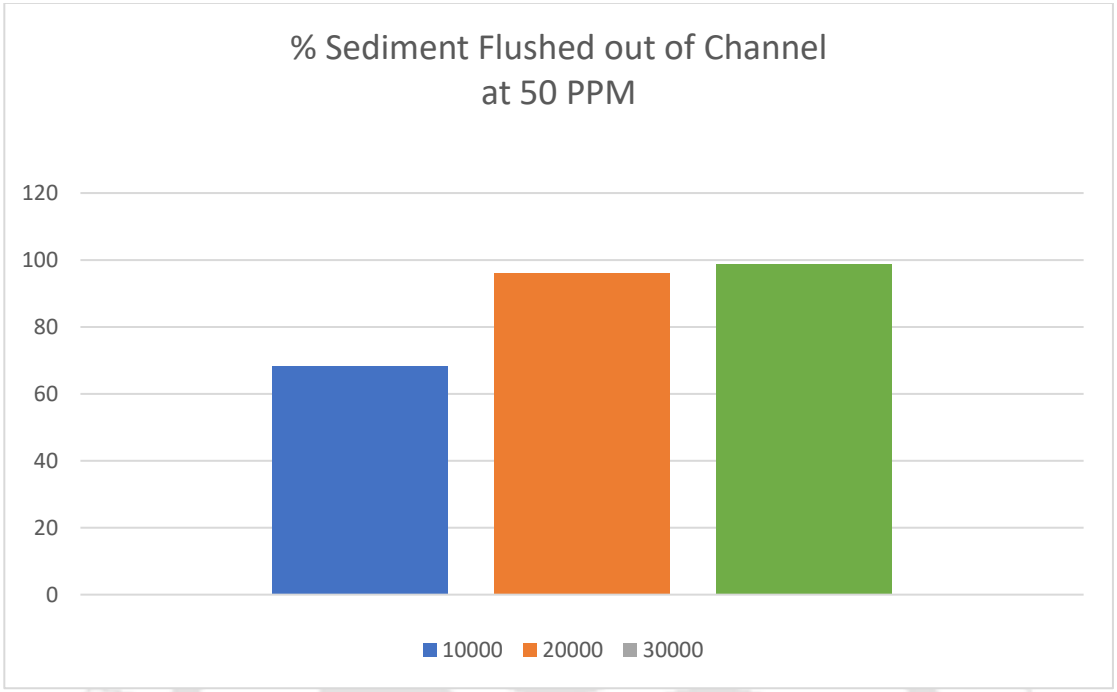

Figure 7.6 Sediment in percentage Flushed out of Channel at 50 PPM

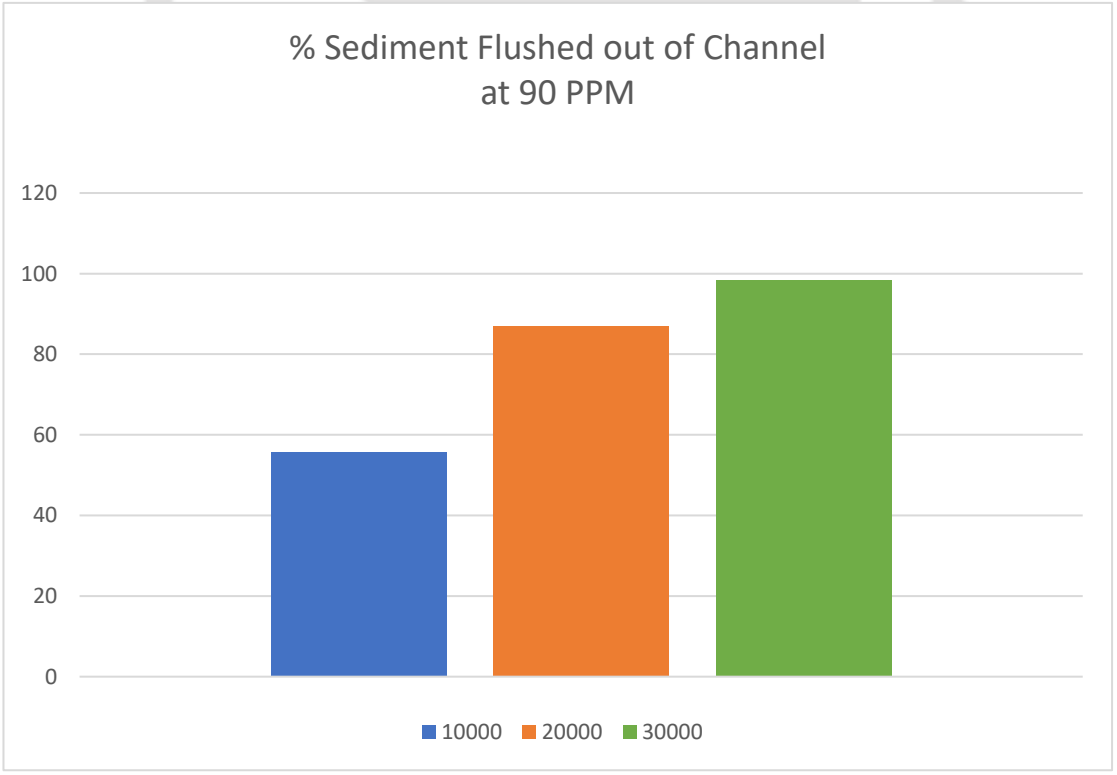

Figure 7.7 Sediment in percentage Flushed out of Channel at 90 PPM

Keeping discharge same, reading at different PPM

Figure 7.8 shows the Collection of PVC at 10000 cumecs discharge and Figure 7.9 shows the collection of Sand at 10000 cumecs discharge

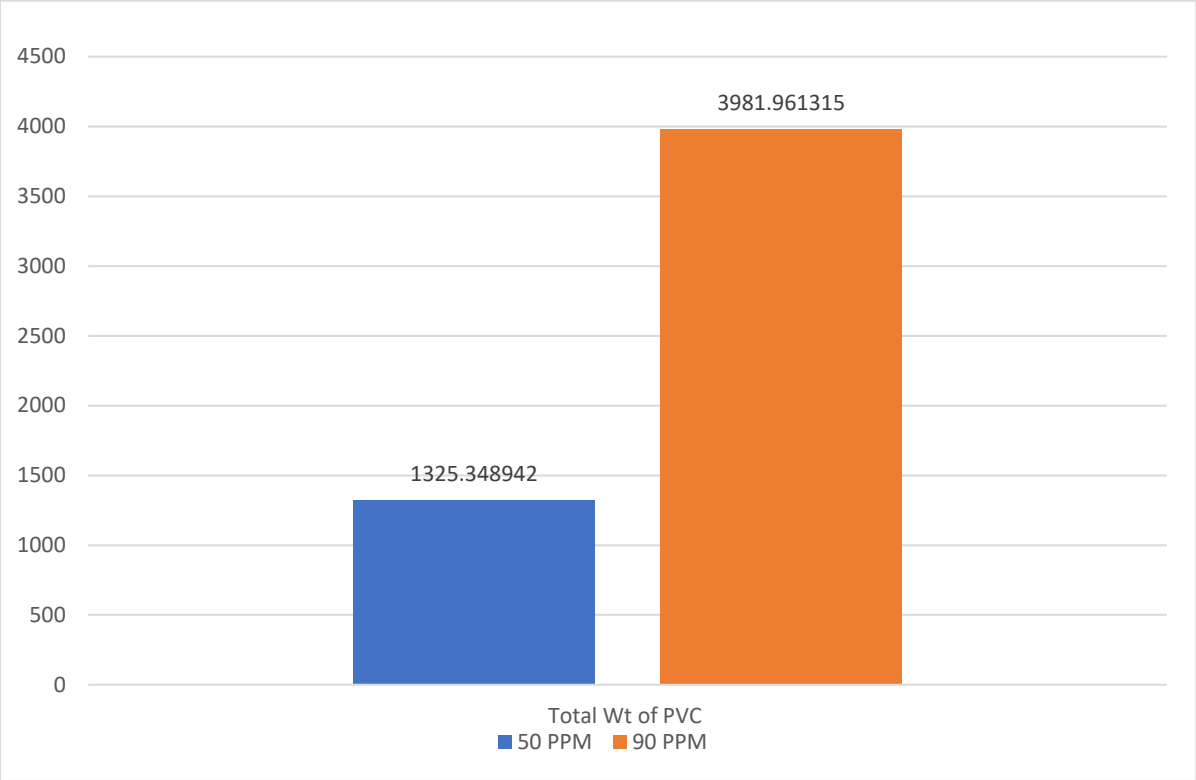

Figure 7.8 Collection of PVC at 10000 cumecs discharge

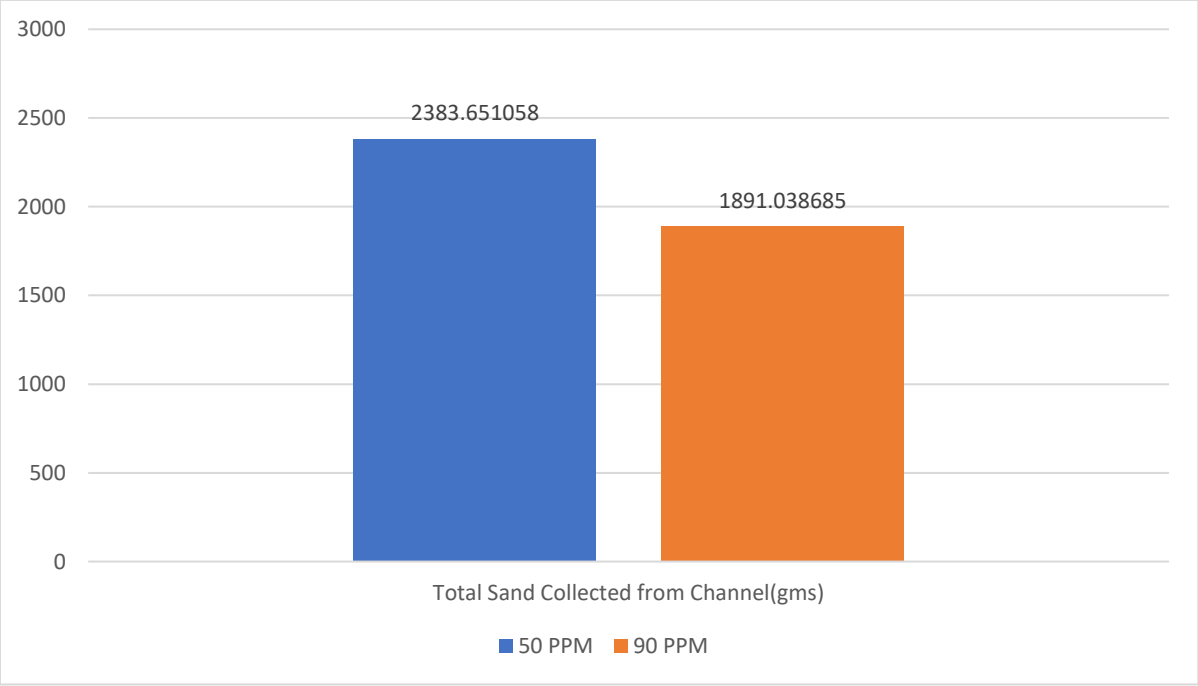

Figure 7.9 Collection of Sand at 10000 cumecs discharge

Keeping discharge same, reading at different PPM

Figure 7.10 shows the collection of PVC at 20000 cumecs discharge and Figure 7.11 shows the collection of sand at 20000 cumecs discharge.

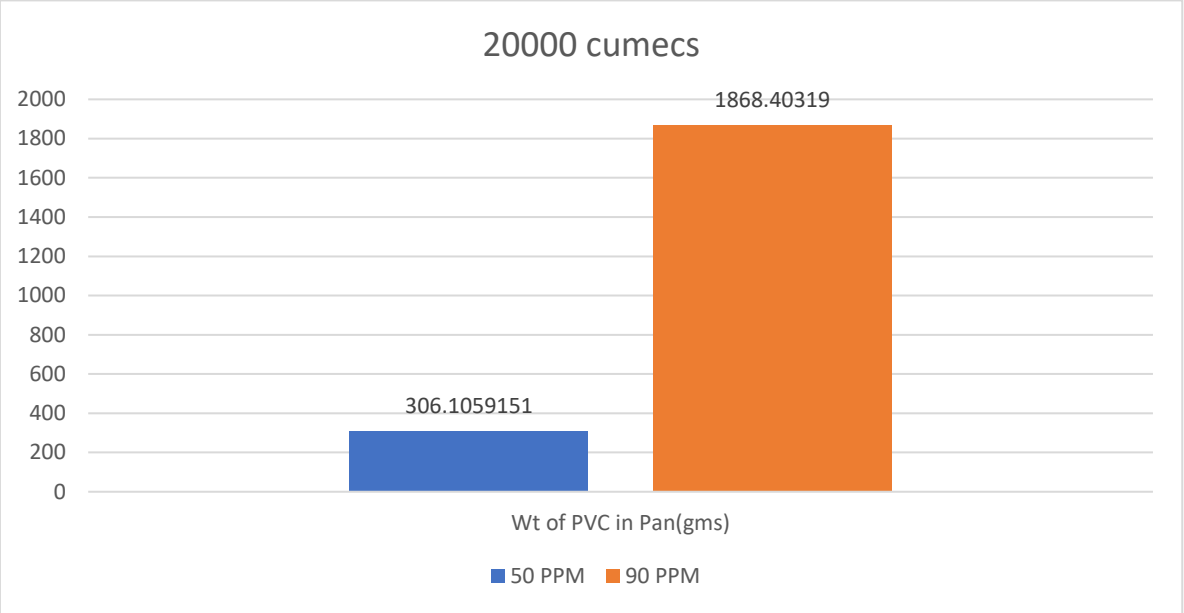

Figure 7.10 Collection of PVC at 20000 cumecs discharge

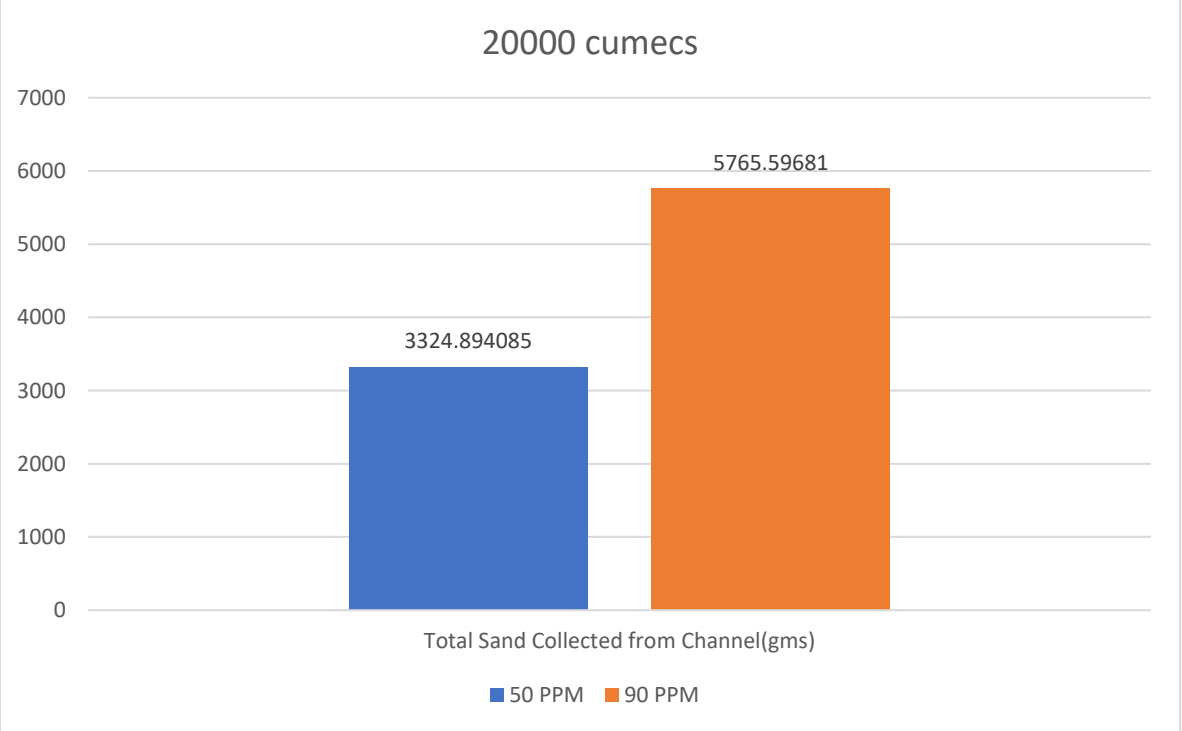

Figure 7.11 Collection of Sand at 20000 cumecs discharge

Keeping discharge same, reading at different PPM

Figure 7.12 shows the collection of PVC at 30000 cumecs discharge and Figure 7.31 shows the collection of sand at 40000 cumecs discharge.

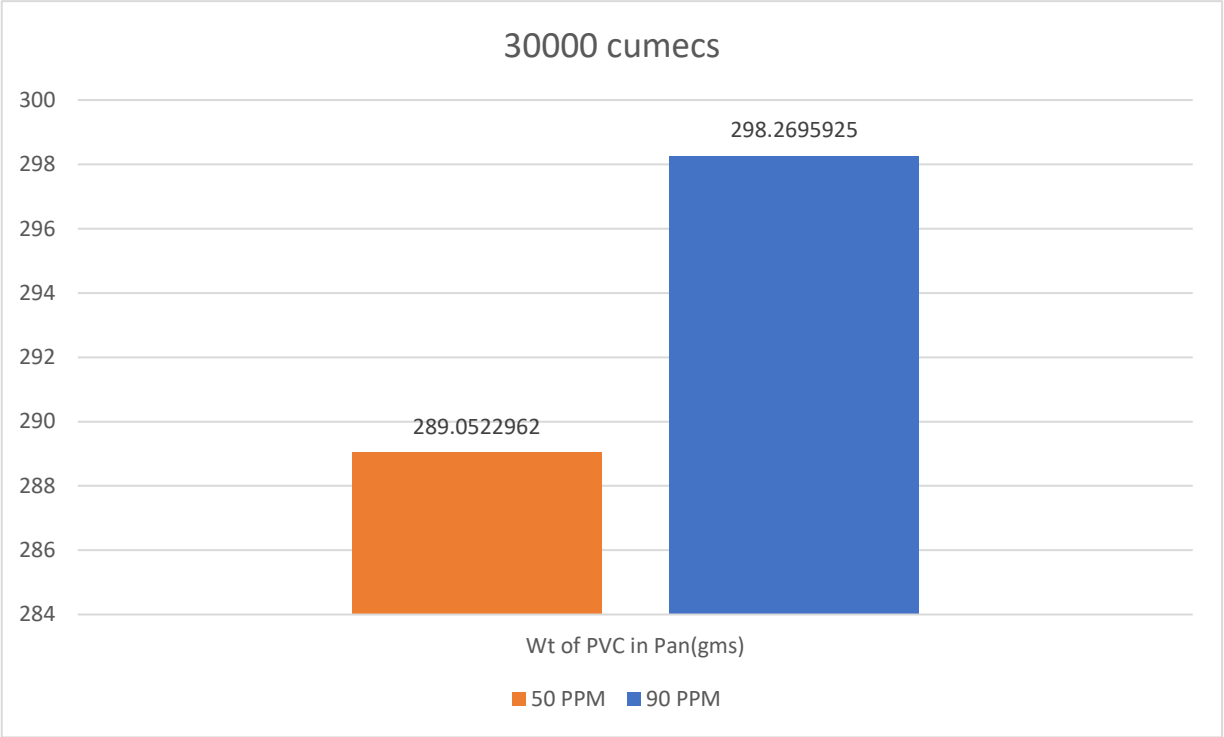

Figure 7.12 Collection of PVC at 30000 cumecs discharge

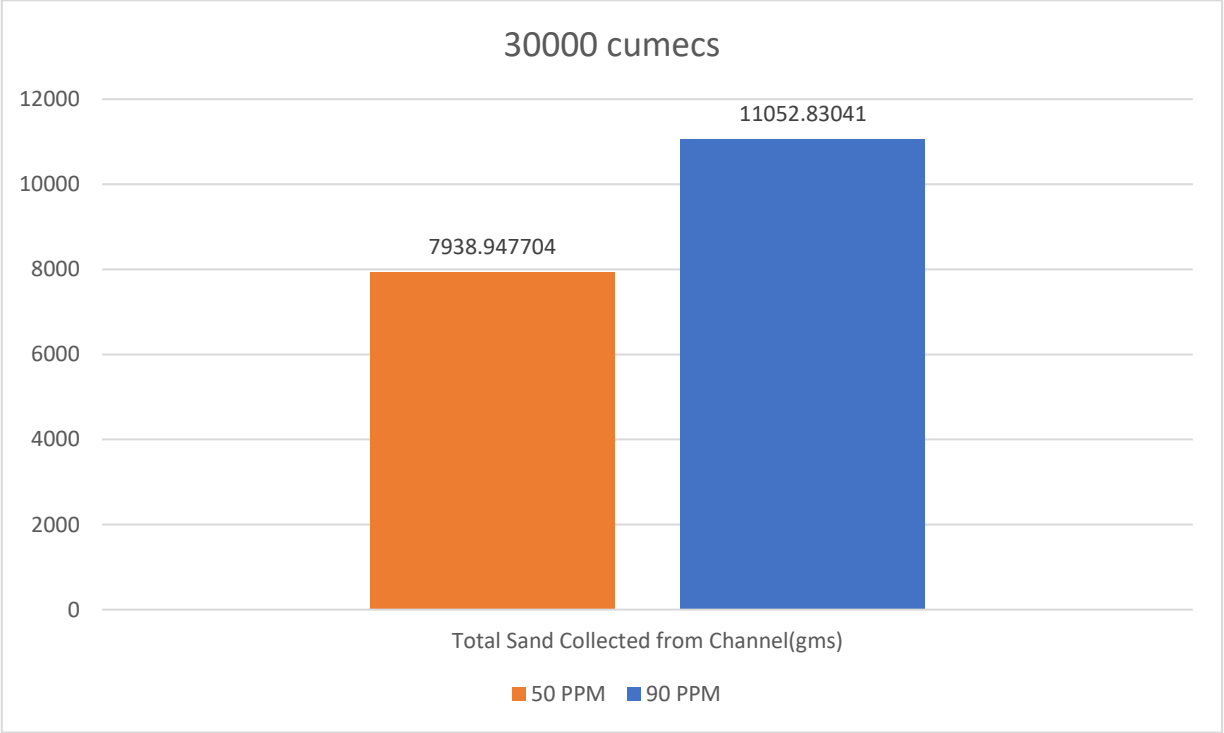

Figure 7.13 Collection of Sand at 30000 cumecs discharge

7.4 Discussion and Conclusion

The design criteria for the movable bed and the settling characteristics of suspended particles have been effectively studied, the settling velocity similarity between the model and the prototype has been established and applied appropriately in the design process. By ensuring that the settling velocity of the model is (67)^0.5 times less than the prototype, the model replicates the sediment transport behaviour of the prototype accurately.

The selection of PVC powder as the suspended sediment material, with its specific gravity matching the calculated requirement, further ensures the similarity between the model and the prototype. Through the injection of sediment in the model channel, scaled according to the prototype sediment load, and the subsequent observations of sedimentation at varying concentrations and discharge levels, valuable insights into the sediment transport process have been gained. The observed sedimentation patterns, recorded weights of sand and PVC in the sieves, and the subsequent analysis of the collected samples provide crucial data for understanding the behaviour of suspended particles in the dredging channel.

Based on the provided table of observations from the physical model, following conclusions can be drawn:

1. Effect of Discharge on Sedimentation: As the discharge increases from 10,000 cumecs to 30,000 cumecs, there is a noticeable change in the distribution of sediment between sand and PVC in the sieves. Specifically, at lower discharges, there is a higher proportion of PVC sediment compared to sand, whereas at higher discharges, this proportion shifts towards more sand sediment. This concludes that, if the concentration of suspended sediment at upstream is kept constant and discharge is varied, with increase in discharge there is decrease in suspended sediment settled and percentage of suspended sediment flushed out increase in dredging channel which further concludes that the dredging channel remains effective even at higher discharges. The total weight of PVC and sand collected from the channel increases with higher discharges, suggesting that higher discharges lead to greater sediment transport and deposition in the channel.

2. Influence of Sediment Concentration: There is a clear impact of sediment concentration (50 PPM vs. 90 PPM) on the sedimentation process. At both 50 PPM and 90 PPM concentrations, the distribution of sand and PVC in the sieves varies significantly, indicating that sediment concentration plays a crucial role in determining sediment deposition patterns. It is observed that keeping discharge

same, with increase in sediment concentration upstream there is increase in suspended sediment settled in channel.

The sediment transport dynamics within dredging channels are paramount for efficient management of hydraulic infrastructure. This study conducts a detailed analysis of sedimentation processes using a physical model approach. By meticulously examining the settling characteristics of suspended particles and establishing a similarity criterion for settling velocity between the model and prototype, this research ensures the accurate replication of sediment transport behaviour. The selection of PVC powder as the suspended sediment material, matched carefully to the specific gravity requirements, further enhances the fidelity of the model. Through scaled sediment injection and systematic observation of sedimentation patterns at varying concentrations and discharge levels, this study provides valuable insights into sediment transport processes.

Analysis of the observed sedimentation patterns and recorded weights of sand and PVC in sieves offers crucial data for understanding the behaviour of suspended particles within dredging channels. Notably, the effect of discharge variations on sedimentation dynamics is profound. With increasing discharge rates from 10,000 cumecs to 30,000 cumecs, a noticeable shift in the distribution of sediment between sand and PVC in the sieves is observed. At lower discharges, there is a higher proportion of PVC sediment compared to sand, while at higher discharges, this proportion shifts towards more sand sediment. This indicates that higher discharges lead to greater sediment transport and deposition in the channel. Furthermore, the total weight of PVC and sand collected from the channel increases with higher discharges, suggesting enhanced sediment transport under these conditions.

Additionally, the influence of sediment concentration on sedimentation dynamics is evident. Analysis reveals significant variations in sediment deposition patterns at different sediment concentrations (50 PPM vs. 90 PPM). Irrespective of discharge rates, an increase in sediment concentration upstream correlates with heightened sediment settlement in the channel. This underscores the critical role of sediment concentration in governing sedimentation dynamics within dredging channels.

8.

Conclusion and General Discussion for Future Studies

8.1 A Brief Review of Work Done

Objective 1:

To Study the Role of Morphology and Soil Properties in Bank Erosion of Brahmaputra River.

From the bank line analysis, it is found that there are five locations which are stable. The first location is the Bogibeel Bridge (Guide Bunds), followed by Salmara, Silghat, Pandu, and Pancharatna. Except at Bessamara (Salmara) point, where there is little erosion, there is no erosion on either of the banks of the Brahmaputra River at these locations. Rocks are available in these locations or guide bunds are constructed in the bank for bridge. Some erosion was reported in Salmara area where clayey soil is available. However, this is now controlled with some, -anti-erosion-measures. There is erosion in every location apart from the above-mentioned stable locations. It is found there is change in discharge distribution and flow direction in sub channel of river Brahmaputra. Soil properties are tested along the bank of river Brahmaputra. Mechanical analysis was done for all the 19 (nineteen) samples. Out of these, 6 (six) samples fall under SP-SM group, 3 (three)samples fall under ML group, 4(four) samples fall under MI group, 6 (six) samples fall under SP group of BIS Soil Classification system. The values of maximum dry density and optimum moisture content vary from 1.50 gm/cc to 1.69 gm/cc and 12.59% to 22.27% respectively. It can be concluded that the bank erosion in large braided river is dependent on flow pattern and direction in channels and it is not much dependent on bank soil properties where clay or rock is not available.

Objective 2.1:

To Study the Formation of Scour Hole in Brahmaputra River and Compare it with the Calculated Scour Depth and Width by Empirical Formula.

The scour depths are measured in the physical model for bridges in river Brahmaputra at Guwahati & Tezpur. The major scour depths at pier are scaled up using Melville & Sutherland equation and compare with the computed scour depth by Lacey's formula. It is found that maximum measured scour depth is just within the calculated scour depth. Therefore, it may be concluded that Melville & Sutherland equation can be used for physical model study for river Brahmaputra. The distances for scour effect are also measured for upstream and downstream of physical model of these two Bridges. The measured distances are scaled up by using horizontal ratio and compared with the computed scour hole influenced distance by the formula given by Singh et. al (2020). It is found that measured distances are at par with the computed distance. Therefore, it may be concluded that the formula given by Singh et. al is applicable for river Brahmaputra.

Objective 2.2:

To Conduct Model Study for Management of River at Downstream of Bridge by Providing Mid Channel.

The reach where Saraighat bridges where were constructed near Guwahati, has constricted with rock out confining the river. The Brahmaputra River has minimum width at this bridge section. The river is widened just downstream of Saraighat bridge. The river is outflanked and has been eroding both North and South Bank. Again, the north bank of river Brahmaputra just downstream of Kolia Bhomora bridge is stable where is the Tezpur town is situated. But there is vast river bank erosion problem at South Bank just downstream of bridge. Field studies are done in these two important reaches of river Brahmaputra downstream of bridges at Guwahati and Tezpur and Physical model studies are conducted. It is found at velocity will decrease near bank due to implementation of proposed channel. But there will be siltation in the channel. Significant siltation happened within 3 days of peak discharge. It is projected that full siltation will happen in the actual channel within 1 year. It is concluded that dredging channel in large braided river can reduce the bank erosion of river but regular maintenance of channel will be required to maintain the channel.

Objective 3:

To Investigate the Possibility of Reduction in River Bank Erosion by Implementing Dredged Channel in Braided River. Also, to Study the Efficacy of Porcupine Screen with Dredging Channel Through Physical Model Study.

The Brahmaputra River is obliquely hitting the river bank at Nimatighat which is situated at opposite side of Majuli Island and a portion of the bank has already eroded by the river. A physical model study of this reach has been conducted to study the effects of the river flow towards Nimatighat in order to find an amicable solution to control the erosion at Nimatighat area. A channel has been dredged in the model of study for widths varying from 100 m to 400 m with an idea to divert the flow of the river away from Nimatighat. Porcupine screens were also laid upstream of the area of study to divert the river flow towards the dredged channel. The readings and observations for different discharges and channel widths (both without and with porcupine screens) are obtained. After detailed study, it is found that the dredging channel with porcupine screen may be the best solution for bank erosion problem in braided river. However, siltation is an issue as discussed earlier.

Objective 4:

To Analyse Radar Data for Planning of Anti-Bank Erosion Work in Braided River.

SAR data from Sentinel-1 were processed with the free software SNAP (Sentinel Application Platform) Tool [http://step.esa.int], created by ESA for the analysis of the data captured by Sentinel satellites. One Sentinel 1 imagery for every month from April'2020 to September'2020 was used to finalized the proposed dredging channel. After analysis, it is found that radar data is very useful for planning of anti-bank erosion work in braided river. During the monsoon season, the planned location is discovered to function as a primary branch channel. Radar data analysis is done with sentinel 1 imagery and the suggested dredging location has been finalised. (Deka and Sarma, 2022). Dredging a channel and constructing a number of permeable spurs close to the eroded bank provided for the conclusion of a numerical modelling study (NEHARI, 2022).

Objective *5*:

To Study the Suspended Sediment Deposition in Proposed Dredging Channel.

Suspended sediment deposition in proposed dredging channel in physical model. The suspended sediment size is scaled down by using settling velocity similarity. The sediment load is induced in a lined channel in physical model proportionality of measured sediment in Brahmaputra River. On

increasing the discharge, keeping same concentration of sediment it is seen that amount of sediment flushed out of channel increases. It is found that there is no significant impact of suspended sediment in the proposed channel during peak discharge. However, further study is required to understand the sedimentation process in large braided river.

8.2 Recommendations for future work

1. The river morphology study of braided river was done using optical image of lean-season and radar image of monsoon season. The methodology can be improved using temporal digital surface model of braided river.

2. The mathematical model study for braided river was done using rigid bed, due to limitation of processing power of computer. The study can be improved by using mobile bed with advancements of better coding of software and processing power of computer in future.

3. Suspended sediment study was done using sediment seeding in dredging channel. This can be further improved by seeding suspended sediment for the entire river.

4. The physical model study for sedimentation in dredging channel is conducted considering 50,000 cumec steady discharge. Time required for sedimentation of the dredge channel is roughly estimated based on this study. However, actual discharge in river will vary in different seasons. Further study can be done by considering variable flow.

References

Archana, S., R. D., G., Nayan, S., 2012. RS-GIS Based Assessment of River Dynamics of Brahmaputra River in India. J. Water Resour. Prot. 2012, 63–72. https://doi.org/10.4236/JWARP.2012.42008

Ashworth, P.J., Best, J.L., Leddy, J.O., Geehan, G.W., 1994. The physical modelling of braided rivers and deposition of fine-grained sediment.

Baynes, E.R.C., van de Lageweg, W.I., McLelland, S.J., Parsons, D.R., Aberle, J., Dijkstra, J., Henry, P.Y., Rice, S.P., Thom, M., Moulin, F., 2018. Beyond equilibrium: Re-evaluating physical modelling of fluvial systems to represent climate changes. Earth-Science Rev. 181, 82–97. https://doi.org/10.1016/j.earscirev.2018.04.007

Bristow, C.S., Best, J.L., 1993. Braided rivers: perspectives and problems. Braided rivers 1–11.

Burele, S.A., Gupta, I.D., Singh, M., Sharma, N., Ahmad, Z., 2012. Experimental study on performance of spurs. ISH J. Hydraul. Eng. 18, 152–161. https://doi.org/10.1080/09715010.2012.695446

Burele, S.A., Sharma, N., Ahmad, Z., Gupta, I.D., 2018. International Journal of Advance Engineering and Research HYDRAULIC MODEL STUDIES FOR CHANNELIZATION OF RIVER KOSI FOR A REACH FROM CHATRA TO KOSI BARRAGE USING 228–240.

Candel, J., Kleinhans, M., Makaske, B., Wallinga, J., 2021. Predicting river channel pattern based on stream power, bed material and bank strength. Prog. Phys. Geogr. 45, 253–278. https://doi.org/10.1177/0309133320948831

Candel, J.H.J., Makaske, B., Storms, J.E.A., Wallinga, J., 2020. Self-constraining of low-energy rivers explains low channel mobility and tortuous planforms 648–669. https://doi.org/10.1002/dep2.112

Cazals, C., Rapinel, S., Frison, P.L., Bonis, A., Mercier, G., Mallet, C., Corgne, S., Rudant, J.P., 2016. Mapping and characterization of hydrological dynamics in a coastal marsh using high temporal resolution Sentinel-1A images. Remote Sens. 8. https://doi.org/10.3390/rs8070570

Chang, H., 2018. EXPERIMENTAL STUDIES ON THE EFFECT OF THE DREDGING ON CHANG- HWA RECLAMATION AREA , TAIWAN.

Chang, H.H., Wiley, J., Bush, G., 1989. AGU Letter to 70, 1989.

Das, T.K., Haldar, S.K., Gupta, I. Das, Sen, S., 2014. River bank erosion induced human displacement and its consequences. Living Rev. Landsc. Res. 8, 1–35. https://doi.org/10.12942/lrlr-2014-3

De, G., 2021. PHYSICAL MODEL AS A TOOL FOR STUDYING RIVER PROBLEMS- A REVIEW.

Deka, R., Sarma, A.K., 2022. Use of Landsat and Sentinel-1 Data for Implementation of Bank Protection Work in Brahmaputra River 235–244. https://doi.org/10.1007/978-981-16-9933-7_15

Dey, S., Basu, A., Banerjee, S.N., Jain, V., 2022. Discharge-driven rapid bank-erosion and its impact on sediment budgeting in the lower Gangetic plains. Episodes 1–9. https://doi.org/10.18814/epiiugs/2022/022027

Die moran, A., El kadi abderrezzak, K., Mosselman, E., Habersack, H., Lebert, F., Aelbrecht, D., Laperrousaz, E., 2013. Physical model experiments for sediment supply to the old Rhine through induced bank erosion. Int. J. Sediment Res. 28, 431–447. https://doi.org/10.1016/S1001-6279(14)60003-2

Dredging for development, 1991.

Duró, G., Crosato, A., Kleinhans, M.G., Winkels, T.G., Woolderink, H.A.G., Uijttewaal, W.S.J., 2020. Distinct patterns of bank erosion in a navigable regulated river. Earth Surf. Process. Landforms 45, 361–374. https://doi.org/10.1002/esp.4736

Egozi, R., Ashmore, P., 2009. Experimental analysis of braided channel pattern response to increased discharge 114, 1–15. https://doi.org/10.1029/2008JF001099

El, K., Abderrezzak, K., Die, A., Mosselman, E., 2014. ScienceDirect A physical , movable-bed model for non-uniform sediment transport , fluvial erosion and bank failure in rivers. J. Hydro-

Environment Res. 8, 95–114. https://doi.org/10.1016/j.jher.2013.09.004

El, K., Abderrezzak, K., Die, A., Mosselman, E., 2013. ScienceDirect A physical , movable-bed model for non-uniform sediment transport , fluvial erosion and bank failure in rivers. J. Hydro-Environment Res. 8, 95–114. https://doi.org/10.1016/j.jher.2013.09.004

Firdaus Zulkefly, Z., Abustan, I., Remy Rozainy, M., Abdul Wahab, K., 2019. An Experience of Hydraulic Physical Model Study in Malaysia. IOP Conf. Ser. Mater. Sci. Eng. 551. https://doi.org/10.1088/1757-899X/551/1/012117

Fischer, S., Pietroń, J., Bring, A., Thorslund, J., Jarsjö, J., 2017. Present to future sediment transport of the Brahmaputra River: reducing uncertainty in predictions and management. Reg. Environ. Chang. 17, 515–526. https://doi.org/10.1007/s10113-016-1039-7

Gorrick, S., Rodríguez, J.F., 2014. Scaling of sediment dynamics in a laboratory model of a sand-bed stream. J. Hydro-Environment Res. 8, 77–87. https://doi.org/10.1016/j.jher.2013.12.001

Haque, S., Ali, M.M., Saiful Islam, A.K.M., Khan, J.U., 2021. Changes in flow and sediment load of poorly gauged Brahmaputra river basin under an extreme climate scenario. J. Water Clim. Chang. 12, 937–954. https://doi.org/10.2166/WCC.2020.219

Harding, J., 2016. A literature review of physical habitats and.

Heller, V., 2011. Scale effects in physical hydraulic engineering models. J. Hydraul. Res. 49, 293–306. https://doi.org/10.1080/00221686.2011.578914

Islam, M.S., 2008. River Bank Erosion and Sustainable Protection Strategies B-11 RIVER BANK EROSION AND SUSTAINABLE. Proc. 4th Int. Conf. Scour Eros. 316–323.

Khan, A., Mujumdar, S., 2021. Assessing the Hydraulic Performance of Proposed Hirpura Barrage on Sabarmati River, Gujarat. J. Inst. Eng. Ser. A. https://doi.org/10.1007/s40030-021-00573-6

Krobicki, M., 2010. Topographical , Geological and Geophysical Measurements in the Diamer Basha Dam Area (Gilgit- Related papers 2010.

Mandal, S., 2017. Assessing the instability and shifting character of the river bank Ganga In

Manikchak Diara Of Malda District, West Bengal Using Bank Erosion Hazard Index (BEHI), RS & GIS. Eur. J. Geogr. 8, 6–25.

Mani, P., Kumar, R., Chatterjee, C., 2003. Erosion study of a part of Majuli river-island using remote sensing data. J. Indian Soc. Remote Sens. 31, 12–18. https://doi.org/10.1007/bf03030747

Maurya, S., Gupta, M., Chitra, R., 2022. Use of Geosynthetics as a Soft Structural Measure to Mitigate Flood Hazard and Bank Erosion Problem, in: Satyanarayana Reddy, C.N. V, Saride, S., Krishna, A.M. (Eds.), Ground Improvement and Reinforced Soil Structures. Springer Singapore, Singapore, pp. 751–763.

Mossa, J., Chen, Y.H., 2021. Geomorphic insights from eroding dredge spoil mounds impacting channel morphology. Geomorphology 376, 107571. https://doi.org/10.1016/j.geomorph.2020.107571

Nath, A., Ghosh, S., 2022. Meandering rivers' morphological changes analysis and prediction - a case study of Barak river, Assam. H2Open J. 5, 289–306. https://doi.org/10.2166/h2oj.2022.003

NEHARI, B.B., 2022. A 2D Hydrodynamic Model Study in Brahmaputra River for Implementation of Bank Protection Work at Nimatighat. Sustain. Water Resour. Manag. Proc. SWARM 2020 92.

Pareta, K., 2021. River morphological modelling of Brahmaputra River , Assam 2, 8–17.

Pareta, K., Pareta, U., 2023. Post-earthquake Sedimentation Changed the Morphology of the Brahmaputra River 12.

RAHMAN, S.A., ISLAM, M.M., SALMAN, M.A., RAFİQ, M.R., 2021. Evaluating bank erosion and identifying possible anthropogenic causative factors of Kirtankhola River in Barishal, Bangladesh: an integrated GIS and Remote Sensing approaches. Int. J. Eng. Geosci. 7, 179–190. https://doi.org/10.26833/ijeg.947493

Sarma, A., 2014. Landscape Degradation of River Island Majuli, Assam (India) due to Flood and Erosion by River Brahmaputra and Its Restoration. J. Med. Bioeng. 3, 272–276. https://doi.org/10.12720/jomb.3.4.272-276

Sarma, D., 2013. Rural Risk Assessment due to Flooding and Riverbank Erosion in Rural Risk Assessment due to Flooding and Riverbank Erosion in Majuli , Assam , India 85.

Sarma, J.N., 2005. Fluvial process and morphology of the Brahmaputra River in Assam, India. Geomorphology 70, 226–256. https://doi.org/10.1016/j.geomorph.2005.02.007

Sarma, N., Dutta, P., 2016. Stability Analysis of Brahmaputra Riverbank at Neulgaon 122–125.

Singh et. al.,2020. Spacing of adjacent bridges based on local bridge scour and stress distribution in surrounding soil - A case study of New Kosi Railway Bridge between Katareah & Kursela Stations on Barauni Katihar 1–9.

Smedes, R., Klaassen, G., Taal, M., Sloff, C., Douben, N., Havinga, H., 2006. Recent training of the lower Rhine River to increase Inland Water Transport potentials. River Flow 2006. https://doi.org/10.1201/9781439833865.ch3

Sultana, P., Uddin, M.I., Analysis, M., 2017. Dredging and Land Reclamation in Bangladesh Perspective : A State-of-the- Art Overview Dredging and Land Reclamation in Bangladesh Perspective : A State-of-the-Art Overview 0–4.

Talchabhadel, R., Nakagawa, H., 2016. EXPERIMENTAL STUDY ON SUSPENDED SEDIMENT TRANSPORT TO REPRESENT TIDAL 1. https://doi.org/10.2208/jscejhe.72.I

Tavus, B., Kocaman, S., Gokceoglu, C., Nefeslioglu, H.A., 2018. CONSIDERATIONS ON THE USE OF SENTINEL-1 DATA IN FLOOD MAPPING IN URBAN AREAS: ANKARA (TURKEY) 2018 FLOODS. Int. Arch. Photogramm. Remote Sens. Spat. Inf. Sci. XLII–5, 575–581. https://doi.org/10.5194/isprs-archives-xlii-5-575-2018

Taylor, P., Heller, V., 2011. Scale effects in physical hydraulic engineering models 37–41. https://doi.org/10.1080/00221686.2011.578914

Twele, A., Cao, W., Plank, S., Martinis, S., 2016. Sentinel-1-based flood mapping: a fully automated processing chain. Int. J. Remote Sens. 37, 2990–3004. https://doi.org/10.1080/01431161.2016.1192304

Valentine, L., Wilson, C.A., 2022. Flood risk of embanked areas and potential use of dredge spoils

as mitigation measures in the southwest region of the Ganges – Brahmaputra – Meghna Delta , Bangladesh 1073–1088. https://doi.org/10.1002/esp.5303

Victor Sapozhnikova, 1996. Self-Affinity in Braided Rivers.pdf, n.d

Wasson, R., Acharjee, S., Rakshit, R., 2022. Towards identification of sediment sources, and processes of sediment production, in the Yarlung-Tsangpo-Brahmaputra River catchment for reduction of fluvial sediment loads. Earth-Science Rev. 226, 103932. https://doi.org/10.1016/j.earscirev.2022.103932

Yang, H., 2020. Numerical investigation of avulsions in gravel-bed braided rivers. Hydrol. Process. 34, 3702–3717. https://doi.org/10.1002/hyp.13837

Zealand, N., 1983. RESPONSE OF BRAIDED RIVERS TO CHANGING DISCHARGE Author (s): M . P . Mosley Published by : New Zealand Hydrological Society Stable URL : https://www.jstor.org/stable/43944509 22, 18–67.

Zhao, K., 2021. A Numerical Model of Bank Collapse and River Meandering Geophysical Research Letters 1–10. https://doi.org/10.1029/2021GL093516

List of Publications

DEKA Ranjit[1], SARMA Arup K.[2] (2020), "A satellite imagery study in Brahmaputra River for implementation of bank protection work at Nimati Ghat" Geospatial application for Natural resources management, (July 9-10,2020) NIRDPR-NERC, Guwahati. ISBN-978-81-8730-584-4

BARUAH Anupal1, DEKA Priyam2, DEKA Ranjit2, SARMA Arup K.2 "A 2D hydrodynamic model study in Brahmaputra River for implementation of bank protection work at Nimati Ghat", International Conference on Sustainable Water Resources Management (SWARM-2020). [Published on18.06.2022] DOI: 10.1007/978-981-16-7535-5_10

Deka Ranjit1, & Sarma, A. K2 "USE OF LANDSAT AND SENTINEL-1 DATA FOR IMPLEMENTATION OF BANK PROTECTION WORK IN BRAHMAPUTRA RIVER", 1st International Conference on River Corridor Research and Management, IIT Jammu, 2021. [Published], DOI: 10.1007/978-981-16-9933-7_15.

DEKA Ranjit[1], SARMA Arup K.[2] (2022), "Observation of physical model for hydraulic research by using UAV", 2nd International Conference on River Corridor Research and Management, IIT Guwahati, 2022. [Presented but not published]

DEKA Ranjit[1], BARMAN Bandita[2] SARMA Arup K. [3], "A Physical Model Study to Investigate the Potential of Dredging in Erosion Reduction at Nimatighat, Brahmaputra River" (At final stage for submission)

Annexure I:

PHOTOGRAPHS TAKEN DURING FIELD VISIT AT MAJULI


26-Jul-2022 1:19:41 pm
26.9166N 94.2991E
45° NE
W78X+FF9
Borboka Pathar
Assam 785110
India
Majuli, Assam
Index number: 2

Annexure II:

PHOTO SHOWING DIFFERENT STAGES OF CONSTRUCTION OF PHYSICAL MODEL FOR A REACH NEAR MAJULI

Construction of boundary of cross-section and it's marking

Laying of Bamboo Pegs at Cross Sections are in Progress

Laying of Bamboo Pegs at Cross Sections are in Progress

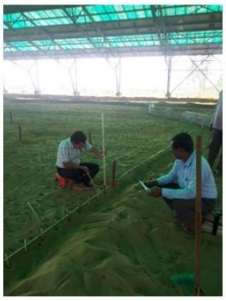

Construction of Spurs at Model

Screening of Bed Materials

Soil Gradation Test at NEHARI

Construction of Arrangement for Entry of Water

Construction of Arrangement for Exit of Water

Construction of Arrangement for Exit of Water

Heading Up Arrangement

Ready to use pump system for Running of Model

Entry of water for Running of Model

Water Running Through the Model

Observation of Model at Spur Area

Observation at field near Spur Area

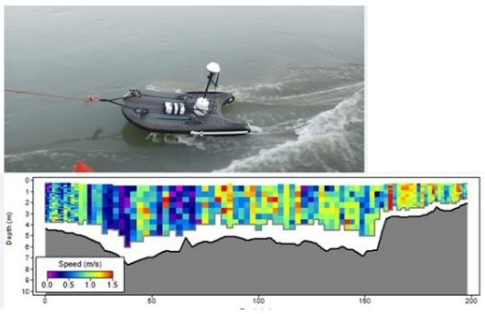

Observation of Model at Spur Area